Design Optimisation of Patient-Specific Implants and Total Joint Replacements in Oral & Maxillofacial Surgery

A Fundamental Approach

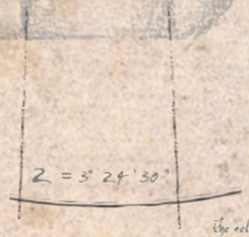

The high tolerances internal angle of the self-locking connection between the stem of the mandibular component and neo-condylus

An exploded view of the mandible component and articulation parts exposing the taper connection between the mandible component and neo-condylus. This connection is the result of metal internal pressure. The neo-hinge envelopes the neo-condylus part's centre point, thereby realising a snap-fit connection.

The human mandible with a reconstruction of a large continuity defect and total joint replacement of the temporomandibular joint (left). The patient-specific reconstructive implant is a topology optimized, organically shaped structure.

The patient-specific total joint replacement, following the 'Groningen principle', is fit to the patient's anatomy and should include a centre of rotation that is lowered and tailored to the specific patient.

A close-up of the underside of the neo-hinge showing opening that seats the neo-condylus. At the applied radiolucent, titanium markers are inserted in the outer hinge, at 12.0° apart.

Bram Merema

Design Optimisation of Patient-Specific Implants and Total Joint Replacements in Oral & Maxillofacial Surgery

A Fundamental Approach

Bram Merema

Unrestricted financial support for publication of this thesis by the following institutions is gratefully acknowledged: University of Groningen (RUG), Graduate School of Medical Sciences (GSMS), University Medical Center Groningen (UMCG), Xilloc Medical, NVMKA, Oceanz, KLS Martin, Witec Medical, Chattering Squirrel, Straumann Group, SORG, Demgy, Formlabs and Materialise.

Layout and printing: Optima Grafische Communicatie, Rotterdam | www.ogc.nl
Cover design: B.J. Merema

ISBN 978-94-6361-919-6

rijksuniversiteit
groningen

Design Optimisation of Patient-Specific Implants and Total Joint Replacements in Oral & Maxillofacial Surgery

A Fundamental Approach

Proefschrift

ter verkrijging van de graad van doctor aan de
Rijksuniversiteit Groningen
op gezag van de
rector magnificus prof. dr. ir. J.M.A. Scherpen
en volgens besluit van het College voor Promoties.

De openbare verdediging zal plaatsvinden op

woensdag 29 november 2023 om 14:30 uur

door

Barteld Jan Merema

geboren op 6 maart 1992
te Assen

Promotores
Prof. dr. F.K.L. Spijkervet
Prof. dr. M.J.H. Witjes
Dr. J. Kraeima

Beoordelingscommissie
Prof. dr. dr. P.A.W.H. Kessler
Prof. dr. ir. G.J. Verkerke
Prof. dr. H.A. Santos

Paranimfen
A.J. Nijman
B.W. Schram
Dr. G. Trentadue

Voor Else

INDEX

Chapter 1

General Introduction

GENERAL INTRODUCTION

The research described in this thesis focuses on the development, implementation, optimisation and evaluation of three-dimensional (3D) virtual surgical planning (VSP) workflows and patient-specific implants (PSI) and temporomandibular joint total joint replacements (TMJ-TJRs) for Oral and Maxillofacial surgery (OMFS) purposes. Despite the focus on OMFS, the suggested and applied techniques in this thesis are translatable, applicable and potentially beneficial to, e.g., other fields of surgery and biomechanics.

3D technology in Oral and Maxillofacial Surgery

Over the past decade, 3D-VSP and patient-specific modelling (PSM) of (reconstructive) implants and surgical tools have gained in popularity and found new applications rapidly. The general availability of software, along with the drastic increase in the computational power of computers, has led to better availability of 3D virtual techniques as well. The use of 3D technology has been incorporated in patient care resulting the number of 3D designed PS or custom implants, often inaccurately referred to as CAD/CAM, and total joint replacement (TJR) prostheses increasing as well. However, despite being an extremely helpful tool, accessible and robust, 3D technology can simultaneously lead to inappropriate use when applied to patient care/healthcare without the required knowledge and pre-clinical testing. This could apply especially to the surgeon who may be familiar with the final product but might not be aware of all the considerations and assumptions taken throughout the design process and the in-silico testing; the in-silico testing might imply, for example, different implant strengths than that seen in the clinical setting. This could harm the patient with respect to implant failure, depending on the nature of the failure and surrounding delicate structures.

Since the introduction of PSM implants and TMJ-TJR prostheses about fifteen years ago, the above described technology has become the current standard in the OMFS department of the University Medical Center Groningen. Based on our own research, numerous indications have emerged for the application of this technology, such as in-house developed surgical drilling and saw guides, reconstructive implants and TMJ-TJR prostheses. With these 'first generation' PSIs, a number of conventional failures have been resolved, however, some have remained. Therefore, the current generation

of PSIs requires more attention and optimisation towards a 'second generation' to raise these applications to a higher level.

With the rapid multiplication of PSM 3D-designed implants and TMJ-TJR prostheses, the demand for properly validated biomechanical virtual models has also increased. Such models are used for, e.g., strength calculations and other digital implant design simulations which means an implant can be tested virtually without actually subjecting the implant to destructive experiments, saving on both costs and time. An example of such a virtual tool that can be used for such purposes is the finite element method, or finite element analysis (FEA).

In the OMFS field, a large variety of osteosynthesis plates and prostheses has been presented in the literature for the treatment of, e.g., trauma-, oncology- or TMJ patients[1-5]. What these applications have in common is failure, e.g., loosening or fracturing of the implanted material, or the screw-fixation of the implant to the patient's bone, often resulting in failure of the reconstruction in its entirety. It appears that, to be successful, the implanted osteosynthesis plate and its fixations should of a matching strength for the patient's specific situation[6]. Mandibular reconstruction failure through either osteosynthesis plate failure or screw loosening are widely reported in the literature as common causes of mechanical failure[7-11], which shows the lack of a truly universal reconstruction solution due to the uniqueness of each patient's specific reconstruction situation. The accessibility and pricing of confection sized and shaped osteosynthesis plates have resulted in their common worldwide implementation. These plates are, however, predominantly associated with the reported osteosynthesis failure in mandibular reconstructions[12-14].

Head and neck reconstructive surgery

Patients who suffer from oral cancer, more specifically, tumours with bone invasion in the mandible (T4), can lose mandibular continuity after the tumour has been resected. This means that the mandible will no longer be connected as one piece after the so called segmental resection. This has major consequences for the oral functions, such as speech and mastication, and generally leads to discomfort for the patient[15]. Therefore, patients who are left with a mandibular bone continuity defect after a segmental resection need the reconstruction to be done in an abiding manner. Preferably, the reconstruction of the defect is carried out with a free vascularised (bone) flap, e.g., a fibula or scapula graft. However, when a patient's general medical condition does

not allow for this type of reconstructive surgery, the mandibular continuity defect can be bridged using solely a conventional reconstruction plate (RP). This type of RP, often made of a titanium alloy, needs manual contouring through bending in order to match the mandible's shape. Repetitive bending of the RP, however, weakens the material and this method has been reported to fail due to screw loosening or plate fracture[13, 14, 16-19]. Plate fracture is seen predominantly in the regions surrounding the screws nearest to the continuity defect and can be caused by fatigue through cyclic in situ loading[17], usually encouraged by residual stress inside the plate as a result of repetitive bending while contouring[19-21]. Previous research found a failure rate of 10% for screw loosening and plate fracture combined[12], while also failure solely due to plate fracture is reported in 10% of the cases[8, 12-14] or only to screw loosening in 18% of the cases[10].

Often, cancer patients who require reconstruction of a mandibular continuity defect also receive postoperative radiotherapy. A common side effect of the consequent scarification of the soft tissues, including around the reconstruction plate, is stiffening and contraction of the tissues. It is not unusual for the foreign RP metallic material becoming dehiscent. This can occur both intra- and extra-orally[22, 23].

Even when the RP is successful and stable, there can be complications related to the osteosynthesis material (OSM) that can develop over time which can reduce its stability or make it fail in-toto. Stress-shielding can, for example, be caused by the application of metallic RPs[24]. An apparent mismatch between the mechanical properties of the RP and the bone it is fixated to can lead to bone resorption around the implant and screws. This is due to a degree of underloading of the bone, causing it to remodel. There is, seemingly, a sophisticated balance between the plates being too weak, causing material failure, or too strong, potentially leading to stress-shielding and thereby disturbance of the natural equilibrium of bone formation, causing resorption of the surrounding bone[24].

Section I of this thesis aims to address these known (bio)mechanical complications following the reconstruction of continuity defects of the mandible by means of mechanical reconsiderations of the current conventional and PS RPs and by developing a finite element based alternative RP.

Temporomandibular joint replacement surgery

Regarding patients who suffer from severe TMJ dysfunction, a TMJ-TJR may be necessary in the form of a prosthesis, especially when joint saving approaches do not suffice. Reported indications include end-stage degenerative joint disease, recurrent ankylosis, and congenital disorders affecting the TMJ[25]. Other indications for TJRs are condylar loss as a result of trauma or neoplasia in or near the joint, or to replace a failed alloplastic or autogenous reconstruction[26]. In most of these patients, mandibular movement is impaired due to either anatomical changes or surgically caused scarification, often resulting in pain, difficulties in speech, impaired oral function, and limited maximum mouth opening.

Already in the 80's of the past century, the value of TMJ-TJRs had become clear[27]. Pain could be drastically reduced in some cases and mandible mobility could be partially restored. Yet, the available TMJ-TJR designs were not up to par for long term use, as was demonstrated by the Vitek-Kent debacle due to its Proplast constituents[27]. To fill in this lack of a proper long-term TMJ-TJR functioning and fulfilment of all the necessary requirements, a developmental project was initiated on a new type of TMJ-TJR prosthesis by the department of Oral and Maxillofacial Surgery in the Groningen University Hospital in 1988 (now University Medical Center Groningen, the Netherlands). The first part of the project was described in Falkenstrom's Ph.D.-thesis [28]. His work was followed up in two successive Ph.D. theses, first by van Loon[29], then by Kraeima[30], which added the necessary steps and led to a clinically applicable prosthesis and actual clinical applications. The current thesis is the fourth in line to (partially) focus on the development of the Groningen TMJ-TJR. This time it is predominantly based on an optimisation perspective based on the experiences in the patients who received these prostheses.

Section II of this thesis aims to increase the amount of patient-specificity of TMJ-TJRs, especially the Groningen TMJ-TJR (G-TMJ-TJR), to optimise the functional qualities of these prostheses.

In-vitro validation of in-silico models

FEA has gained ground in the biomedical field since the 1970s and has proven to be valuable due to its non-destructive character and ease in evaluating multiple scenarios[31]. This tool can be used to virtually load digital objects and in order to predict and study their static or dynamic response to the loads it is subjected to. Typical

necessary variables that need to be assigned to the analysed object(s) depend on the type of FEA performed but include material properties such as Young's modulus of elasticity and Poisson's ratio. Furthermore, the object(s) need to be constrained in space and need to be loaded using internally or externally exerted forces. The engineer needs to carefully consider all the input variables and assumptions whilst setting up the analysis as these strongly affect the outcome of the FEA. Accurate FEA models help to predict a material's behaviour without the need for destructive tests and could replace in-vivo tests whereas inaccurate models provide a false sense of security and can have catastrophic consequences.

To be able to rely sufficiently on the strength of a PSI or TMJ-TJR, which has been calculated and simulated virtually with, e.g., FEA, the used biomechanical model must be endorsed by means of a thorough validation process. To make this possible, the patient's biomechanical situation should be transferred as accurately as possible to the physical validating process. Many FEA based PSIs and TMJ-TJRs have now been presented in the OMFS related literature, especially PS devices. Although the FEA tool is perfectly suited for complex strength calculations of such PSIs and TMJ-TJRs, what often stands out is that the FEA input variables and assumptions are not patient-specific. The mechanical properties of the bone and the muscular system, i.e., absolute forces, force directions and attachment sites to the mandible, are often based on dated generic models or information that was acquired from a number of cadaveric dissections[32-34]. Such PSIs and TMJ-TJRs could be drastically over- or under dimensioned without the engineer or surgeon knowing, resulting in possible short or long-term failure of the implant.

Current literature lacks both validation of the old assumptions and consensus on the input variables that should be applied to representative FEA models of the human mandible[6].

In section III of this thesis, an attempt is made to suggest a complete validated work-flow for PS mechanical testing of the mandible, both intact or reconstructed with a PSI or TMJ-TJR. This method can be used to directly compare anatomically correct PS in-silico models of the mandible with an identical physical in-vitro copy. As mentioned, the in-silico methods used for PSI designs have not been fully validated[6]. Included are in-silico models such as FEA, presented in the literature in relation to designing critical implants, and they have seldomly been confirmed in-vitro[2, 3, 35, 36].

Moreover, whenever an in-silico model is validated in-vitro, it is typically performed in a rather primitive and far from anatomically realistic setting[5, 37-40]. The muscle models, for example, used in the majority of FEAs and, if available, their matching validation testing, generally consist of muscular forces and directions that are based on a generic or mean model found through a handful of dissections many years ago, and were then assumed to be uniformly applicable over time[33]. The mechanical potential of a muscle model on the outcome of PSIs designed through FEA could be substantial and should be explored.

This section presents a dedicatedly developed mandibular dynamic bite simulator (MANDYBILATOR) apparatus together with a more straight forward mandibular uniaxial compression testing apparatus (MUNACAPP). The combination of both devices enables close in-vitro validation of in-silico experiments of the mandible, both intact and reconstructed, and can be applied to both static and dynamic / cyclic load testing scenarios in a truly PS manner.

As a proof of principle, these validation instruments, together with topology optimisation, were used to develop and mechanically test a load bearing non-metallic polyetheretherketone (PEEK) PSI for the reconstruction of a large mandibular continuity defect. This was considered until now as impossible and therefore presents a perfect example of the value of these matching in-silico and in-vitro validations.

General aim of the thesis

The general aim of the research presented in this Ph.D. thesis is to develop, implement, validate and optimise 3D virtual surgical planning workflows and PSIs for two main clinical challenges in Oral and Maxillofacial Surgery. It is geared at the next generation of PSIs with a higher level of patient specificity than the current generation.

The studied fields are: head and neck reconstructive surgery and temporomandibular joint replacement surgery. ***Section I*** of this thesis covers a review of the literature on FEA models of the mandible and applies FEA to develop an implant for reconstructive surgery to bridge a continuity defect of the mandible. ***Section II*** covers the development, validation, implementation and optimisation of the Groningen TMJ-TJR prosthesis. ***Section III*** presents the workflows, devices and validations which can be generally used in the development of PSIs and TMJ-TJR prostheses applied

during OMFS to increase patient-specificity. Furthermore, a method is presented for patient specific determination of the individual forces of the presented muscle model of the mandible, which can be used to increase the patient specificity of FEA models. In Chapter 8, all the knowledge obtained in sections I, II and III are amalgamated, resulting in a non-metallic PEEK PSI for the reconstruction of a large mandibular continuity defect.

The specific aims are:

- To find consensus on how to define the input parameters for a representative FEA model of the human mandible. **(Chapter 2)**
- To design and analyse PS-RPs to bridge mandibular gaps and to minimise plate fracture and screw pull-out-related failure. **(Chapter 3)**
- To optimise the design of the Groningen TMJ prosthesis, by means of implementation of patient-specific planning and customisation. **(Chapter 4)**
- To validate the accuracy of placement of the patient-specific G-TMJ-TJR in the clinical setting. **(Chapter 5)**
- To develop a 4D-workflow to ascertain the PS mean axis of rotation, or fixed hinge, that mimics the patient's specific physiological mouth opening. **(Chapter 6**)
- To propose a contemporary method to determine the patient-specific intrinsic strength value of the elevator muscles. **(Chapter 7)**
- To develop a universal apparatus that mechanically loads the (un)implanted mandible, both synthetic and cadaveric, in a patient-specifically correct manner (**Chapter 8)**.
- To develop a non-metallic load bearing reconstruction of a continuity defect in the human mandible (**Chapter 8).**

REFERENCES

1. Elledge, R., Mercuri, L. G., Attard, A., Green, J. & Speculand, B. Review of emerging temporomandibular joint total joint replacement systems. *Br. J. Oral Maxillofac. Surg.* **57**, 722-728 (2019).
2. Li, P. *et al*. Optimal design of an individual endoprosthesis for the reconstruction of extensive mandibular defects with finite element analysis. *J. Craniomaxillofac. Surg.* **42**, 73-78 (2014).
3. Luo, D., Xu, X., Guo, C. & Rong, Q. *Fracture Prediction for a Customized Mandibular Reconstruction Plate with Finite Element Method* (Advanced Computational Methods in Life System Modeling and Simulation, Springer Singapore, Singapore, 2017).
4. Narra, N. *et al*. Finite element analysis of customized reconstruction plates for mandibular continuity defect therapy. *J. Biomech.* **47**, 264-268 (2014).
5. van Kootwijk, A. *et al*. Semi-automated digital workflow to design and evaluate patient-specific mandibular reconstruction implants. *J. Mech. Behav. Biomed. Mater.* **132**, 105291 (2022).
6. Merema, B. B. J., Kraeima, J., Glas, H. H., Spijkervet, F. K. L. & Witjes, M. J. H. Patient-specific finite element models of the human mandible: Lack of consensus on current set-ups. *Oral Dis.* **27**, 42-51 (2021).
7. Freitag, V., Hell, B. & Fischer, H. Experience with AO reconstruction plates after partial mandibular resection involving its continuity. *Journal of Cranio-Maxillofacial Surgery* **19**, 191-198 (1991).
8. Irish, J. C. *et al*. Primary mandibular reconstruction with the titanium hollow screw reconstruction plate: evaluation of 51 cases. *Plast. Reconstr. Surg.* **96**, 93-99 (1995).
9. Kimura, A. *et al*. Adaquate fixation of plates for stability during mandibular reconstruction. *J. Craniomaxillofac. Surg.* **34**, 193-200 (2006).
10. Markwardt, J., Pfeifer, G., Eckelt, U. & Reitemeier, B. Analysis of complications after reconstruction of bone defects involving complete mandibular resection using finite element modelling. *Onkologie* **30**, 121-126 (2007).
11. van Gemert, J. T. *et al*. Free vascularized flaps for reconstruction of the mandible: complications, success, and dental rehabilitation. *J. Oral Maxillofac. Surg.* **70**, 1692-1698 (2012).
12. Maurer, P., Eckert, A. W., Kriwalsky, M. S. & Schubert, J. Scope and limitations of methods of mandibular reconstruction: a long-term follow-up. *Br. J. Oral Maxillofac. Surg.* **48**, 100-104 (2010).
13. Schoning, H. & Emshoff, R. Primary temporary AO plate reconstruction of the mandible. *Oral Surg. Oral Med. Oral Pathol. Oral Radiol. Endod.* **86**, 667-672 (1998).
14. Shibahara, T., Noma, H., Furuya, Y. & Takaki, R. Fracture of mandibular reconstruction plates used after tumor resection. *J. Oral Maxillofac. Surg.* **60**, 182-185 (2002).
15. Lindqvist, C., Soderholm, A. L., Laine, P. & Paatsama, J. Rigid reconstruction plates for immediate reconstruction following mandibular resection for malignant tumors. *J. Oral Maxillofac. Surg.* **50**, 1158-1163 (1992).
16. Gellrich, N. C. *et al*. Comparative study of locking plates in mandibular reconstruction after ablative tumor surgery: THORP versus UniLOCK system. *J. Oral Maxillofac. Surg.* **62**, 186-193 (2004).
17. Katakura, A., Shibahara, T., Noma, H. & Yoshinari, M. Material analysis of AO plate fracture cases. *J. Oral Maxillofac. Surg.* **62**, 348-352 (2004).

18. Lopez, R., Dekeister, C., Sleiman, Z. & Paoli, J. R. Mandibular reconstruction using the titanium functionally dynamic bridging plate system: A retrospective study of 34 cases. *J. Oral Maxillofac. Surg.* **62**, 421-426 (2004).
19. Maurer, P., Eckert, A. W., Kriwalsky, M. S. & Schubert, J. Scope and limitations of methods of mandibular reconstruction: a long-term follow-up. *Br. J. Oral Maxillofac. Surg.* **48**, 100-104 (2010).
20. Lindqvist, C. *et al*. A comparative study on four screw-plate locking systems in sheep: a clinical and radiological study. *Int. J. Oral Maxillofac. Surg.* **30**, 160-166 (2001).
21. Martola, M., Lindqvist, C., Hanninen, H. & Al-Sukhun, J. Fracture of titanium plates used for mandibular reconstruction following ablative tumor surgery. *J. Biomed. Mater. Res. B. Appl. Biomater.* **80**, 345-352 (2007).
22. Wei, F. *et al*. Complications after reconstruction by plate and soft-tissue free flap in composite mandibular defects and secondary salvage reconstruction with osteocutaneous flap. *Plast. Reconstr. Surg.* **112**, 37-42 (2003).
23. Onoda, S. *et al*. Prevention points for plate exposure in the mandibular reconstruction. *J. Craniomaxillofac. Surg.* **40**, 310 (2012).
24. Kennady, M. C., Tucker, M. R., Lester, G. E. & Buckley, M. J. Stress shielding effect of rigid internal fixation plates on mandibular bone grafts. A photon absorption densitometry and quantitative computerized tomographic evaluation. *Int. J. Oral Maxillofac. Surg.* **18**, 307-310 (1989).
25. Sidebottom, A. J. Current thinking in temporomandibular joint management. *Br. J. Oral Maxillofac. Surg.* **47**, 91-94 (2009).
26. Johnson, N. R., Roberts, M. J., Doi, S. A. & Batstone, M. D. Total temporomandibular joint replacement prostheses: a systematic review and bias-adjusted meta-analysis. *Int. J. Oral Maxillofac. Surg.* **46**, 86-92 (2017).
27. van Loon, J. P., de Bont, G. M. & Boering, G. Evaluation of temporomandibular joint prostheses: review of the literature from 1946 to 1994 and implications for future prosthesis designs. *J. Oral Maxillofac. Surg.* **53**, 984-7 (1995).
28. Falkenström, C. H. Biomechanical design of a total temporomandibular joint replacement. (1993).
29. van Loon, J. P. The Groningen temporomandibular joint prosthesis. *Ph.D Thesis. University of Groningen, Groningen, The Netherlands* (1999).
30. Kraeima, J. Three dimensional virtual surgical planning for patient specific osteosynthesis and devices in oral and maxillofacial surgery. *Ph.D Thesis. University of Groningen, Groningen, The Netherlands* (2019).
31. Huiskes, R. & Chao, E. Y. A survey of finite element analysis in orthopedic biomechanics: the first decade. *J. Biomech.* **16**, 385-409 (1983).
32. Baron, P. & Debussy, T. A biomechanical functional analysis of the masticatory muscles in man. *Arch. Oral Biol.* **24**, 547-553 (1979).
33. Korioth, T. W., Romilly, D. P. & Hannam, A. G. Three-dimensional finite element stress analysis of the dentate human mandible. *American journal of physical anthropology* **88**, 69-96 (1992).
34. Nelson, G. J. Three dimensional computer modeling of human mandibular biomechancis. *M.Sc Thesis. The University of British Columbia, Vancouver.* (1986).
35. Shi, Q. *et al*. Failure analysis of an in-vivo fractured patient-specific Ti6Al4V mandible reconstruction plate fabricated by selective laser melting. **124** (2021).

36. Huo, J., Derand, P., Rannar, L., Hirsch, J. & Gamstedt, E. K. Failure location prediction by finite element analysis for an additive manufactured mandible implant. *Med. Eng. Phys.* **37**, 862-869 (2015).
37. Koper, D. C. *et al*. Topology optimization of a mandibular reconstruction plate and biomechanical validation. *J. Mech. Behav. Biomed. Mater.* **113**, 104157 (2021).
38. Schupp, W., Arzdorf, M., Linke, B. & Gutwald, R. Biomechanical testing of different osteosynthesis systems for segmental resection of the mandible. *J. Oral Maxillofac. Surg.* **65**, 924-930 (2007).
39. Gutwald, R., Jaeger, R. & Lambers, F. M. Customized mandibular reconstruction plates improve mechanical performance in a mandibular reconstruction model. *Comput. Methods Biomech. Biomed. Engin.* **20**, 426-435 (2017).
40. Gateno, J. *et al*. Biomechanical evaluation of a new MatrixMandible plating system on cadaver mandibles. *J. Oral Maxillofac. Surg.* **71**, 1900-1914 (2013).

Section I

Chapter 2

Patient-specific finite element models of the human mandible:

Lack of consensus on current set-ups

Bram Barteld Jan Merema, Joep Kraeima, Haye H. Glas,
Fred K. L. Spijkervet, Max J. H. Witjes

Department of Oral and Maxillofacial Surgery, University Medical Center Groningen,
University of Groningen, Hanzeplein 1, 9700 RB Groningen, The Netherlands

Published:
Oral Diseases, 2021; 27(1): 42-51

ABSTRACT

The use of finite element analysis (FEA) has increased rapidly over the last decennia and has become a popular tool to design implants, osteosynthesis plates and prostheses. With increasing computer capacity and the availability of software applications, it has become easier to employ the FEA. However, there seems to be no consensus on the input variables that should be applied to representative FEA models of the human mandible. This review aims to find a consensus on how to define the representative input factors for a FEA model of the human mandible.

A literature search carried out in the PubMed and Embase database resulted in 137 matches. Seven papers were included in this current study. Within the search results, only a few FEA models had been validated. The material properties and FEA approaches varied considerably, and the available validations are not strong enough for a general consensus.

Further validations are required, preferably using the same measuring workflow to obtain insight into the broad array of mandibular variations. A lot of work is still required to establish validated FEA settings and to prevent assumptions when it comes to FEA applications.

INTRODUCTION

Over the last decennia, a large variety of osteosynthesis plates and prostheses has been presented in the literature for the treatment of, for example, trauma, oncology or TMJ patients. These applications have in common that failure (loosening or fracturing) of the implanted material, or the screw-fixation of the implant to the patient's bone will often result in failure of the application. It appears crucial for success that the implanted osteosynthesis plates and its fixations are of a matching strength for the patient's specific situation.

Mandibular reconstruction failure through either osteosynthesis plate failure or screw loosening are widely reported in the literature as the most common causes of mechanical failure[1-5], which shows the lack of a truly universal reconstruction solution due to the uniqueness of each patient's reconstruction situation. The accessibility and pricing of confection sized and shaped osteosynthesis plates have resulted in them being commonly adopted worldwide. These plates, however, are associated with the reported osteosynthesis failure in mandibular reconstructions[6-8]. There is seemingly a sophisticated balance between plates being too weak, causing material failure, or too strong, potentially leading to stress-shielding or disturbance of the natural equilibrium of bone formation, causing resorption of the surrounding bone[9].

The development of biomechanical models to describe the forces acting on the mandible, using specifically the finite element analysis (FEA), has been underway over the last decennia in for example automotive or aviation engineering. Accurate FEA models help to predict material behaviour without the need for destructive tests and could replace in vivo tests. With the increase in computer capacity and the availability of software applications, FEA has gained ground in the biomedical field since the 1970s and has proven valuable due to its non-destructive character and ease in evaluating multiple scenarios[10].

There are great variations between the FEA models due to differences in the input factors such as constraints, load application, mechanical properties of the bone, muscle forces and muscle force directions. Xin et al.[11] describe three different material composition options to approach the mandible mechanically, namely a solid model with homogeneous material properties[12] and two solid models composed of cortical and cancellous volume, each with their own homogeneous material properties[13,14] and

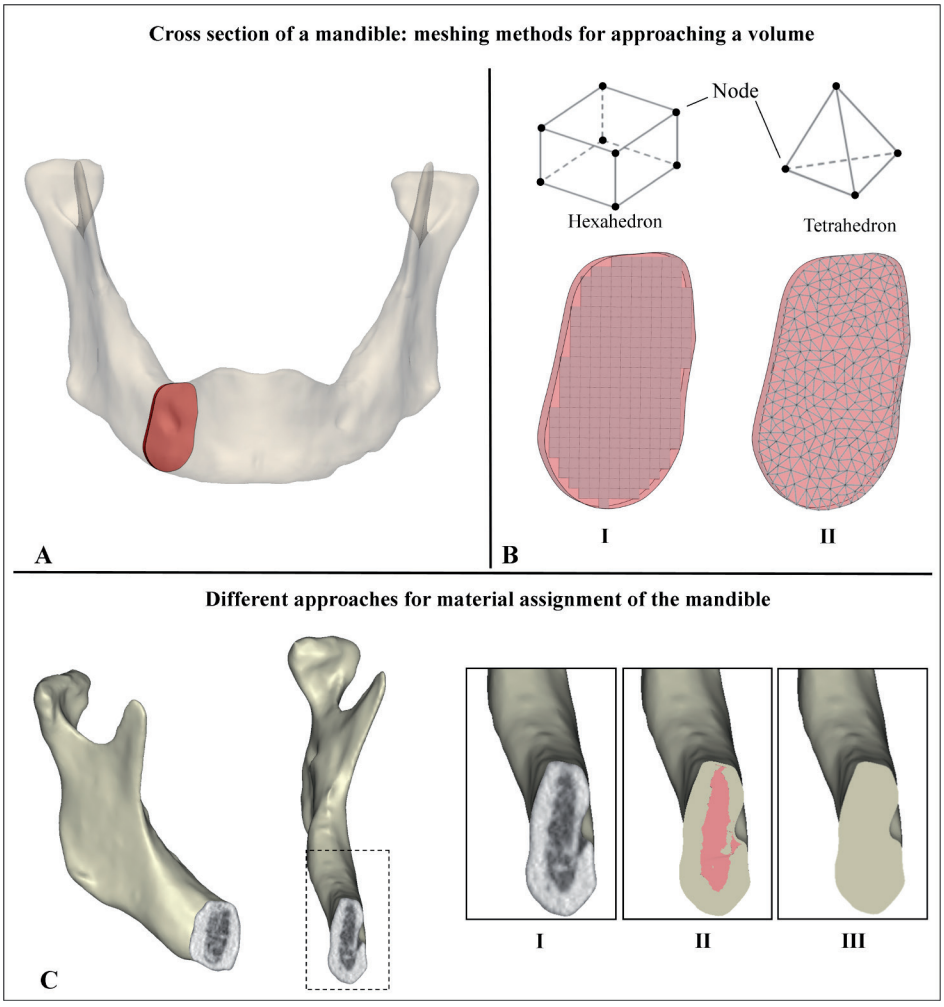

FIGURE 1 | (a) Indication of the position of the red coloured slice, used in (b) to illustrate the approximation of the shape of this slice using hexahedal (b-I) and tetrahedral (b-II) meshes with the same dimensions. The number of nodes is highly influenced by this and this is reflected in the outcome of the FEA. (c) A 3D model of a mandible showing the CT pixels with material information on the cut planes. Approach c-I represents material assignment per voxel, approach c-II shows the assumption of two different materials (cortical and cancellous) and approach c-III illustrates a solid uniform (cortical only) material assignment of the mandible. These settings affect the outcome of the FEA.

a heterogeneous or orthotropic material assignment, meaning the bulk material properties are not the same in all directions[15-17] (Figure 1). Generally, loads are approached with simplified muscle models, of only one muscle group or resultant force. Other studies have created a more extensive and complex model consisting of four or more

muscle groups[18-20]**.** In the latter, the masseter (deep and superficial or combined), temporalis (anterior and medial or combined), lateral pterygoid and medial pterygoid are typically defined. The force magnitudes and working directions are, however, not commonly agreed upon and vary considerably[21-25]. Muscle forces and directions are subject-specific; yet, most authors describe a universal and simplified muscle model which should represent a maximum loading. In static engineering, this might seem a safe solution to a structural problem; but, for a mandible, this could result in unnecessarily strong and bulky plates which do not fit the specific patient (e.g. a small, resorbed mandible due to an edentulous situation does not allow placement of a bulky implant).

Current literature lacks consensus on the input variables that should be applied to representative FEA models of the human mandible. Thus, the aim of this review was to find a consensus on how to define the input factors for a representative FEA model of the human mandible.

METHODS

A computer database search was carried out in PubMed on the 1 November 2019. The applied search term was created using both MeSH and Boolean terms: *("Mandible"[Mesh]* ***OR*** *mandible[tiab]* ***OR*** *jaw*[tiab])* ***AND*** *(finite element*[tiab]* ***OR*** *fea[tiab])* ***AND*** *("Laboratory"[Mesh]* ***OR*** *"*In Vitro*Techniques"[Mesh]* ***OR*** *"Validation Studies as Topic"[Mesh]* ***OR*** *validation*[tiab]* ***OR*** in vitro*[tiab]* ***OR*** in-vitro*[tiab]* ***OR*** *test[tiab]* ***OR*** *assess[tiab]* ***OR*** *verification[tiab])* ***NOT*** *(dental* ***AND*** *Humans[Mesh])*. Subsequently, a search was performed in the Embase database using the same separated terms.

The resulting abstracts, or entire content when the abstract did not provide sufficient information for inclusion or exclusion, were assessed by one author (BJM). No criterion was set regarding the date of publication. The applied criteria were as follows:

Inclusion criteria

1. Written in the English language
2. Assessment of one or more human mandible(s); only human models were taken into account in order to make comparison of multiple studies possible.

3. In vitro model with matching finite element model; the study should compare in vitro mechanical testing with a FEA model of the matching mandible(s).

Exclusion criteria

1. Use of synthetic or phantom mandibles**;** the aim of this study was to extract representative material properties for the mandible. Synthetic bone substitutes introduce assumptions and confounders to the models.
2. Focus on soft tissue; our study focuses on hard tissue as most FEA models are used to design osteosynthesis materials or implants.

RATIONALE

A FEA model is typically composed of an object, referred to as a geometry, to which material properties, boundary conditions and loads are assigned. Material characteristics, such as yield properties, elastic behaviour or Young's Modulus and Poisson's ratio, are important input parameters and should be considered carefully in order to obtain a representative reflection of the anatomical situation. The Young modulus (YM), expressed as E [GPa], measures elasticity; the higher the YM the stiffer the material becomes. The Poisson ratio (PR) [dimensionless] of a material describes the deformation behaviour under a load and is calculated by dividing the amount of transversal expansion by the amount of axial compression. Also, relevant to a FEA are yield properties. These indicate a stress value where a material will start to yield and, in order to avoid this, the minimal value must be known.

Boundary conditions relate to the constraints that are applied to the geometry, in this case the mandible. When it comes to a FEA of the mandible, fixation in an area of the mandible at, for example, both condyles, and a limitation in the freedom of movement at the occlusal site are typical examples of boundary conditions. Another type of boundary condition that often needs to be applied in a FEA is a contact set. Contact sets are required when multiple geometries or parts of a geometry are in contact and they define how the FEA software should treat the contacting sites. For example a mandible that is considered to consist of a cortical shell with a cancellous inner volume (Figure 1c-II). If both materials have different properties, these will have the tendency to deform differently at the sites of contact. During a FEA, the user has to decide whether to treat the two materials as fixed, thus, prohibiting interbody

movement, or to apply a bearing contact set and allowing for shear movement at the contact site.

Mesh creation (meshing) is the discretisation step of FEA in which the analysed object is described as a finite number of blocks or elements (Figure 1a,b). This step is responsible for the division of the greater numerical problem into a finite number of smaller problems and is of great importance since the mesh parameterisation can drastically influence the approximation of the input geometry and thus the quality of the FEA's results[26].

Forces are generally applied by assigning loads, or loading conditions. In order to assign a load, a force origin and direction are required alongside the force magnitude. The mandible's loading conditions, representing the muscle system, could be approached in this manner.

When performing a FEA, it is important to pay attention to any occurring stress and strain. In order to understand whether or not the results are within acceptable limits, the limitations of the acceptable magnitudes of stress and strain should be clear. These limitations have been known for years for the vast majority of engineering materials but appear to be complex for a natural and dynamic material such as bone due to its heterogeneous and individual character[27-29]**.** For FEA, it would be interesting to know what yield strength and fatigue strength should be taken into account.

In accordance with the above, six main categories were formulated and used to assess all the included papers:

- Bone geometry and property acquisition
- Acceptable bone stress values
- Muscle model and fixtures
- Applied finite element settings
- In vitro validation method
- In vitro and FEA results conformity

RESULTS

The PubMed electronic database search resulted in a total of 137 papers matching our search term, published between 1992 and 2019. Seven papers complied with the inclusion criteria, as shown in Table 1[30-37]. Of these, four papers were written by the same authors (Ramos & Mesnard)[34-37] who used of the same or a very similar FEA model and validation method, resulting in a total of four unique study models to compare. The Embase search that followed the PubMed search did not result in any additional unique studies.

Bone geometry and property acquisition

The mandibular geometry in all the seven papers included in this study was obtained through segmentation of computed tomography (CT) or cone beam CT (CBCT) im-

TABLE 1 | The finite element and in vitro approaches of all the included papers

Author	FEA-model approach	Cortical		Cancellous		In-vitro method	Conformity FEA & in-vitro results
		E [GPa]	v [-]	E [GPa]	v [-]		
Vollmer et al. 2000[38]	Homogeneous, cortical & cancellous	NS	NS	NS	NS	Load applying apparatus & strain gauge measurement	0.992 correlation coefficient
Clason et al. 2004[31]	Homogeneous, cortical & cancellous	dry 5.466	0.246	0.646	0.246	Load applying apparatus & optical measurements method	Average relative mean square deviations of the marker positions: 0.29, 0.28 and 0.29 mm for 3 load cases
		soaked 5.658	0.273	0.785	0.269		
Gröning et al. 2009[32]	Homogeneous, cortical	17	0.3	NA	NA	Load applying apparatus & Digital Speckle Pattern Interferometry measurement	Most predicted values lie within 2 SD
Ramos et al. 2016[34]	Homogeneous, cortical & cancellous	14.7	0.3	0.4	0.35	Load applying apparatus & strain gauge measurement	R^2: 0.931, slope: 1.05, NRMSD: 10.4%
Mesnard et al. 2016[35]	Homogeneous, cortical & cancellous	14.7	NS	0.4	NS	Load applying apparatus & strain gauge measurement	R^2: 0.935 ,slope: 1.045, NRMSD: 10.3%
Ramos et al. 2017[36]	Homogeneous, cortical & cancellous	13.7	0.3	0.4 -13.7	0.3	Load applying apparatus & strain gauge measurement	R^2 slope: 0.953, NRMSD: 9.7%
Ramos et al. 2019[37]	Homogeneous, cortical & cancellous	14.7	0.3	0.4	0.35	Load applying apparatus & strain gauge measurement	R^2: 0.95, slope: 0.899, NRMSD: 6.5%

E, Young's modulus; GPa, $1*10^9$ Pascal; NA, not-applicable; NRMSD, normalised root-mean-square deviation; NS, not specified; R^2, correlation value; *SD*, standard deviation; *v*, Poisson's ratio.

aging. Ramos and Mesnard chose to perform a micro-CT scan of the mandibles[34-37], whereas all other authors used regular CT scans[31,38]. Gröning et al.[32] performed both a micro-CT and a regular CT and created a high-resolution and lower resolution model with element counts and sizes of 19.6 million and 0.135 mm/450.000 and 0.488 mm, respectively. They found that both their models predicted similar strains and noted that a relatively low-resolution scan is sufficient for FEA-model creation. However, the resolution of the scan must be increased when assessing strain gradients in small structures. Thus, a regular (CB)CT could be sufficient for modelling a human mandible in toto when the region of interest of the mandible is not at micro level.

The (CB)CT data (DICOM files) possess information on both geometry and local radiographic attenuation. Local density values can be assigned mathematically to the latter. Through mathematical formulae, the attenuation values, expressed in Hounsfield unit (HU) or grey value (GV), and material properties such as YM and PR can be extracted. The formulae used in the literature for this extraction were empirically determined and differ from each other since the tested samples origin from different anatomical positions[33,39,40].

All the seven papers included in this study describe an in silico model where the material properties are considered homogeneous[31,32,34-38]. Clason et al., Ramos and Mesnard, Mesnard and Ramos and Vollmer et al. assigned two material groups, related to HU, in conformation with the Ciarelli et al.[41] study and created a cortical and a cancellous mandibular portion. Ramos et al.[36] assumed the teeth are part of the cortical volume, stating this would have marginal influence on mandible behaviour. Gröning et al.[32] left the cancellous portion out of their model and used a single pair of material properties for cortical bone instead. Their studied mandible was assumed to be fully cortical even though it was dentate. A relatively wide range of YM was applied to the homogeneous models. Clason et al.[31] applied the most flexible value, namely 5.46 [GPa] while Gröning et al.[32] used the stiffest value, 17 [GPa]. The PR of mandibular (cortical) bone was often chosen 0.3[42-50]. The studies that mechanically tested the PR of the mandible in different directions showed values ranging from 0.18 to 0.53[29,51]. We found that five of the selected studies had a PR of 0.3 or close to it[32,34-37]. Clason et al.[31] deviated from this with their values of 0.25–0.27 for cortical bone and as much as 0.65–0.79 for cancellous bone. Clason et al.[31] studied the mechanical properties of mandibular bone in an inverse manner. They performed measurements on a cadaveric mandible prior to setting up an in silico model and

adjusted the mechanical property settings to fit the in vitro measurements. Ramos used the cortical and cancellous bone values (PR 0.3 and 0.35, respectively) in one paper but applied the value of 0.3 to both the cortical and cancellous bone in a later study[34,36]. The effect of which is expected to be marginal.

Acceptable bone stress values

None of the included papers paid attention to a maximum acceptable bone stress, yield properties or fatigue limits and thus did not state maximum values.

Muscle models

The description of the muscle models used in the included studies was in most cases rather brief. In order to simplify their mathematical model, Clason et al.[31] chose to only apply a pterygo-masseter sling which looped around the mandibular anguli and pulled upwards. The force applied to this sling went up to 650 [N] which, according to Clason et al., covers the reasonable physiological range reported in the literature[52,53]. The simplification with such an approach makes comparison of the FEA model with the in vitro measurements easier, with less introduction of errors, while loading the mandible in a non-physiological manner. Gröning et al.[32] loaded their in vitro model by resting the mandible on both condyles and the lower incisors while vertically applying a force to the mandibular angles, which is comparable to Clason's et al.'s loading. Mesnard et al.[35] and Ramos et al.[34] on the other hand did not add a physiologically complete muscle model to their experiment but chose to apply a resultant force to the condyle since the condyle and mandibular ramus were their regions of interest. Vollmer et al.[38] applied a load of 130 N to both coronoid processes to imitate mastication through the temporalis muscle only. Ramos et al.[36] used the most extensive muscle model. It involved five pairs of muscle forces, including all the previously studied vector directions[54]. All the selected studies agree on the exclusion of the lateral pterygoid muscle from the analysis because this muscle is located at the condyle; all their mandibles were either fixed or loaded with a resultant TMJ force at the condyles.

Applied finite element settings

Clason et al.[31] and Gröning et al.[32] describe a vertical rigid fixation of the condyle surfaces, which was the direction of load application. Gröning et al.[32] also fixed the tips of the anterior teeth, preventing movement in this direction. The highly similar models used by Mesnard et al.[35] and Ramos et al.[34] focused on the mandibular ramus

and condyle. The hemi-mandible was fixed at the mandibular body, by cementation to the testing apparatus. Therefore, the applied fixture in the FEA was matched to the physical situation. Ramos et al.[36] fixed a hemi-mandible to his in vitro tool by cementation but created a FEA model which included a muscle model and boundary conditions to the intact mandible. The condyles were fixed in the craniocaudal and anteroposterior direction while a lower incisive tooth was fixed in mediolateral and craniocaudal direction. Vollmer et al.'s description[38] of the FEA-model set-up was very minimal. They did not give any specific details of the FEA fixation of the tested mandible other than that the condyles of the mechanically tested mandible were fixed and this was simulated in the FEA model.

Vollmer et al.[38] and Gröning et al.[32] used voxel(3D pixel)-to-voxel material assignment. That is, for every single voxel, or group of voxels in the CT data, one was created in the FEA mesh (Figure 1c-I). This resulted in linear hexahedral elements with 8 connective corner points between elements, called nodes (Figure 1b-I). Clason et al.[31], Ramos et al.[34,36,37] and Mesnard et al.[35] made use of linear tetrahedral elements which consist of 4 corner nodes and can be presented as a pyramid shape (Figure 1b-II). Linear tetrahedral elements can be fit into complex geometries more accurately with relatively bigger element dimensions due to their pyramid shape. An organically shaped mandible for example would need a relatively high number of hexahedral elements in order to follow the outer surface accurately (Figure 1b). Moreover, wherever there are sharp angled boundaries between elements (sharp edges), it is likely the peak stresses will be concentrated. A typical linear hexahedral mesh shows these peak stress concentrations when the element's dimensions are too big.

Interbody contact sets are applied wherever there are multiple objects coinciding. Of the four authors that actually made use of multiple contacting bodies (Vollmer et al.[38], Clason et al.[31], Ramos et al.[34,36,37] and Mesnard et al.[35]), only Mesnard and Ramos described the applied interbody contact for the cortical and cancellous volumes. They reported a "glue contact" which allows for interface separation. Furthermore, they mentioned a friction contact for the mandible-implant and screw-implant interfaces. Ramos and Mesnard described a comparable contact between the mandible and implant[34].

The software used for the FEA varied in the included papers from in-house code (Clason et al.[31]) to non-commercially available VOX-FE software[32] and commercially

available software. Ramos et al.[34,36,37] and Mesnard et al.[35] used a separate pre-processor (Hyperworks 12, Altair Engineering, Troy, MI, USA) and performed their analysis in MSc MARC 2015 (MSc Software, Newport Beach, CA, USA). Vollmer[38] chose to combine an in-house pre-processor to mesh the CT data with a commercially available solver (Cosmos V2.0).

In vitro validation methods

In most included studies, in vitro measurements of the mandibles are carried out by strain gauges. Usually, a series of strain gauges is applied to the surface of the region of interest by means of an adhesive. When the studied object is subject to surface deformation, the strain gauges will change length and width thereby changing the electrical resistance, which can be measured. In Vollmer et al.[38], Ramos et al.[34,36,37] and Mesnard et al.'s[35] method, a series of strain gauges were applied to the mandibular surface in the regions of interest and the measured values were mathematically converted into local strain values. In all cases, the in vitro loads were applied by means of a compression or tensile testing machine. Also, Gröning et al.[32] used a tensile testing machine for the load applications but, instead of strain gauges, applied digital speckle pattern interferometry (DSPI) in order to optically perform their measurements.

Clason et al.[31] describe an in vitro experiment that measured the displacement of specific points of interest on the mandible. A number of tracer spheres were applied to the mandibular surface and the displacement was recorded using a camera. Contrary to the afore-mentioned studies, the loads were applied by a series of hydraulic actuators.

They preserved the mandible in alcohol and measurements were performed under dry conditions. Ramos and Mesnard also first used a cleaned fresh frozen mandible[34,35], but the teeth were removed. However, in their follow-up study[36], the teeth were left in the mandible. Vollmer et al.[38] chose to store their five mandibles in a humid 20°C atmosphere by soaking the mandibles in a physiological sodium chloride solution one hour prior to mechanical testing.

In vitro and FEA results conformity

All the studies claim a good correlation between the FEA outcome and in vitro results. The results of the studies however are difficult to compare since the raw data are unavailable and most of the studies scored their results differently. The studies that

present a correlation coefficient show good correlations of 0.992 (Vollmer et al.[38]), 0.931 (Ramos et al.[34]), 0.935 (Mesnard et al.[35]), 0.953 (Ramos et al.[36]) and 0.95 (Ramos et al.[55]). Most of the FEA results obtained by Gröning et al.[32] lie within two standard deviations from the in vitro values. The results by Clason et al.[31] are expressed as average relative mean square errors between the predicted and measured displacement. The calculated errors were 0.29 mm, 0.28 mm and 0.29 mm for their first, second and third load cases, respectively.

DISCUSSION

Finite element studies are currently recognised as a necessary part of designing personalised osteosynthesis. However, the approaches vary greatly and the assumptions, concerning for example material properties and boundary conditions, are not fully understood. We aimed to find a consensus on how to approach a representative FEA model of the human mandible within the literature.

Many studies used FEA to develop and design osteosynthesis and prostheses for patients but surprisingly, only seven papers describe how they validated the applied FEA on human mandibles. This simulation technique supplies the user with results that match the input problem as formulated by the user, even if this input problem is not an accurate one. Thus, the reader should be critical towards the used approach.

The papers included in this current study applied similar simplifications regarding bone geometry and material properties. They all describe homogeneous materials with either only a cortical portion or a cortical portion with cancellous volume. The properties required for an FEA, that is YM and PR, were mentioned by every study and they generally agreed with prior experiments[29,51]. The majority of reported PR vary marginally and ranged from 0.25–0.30 to 0.25–0.35 for cortical and cancellous bone, respectively. Clason et al.[31] calculated PR and YM, however, both seem to stand out (Table 1). However, the majority of the YM ranged from 13.7 to 17 [GPa], Clason et al. calculated values of 5.5–5.7 [GPa] for the cortical bone, resulting in a much stiffer material[36]. This study involved only one test subject and the diverging results could have been caused by individual variables (age, porosity or geometry, etc.), or measuring variables. For such outlying results, we find the support too weak to use

their measured material properties over the properties used in the rest of the included studies.

Xin et al.[33] applied heterogeneous material properties whereby the material property assignment was matched to the local attenuation properties. They divided the CT GV range into ten equally distributed intervals and assigned a set of material properties to each of these intervals, creating ten different materials. They describe in vitro measurements of mandibular segments in three different directions. Their results show property independency in all the measured directions and specimen locations. Hart et al.[56] however, describe that even on taking the anisotropy of the mandible into account, two out of three directions show similar properties. Schwarz et al.[51] show the varying properties of cortical bone related to the location in the mandible. This method should be applied patient-specifically due to the great individuality of the mandibular shape and bone quality. However, validations of this method are still lacking.

The focus of the seven included papers was clearly not on the application of a representative muscle model in either the FEA or in vitro experiments. Except for Ramos et al.[36], who describe five muscle groups per side, all the authors simplified their model to one force. This might be sufficient when analysing only a part of the mandible but the lack of use of the entire mandible should be acknowledged. Only applying a resultant force, calculated for a specific region, could result in overlooking the internal force transmission. All the authors agree on the elimination of the lateral pterygoid muscle from the analysis and using the condyles to either fixate the mandible in space[31,32,38], or to apply a resultant force[34-36,55].

Most of the FEA-related publications do not describe the maximum bone performance values in terms of yield or fatigue properties. Since bone is a dynamic material, subject to a number of factors influencing its properties and with a continuous (de)formation, it is imaginable that it is not possible to measure true in vivo properties such as fatigue in vitro. Zioupos & Casinos (1998) studied fatigue damage in cadaveric femoral bone in an in vitro setting and show the influence of order in which non-uniform repetitive loadings are applied, indicating simple stress against cycles to failure (S-N) fatigue tests do not suffice for ex vivo bone. They conclude it is an extremely difficult task to predict in vivo bone fatigue under variable loading. Yield information can be obtained but is strongly dependant on the assumed material YM and PR. We found only two

studies that state the yield strength and/or ultimate strength of the cortical and cancellous bone[57,58]. These values, however, vary considerably. A third study extracted these ultimate values from experiments conducted with vertebral and femoral specimens and used this to calculate the values for the mandible[59] . Of the seven included papers, only Ramos et al.[34,36,37] and Mesnard et al.[35] refer to fatigue, and relate this to strain instead of stress. The same strain focus was applied in the Bujtar et al.[15] and Chen et al.[57] studies which are related to the Frost's 'Mechanostat' principle[60], a principle in which bone formation and resorption are linked to the bone's strain values.

In vitro testing of mandibles can be approached with different measurement techniques, all with their own strengths and limitations. The optical techniques are "non-invasive" and do not require the attachment of materials to the bone but are sensitive to vibration and light and require high-resolution optical cameras. The use of gauges requires bone preparation, that is fixation of the sensor, and covers only one-directional measurements. It should be mentioned that both techniques are only capable of surface measurements. Ramos et al.[34,36,37] and Mesnard et al.[35] could reproduce their FEA measurements in vitro multiple times. It is valuable that four papers included in this study applied the same in vitro method and calculated comparable and good regression values with their strain gauge workflow.

The small number of inclusions is the biggest limitation of this current study. The information available regarding validated FEA of the human mandible is scarce and that is worrying knowing how widely FEA are performed and used for the design of medical devices. FEA models could be more individual in order for patient-specific plates and prostheses to better fit the patient in terms of bulkiness and in situ performance. A technique that should be considered is topology optimisation (TO). TO is a mathematical method applied in the FEA phase and is capable of removing material that dependant to the input variables, is unnecessary[61,62]. Instead of testing a man-made design with FEA, we can have the TO calculate the ideal design by removing material from a volume, given certain boundary conditions.

In conclusion, we carried out a literature search to find a possible consensus on how to perform a FEA on the human mandible. The available validations provide a lot of information but appear insufficient for reaching a general consensus. Further validations are required, preferably using the same measuring workflow and multiple mandibles to obtain insight into the broad range of mandibular characteristics. We

believe the models suggested by Ramos et al.[34,36,37] and Mesnard et al.[35] over the years are the most complete and best validated.

Conflict of Interest

None.

REFERENCES

1. Freitag, V., Hell, B. & Fischer, H. Experience with AO reconstruction plates after partial mandibular resection involving its continuity. *Journal of Cranio-Maxillofacial Surgery* **19**, 191-198 (1991).
2. van Gemert, J. T. *et al*. Free vascularized flaps for reconstruction of the mandible: complications, success, and dental rehabilitation. *J. Oral Maxillofac. Surg.* **70**, 1692-1698 (2012).
3. Kimura, A. *et al*. Adaquate fixation of plates for stability during mandibular reconstruction. *J. Craniomaxillofac. Surg.* **34**, 193-200 (2006).
4. Irish, J. C. *et al*. Primary mandibular reconstruction with the titanium hollow screw reconstruction plate: evaluation of 51 cases. *Plast. Reconstr. Surg.* **96**, 93-99 (1995).
5. Markwardt, J., Pfeifer, G., Eckelt, U. & Reitemeier, B. Analysis of complications after reconstruction of bone defects involving complete mandibular resection using finite element modelling. *Onkologie* **30**, 121-126 (2007).
6. Maurer, P., Eckert, A. W., Kriwalsky, M. S. & Schubert, J. Scope and limitations of methods of mandibular reconstruction: a long-term follow-up. *Br. J. Oral Maxillofac. Surg.* **48**, 100-104 (2010).
7. Schoning, H. & Emshoff, R. Primary temporary AO plate reconstruction of the mandible. *Oral Surg. Oral Med. Oral Pathol. Oral Radiol. Endod.* **86**, 667-672 (1998).
8. Shibahara, T., Noma, H., Furuya, Y. & Takaki, R. Fracture of mandibular reconstruction plates used after tumor resection. *J. Oral Maxillofac. Surg.* **60**, 182-185 (2002).
9. Kennady, M. C., Tucker, M. R., Lester, G. E. & Buckley, M. J. Stress shielding effect of rigid internal fixation plates on mandibular bone grafts. A photon absorption densitometry and quantitative computerized tomographic evaluation. *Int. J. Oral Maxillofac. Surg.* **18**, 307-310 (1989).
10. Huiskes, R. & Chao, E. Y. A survey of finite element analysis in orthopedic biomechanics: the first decade. *J. Biomech.* **16**, 385-409 (1983).
11. Xin, P. *et al*. Material assignment in finite element modeling: heterogeneous properties of the mandibular bone. *The Journal of craniofacial surgery* **24**, 405-410 (2013).
12. Kavanagh, E. *et al*. Use of finite element analysis in presurgical planning: treatment of mandibular fractures. *Ir J Med Sci* **177**, 325-331 (2008).
13. Xiangdong, Q. I., Limin, M. A. & Shizhen, Z. The influence of the closing and opening muscle groups of jaw condyle biomechanics after mandible bilateral sagittal split ramus osteotomy. *J. Craniomaxillofac. Surg.* **40**, 159 (2012).
14. Gautam, P., Zhao, L. & Patel, P. Biomechanical response of the maxillofacial skeleton to transpalatal orthopedic force in a unilateral palatal cleft. *Angle Orthod.* **81**, 503-509 (2011).
15. Bujtar, P., Simonovics, J., Varadi, K., Sandor, G. K. & Avery, C. M. The biomechanical aspects of reconstruction for segmental defects of the mandible: a finite element study to assess the optimisation of plate and screw factors. *J. Craniomaxillofac. Surg.* **42**, 855-862 (2014).
16. Huang, H. L., Tsai, M. T., Lin, D. J., Chien, C. S. & Hsu, J. T. A new method to evaluate the elastic modulus of cortical bone by using a combined computed tomography and finite element approach. *Comput. Biol. Med.* **40**, 464-468 (2010).
17. Taylor, W. R. *et al*. Determination of orthotropic bone elastic constants using FEA and modal analysis. *J. Biomech.* **35**, 767-773 (2002).
18. Korioth, T. W. & Hannam, A. G. Deformation of the human mandible during simulated tooth clenching. *J. Dent. Res.* **73**, 56-66 (1994).

19. Vajgel, A. *et al*. Comparative Finite Element Analysis of the Biomechanical Stability of 2.0 Fixation Plates in Atrophic Mandibular Fractures. *Journal of Oral and Maxillofacial Surgery* **71**, 335-342 (2013).
20. Commisso, M. S., Martinez-Reina, J., Ojeda, J. & Mayo, J. Finite element analysis of the human mastication cycle. *J. Mech. Behav. Biomed. Mater.* **41**, 23-35 (2015).
21. Koolstra, J. H., van Eijden, T. M. G. J., Weijs, W. A. & Naeije, M. A three-dimensional mathematical model of the human masticatory system predicting maximum possible bite forces. *Journal of Biomechanics* **21**, 563-576 (1988).
22. Koolstra, J. H. & van Eijden, T. M. G. J. Three-dimensional dynamical capabilities of the human masticatory muscles. *Journal of Biomechanics* **32**, 145-152 (1999).
23. Koolstra, J. H. & van Eijden, T. M. G. J. A method to predict muscle control in the kinematically and mechanically indeterminate human masticatory system. *Journal of Biomechanics* **34**, 1179-1188 (2001).
24. May, B., Saha, S. & Saltzman, M. A three-dimensional mathematical model of temporomandibular joint loading. *Clin. Biomech. (Bristol, Avon)* **16**, 489-495 (2001).
25. Meyer, C., Kahn, J., Boutemy, P. & Wilk, A. Determination of the external forces applied to the mandible during various static chewing tasks. *Journal of Cranio-Maxillofacial Surgery* **26**, 331-341 (1998).
26. Ramos, A. & Simoes, J. A. Tetrahedral versus hexahedral finite elements in numerical modelling of the proximal femur. *Med. Eng. Phys.* **28**, 916-924 (2006).
27. Keller, T. S. Predicting the compressive mechanical behavior of bone. *J. Biomech.* **27**, 1159-1168 (1994).
28. Rho, J. Y., Hobatho, M. C. & Ashman, R. B. Relations of mechanical properties to density and CT numbers in human bone. *Medical Engineering and Physics* **17**, 347-355 (1995).
29. Dechow, P. C., Nail, G. A., Schwartz-Dabney, C. L. & Ashman, R. B. Elastic properties of human supraorbital and mandibular bone. *Am. J. Phys. Anthropol.* **90**, 291-306 (1993).
30. Vollmer, D., Meyer, U., Joos, U., Vègh, A. & Piffkò, J. Experimental and finite element study of a human mandible. *Journal of Cranio-Maxillofacial Surgery* **28**, 91-96 (2000).
31. Clason, C., Hinz †, A. M. & Schieferstein ‡, H. A Method for Material Parameter Determination for the Human Mandible Based on Simulation and Experiment. *Computer Methods in Biomechanics and Biomedical Engineering* **7**, 265-276 (2004).
32. Gröning, F., Liu, J., Fagan, M. J. & O'Higgins, P. Validating a voxel-based finite element model of a human mandible using digital speckle pattern interferometry. *Journal of Biomechanics* **42**, 1224-1229 (2009).
33. Xin, P. *et al*. Material assignment in finite element modeling: heterogeneous properties of the mandibular bone. *The Journal of craniofacial surgery* **24**, 405-410 (2013).
34. Ramos, A. & Mesnard, M. A new condyle implant design concept for an alloplastic temporomandibular joint in bone resorption cases. *J. Craniomaxillofac. Surg.* **44**, 1670-1677 (2016).
35. Mesnard, M. & Ramos, A. Experimental and numerical predictions of Biomet((R)) alloplastic implant in a cadaveric mandibular ramus. *J. Craniomaxillofac. Surg.* **44**, 608-615 (2016).
36. Ramos, A., Nyashin, Y. & Mesnard, M. Influences of geometrical and mechanical properties of bone tissues in mandible behaviour - experimental and numerical predictions. *Computer Methods in Biomechanics and Biomedical Engineering* **20**, 1004 (2017).
37. Ramos, A., Gonzalez-Perez, L. M., Infante-Cossio, P. & Mesnard, M. Ex-vivo and in vitro validation of an innovative mandibular condyle implant concept. *J. Craniomaxillofac. Surg.* **47**, 112-119 (2019).
38. Vollmer, D., Meyer, U., Joos, U., Vègh, A. & Piffkò, J. Experimental and finite element study of a human mandible. *Journal of Cranio-Maxillofacial Surgery* **28**, 91-96 (2000).

39. Cioffi, I. *et al*. Regional variations in mineralization and strain distributions in the cortex of the human mandibular condyle. *Bone* **41**, 1051-1058 (2007).
40. van Ruijven, L. J., Mulder, L. & van Eijden, T. M. Variations in mineralization affect the stress and strain distributions in cortical and trabecular bone. *J. Biomech.* **40**, 1211-1218 (2007).f
41. Ciarelli, M. J., Goldstein, S. A., Kuhn, J. L., Cody, D. D. & Brown, M. B. Evaluation of orthogonal mechanical properties and density of human trabecular bone from the major metaphyseal regions with materials testing and computed tomography. *J. Orthop. Res.* **9**, 674-682 (1991).
42. Gallas Torreira, M. & Fernandez, J. R. A three-dimensional computer model of the human mandible in two simulated standard trauma situations. *J. Craniomaxillofac. Surg.* **32**, 303-307 (2004).
43. Ozan, O. & Ramoglu, S. Effect of Implant Height Differences on Different Attachment Types and Peri-Implant Bone in Mandibular Two-Implant Overdentures: 3D Finite Element Study. *J. Oral Implantol.* **41**, 50 (2015).
44. Santos, L. S. *et al*. Finite-element analysis of 3 situations of trauma in the human edentulous mandible. *J. Oral Maxillofac. Surg.* **73**, 683-691 (2015).
45. Korioth, T. W., Romilly, D. P. & Hannam, A. G. Three-dimensional finite element stress analysis of the dentate human mandible. *American journal of physical anthropology* **88**, 69-96 (1992).
46. Borchers, L. & Reichart, P. Three-dimensional stress distribution around a dental implant at different stages of interface development. *J. Dent. Res.* **62**, 155-159 (1983).
47. Meijer, H. J., Kuiper, J. H., Starmans, F. J. & Bosman, F. Stress distribution around dental implants: influence of superstructure, length of implants, and height of mandible. *J. Prosthet. Dent.* **68**, 96-102 (1992).
48. Nagasao, T., Kobayashi, M., Tsuchiya, Y., Kaneko, T. & Nakajima, T. Finite element analysis of the stresses around fixtures in various reconstructed mandibular models--part II (effect of horizontal load). *J. Craniomaxillofac. Surg.* **31**, 168-175 (2003).
49. Liu, Z., Fan, Y. & Qian, Y. Comparative evaluation on three-dimensional finite element models of the temporomandibular joint. *Clin. Biomech. (Bristol, Avon)* **23 Suppl 1**, 53 (2008).
50. Ichim, I., Swain, M. V. & Kieser, J. A. Mandibular stiffness in humans: numerical predictions. *J. Biomech.* **39**, 1903-1913 (2006).
51. Schwartz-Dabney, C. L. & Dechow, P. C. Variations in cortical material properties throughout the human dentate mandible. *Am. J. Phys. Anthropol.* **120**, 252-277 (2003).
52. Gay, T., Rendell, J., Majoureau, A. & Maloney, F. T. Estimating human incisal bite forces from the electromyogram/bite-force function. *Arch. Oral Biol.* **39**, 111-115 (1994).
53. Kampe, T., Haraldson, T., Hannerz, H. & Carlsson, G. E. Occlusal perception and bite force in young subjects with and without dental fillings. *Acta Odontol. Scand.* **45**, 101-107 (1987).
54. Mesnard, M. *et al*. Biomechanical Analysis Comparing Natural and Alloplastic Temporomandibular Joint Replacement Using a Finite Element Model. *Journal of Oral and Maxillofacial Surgery* **69**, 1008-1017 (2011).
55. Ramos, A., Gonzalez-Perez, L. M., Infante-Cossio, P. & Mesnard, M. Ex-vivo and in vitro validation of an innovative mandibular condyle implant concept. *J. Craniomaxillofac. Surg.* **47**, 112-119 (2019).
56. Hart, R. T., Hennebel, V. V., Thongpreda, N., Van Buskirk, W. C. & Anderson, R. C. Modeling the biomechanics of the mandible: A three-dimensional finite element study. *Journal of Biomechanics* **25**, 261-286 (1992).
57. Chen, X. *et al*. Biomechanical evaluation of Chinese customized three-dimensionally printed total temporomandibular joint prostheses: A finite element analysis. *J. Craniomaxillofac. Surg.* **46**, 1561-1568 (2018).

58. Hoefert, S. & Taier, R. Mechanical stress in plates for bridging reconstruction mandibular defects and purposes of double plate reinforcement. *J. Craniomaxillofac. Surg.* **46**, 785-794 (2018).
59. Kharmanda, G. & Kharma, M. Y. Evaluating the Effect of Minimizing Screws on Stabilization of Symphysis Mandibular Fracture by 3D Finite Element Analysis. *J. Maxillofac. Oral Surg.* **16**, 205-211 (2017).
60. Frost, H. M. Bone's mechanostat: a 2003 update. *The anatomical record. Part A, Discoveries in molecular, cellular, and evolutionary biology* **275**, 1081-1101 (2003).
61. Sutradhar, A. *et al*. Designing patient-specific 3D printed craniofacial implants using a novel topology optimization method. *Med Biol Eng Comput* **54**, 1123-1135 (2016).
62. Iqbal, T. *et al*. A general multi-objective topology optimization methodology developed for customized design of pelvic prostheses. *Med. Eng. Phys.* **69**, 8-16 (2019).

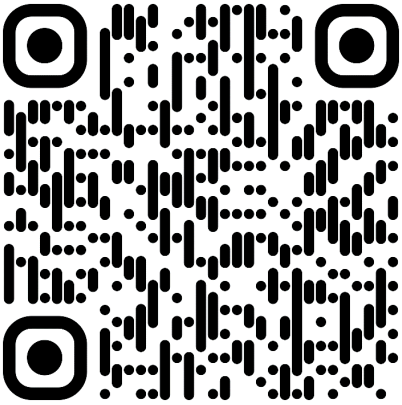

Supplementary video

Chapter 3

Novel finite element-based plate design for bridging mandibular defects:
Reducing mechanical failure

Bram B. J. Merema, Joep Kraeima, Sebastiaan A. H. J. de Visscher, Baucke van Minnen, Fred K. L. Spijkervet, Kees-Pieter Schepman, Max J. H. Witjes

Department of Oral and Maxillofacial Surgery, University Medical Center Groningen, University of Groningen, Hanzeplein 1, 9700 RB Groningen, The Netherlands

Published:
Oral Diseases, 2020; 26(6): 1265-1274

ABSTRACT

Introduction

When the application of a free vascularised flap is not possible, a mandibular continuity defect is often reconstructed using a conventional reconstruction plate. Mechanical failure of such reconstructions is mostly caused by plate fracture and screw pull-out. This study aims to develop a reliable, mechanically superior, yet slender patient-specific reconstruction plate that reduces failure due to these causes.

Patients and Methods

Eight patients were included in the study. Indications were as follows: fractured reconstruction plate (2), loosened screws (1) and primary reconstruction of a mandibular continuity defect (5). Failed conventional reconstructions were studied using finite element analysis (FEA). A 3D virtual surgical plan (3D-VSP) with a novel patient-specific (PS) titanium plate was developed for each patient. Postoperative CBCT scanning was performed to validate reconstruction accuracy.

Results

All PS plates were placed accurately according to the 3D-VSP. Mean 3D screw entry point deviation was 1.54 mm (SD: 0.85, R: 0.10–3.19), and mean screw angular deviation was 5.76° (SD: 3.27, R: 1.26–16.62). FEA indicated decreased stress and screw pull-out inducing forces. No mechanical failures appeared (mean follow-up: 16 months, R: 7–29).

Conclusion

Reconstructing mandibular continuity defects with bookshelf-reconstruction plates with FEA underpinning the design seems to reduce the risk of screw pull-out and plate fractures.

INTRODUCTION

Patients who require a continuity resection of the mandible due to, for example, head and neck cancer often receive a reconstruction preferably including a free vascularised flap (e.g. fibula graft). However, when a patient's general medical condition does not allow for this type of reconstructive surgery, the mandibular continuity defect can be bridged using solely a conventional reconstruction plate (RP). This type of RP usually needs manual bending to match the contour of the mandible. This method, however, has been reported to fail due to screw loosening or plate fracture[1-6]. Maurer et al.[1] describe a failure rate of 10% for screw loosening and plate fracture combined, while others report failure solely due to plate fracture in 10% of the cases[2,3,8] or to screw loosening alone in 18% of the cases[9]. According to Maurer et al., (2010), all screw loosening occurred within the first 6 months postoperatively[7].

Plate fracture is seen predominantly in the regions surrounding the screws nearest to the continuity defect and can be caused by fatigue through cyclic in situ loading[4], usually encouraged by residual stress inside the plate as a result of repetitive bending while contouring[10,11]. It seems to occur mostly in continuity defects that do not cross the midline and in the presence of relatively many remaining occlusal units[3]. Failure of a bridging RP leads to severe discomfort and impaired oral function for the patient[12]. In most cases, an additional surgical procedure involving a secondary reconstruction is needed[11].

Numerous studies applied patient-specific reconstruction plates (PS-RP) to prevent plate fracture by changing the material or design of conventional RP[13-16] but did not look at screw pull-out and its prevention. In order to prevent failure in further developed PS-RP, it is necessary to assess current conventional reconstructions biomechanically. Therefore, this study focused on an analysis of conventional RPs with the finite elements method (FEM), to obtain insight into any weaknesses and to exclude them in further patient-specific designs.

The aim of this phase 1 study was to design and analyse PS-RPs to bridge mandibular gaps and to minimise plate fracture and screw pull-out-related failure. This was achieved through the development and clinical application of a reconstructive method using a PS-RP, based on a 3D virtual surgical planning (VSP) and FEM supported individual design.

PATIENTS AND METHODS

Patients

All the patients included in this study required a reconstruction of either a primary or a secondary mandibular continuity defect due to a fractured or loosened conventional RP. None of these patients' mandible could be reconstructed with a free vascularised bone flap due to the poor quality of the donor site vascularisation, an impaired medical condition or refusal to undergo major free vascularised bone flap surgery. The study was approved by the Medical Ethical board of our centre (no. METc-2019/301), and informed consent was obtained for all patients.

In the secondary cases, we started by assessing the mechanically failed conventional RPs retrospectively, following plate fracture or screw pull-out. Postoperative CT scans were used for the segmentation, and 3D models of the mandibular segments were obtained using Mimics 19.0 software (Materialise). In order to perform finite element analysis (FEA) on the failed primary reconstructions, we digitalised the conventional reconstruction plates, which had been bent to follow the mandible's contour. Using the postoperative CT scans of primary reconstructions, we obtained the contours the plates were bent to, and using the manufacturer's dimensions, we designed matching plates for analysis. This was necessary since the quantity of metal artefacts or scatter in the CT data would not allow for proper segmentation of the osteosynthesis material.

3D FEA (performed with Solidworks Professional 2017 software, Dassault Systèmes Solidworks Corp.) of the conventional reconstructions enabled assessment of the local stress values in the conventional reconstruction plates. The typical defect size used in our general design process was a continuity defect spanning from the mandibular angle up to the approximate midline of the mandible while not crossing it. This represents a L-defect according to Jewer's HCL classification[17] or a class II defect according to Brown's[18] (Figure 1) and is reported to be the most prone to RP failure[3]. In our FEA, we applied the bone material properties and the muscle system as described by Mesnard and Ramos[19-23]. Their models are based on in vivo muscle force measurements and musculature information derived from dissections. They were validated by comparing in silico models to in vitro models of the same human mandibles. In accordance with these studies, incisal bite was simulated since this would ultimately load the mandible. Fixtures were applied to both condyles; thus, the lateral pterygoid muscles were not taken into account. The mandible was assumed to consist of an

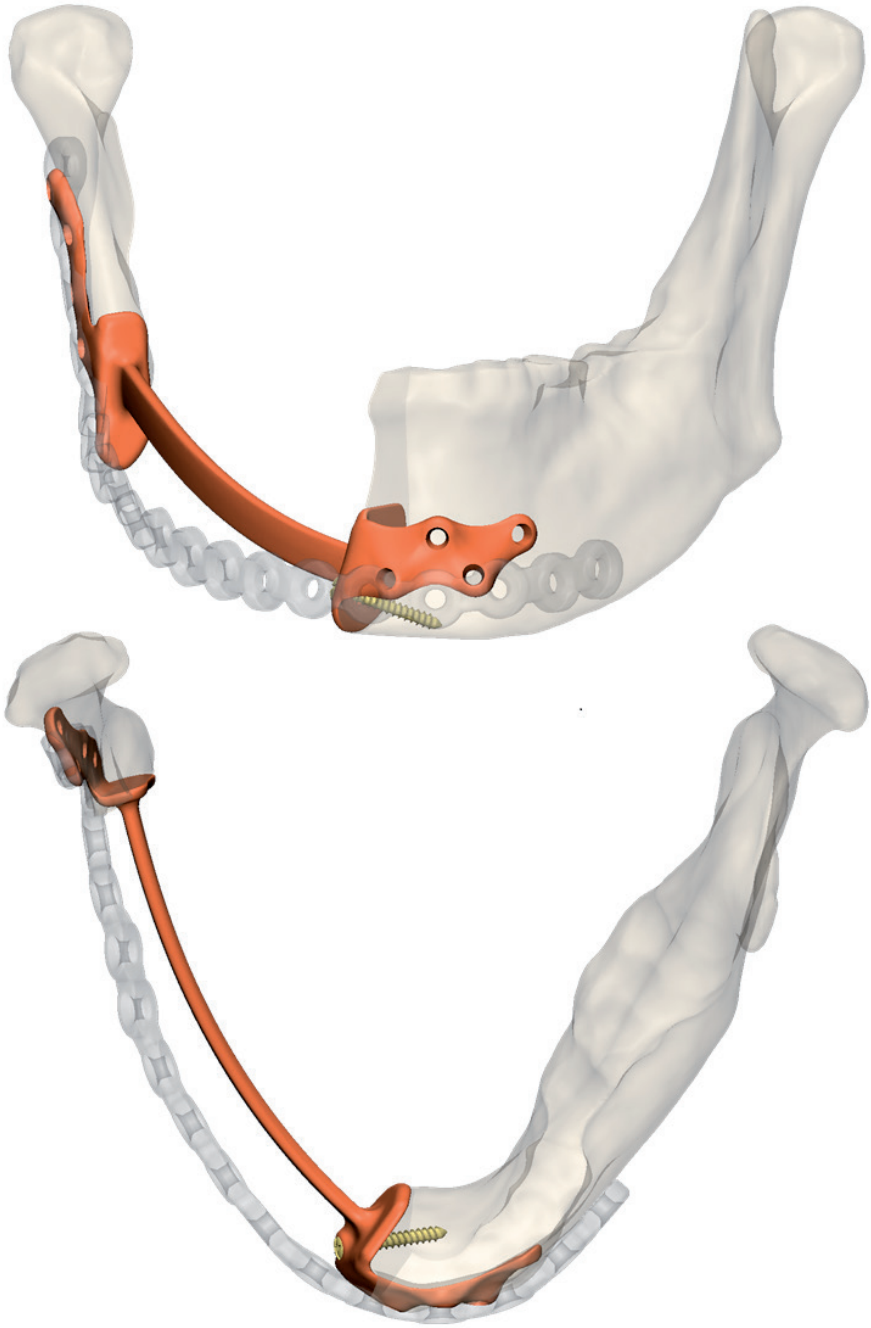

Figure 1 | The primary and secondary reconstructions for patient 2. Notice the under-contouring of the patient-specific secondary reconstruction plate (orange) compared to the failed primary reconstruction plate (transparent).

isotropic cancellous portion, with a cortical outer layer whereby the elastic properties are presented as Young's moduli (Young's modulus measures the stiffness of a solid material) of 400 MPa and 14,700 MPa, respectively[22] (Mesnard & Ramos, 2016). Poisson's ratio, a measure of how a material constricts or expands to a tensile or compressive load, was assumed to be 0.3 for both the cortical and cancellous bone[22]. All the conventional RPs were considered commercially pure grade 2 titanium, with a Young modulus of 102,000 MPa and a Poisson ratio of 0.34, while the PS-RPs and all the applied screws were assigned 113,800 MPa and 0.34 for Young's modulus and Poisson's ratio, respectively, representing titanium grade 5 alloy[24,25]. We used this titanium alloy because of its higher resistance against fatigue, or endurance limit.

Design and production

After analysing the conventional RP, an alternative PS reconstruction method was developed consisting of a 3D virtual surgical plan (VSP) that combines both CT data (i.e. bone segmentation and nerve canal delineation) and fused with MRI-based tumour delineation for osteotomy placement[26]. The aim was to overcome screw pull-out and high stresses which could lead to plate fracture.

Contrary to the majority of PS-RP suggested in the literature, which typically consist of a strip-like plate following the buccal contour of the mandible, we focused on incorporating the osteotomy sites of the mandibular segments for stable fixation of the plate. Bookshelf-like flanges situated against the osteotomy planes of the mandibular segments were added to a bridging section. To mitigate the chance of dehiscence of the plate due to contraction of the covering soft tissues, the bridging section was under-contoured with respect to the lateral and caudal boundaries of the preresected mandible (Figure 1). Fixation of the plate was obtained through bi-cortical screw placement and, whenever possible, mono-cortically in the flanges supporting the osteotomy sites. The design was carried out in 3-Matic Medical 11.0 (Materialise). Once finished, the STL file of the plate was exported and converted into a non-uniform rational basis spline (NURBS) object using Geomagic software (3D Systems). Subsequently, screw threads, compatible with 2.3 locking screws (KLS Martin), were inserted into the NURBS file using the Solidworks Professional 2017 software. Subsequently, the finalised CAD files were sent to the manufacturer (Witec Fijnmechanische Techniek BV) to mill the PS plates from medical grade 5 titanium alloy.

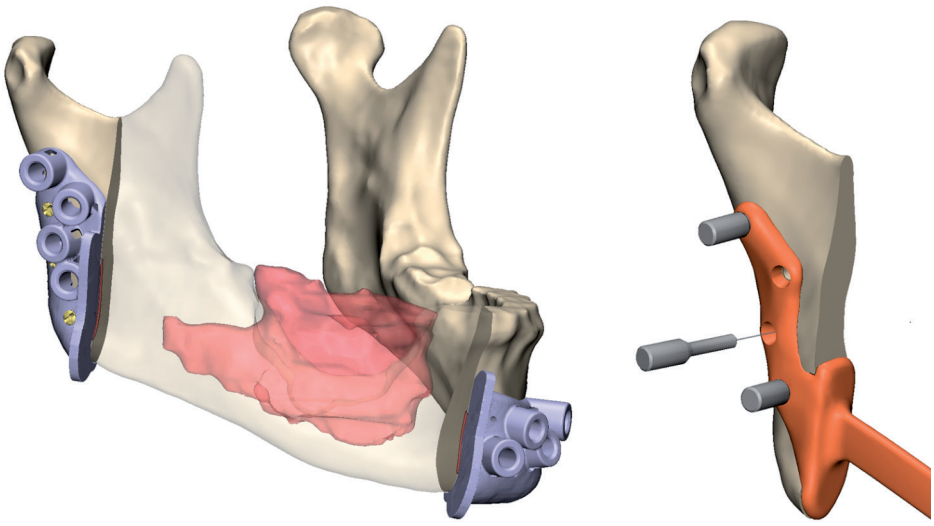

Figure 2 | This figure shows an example of the type of surgical guides (top right) and temporary centring pins (lower right) that were used in this study.

In order to accurately translate the VSP to the operating theatre, surgical drill and cutting guides were designed in house and 3D printed by Oceanz (Oceanz BV) from medical grade polyamide powder (Figure 2). Cylinders in the guide indicate the position and direction of the planned screws and function as a pilot drill support when an additional metallic drill sleeve is inserted. Comparable guide designs were applied in previous studies and proved to be an accurate translator of surgical plans[27-30]. In addition, centring pins were designed to function as intraoperative plate positioning devices and inserted into the drilled screws pilot holes (Figure 2).

Measurements

All the patients underwent a postoperative CBCT scan (120 kV/5 mA with a field of view of 130–230 mm and 0.2–0.4 mm voxel size) to assess the accuracy of implant placement by means of screw entry point deviation and angular screw deviation. Manual alignment of the planned 3D objects of the mandibular segments and screw cylinders with the postoperative CBCT was performed with the Mimics Medical 19.0 software. Two observers executed the alignment independently (BJM and JK). The in situ plate was segmented in order to assess angular screw deviation and subsequently matched to the plate's design file, while the manually aligned screw cylinders were moved along. The Geomagic Studio 2012 (3D Systems) software was used for the matching through a best-fit surface alignment procedure.

Screw entry point deviation was measured between the entry points in the virtual planning, and the cylinders were matched to the postoperative CBCT by means of Euclidean distance (3D) measurements in the 3-Matic Medical 11.0 software. Prior to these measurements, all the manually aligned mandibular segments and corresponding cylinders were matched to the virtual planning using the global alignment function in 3-Matic Medical 11.0.

Data analysis was performed using MedCalc for Windows, version 19.0.5 (MedCalc Software). The inter-observer variability was supported by the calculation of the interclass correlation coefficient (ICC) for every screw entry point, placed by both observers. A value of <.40 is reported as poor, .40–.59 fair, .60–.74 good and .75–1.00 as excellent[31].

RESULTS

Patients

A total of eight patients who had either already undergone reconstruction of a continuity resection of the mandible or were scheduled to undergo one presented to our centre (n = 8). This group required either primary treatment of tumours (n = 5) or replacement of a mechanically failed conventional reconstruction plate (n = 3). The latter consisted of two patients with a broken conventional 2.7 RP and one patient with pulled out screws, causing loosening of the conventional 2.7 RP and the locking screws. Table 1 shows the detailed overview of these patients. Patients 7 and 8 received postoperative radiotherapy (66 Gy), starting within six weeks after reconstruction with the PS-RP.

We created comparative FEA of our PS reconstructions for the three patients with failed hand-bent reconstruction plates. Mandibular segments, loading situations and boundary conditions remained unchanged. The comparative FEA considered the resultant forces on the bone–screw interface, as well as the von Mises or resultant stress occurring in the reconstruction plates. This von Mises stress was used to predict whether or not materials will yield under loading.

Table 1. Patient overview.

	Patient	Age	Sex	Diagnosis	Indication	PM flap	Follow up (months)	Number of screws	Screw entry point dev. [mm]	Screw angular dev. [°]
1		49	♂	Metastasis melanoma mandible	Broken 2.7 OSM plate	No	29	13	2.20 (± 0.51)	5.41 (± 3.32)
2	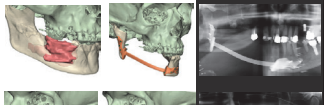	85	♂	T4N0 SCC	Broken 2.7 OSM plate	Yes	25	9	1.49 (± 0.42)	4.81 (± 2.56)
3	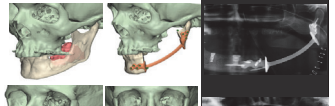	58	♀	T4N0 SCC	Primary recon.	Yes	21	9	1.31 (± 0.30)	5.99 (± 3.52)
4	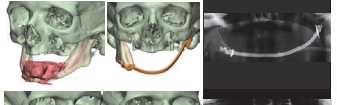	72	♀	T4N0 SCC	Primary recon.	Yes	18	8	0.35 (± 0.22)	4.26 (± 2.29)
5	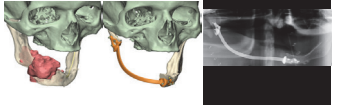	85	♂	T4Nx SCC	Primary recon.	Yes	NA	8	NA	NA
6	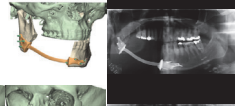	70	♂	Ameloblastoma mandible	Loosened screws 2.7 OSM plates	No	8	8	2.04 (± 0.75)	7.49 (± 4.27)
7	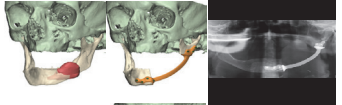	80	♀	T4N0 SCC mandible	Primary recon.	Yes	7	7	0.87 (± 0.59)	4.94 (± 3.46)
8	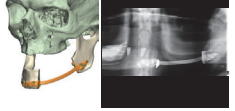	78	♂	Metastasis T2N2 SCC mandible	Primary recon.	Yes	7	10	1.83 (± 0.96)	6.29 (± 3.20)
	Mean	72					16 (R: 7-29)	9 (R: 7-13)	1.54 (± 0.85)	5.76 (± 3.27)

Abbreviations: ♀, female; ♂, male; OSM, osteosynthesis material; PM, pectoralis major; SCC, squamous cell carcinoma.

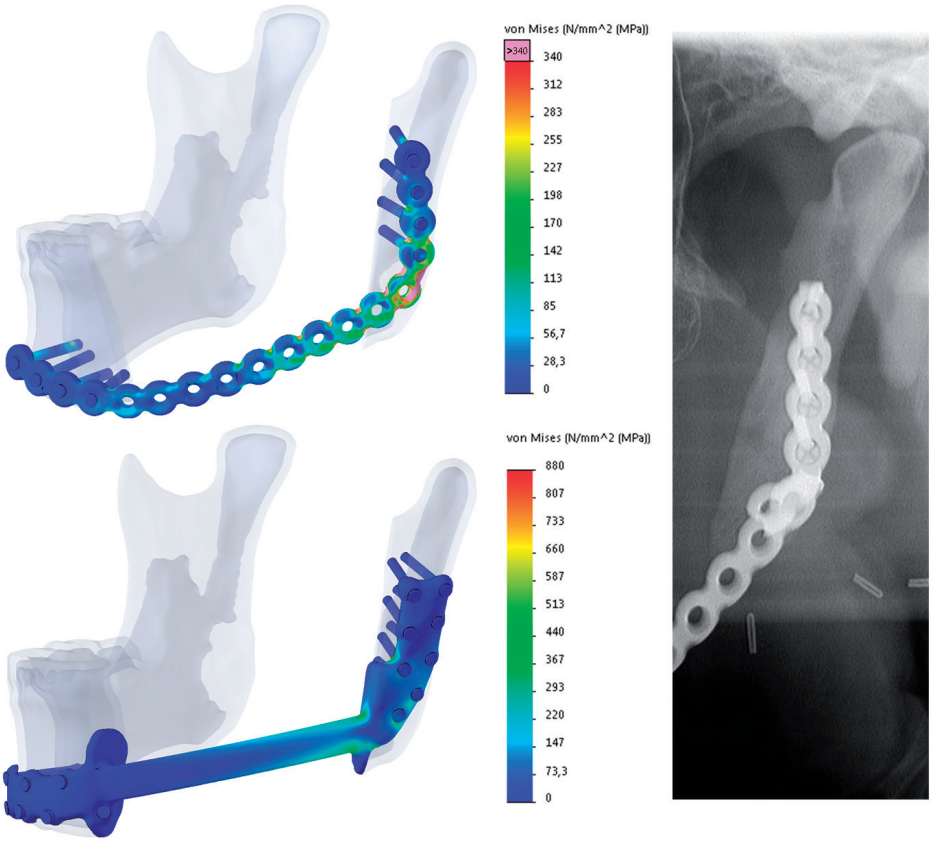

Figure 3 | Finite element analysis shows the maximum occurring von Mises stress in both the failed conventional (primary) reconstruction plate (top left) and the PS reconstruction plate (lower left) in patient one and illustrates the resemblance between the highest stress region of the conventional reconstruction plate in silico (note the overloaded pink region in the top left image) and the actual location of the in situ plate fracture (panorex).

Plate fracture

The FEA results showed that the maximum von Mises stresses in all the analysed conventional RPs exceeded their yield strength (YS), by 42% up to 153%, indicating plastic deformation would occur on applying the load case. The plates would therefore not return to their original shape after loading. Furthermore, the stress in these plates exceeded the material's ultimate strength (US) value by 13% up to 100%, indicating a high risk of plate fracture. The application of our PS reconstruction to the latter patient resulted in a decrease in the YS and US percentages, going from 253% to 59% and 200% to 55%, respectively (Figure 3). In patient number two, who suffered from

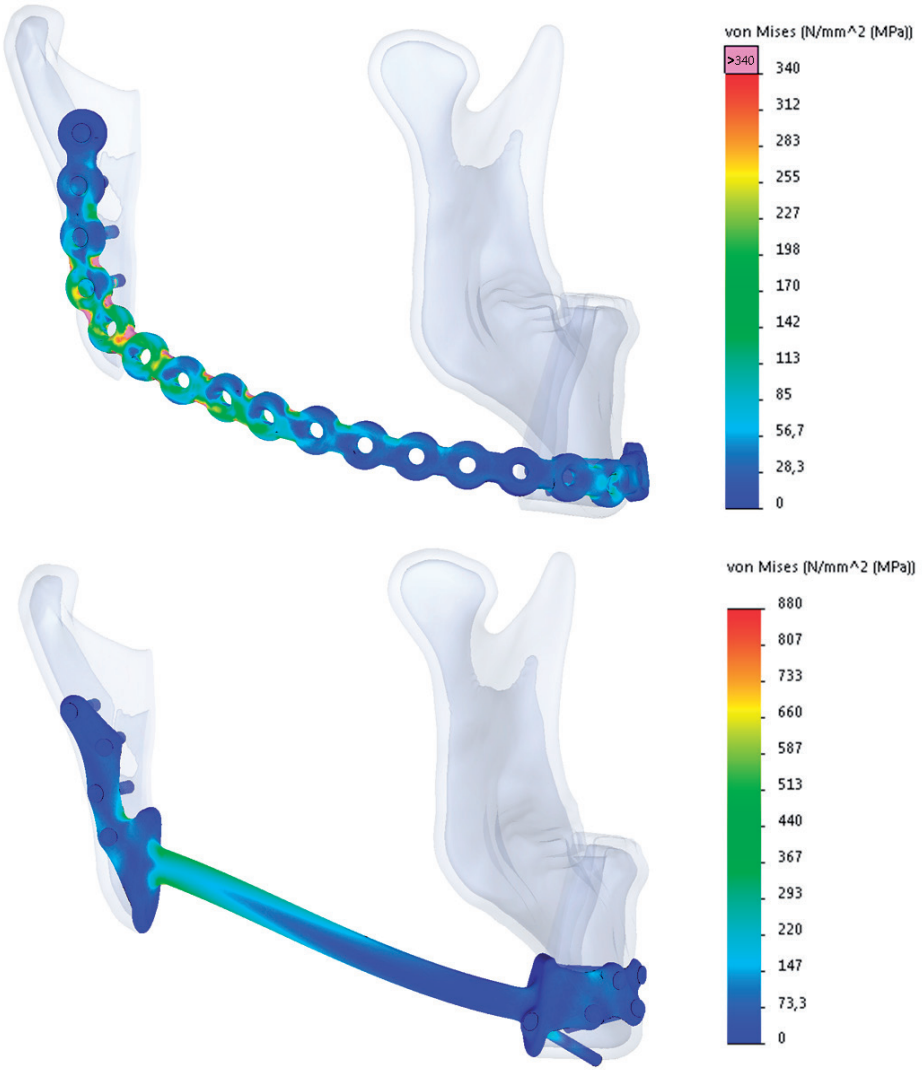

Figure 4 | Finite element analysis von Mises stress results for the failed conventional reconstruction (top left) and patient-specific solution (lower left) for patient 2. The Bridging part height was reduced compared to the first application of our patient-specific plate, as shown in Figure 2, and remained at this height throughout this study's series.

a fractured conventional RP, we saw a decrease in YS and US percentages, going from 188% to 67% and 149% to 62%, respectively (Figure 4), thereby staying well within acceptable boundaries.

Screw pull-out

The results of our FEA of the primary conventional reconstruction that failed due to screw pull-out showed that high resultant forces were acting on these screw surrounding areas. In this case, the RP was fixed at the ventral side of the defect with three screws. Screw one, two and three, counting away from the defect, which had loosened over time, were loaded with 438 N, 416 N and 112 N, respectively. The comparative FEA of our bookshelf-plate design showed that adding a screw in the ventral bookshelf flange (205 N) would lower the resultant screw forces to 184 N, 144 N and 90 N, respectively, which represents a minimisation of 58%, 66% and 20%. The axial pull-out force components, the forces along the longitudinal screw directions, did not exceed 180 N for the conventional reconstructions or 90 N for the PS reconstructions.

Surgical procedure

All the PS bookshelf-reconstruction plates were inserted in accordance with the 3D-VSP. The surgical procedures were uneventful. During surgery, prior to the drilling of screw pilot holes, the mandibular bone was denuded and the guides were positioned and fixed using 1.5-mm mini screws (KLS Martin). Subsequently, the osteotomies were performed. Thereafter, the plate was inserted and fitted to the mandibular segments using several centring pins. Once properly aligned, these pins were replaced one by one by 2.3-mm locking screws with a length in agreement with the surgical planning. Primary closure was performed according to plan in two patients. In the remaining six patients, a pectoralis major flap was used to reconstruct the soft tissue defect and to cover the plate.

Postoperative

Recovery was uneventful from a mechanical point of view for seven patients with a mean of 11.4 days of hospitalisation (SD: 9.3, R: 3–29). One patient, however, patient 5 in Table 1, deceased in the fourth week postoperatively due to complications related to a PRG probe and therefore could not be followed up. All patients underwent a CBCT scan 6–27 days (mean 12 days) postoperatively. The mean follow-up period of the 7 patients alive is 16 months (R: 7–29) and was uneventful with regard to plate failure or screw pull-out.

Measurements

Screw entry point deviation (3D) resulted in a mean value of 1.54 mm (SD 0.85, R: 0.10–3.19) for a total of 64 screws. The mean angular screw deviation was 5.76 degrees (SD: 3.27, R: 1.26–16.62). The 95% confidence interval of the inter-observer variability for our measurements was 0.15–0.26 mm with a P-value of .05. The inter-class correlation coefficient (two-way mixed) was 0.97, indicating an excellent match of measurements by both observers.

Dehiscence

The ventral bookshelf-like flange of our PS-RPs in the first and third operated patients became partially dehiscent intra-oral approximately 14 and 4 months postoperatively, respectively. Patient 1 lost 16 kg of bodyweight over a short period of time prior to the intra-oral dehiscence, which could have played a role in this development. One of these two patients had received a pectoralis major flap, while the other patient underwent primary closure. It was assessed that the design of the flange was too high. The dehiscent cranial part of this flange was surgically removed with some margin (23 and 19 months postoperatively, respectively), and the surrounding soft tissue could be closed (Figure 5). By comparing the 6 days postoperative panorex image of patient 1 to its 18-month follow-up, a gradual resorption of the left mandibular angle up to the caudal contour of the plate was observed. There have been no further complications to date.

DISCUSSION

In this pilot study, we present a unique patient-specific bookshelf-reconstruction plate for accurate bridging of mandibular continuity defects. The novel design was based on the FEA of the conventional reconstruction plate failure, with regard to plate fractures and screw loosening. Application of bookshelf-like flanges, with a screw fixation in the osteotomy sites, resulted in substantial reduction of resultant screw pull-out inducing forces and, in combination with a change in material, lowered plate stress to within satisfactory levels. Therefore, the chances of the widely reported mechanical problems seen with conventional RPs, which are responsible for 5%–10% of reconstruction failures, were reduced [1-6].

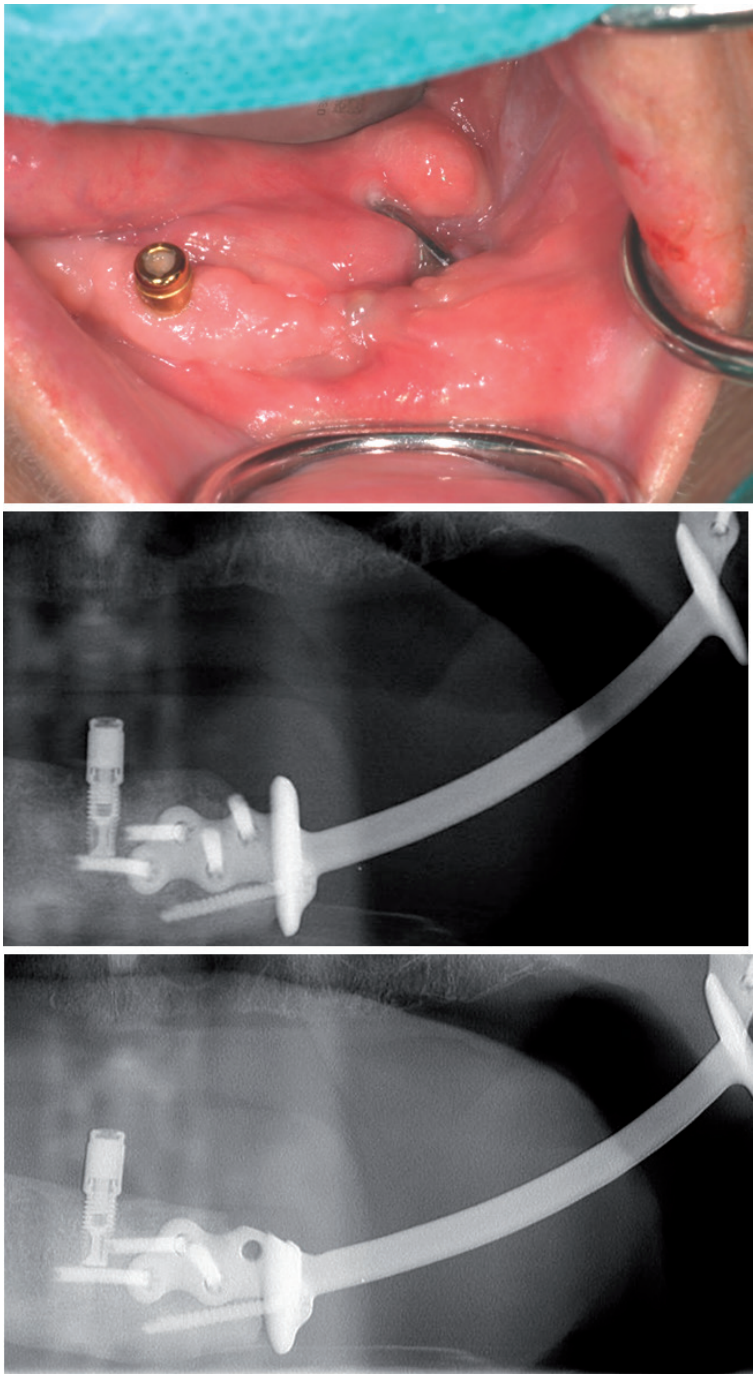

Figure 5 | Dehiscence of the cranial section of the ventral bookshelf-flange in patient 3. The top and middle images are intra-oral and panorex images, respectively, before surgical bookshelf-flange modification. The lower panorex image shows the postoperative situation.

Our comparative FEA focused on resultant screw forces rather than the force components in axial screw direction. Most studies found in the literature that look into screw pull-out describe in vitro results of axial single screw pull-out. This observation of axial pull-out could occur with compression screws but not with locking screws, since these have the tendency to be pulled out en bloc with the RP rather than axially, due to their semi-rigid connection with the RP[32]. We do know, however, that the axial force components regarding the screws in our study did not exceed 180 N for the conventional reconstructions and 90 N for the PS reconstructions.

The addition of our bookshelf-flange concept is only of value, in terms of mechanical stability and reduction of the risk of failure, when applied accurately to the planned position. First, a per-operative visual inspection after guided placement confirmed that no gap remained between the flange and the mandibular bone at the osteotomy sites. Second, postoperative analysis of CBCT scans showed a high accuracy of placement, with 3D deviations comparable to our prior studies and of others, using surgical guides[29,30,33-35]. Additionally, careful inspection of the postoperative CBCT scans confirmed contact between the osteotomy sites and bookshelf-like flanges of the RPs as well as the remainder bone–plate interface, which indicates proper positioning with a small potential shift in the osteotomy plane. The measured screw entry point deviation of 1.58 mm (SD 0.82) and angular screw deviation of 5.77 degrees (SD 3.33) indicate this method could be applied as a reliable one-phase procedure for resection and direct reconstruction of a tumour in the mandible. These results represent the accumulation of errors in all visualisation and segmentation steps as well as geometrical errors of the guides and plate and the actual surgical procedure.

Over the last two decades, a rapidly increasing number of PS-RPs have been presented in the literature with an equal increase in varying finite element analysis models. Applying FEA is of great importance in the design process, since PS-RPs can still fail mechanically when designed using incorrect assumptions[15,36]. Only a very small selection of these FEA models has actually been validated through in vitro and in vivo experiments. Engineers should be always careful when setting up a FEA model, especially complex anatomical models, and all the necessary assumptions that come with it. Also, PS-RP's should be designed to withstand repetitive loading and the material's fatigue properties for FEA should be chosen accordingly, like we did in this study. Often, only the ultimate or yield properties of a material are taken into account, while the fatigue properties are lower, which could lead to early material

failure. We decided to use the most extensively validated model we could find in the literature. However, even this model has its limitations and assumptions. We found that most of the PS-RPs designs in the literature rely on a strip-like plate which is positioned and fixated at the buccal contour of the mandible[14,15,36-39]. We decided to make use of the osteotomy site as well and trap the mandibular segment in between the plate design, which is more stable biomechanically, according to our FEA results.

We expect the dehiscence of the cranial section of the ventral flanges, that occurred in two patients, to be caused by the height of the flanges in combination with contraction of the covering soft tissue. Minimising the bulkiness and height of these flanges might exclude this occurrence. A gradual remodelling of the mandibular angle was observed in one patient past the implant border. The reconstruction plate could have shielded this particular region of the mandible mechanically, causing bone remodelling to occur. Stress-shielding, also seen in conventional reconstruction plate reconstructions, might explain this resorption. Future application of the topology optimisation technique[40] could play a key role in minimising the occurrence of, or potentially totally exclude, both stress-shielding and dehiscence. This engineering technique removes unloaded or unnecessary material and is applied in the FEA phase of the design. It could be used to create geometrically minimalistic designs, while approaching displacement or stress limits, and could prevent a RP from being too stiff, which can cause stress-shielding, and plates becoming bulky. This study describes a first step in the optimisation of patient-specific plate design. By allowing for freeform organic structures through topology optimisation, we expect we can lift our patient-specific reconstructions to a higher level of patient specificity in the near future. Also, based on the results of this phase-one study we aim to start a multicentre phase-two study in which we can further validate the effect of our reconstruction method in more patients and over a longer follow-up period.

Conclusion

Using the finite element method, we retrospectively analysed mechanically failed conventional reconstruction plates and developed an alternative reconstruction plate for the mandible that reduces the chance of screw pull-out and plate fracture. During this phase-one study, we successfully reconstructed mandibular continuity defects using our bookshelf-reconstruction plate concept in eight patients and no mechanical failures have occurred in the study cohort. This novel design of reconstructive plates seems to reduce the risk of screw pull-out and plate fractures.

Acknowledgements

The materials used in this study were unrestrictedly supported by an Innovative Action programme Groningen-4 (IAG4) grant from the Province of Groningen, The Netherlands.

Conflict of Interest

There is no conflict of interest to report.

REFERENCES

1. Maurer, P., Eckert, A. W., Kriwalsky, M. S. & Schubert, J. Scope and limitations of methods of mandibular reconstruction: a long-term follow-up. *Br. J. Oral Maxillofac. Surg.* **48**, 100-104 (2010).
2. Schoning, H. & Emshoff, R. Primary temporary AO plate reconstruction of the mandible. *Oral Surg. Oral Med. Oral Pathol. Oral Radiol. Endod.* **86**, 667-672 (1998).
3. Shibahara, T., Noma, H., Furuya, Y. & Takaki, R. Fracture of mandibular reconstruction plates used after tumor resection. *J. Oral Maxillofac. Surg.* **60**, 182-185 (2002).
4. Katakura, A., Shibahara, T., Noma, H. & Yoshinari, M. Material analysis of AO plate fracture cases. *J. Oral Maxillofac. Surg.* **62**, 348-352 (2004).
5. Lopez, R., Dekeister, C., Sleiman, Z. & Paoli, J. R. Mandibular reconstruction using the titanium functionally dynamic bridging plate system: A retrospective study of 34 cases. *J. Oral Maxillofac. Surg.* **62**, 421-426 (2004).
6. Gellrich, N. C. *et al*. Comparative study of locking plates in mandibular reconstruction after ablative tumor surgery: THORP versus UniLOCK system. *J. Oral Maxillofac. Surg.* **62**, 186-193 (2004).
7. Maurer, P., Eckert, A. W., Kriwalsky, M. S. & Schubert, J. Scope and limitations of methods of mandibular reconstruction: a long-term follow-up. *Br. J. Oral Maxillofac. Surg.* **48**, 100-104 (2010).
8. Irish, J. C. *et al*. Primary mandibular reconstruction with the titanium hollow screw reconstruction plate: evaluation of 51 cases. *Plast. Reconstr. Surg.* **96**, 93-99 (1995).
9. Markwardt, J., Pfeifer, G., Eckelt, U. & Reitemeier, B. Analysis of complications after reconstruction of bone defects involving complete mandibular resection using finite element modelling. *Onkologie* **30**, 121-126 (2007).
10. Lindqvist, C. *et al*. A comparative study on four screw-plate locking systems in sheep: a clinical and radiological study. *Int. J. Oral Maxillofac. Surg.* **30**, 160-166 (2001).
11. Martola, M., Lindqvist, C., Hanninen, H. & Al-Sukhun, J. Fracture of titanium plates used for mandibular reconstruction following ablative tumor surgery. *J. Biomed. Mater. Res. B. Appl. Biomater.* **80**, 345-352 (2007).
12. Lindqvist, C., Soderholm, A. L., Laine, P. & Paatsama, J. Rigid reconstruction plates for immediate reconstruction following mandibular resection for malignant tumors. *J. Oral Maxillofac. Surg.* **50**, 1158-1163 (1992).
13. Li, P. *et al*. Establishment of sequential software processing for a biomechanical model of mandibular reconstruction with custom-made plate. *Comput. Methods Programs Biomed.* **111**, 642-649 (2013).
14. Narra, N. *et al*. Finite element analysis of customized reconstruction plates for mandibular continuity defect therapy. *J. Biomech.* **47**, 264-268 (2014).
15. Luo, D., Xu, X., Guo, C. & Rong, Q. *Fracture Prediction for a Customized Mandibular Reconstruction Plate with Finite Element Method* (Advanced Computational Methods in Life System Modeling and Simulation, Springer Singapore, Singapore, 2017).
16. Singare, S., Shenggui, C. & Sheng, L. The use of 3D printing technology in human defect reconstruction-a review of cases study. *Medical Research and Innovations* **1** (2017).
17. Jewer, D. D. *et al*. Orofacial and mandibular reconstruction with the iliac crest free flap: a review of 60 cases and a new method of classification. *Plast. Reconstr. Surg.* **84**, 391-5 (1989).
18. Brown, J. S., Barry, C., Ho, M. & Shaw, R. A new classification for mandibular defects after oncological resection. *Lancet Oncol.* **17**, 23 (2016).

19. Mesnard, M. *et al*. Biomechanical Analysis Comparing Natural and Alloplastic Temporomandibular Joint Replacement Using a Finite Element Model. *Journal of Oral and Maxillofacial Surgery* **69**, 1008-1017 (2011).
20. Ramos, A., Ballu, A., Mesnard, M., Talaia, P. & Simões, J. Numerical and Experimental Models of the Mandible. *Exp Mech* **51**, 1053-1059 (2011).
21. Ramos, A. M. & Mesnard, M. The stock alloplastic temporomandibular joint implant can influence the behavior of the opposite native joint: A numerical study. *Journal of Cranio-Maxillofacial Surgery* **43**, 1384-1391 (2015).
22. Mesnard, M. & Ramos, A. Experimental and numerical predictions of Biomet((R)) alloplastic implant in a cadaveric mandibular ramus. *J. Craniomaxillofac. Surg.* **44**, 608-615 (2016).
23. Ramos, A., Nyashin, Y. & Mesnard, M. Influences of geometrical and mechanical properties of bone tissues in mandible behaviour - experimental and numerical predictions. *Computer Methods in Biomechanics and Biomedical Engineering* **20**, 1004 (2017).
24. Boyer R., Welsch G., Collings E. W. in *Materials Properties Handbook: Titanium Alloys* , 1994).
25. Holt, J. M. & Ho, C. Y. in *Structural Alloys Handbook* , 1996).
26. Kraeima, J. *et al*. Multi-modality 3D mandibular resection planning in head and neck cancer using CT and MRI data fusion: A clinical series. *Oral Oncol.* **81**, 22-28 (2018).
27. Kraeima, J., Merema, B. J., Witjes, M. J. H. & Spijkervet, F. K. L. Development of a patient-specific temporomandibular joint prosthesis according to the Groningen principle through a cadaver test series. *J. Craniomaxillofac. Surg.* **46**, 779-784 (2018).
28. Schepers, R. H. *et al*. Accuracy of fibula reconstruction using patient-specific CAD/CAM reconstruction plates and dental implants: A new modality for functional reconstruction of mandibular defects. *J. Craniomaxillofac. Surg.* **43**, 649-657 (2015).
29. Schepers, R. H. *et al*. Accuracy of secondary maxillofacial reconstruction with prefabricated fibula grafts using 3D planning and guided reconstruction. *J. Craniomaxillofac. Surg.* **44**, 392-399 (2016).
30. Vosselman, N., Merema, B. J., Schepman, K. P. & Raghoebar, G. M. Patient-specific sub-periosteal zygoma implant for prosthetic rehabilitation of large maxillary defects after oncological resection. *Int. J. Oral Maxillofac. Surg.* (2018).
31. Cicchetti, D. in *Guidelines, Criteria, and Rules of Thumb for Evaluating Normed and Standardized Assessment Instrument in Psychology* 284-290, 1994).
32. Cronier, P. *et al*. The concept of locking plates. *Orthop. Traumatol. Surg. Res.* (2010).
33. Kraeima, J., Merema, B. J., Witjes, M. J. H. & Spijkervet, F. K. L. Development of a patient-specific temporomandibular joint prosthesis according to the Groningen principle through a cadaver test series. *J. Craniomaxillofac. Surg.* **46**, 779-784 (2018).
34. Pietruski, P. *et al*. Supporting mandibular resection with intraoperative navigation utilizing augmented reality technology - A proof of concept study. *J. Craniomaxillofac. Surg.* (2019).
35. van Baar, G J C, Forouzanfar, T., Liberton, N P T J, Winters, H. A. H. & Leusink, F. K. J. Accuracy of computer-assisted surgery in mandibular reconstruction: A systematic review. *Oral Oncol.* **84**, 52-60 (2018).
36. Li, P. *et al*. Optimal design of an individual endoprosthesis for the reconstruction of extensive mandibular defects with finite element analysis. *J. Craniomaxillofac. Surg.* **42**, 73-78 (2014).
37. Mazzoni, S. *et al*. Prosthetically guided maxillofacial surgery: evaluation of the accuracy of a surgical guide and custom-made bone plate in oncology patients after mandibular reconstruction. *Plast. Reconstr. Surg.* **131**, 1376-1385 (2013).
38. Wu, C. H., Lin, Y. S., Liu, Y. S. & Lin, C. L. Biomechanical evaluation of a novel hybrid reconstruction plate for mandible segmental defects: A finite element analysis and fatigue testing. *J. Craniomaxillofac. Surg.* **45**, 1671-1680 (2017).

39. Gutwald, R., Jaeger, R. & Lambers, F. M. Customized mandibular reconstruction plates improve mechanical performance in a mandibular reconstruction model. *Comput. Methods Biomech. Biomed. Engin.* **20**, 426-435 (2017).
40. Iqbal, T. *et al*. A general multi-objective topology optimization methodology developed for customized design of pelvic prostheses

Section II

Chapter 4

Development of a patient-specific temporomandibular joint prosthesis according to the Groningen principle through a cadaver test series

J. Kraeima, B.J. Merema, M.J.H. Witjes, F.K.L. Spijkervet

Department of Oral and Maxillofacial Surgery, University Medical Centre Groningen, Hanzeplein 1, P.O. Box 30.001, 9700, RB Groningen, The Netherlands

Published:
Journal of Cranio-Maxillofacial Surgery, 2018; 46(5): 779-784

ABSTRACT

Objectives

Patients suffering from osteoarthritis, ankylosis (e.g. post-trauma or tumour) in the temporomandibular joint (TMJ) can present with symptoms such as severely restricted mouth opening, pain or other dynamic restrictions of the mandible. To alleviate the symptoms, a total joint prosthesis can be indicated, such as the Groningen TMJ prosthesis. This was developed as a stock device with a lowered centre of rotation for improved translational and opening capacity. This study aimed to improve the design of the prosthesis, and produce a workflow for a customized Groningen TMJ prosthesis, in order to make it more accurate and predictable.

Methods

The fossa and mandibular components of the Groningen TMJ prosthesis were customized. A series of five human cadavers was operated and bilateral TMJ prostheses were placed using custom cutting and drilling guides. Placement accuracy was evaluated based on post-operative CT data.

Results

A total of N = 10 prostheses were placed and analysed. The average Euclidean distance deviation from planned to actual position was 0.81 mm (SD 0.21). All prostheses were placed according to the routine surgical approaches and had an excellent alignment with the bony structures.

Conclusion

The newly developed custom Groningen TMJ prosthesis can be placed with great accuracy and is the first step for improving TMJ total joint replacement surgery.

INTRODUCTION

Patients suffering from osteoarthritis, ankylosis, post-traumatic ankylosis or tumours in the temporomandibular joint (TMJ) area can present with symptoms such as severely restricted mouth opening, pain or other dynamic restrictions of the mandible. If conservative treatments or regular open joint surgery (gap-osteotomy with arthroplasty) do not suffice, a total joint prosthesis may be indicated[1]. Previous studies have reported that placement of total joint prostheses can also improve the maximum mouth opening and reduce pain[1, 2]. Moreover, the total joint prosthesis was reported to be a predictable and flexible instrument for reconstruction of the TMJ[2].

One of the challenges in replacing the TMJ is the imitation of the complex movements of the natural TMJ, including both a rotational and translational component. Multiple TMJ prosthesis variants have been produced, which were reported to have limitations with regards to the translational component of the joint movement[3-5]. As a result of the design of the prosthesis and the lacking attachment of the lateral pterygoid muscle to the condyle, the translational freedom was substantially restricted to a few millimetres only. The natural translation movement of the TMJ was reported to be in the order of 16 mm[6]. As was described by van Loon et al., the optimal position for a fixed centre of rotation (CR) in TMJ prostheses, thereby mimicking the physiological movement, is 15 mm inferior to the natural CR[6].

This inferiorly located CR was incorporated in the Groningen TMJ prosthesis, which was developed between 1983 and 1999 as a stock prosthesis[7, 8]. A series of eight patients who received this prosthesis was analysed after a period of eight years of follow-up. This follow-up study of Schuurhuis et al. reported that patients were satisfied, despite the limited improvement of the maximum mouth opening due to continuation of their pre-operative chronic[3].

Stock prostheses can however have a suboptimal fit; requiring per-operative bone re-contouring or resulting in post-operative dis-occlusion due to inadequate condylar length[2]. Moreover the TMJ prostheses require osseo-integration in order to remain functional on the long-term, and this can only be achieved as long as the fossa and mandibular parts are in proper and primary stable contact with the host bone[9, 10]. In general, a stock prosthesis is reported to be hard to fit, as the target area is usually mutilated especially at the fossa level[5]. The customisation of the TMJ prosthesis,

adaption of the bone connective surfaces to the anatomy of the individual patient, can contribute to overcome these problems. In addition, the use of custom prostheses and the use of placement surgical guides can save time within the surgical procedure, as for example the exact location, angulation and length of the screws are pre-determined.

As already used in other applications of patient-specific implants for oral and maxillofacial surgery[11-13], the current techniques for 3D planning, design and manufacturing, e.g. 3D milling and printing, enable accurate customised implants. Due to these developments, the customisation of the prostheses and production of custom placement/drilling guides is now readily available. However, to our knowledge, no combined cutting, drilling and placement guides are included in current available (custom) TMJ prostheses[14, 15].

As the Groningen TMJ prosthesis was developed and placed as a stock prosthesis, it was not fitted with the use of individual placement guides. This might have caused a suboptimal placement and realisation of the pre-determined CR, 15 mm inferior to the natural CR. For the previously placed Groningen TMJ prostheses, no accuracy analyses were performed of the placement accuracy. Therefore no exact comparison between the theoretical model of patient-specific planning and the actual post-operative result could be made. For other (stock or custom) prosthesis, to our knowledge, no additional accuracy analysis was performed either. In order to effectuate the concept of lowering the pivot point of the patient, and thereby improving the simulation of the rotation/translational movement, the prosthesis should be placed as it was planned.

The aim of this study is optimise the design of the Groningen TMJ prosthesis, by means of implementation of patient-specific planning and customisation. This should lead to an accurate placement in a cadaver series. It is hypothesized that the customized TMJ prosthesis and the introduction of custom placement guides provides an accurate translation of the virtual planning towards the cadaver. The design and fabrication is described in this manuscript, as well as the validation of the placement accuracy using the guides, including inter-observer variation. The results are based on analysis of planning and post-operative imaging of 5 human cadavers.

MATERIALS AND METHODS

The original Groningen TMJ prosthesis consisted of a total of six parts of which four parts were available in multiple sizes to ensure a close fit to the patient's anatomy. The overview, together with an exploded view, of this original design is presented in Fig. 1A. Titanium was used for the fossa part (1B part B), fitting member (1B part A) and mandibular part (1B part F) while the condylar sphere (1B part E) and translation plate (1B part C) were manufactured from zirconia. An Ultra-High Molecular Weight Polyethylene (UHMWPE) disc (1B part D) formed the counter bearing surface to the zirconia parts, as is presented in Fig. 1B.

Two types of movements in this TMJ prosthesis were distinguished: translational and rotational movements. This took place on separate sites. The rotational movement was achieved by a ball and socket joint whereas the translational articulation was

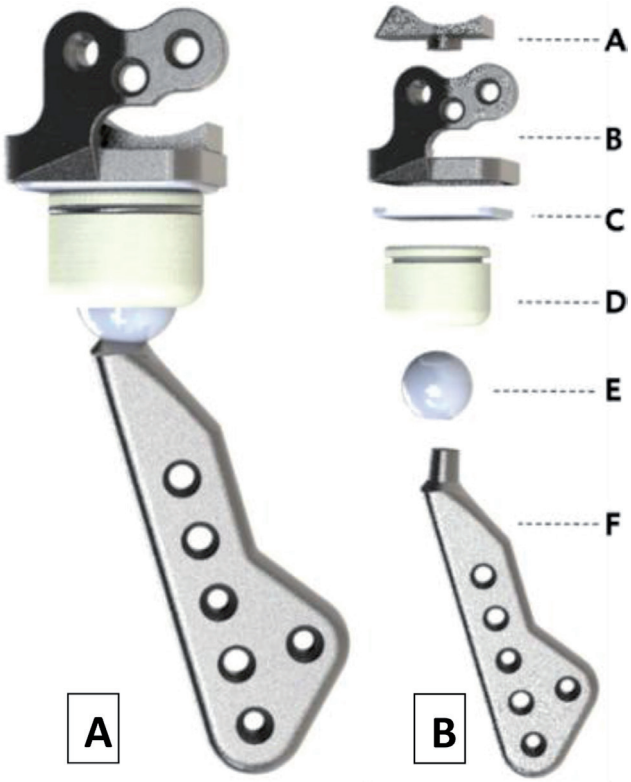

Fig. 1 | A. Stock Groningen TMJ prosthesis **B.** exploded view of stock Groningen TMJ prosthesis: a fitting member (titanium), b fossa part (titanium), c ceramic plateau, d UHMWPE disc, e ceramic condylar head, mandibular part (titanium).

obtained through an artificial disc which could freely slide over a translation site, to the inferior side of the fossa part. The separation of these articulating sites is unique in TMJ prostheses and enables the use of relatively large load-bearing areas for both articulations, resulting in low contact stress and therefore low wear rates[16, 17].

In order to customise the design the technical drawings were retrieved from the original manufacturer to function as a base for the 3D design of the patient specific prosthesis. In this customised TMJ prosthesis, the concepts of the original Groningen prosthesis where maintained -i.e., the inferiorly located CR and the separated articulation sites for rotational and translational movements. A prosthesis that consists of a customised fossa and mandibular part was designed in order to match the individual patient's anatomical geometry. Fig. 2 presents an example of the custom Groningen TMJ prosthesis, including an exploded view (2B) for a detailed description per part. For this customised prosthesis titanium alloy was used for the fossa-(2B part A) and

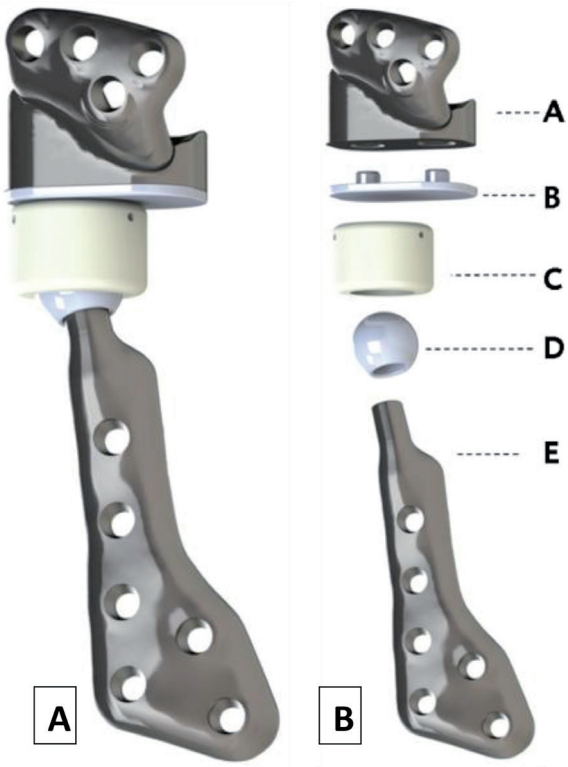

Fig. 2 | A. Customized Groningen TMJ prosthesis **B.** Exploded view of the custom Groningen TMJ prosthesis: a printed titanium fossa part, b ceramic gliding part (tapered fixation to fossa part), c UHMWPE disc, ceramic condylar head (tapered fixation to mandibular part).

mandibular part (2B part E). Zirconia for used for both the condylar sphere (2B part B) and translation plate (2B part D) while the disc (2B part C) is made of UHMWPE.

In addition to the customised prosthesis design, surgical guides for per-operative placement where designed, matching the prosthesis design and the individual anatomy (Fig. 3). These surgical guides were designed to implement the virtual planning in the actual surgical procedure, and consisted of a condylectomy guiding flange and drill guiding cylinders for creating screw pilot holes. Guides were manufactured from Polyamide by means of Additive Manufacturing using an EOS P396 SLS printer (EOS, Krailling, Germany). The drill guiding cylinders were machined from stainless steel (316L) in order to minimise wear particles due to high-speed drill contact. All titanium parts used during this study were 3D printed from medical grade titanium alloy powder (Ti-6Al-4V ELI/Grade 23) using an EOS M 290 Direct Metal Laser Sintering printer (EOS, Krailling, Germany). In the original Groningen TMJ prostheses, commercially pure titanium (Ti-CP) was used. In current TMJ prosthesis, the mechanically superior medical grade 23 titanium alloy was used as material for the fossa part and mandibular part. Ti-CP is reported to have a lower strength and resistance to fatigue than (3D printed) grade 23 titanium[18, 19]. In order to obtain a

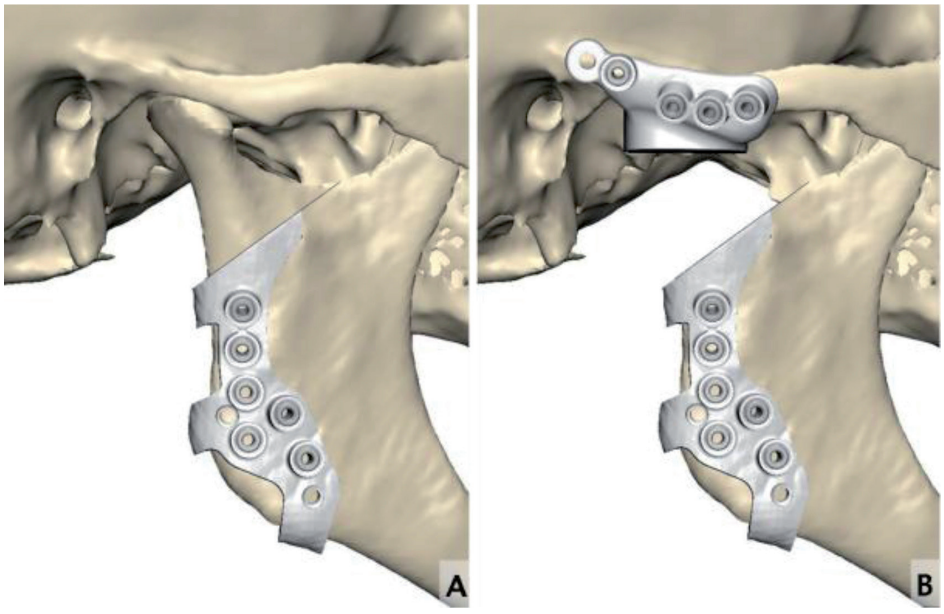

Fig. 3 | A. Custom polyamide surgery guides with stainless steel bur inserts used for cutting, drilling and placement indication of the prosthesis. **B.** Condylectomy performed according to the guide. Fossa guide applied to the bone as well.

smooth surface finish to all soft-tissue facing sites of the printed titanium parts, the parts were milled after printing. The articulating zirconia and UHMWPE parts were milled using high precision milling machines.

In order to produce the prosthesis, all connected parts were fixed through mechanical connections. No additional adhesives were required. For fixating the condylar sphere, a self-locking taper connection was used. For fixation of the translation plate an interference-fit was chosen. The resulting force, when functioning in the patient, for these mechanical connections is mainly compressive. This is comparable to the original design[8]. Both connections are illustrated in Fig. 2B, exploded view. The Groningen TMJ prosthesis as well as the surgical guides where provided by Xilloc Medical, (Sittard-Geleen, The Netherlands). The produced TMJ prosthesis consists of three parts: fossa part, mandibular part, and the UHMWPE disk.

A cadaver test was set up to validate the surgical procedure and accuracy of the surgical implantation of the customise TMJ total joint prosthesis. A total of five fresh-frozen human cadaver heads (n = 10 prostheses, = 20 fixed prosthesis parts) were individually operated and received a bilateral patient specific TMJ prosthesis. In order to make a virtual planning and design, a CT scan of the cadaver heads was made in frozen condition. Anatomical 3D-models of the skull, mandible and mandibular nerve were acquired using Mimics 19.0 (Materialise, Leuven, Belgium) software. Based on these models, the fossa and mandibular prosthesis parts where designed using 3-Matic 11.0 (Materialise, Leuven, Belgium). The virtual planning included the anatomical CR of the mandible, the inferiorly located prosthesis CR, resection planes for condylectomies, screw positions and screw lengths. For all parts that required screw fixation a surgical guide/template was designed to translate the virtual 3D-planning towards per-operative guidance for the surgeon.

The patient specific parts of the prosthesis are fixed to the bone using 2.0 mm cortical locking screws (KLS Martin, Tuttlingen, Germany), therefore matching internal threads were integrated into the design.

Surgery

The cadaver heads were thawed several days before surgery. Implantation was performed according to regular pre-auricular and retro-mandibular approaches. The surgical guides were fixed to the skull and mandible using 2.0 mm surgical screws.

After drilling of the screw pilot holes through the guides, guides were removed and the prosthesis parts were positioned with a set of three centring pins before screw fixation, see Fig. 4A and B. This allowed for an exact alignment of these particular prosthesis parts to the pilot holes, therefore making sure the prosthesis is already in place before final screw fixating. Furthermore, alignment using centring pins provides the surgeon a visual check to see whether or not all pilot holes line up properly with the prosthesis

Fig. 4 | Per-operative images of the custom prosthesis placement. **A.** The mandibular and fossa guides are placed. **B.** The prosthesis (fossa part) is aligned using the centring pins (orange arrows). Note the glass marker sphere for post-operative analysis (yellow arrow). **C.** The fossa part is placed by screw fixation. **D.** Final result of prosthesis placement.

parts. After bilateral implantation the heads underwent a post-operative CT scan for analysis as presented in Fig. 4C and D.

Placement accuracy

On CT images titanium causes streak artefacts, thereby it can obstruct a reliable post-operative analysis. To enable accurate post-operative evaluation, all skull- and mandibular parts were supplied with three 2.0 mm spherical glass radiopaque markers, with an offset from the titanium main parts (see Fig. 4B, yellow arrow for an example).

The accuracy of implantation was evaluated after each cadaver test. This accuracy was derived by superimposing our final design file (STL format) onto the post-operative CT scan, using the glass tracer spheres as a reference. This placement was performed by 2 independent observers (JK, BM) in random order. The inter-observer variation is determined for all 20 prostheses parts (both fossa and mandibular). A post-operative segmentation was carried out and matching of the post-operative result to the pre-operative planning was performed. Skull and mandible, including the corresponding prosthesis part, were matched separately. Using a best fit alignment function in Geomagic Studio 2012 (3D Systems, Rock Hill, USA) based on an iterative closest point algorithm, both the planned and post-operative situations where matched.

The deviation between the planning and post-operative result was registered by centre point distances, the Euclidean distances based on the x, y, z coordinates of all glass tracer spheres. From these three values, a mean Euclidean error value and standard deviation for all fixed prosthesis parts was derived.

Data analysis was performed using IBM SPSS statistics version 23 (IBM corp., Armonk, NY, USA). Both the mean and standard deviation where calculated for the difference between the identified landmarks. The inter-observer variability was supported by the calculation of the intra class coefficient (ICC), in which the value of <0.40 is reported as poor, 0.4–0.59 fair, 0.60–0.74 good and 0.75–1.00 as excellent[20].

RESULTS

All planned prostheses were successfully implanted, resulting in the total series of 10 implanted prostheses (=20 fixed implanted prosthesis parts –i.e., fossa and mandibular). After matching with the post-operative CT data, a mean Euclidean error of 0.81 [mm] (SD 0.29, R: 0.49–1.60) was found. The mean difference on the fossa parts was 0.80 mm (SD 0.29) and for the mandibular parts was 0.82 mm (SD 0.31). The values for all implanted prosthesis parts are presented in Table 1.

The inter-observer variation was found to be 0.39 mm Euclidean distance, with an inter class correlation (two-way mixed) of 0.99. The mean deviation between the two observers was 0.23 mm, 0.17 mm and 0.16 mm in the x, y, z axis respectively.

The surgical approach used for the total joint insertion comprising a pre-auricular and retro-mandibular incision provided sufficient exposure, resulting in proper implantation of the prostheses using surgical guides, according to our pre-operative virtual plan. Fig. 4 presents a per-operative impression of the surgical procedure. After guide removal and positioning of to be fixed prosthesis parts using our centring pins, a clear visual check was acquired by the surgeon, as well as proper pre-fixation positioning of the prostheses. Fig. 4 shows this per-operative pre-fixation visual check.

Table 1 | Result of post-operative analysis.

Prosthesis	Mean Euclidean dist. [mm]	
	Fossa	Mandibular
I-L	1.42	0.64
I-R	0.69	0.84
II-L	0.49	0.69
II-R	1.17	1.04
III-L	0.68	0.70
III-R	0.63	1.60
IV-L	0.68	0.71
IV-R	0.77	0.89
V-L	0.91	0.62
V-R	0.60	0.49
Mean	**0.80**	**0.82**
SD	**0.29**	**0.31**
Total of n=20 prostheses		
Mean	**0.81**	
SD	**0.29**	

DISCUSSION

We developed and validated a customized TMJ prosthesis, based on the previous Groningen principles, of the stock prosthesis, in a humane cadaver series (N = 10 prostheses). The virtual planning was directly translated to the cadaver using a newly developed surgical custom made template. This template includes bony fixation, guidance for the condylectomy and pre drilling of the screw-holes. An exact translation of the planning was realised and confirmed by post-operative analysis based on CT imaging.

The Groningen TMJ prosthesis, as it was described in this manuscript, combines both a validated concept of the previous Groningen TMJ prosthesis and approved methods for 3D virtual planning and design. In addition the translation from virtual planning to the surgical procedure and post-operative analysis were derived from an oncologic reconstructive surgery workflow as was described by Schepers et al.[12].

The design of the Groningen TMJ prosthesis includes a lowered CR, which simulates the anatomical combination of both rotational- and translational movements of the condyle[6]. In comparison to other commercially available TMJ prostheses, this is a unique feature[2, 15, 21]. In order to realise the planned location of the lowered CR, accurate translation from planning towards surgical procedure is required. Therefore the proven methods for placement and drilling guides were used[12], supplemented with the described centring pins.

In this study we validated the guided placement of the Groningen TMJ prosthesis, resulting in a mean Euclidean distance deviation of 0.81 mm. Multiple studies have reported patient-related outcome measures, e.g. pain, mouth opening, however no detailed description of the placement accuracy was found[15, 22, 23]. The study of Haq et al., (2014) reported the use of patient specific cutting guides in order to place a custom TMJ prosthesis as treatment for ankylosis of the TMJ, in a single stage surgical procedure. The described concept of the cutting guides is comparable to the methods described in this manuscript, however the report from Haq et al.[24] did not state the use of guides for pre-drilling the fixation screw holes in the fossa part, nor positioning check with the use of centring pins. The accuracy of placement of the custom TMJ prostheses was not reported[24].

The use of customized TMJ prostheses has been reported to have advantages over stock prostheses. In previous studies, the fitting and placement by guides realised accurate fit to the bone and stability, which improves osseointegration and thereby the long-term success[2, 9]. Moreover, custom TMJ prostheses are less likely to exhibit micro movement when in situ and subject to forces of normal physiology. This is expected to contribute to an extended lifespan and reduced failure rate[24], and concluded to be a safe and predicable treatment[25].

This study presents a customised prosthesis that was optimised and validated in a human cadaver series. After this successfully completed pre-clinical phase and the recently obtained permission by the local medical ethics board, it can be applied in patients. At this stage however, no validation of clinical outcome in terms of improvement or consolidation of the opening of the mouth, decrease in reported pain of jaw function can be reported. Application of the custom Groningen TMJ prosthesis in a clinical series of patient will provide information with regard to these functional parameters and is currently approved by our medical ethical board.

Conclusion

This study presents an optimised design for the custom Groningen TMJ prosthesis. The workflow was validated in a series of 5 human cadavers, resulting in high accurate placement by using a routine surgical approach.

We conclude that the use of 3D virtual planning and custom production of the TMJ prosthesis enables accurate surgical placement, and thereby providing the first step in improvement of treatment options for patients suffering from restricted mouth opening or pain as a result of TMJ-related ankylosis.

Disclosures

The materials used in this study were unrestrictly sponsored by Xilloc Medical (Sittard-Geleen, The Netherlands) and KLS-Martin (Tüttlingen, Germany).

No financial support was received.

Acknowledgements

The authors thank Wim Tukker, CT-specialist from the radiology department of the University Medical Centre Groningen for his help with the scanning procedures. Furthermore the authors thank the department of Anatomic pathology in the UMCG for facilitating the cadaver-test setting.

REFERENCES

1. Sidebottom AJ. Current thinking in temporomandibular joint management. Br J Oral Maxillofac Surg. 2009 March 01;47(2):91-4.
2. Kanatas AN, Needs C, Smith AB, Moran A, Jenkins G, Worrall SF. Short-term outcomes using the Christensen patient-specific temporomandibular joint implant system: a prospective study. British Journal of Oral and Maxillofacial Surgery. 2012;50(2):149-53.
3. Schuurhuis JM, Dijkstra PU, Stegenga B, de Bont, Lambert G M, Spijkervet FKL. Groningen temporomandibular total joint prosthesis: An 8-year longitudinal follow-up on function and pain. Journal of Cranio-Maxillofacial Surgery. 2012;40(8):815-20.
4. Mercuri LG, Wolford LM, Sanders B, White RD, Hurder A, Henderson W. Custom CAD/CAM total temporomandibular joint reconstruction system: preliminary multicenter report. J Oral Maxillofac Surg. 1995 February 01;53(2):6.
5. Driemel O, Braun S, Muller-Richter UD, Behr M, Reichert TE, Kunkel M, et al. Historical development of alloplastic temporomandibular joint replacement after 1945 and state of the art. Int J Oral Maxillofac Surg. 2009 September 01;38(9):909-20.
6. van Loon JP, Falkenstrom CH, de Bont LG, Verkerke GJ, Stegenga B. The theoretical optimal center of rotation for a temporomandibular joint prosthesis: a three-dimensional kinematic study. J Dent Res. 1999 January 01;78(1):43-8.
7. Falkenström CH. Biomechanical design of a total temporomandibular joint replacement [dissertation]. University of Groningen; 1993.
8. van Loon JP, de Bont LG, Stegenga B, Spijkervet FK, Verkerke GJ. Groningen temporomandibular joint prosthesis. Development and first clinical application. Int J Oral Maxillofac Surg. 2002 February 1,;31(1):44-52.
9. Mercuri LG, Anspach WE. Principles for the revision of total alloplastic TMJ prostheses. Int J Oral Maxillofac Surg. 2003 August 01;32(4):353-9.
10. Mercuri LG, Giobbie-Hurder A. Long-term outcomes after total alloplastic temporomandibular joint reconstruction following exposure to failed materials. J Oral Maxillofac Surg. 2004 September 01;62(9):1088-96.
11. Kraeima J, Jansma J, Schepers RH. Splintless surgery: does patient-specific CAD-CAM osteosynthesis improve accuracy of Le Fort I osteotomy? Br J Oral Maxillofac Surg. 2016 December 01;54(10):1085-9.
12. Schepers RH, Raghoebar GM, Vissink A, Stenekes MW, Kraeima J, Roodenburg JL, et al. Accuracy of fibula reconstruction using patient-specific CAD/CAM reconstruction plates and dental implants: A new modality for functional reconstruction of mandibular defects. Journal of Cranio-Maxillofacial Surgery. 2015;43(5):649-57.
13. Roser SM, Ramachandra S, Blair H, Grist W, Carlson GW, Christensen AM, et al. The accuracy of virtual surgical planning in free fibula mandibular reconstruction: comparison of planned and final results. J Oral Maxillofac Surg. 2010 November 01;68(11):2824-32.
14. Bai G, He D, Yang C, Chen M, Yuan J, Wilson JJ. Application of Digital Templates to Guide Total Alloplastic Joint Replacement Surgery With Biomet Standard Replacement System. Journal of Oral and Maxillofacial Surgery. 2014;72(12):2440-52.
15. Aagaard E, Thygesen T. A prospective, single-centre study on patient outcomes following temporomandibular joint replacement using a custom-made Biomet TMJ prosthesis. International Journal of Oral and Maxillofacial Surgery. 2014;43(10):1229-35.

16. van Loon JP, Verkerke GJ, de Vries MP, de Bont LG. Design and wear testing of a temporomandibular joint prosthesis articulation. J Dent Res. 2000 February 01;79(2):715-21.
17. Van Loon JP, Verkerke GJ, de Bont LG, Liem RS. Wear-testing of a temporomandibular joint prosthesis: UHMWPE and PTFE against a metal ball, in water and in serum. Biomaterials. 1999 August 1,;20(16):1471-8.
18. Papakyriacou M, Mayer H, Pypen C, Plenk Jr H, Stanzl-Tschegg S. Effects of surface treatments on high cycle corrosion fatigue of metallic implant materials. International Journal of Fatigue. 2000;22(10):873-86.
19. Rafi HK, Karthik NV, Gong H, Starr TL, Stucker BE. Microstructures and Mechanical Properties of Ti6Al4V Parts Fabricated by Selective Laser Melting and Electron Beam Melting. Journal of Materials Engineering and Performance. 2013;22(12):3872-83.
20. Cicchetti DV. Guidelines, criteria, and rules of thumb for evaluating normed and standardized assessment instruments in psychology. Psychological Assessment. 1994 Dec;6 (4):284-90.
21. Mercuri LG. The role of custom-made prosthesis for temporomandibular joint replacement. Revista Española de Cirugía Oral y Maxilofacial. 2013;35(1):1-10.
22. Gonzalez-Perez LM, Fakih-Gomez N, Gonzalez-Perez-Somarriba B, Centeno G, Montes-Carmona JF. Two-year prospective study of outcomes following total temporomandibular joint replacement. International Journal of Oral and Maxillofacial Surgery. 2016;45(1):78-84.
23. Wolford LM, Rodrigues DB, McPhillips A. Management of the infected temporomandibular joint total joint prosthesis. J Oral Maxillofac Surg. 2010 November 01;68(11):2810-23.
24. Haq J, Patel N, Weimer K, Matthews NS. Single stage treatment of ankylosis of the temporomandibular joint using patient-specific total joint replacement and virtual surgical planning. British Journal of Oral and Maxillofacial Surgery. 2014;52(4):350-5.
25. Wolford L, Movahed R, Teschke M, Fimmers R, Havard D, Schneiderman E. Temporomandibular Joint Ankylosis Can Be Successfully Treated With TMJ Concepts Patient-Fitted Total Joint Prosthesis and Autogenous Fat Grafts. Journal of Oral and Maxillofacial Surgery. 2016;74(6):1215-27.

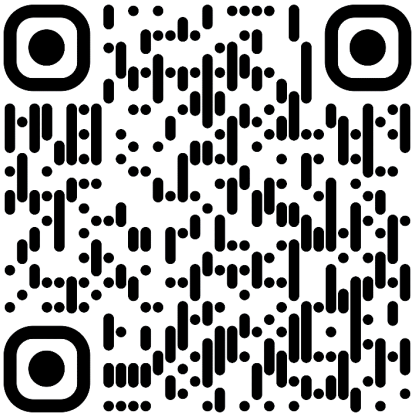

Supplementary video

Chapter 5

Accuracy of fit analysis of the patient-specific Groningen temporomandibular joint prosthesis

B.J. Merema, J. Kraeima, M.J.H. Witjes, N.B. van Bakelen, F.K.L. Spijkervet

Department of Oral and Maxillofacial Surgery, University Medical Center Groningen, University of Groningen, Groningen, The Netherlands

Published:
International Journal of Oral and Maxillofacial Surgery, 2021; 50(4): 538-545

ABSTRACT

Total joint replacement (TJR) with a prosthesis can be indicated for patients with severe temporomandibular joint (TMJ) dysfunction. Surgical accuracy is necessary for correct translation of the preoperatively predicted functional outcome, wear, and biomechanical behaviour of the patient-specific TMJ-TJR prosthesis. This study describes the first clinical applications of the patient-specific TMJ-TJR prosthesis according to the Groningen principles (G-TMJ-TJR), which was developed and validated in a prior human cadaver test study. The aim of this study was to validate the accuracy of placement of the patient-specific G-TMJ-TJR in the clinical setting. It was hypothesized that a virtual surgical plan (VSP) combined with guided placement of the patient-specific G-TMJ-TJR would be performed as predictably and accurately as in the prior cadaver series.

All patients who received a VSP-based patient-specific G-TMJ-TJR between December 2017 and March 2020 were included in this study. The accuracy analysis was based on postoperative cone beam computed tomography (CBCT) data.

All 11 prostheses could be inserted using routine pre-auricular and retromandibular surgical approaches. Analysis of the VSPs and postoperative CBCTs showed an average three-dimensional deviation of 1.07 mm (standard deviation 0.46 mm, range 0.33–1.91 mm) for all of the fossa and mandibular components.

The patient-specific G-TMJ-TJR can be applied predictably and accurately in a clinical setting.

INTRODUCTION

For patients with severe temporomandibular joint (TMJ) dysfunction, a total joint replacement (TJR) of the TMJ using a prosthesis may be considered. Reported indications are end-stage degenerative joint disease, recurrent ankylosis, and congenital disorders affecting the TMJ, if conservative treatment or regular open joint surgery do not suffice[1]. Moreover, condylar loss due to neoplasia or trauma, or the need for a revision of a failed alloplastic or autogenous reconstruction, are reported indications for TMJ-TJR[2]. Mandibular movement is impaired for most of these patients, due to anatomical changes or surgically caused scarification. This often results in pain, difficulties in speech, and impaired oral function.

Replacement of a TMJ with a total joint prosthesis can have a great impact on the biomechanical aspect of the contralateral joint and can affect the complex mandibular movements, which consist of both rotational and translational components[3, 4, 5]. Over the last few decades, a number of prostheses have been developed with the aim of reconstructing the TMJ and restoring its physiological movements, especially over the last 2 years[6]. Most of the currently available TMJ-TJRs are produced using computer-aided design and manufacturing (CAD/CAM) techniques, enabling virtual patient-specific modelling. Generally, designs are based on two commercially available prostheses[7, 8] consisting of both a skull and mandibular component, which are fixed separately to the glenoid fossa and mandibular ramus, respectively. These parts have the freedom to articulate relative to each other, enabling movement between a concave and convex body. The designs of these prostheses, however, do not seem to mimic the natural TMJ movement properly in all cases[5].

The value of patient-specific prostheses has been widely recognized and should increase treatment predictability and improve long-term success, due to the close fit of the prosthesis, which improves osseointegration[9, 10, 11]. Several CAD/CAM prostheses have been placed with the aid of surgical guides to translate the virtual surgical plan (VSP) to the operating theatre[12, 13, 14, 15,16]. However, data on the surgical accuracy of implementing TMJ-TJRs with surgical guides are scarce.

Between 1983 and 1999, a unique device – the Groningen TMJ-TJR (G-TMJ-TJR) – was developed at the University Medical Center Groningen (Groningen, The Netherlands). This prosthesis makes use of a lowered centre of rotation compared to

the anatomical situation, which is mathematically determined and mimics both the translational and rotational components of the healthy joint, without the need for actual translational movement[3, 4, 17, 18,19, 20]. As a result, both the loading and movement of the contralateral joint in the case of a unilateral prosthesis remain within the natural boundaries[3, 4, 17, 18,19, 20]. The G-TMJ-TJR has separate rotation and translation sites, allowing for free translation in both mediolateral and anteroposterior directions, an aspect necessary for proper mastication. Furthermore, this separation allows for improved bearing surfaces, unlike the conventional concave–convex designs with sliding point contacts instead of ball–socket principles with relatively large contact surfaces, and enables the optimization of both the rotation and translation articulations and low wear rates[3, 4, 17, 18,19, 20].

The first clinical application of the G-TMJ-TJR was in 1999 as a stock prosthesis, and an 8-year clinical follow-up study was conducted to assess the first series of patient applications[21]. This study showed an improvement in mouth opening and a reduced pain score, but the authors also mentioned that the stock device was difficult to position and fit to the damaged TMJ region that is often found in TMJ disorders, and concluded that a patient-specific prosthesis would be preferred.

After the patient-specific version of the G-TMJ-TJR was developed, it was validated with the corresponding digital workflow through a human cadaver test series. Due to its fit, it appeared to be a good successor to the stock prosthesis, with sub-millimetre accuracy[22]. The G-TMJ-TJR was subsequently available for use in patients and the first patient-specific clinical application occurred in December 2017. Since then, a series of 11 prostheses have been placed and are now available for analysis.

The aim of this study was to validate the accuracy of placement of the patient-specific G-TMJ-TJR in the clinical setting. It was hypothesized that a VSP combined with guided placement of the patient-specific G-TMJ-TJR would be performed predictably and accurately, in a similar way to the previous cadaver series results.

MATERIALS AND METHODS

G-TMJ-TJR prosthesis

All of the patients in need of a TMJ-TJR underwent a computed tomography (CT) scan preoperatively (bone kernel, 0.6-mm slice interval), with the mouth closed and in maximum occlusion; this was used for the VSP and prosthesis design. The design was conducted in-house and the screw positions were based on local cortical thickness and the position of the mandibular nerve. The chosen lowered point of rotation and screw positions were paramount in the prosthesis design process. The G-TMJ-TJR, manufactured and assembled by Xilloc Medical (Geleen, The Netherlands), consists of a patient-specific grade 23 titanium fossa component, which is fixed to the glenoid fossa with 2-mm locking screws (Medicon, Tuttlingen, Germany), a patient-specific grade 23 titanium mandibular component, which is fixed bicortically to the mandibular ramus with 2-mm locking screws (Medicon, Tuttlingen, Germany), and an ultra-high-molecular-weight polyethylene (UHMWPE) neo-disc that is placed in between the other two components. Zirconia to UHMWPE bearing couples are realized by connecting a zirconia translation plate and sphere, adhesive-free through press-fitting,

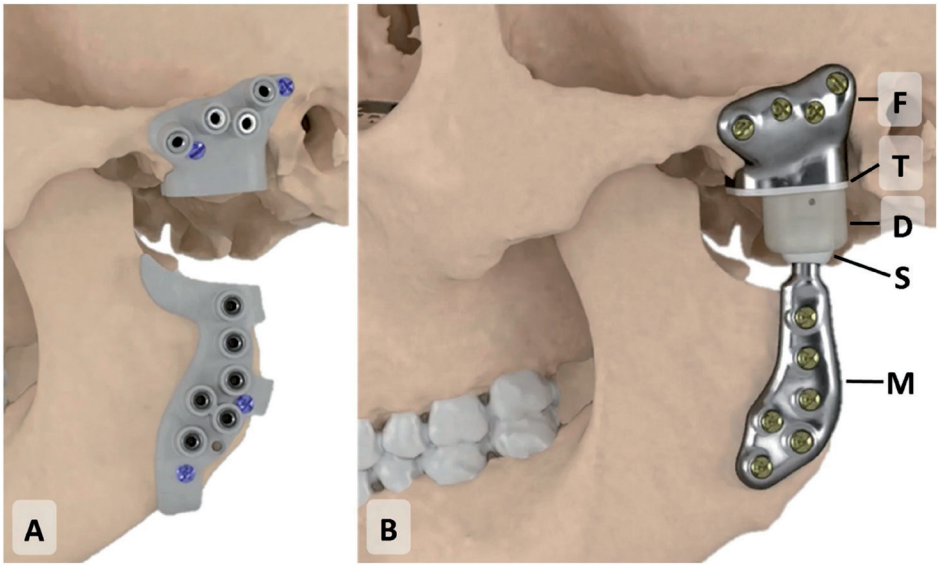

Fig. 1 | Rendering of the Groningen temporomandibular joint prosthesis, illustrating the use of fixed surgical guides for drilling and cutting (**A**). The guides are fixed using compression screws (blue) and are provided with stainless steel drill sleeves. The planned condylectomy is indicated by the cranial edge of the mandibular guide. (**B**) All the separate prosthesis components are labelled: **F**: titanium fossa component; **T**: zirconia translation plate; **D**: UHMWPE neo-disc; **S**: zirconia condylar sphere; **M**: titanium mandibular component.

to the fossa and mandibular components, respectively, during fabrication (Fig. 1)[22]. The neo-disc is locked on the zirconia sphere at the mandibular component using a snap connection and can freely translate along the translation plate of the skull component. All of the fixed parts are placed using patient-specific medical-grade polyamide surgical guides, which are fixed to the bone using 2-mm screws. The surgical guides are used to both drill all the pilot screw holes and to perform the planned condylectomy at the condylar neck level[22].

Patients

All of the patients who received a patient-specific G-TMJ-TJR prosthesis between December 2017 and March 2020 were included in this study.

Surgical procedure

A single-stage implantation is indicated when the patient's fossa and condyle are clearly separated at the bone level on the CT. When this is not the case, or the patient already has a prosthesis or other object in situ that does not allow reliable scanning of the bony recipient area, a two-stage surgical procedure is necessary. In such cases, the fossa is freed up or the obstructing object is removed in the first surgery. A CT scan for VSP and prosthesis design is then conducted following the first surgery.

Implantation was performed according to routine pre-auricular and retromandibular approaches. During surgery, intermaxillary fixation was applied to the preoperatively inserted surgical tooth brackets with elastics. The surgical guides were inserted and fixed independently to the mandible or skull using 2.0-mm surgical screws prior to drilling the pilot screw holes and performing the condylectomy. Multiple fixation screws were planned as a backup in case of poor grip. Subsequently, the guides were removed and the pre-assembled titanium–zirconia fossa and mandibular components were aligned to the pre-drilled pilot screw holes. The prosthesis was aligned with the pre-drilled pilot screw holes, and stainless steel (316 L) centring pins were inserted (Xilloc Medical, Geleen, The Netherlands) through the screw holes in the prosthesis into the drilled pilot screw holes. Since the planned screw paths are not parallel, the centring pins only fit in one manner, resulting in a tight fit of the prosthesis to the bone. Next, the pins were replaced one by one with 2.0-mm locking screws (Medicon, Tuttlingen, Germany) and the UHMWPE neo-disc was snapped into place over the neo-condyle with a distinct popping sound, indicating a good retention of the disc (supplementary video).

Analysis of accuracy

All of the study patients underwent a routine postoperative cone beam computed tomography scan (CBCT) within 16 days after surgery, which was used to evaluate the accuracy of the prosthesis placement. The computer-aided design (CAD) files in STL format of the patient-specific titanium components were superimposed onto the

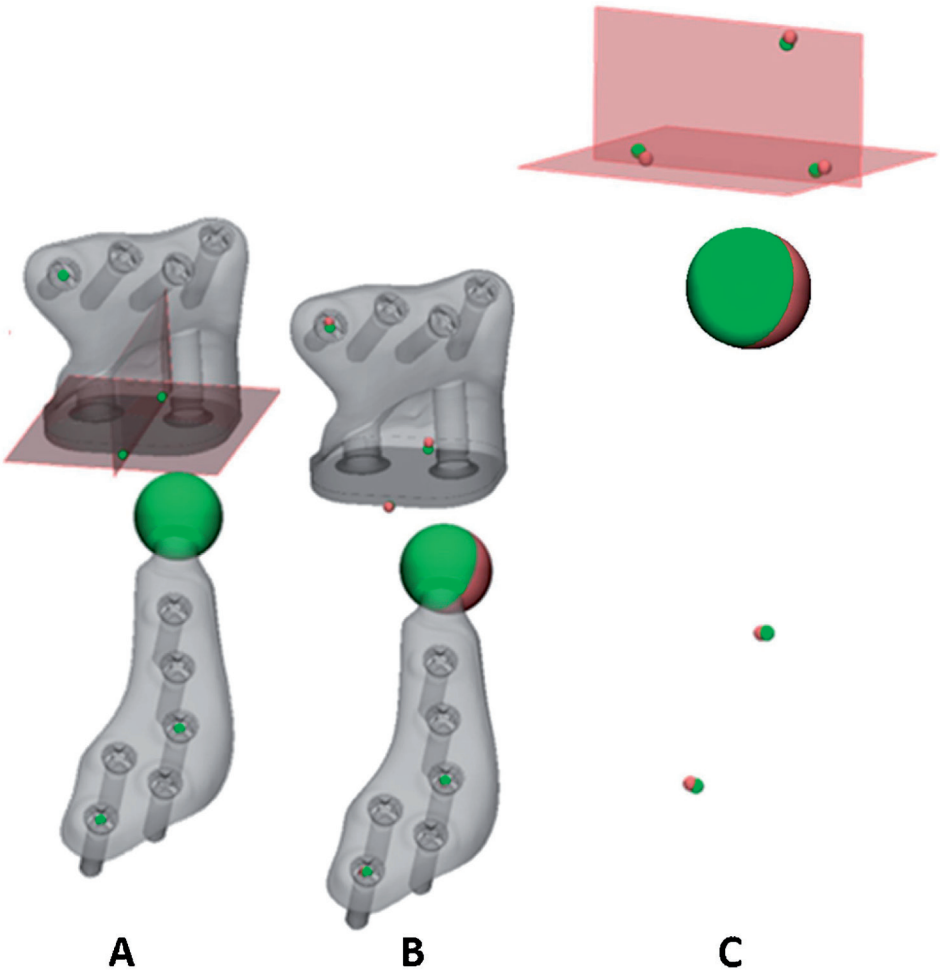

Fig. 2 | The exact same design files were used to select both the planned and postoperative marker positions. Superimposing the design files enables a coordinate comparison. The midpoints of both the medial and lateral edges of the translation plate for the skull component were selected, as was the centre of the most ventral screw head recess. The midpoint of the sphere/neo-condyle was chosen for the mandibular component, together with the centre points of the screw head recesses in the most ventral screw and the third cranial screw along the posterior border (A). The planned marker positions in green and the postoperative superimposed marker positions in red were used for postoperative analysis (B). A clearer view of the marker deviation is visible when the planned prosthesis is hidden (C).

postoperative CT data, and a comparison was made with the planned positions. This alignment was performed by two observers independently (BM, JK) using ProPlan CMF 3.0 software (Materialise, Leuven, Belgium); the inter-observer variation was determined for all fossa and mandibular components separately. The skull and mandible were segmented postoperatively and matched individually to the preoperative segmentations, whilst moving along the matched CAD files. Matching was conducted in the 3-Matic 11.0 software (Materialise, Leuven, Belgium) using a surface-based alignment function.

In order to assess the deviation between the planned and postoperative prosthesis positions, three landmarks were assigned to both the fossa and mandible parts. To analyse the fossa part, two coordinates were chosen on the lateral and medial sides of the translation plate, in the exact middle of its length (anteroposterior direction). A third coordinate was assigned to the recess of the most anterior screw head, which is meant to receive the centre of a screwdriver. The landmarks used for the mandibular parts were assigned to the centre of the neo-condyle and recesses in the screw heads of the most anterior screw and the most caudal screw along the posterior border of the mandible (Fig. 2). Since all of the translation plate, neo-condyle, and screw CAD files are exactly the same, the landmarks are reproducible and can be assigned objectively. The deviation of each landmark couple was measured as a Euclidean or three-dimensional (3D) distance, and the mean Euclidean error and standard deviation (SD) were calculated for three landmark deviations per prosthesis.

Statistical analysis

Calculation of the inter-observer variability was performed in IBM SPSS Statistics version 23 (IBM Corp., Armonk, NY, USA). The inter-observer variability was determined by calculating the inter-class correlation coefficient (ICC), whereby a reported value of <0.40 is poor, 0.40–0.59 is fair, 0.60–0.74 is good, and 0.75–1.00 is excellent[23].

Approval for this study was obtained from the Medical Ethics Board of the University Medical Center Groningen (METc 2016/568).

RESULTS

Over the duration of this study, a total of 11 prostheses were placed in 10 female patients who required either a primary (n = 8) or secondary (n = 2) TMJ-TJR. The patients in the primary TMJ-TJR group suffered from recurring ankylosis, which had resulted in poor mouth opening, pain, and impaired speech and chewing abilities. The two patients who needed a secondary TJR had received stock G-TMJ-TJR prostheses during the 1999–2000 period but still had pain complaints, which were assumed

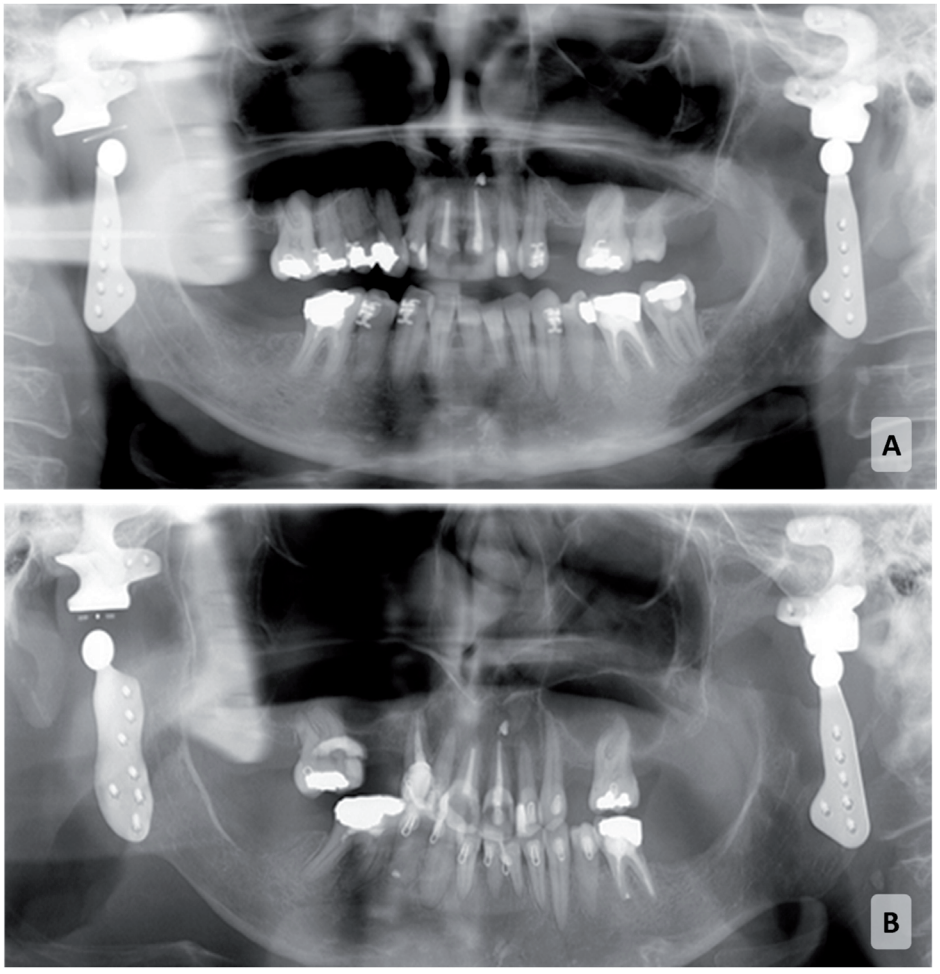

Fig. 3 | Panoramic radiographs obtained (A) pre-revision and (B) post-revision of the right-side TMJ-TJR in patient 1. Due to prior suboptimal positioning of the mandibular component, the stock G-TMJ-TJR was not satisfactory. This indicates the difficulty that can present with stock prostheses and/or without the use of surgical guides.

to be related to a suboptimal fit. One of the secondary TJR patients only required a mandibular component restoration to correct a suboptimally positioned stock mandibular component (Fig. 3). Accordingly, a VSP was designed that incorporated the new mandibular component – including a new zirconia neo-condyle – that matched the original 15-year-old stock fossa component.

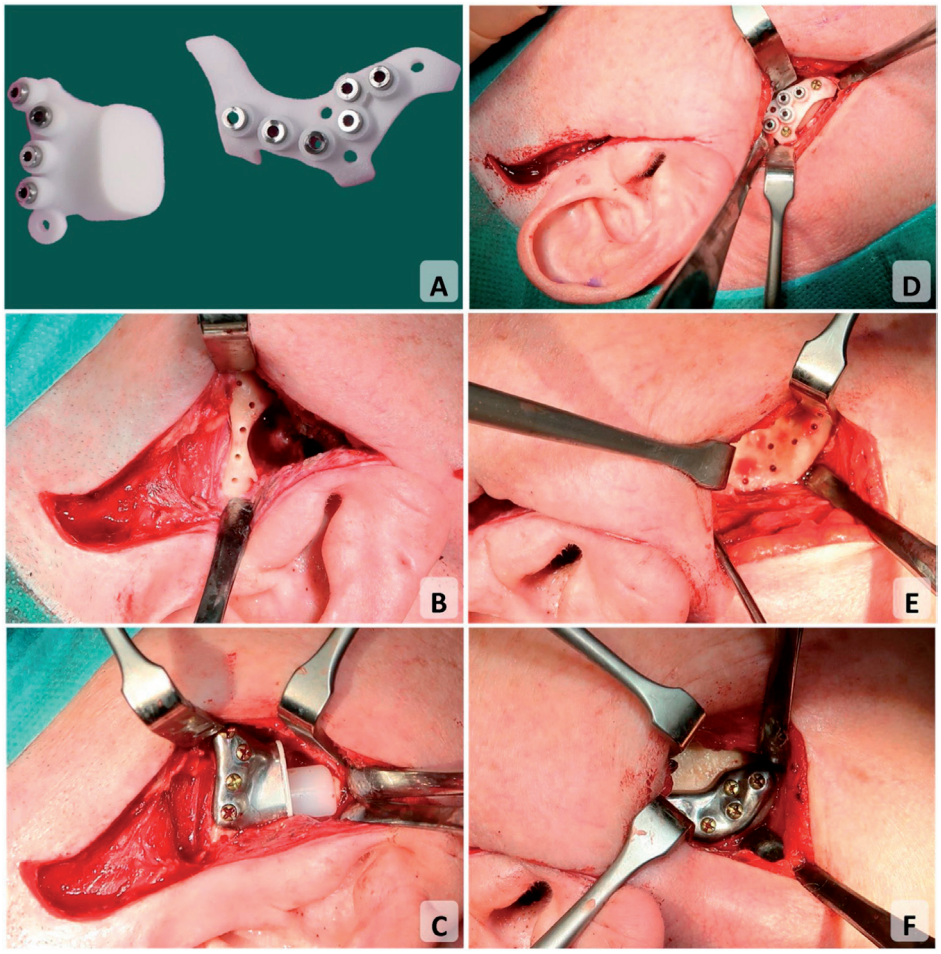

Fig. 4 | Intraoperative pictures showing the use of the surgical guides. (**A**) The separate fossa and mandibular guides are designed and assembled with drill sleeves. (**B**) The pilot screw holes drilled under guidance seen after fossa guide removal. (**C**) The fossa component with the TJR in place. (**D**) The mandibular resection and drilling guide in place; note the two fixation screws applied to ensure the correct drill pattern. (**E**) The pilot screw holes drilled under guidance seen after mandibular guide removal. (**F**) The mandibular component in place.

The surgical procedures were uneventful and all prostheses could be inserted according to the VSP using the routine pre-auricular and retromandibular surgical approaches. This resulted in a total of 21 separate components (10 fossa and 11 mandibular) placed under guidance that were available for analysis. Figure 4 shows the intraoperative use of the surgical guides for patient 2.

The analysis of accuracy showed a mean Euclidean deviation of 1.10 mm (SD 0.55 mm, range 0.33–1.91 mm) for the fossa component and of 1.05 mm (SD 0.38 mm, range 0.45–1.60 mm) for the mandibular component. When combined, an overall mean Euclidean deviation of 1.07 mm (SD 0.46 mm) was calculated for all of the 21 separately placed components. Table 1 describes the deviation of all of the separate components. The inter-observer variation was a mean Euclidean distance of 0.20 mm with an ICC (two-way mixed) of 0.93, indicating an excellent matching of the measurements made by the two observers.

Table 1 | Overview of the patients included in this study. The mean deviation for each separate prosthesis component placed under guidance is presented for all of the patients.

Patient	Age	Sex	Indication	Lat.	FP	MP
1	56	F	Revision of stock prosthesis	R	NA*	0,87
2	51	F	Ankylosis	L	0,70	0,45
3	53	F	Bilateral ankylosis	L	1,64	1,05
4	55	F	Ankylosis	R	1,91	1,55
5	72	F	Condylar neck fracture malunion	R	1,64	1,52
6	68	F	Ankylosis	L	1,57	0,94
7	52	F	Ankylosis	R	0,33	1,60
8	59	F	Revision of stock prosthesis	L	0,84	1,04
9	68	F	Ankylosis	L	0,83	0,63
10	56	F	Ankylosis	R	0,52	0,76
Mean	**59**				**1,10**	**1,05**
sd					0,55	0,38
Range					0.33-1.91	0.45-1.60

F, female; R, right; L, Left; NA, not applicable; SD, standard deviation.

[a] Patient1 only received a mandibular component.

DISCUSSION

In this first prospective series of clinical applications of the patient-specific G-TMJ-TJR, all prostheses were placed successfully with high predictability and good initial stability. Postoperative analysis showed highly accurate positioning of the G-TMJ-TJR prostheses using fixed surgical guides as a tool to translate the VSP to the intraoperative setting.

Only two prior studies have analysed the deviation between the VSP and the postoperative positions in guided placement of patient-specific TMJ prostheses[22, 24]. The first publication on this subject was a study performed by the present authors, in which the patient-specific G-TMJ-TJR was validated in a series of human cadavers[22]. An overall mean 3D deviation of 0.81 mm (SD 0.29 mm) was observed in the cadaver series, compared to 1.07 mm (SD 0.46 mm) in the current study. The difference, even though marginal, could be related to the fact that the positions of the three landmarks for each prosthesis component were adapted in the patients and placed in the extremities of the prostheses, where the deviations were expected to be greatest. This was necessary because the glass tracer spheres that were used in the cadaver series could not be used in patients.

The second publication on this subject was by Sembronio et al.[24]. They placed a patient-specific VSP-based prosthesis using surgical guides. Since the VSP, guides, and prostheses had similarities in their setup and function, the results of the deviation analysis were expected to be comparable. However, it appears that they only used a surgical guide to position the mandibular component and it is not clear to us whether they fixed their surgical guides to the bone prior to drilling. A mean value of the absolute deviations was not mentioned, but a scatter plot was presented instead. Based on the information provided in their paper, an approximate range of 0.0 to 2.6 mm and a standard deviation of approximately 0.8 mm could only be guessed for their two-dimensional measurements. Their results, however, are not directly comparable to the measurements presented in our previous study or the present study. The authors presented their measured deviation on the midsagittal plane. Therefore, only two out of three deviation directions were taken into account, meaning the actual 3D deviation would have been greater than that described in their paper, unless the third direction was 0 mm for all of the measured points. Moreover, the measurements were

performed by only one observer. Therefore, it remains unclear how user-dependent their measurements were.

The surgical accuracy of patient-specific TMJ-TJRs is required for a correct translation of the preoperatively predicted functional outcome, wear, and biomechanical behaviour. Discrepancies between the planned and postoperative position of a TMJ-TJR prosthesis can affect the above and the proposed function of the device[4], and cause malocclusions[25], resulting in unforeseen and increased loading conditions, especially when the device does not make use of a spherically shaped contact set at both the neo-condyle and fossa level[7, 14, 26.] Malpositioning a non-spherical fossa–condyle contact can initiate point contacts where two non-matching shapes meet and potentially could affect condylar seating in the contralateral joint (Fig. 5). The occurring material stress in such point contacts can exceed the theoretically assessed values and, in turn, drastically increase UHMWPE wear[27]. The flat sliding contact of the G-TMJ-TJR neo-disc, one of the Groningen principles, ensures a constant load-bearing surface to avoid such point contacts and maintain a relatively large surface area to reduce wear[17]. Studying the surgical accuracy provides valuable information regarding accurate boundary conditions and worst-case scenarios and can be used for biomechanical calculations. When a prosthesis is accurately positioned according to the VSP, predicting the in situ loading becomes more accurate as well.

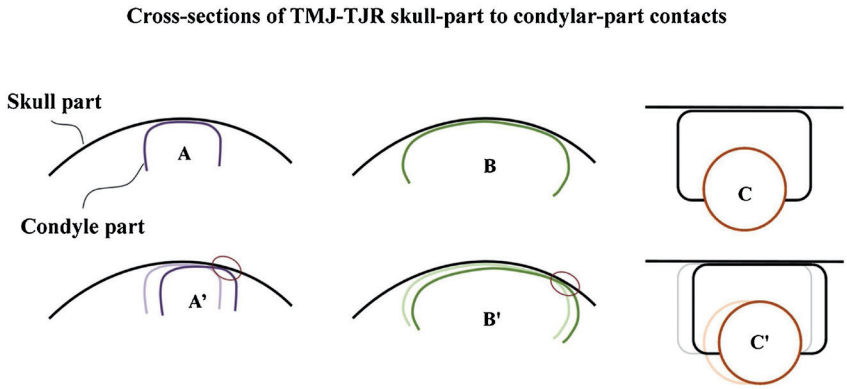

Fig. 5 | Schematic examples of two prostheses with a non-spherical/non-matching contact set (A and B) at the neo-condyle to fossa component articulation site and the G-TMJ-TJR (C) with a spherical/matching contact set. The cross-sectional views illustrate the effect of a marginal shift of the neo-condylar position (A′, B′ and C′) relative to the neo-fossa, which results in a point contact (circle) in A′ and B′, and increasing material stress. Note the shifting has no influence on the contact in situation C′.

The important factors for an accurate execution of a VSP using surgical guides are comprehensive preparation and denudation of the bone surfaces in contact with the guides and the fixation of the surgical guides to the bone using screws. The latter is necessary to ensure that planned inter-screw relationships are maintained during pilot screw hole drilling, which is especially important when using locking screws. In the absence of surgical guides, the final prosthesis could be used as a template to drill through. However, not having any protective drill sleeves can result in damage to the prosthesis, thereby leaving metal particles in the surrounding tissues and off-centred screws.

Knowing the surgical accuracy of the G-TMJ-TJR procedure enables the worst-case positioning scenario to be taken into account. In such a case, the pressure of the mandibular component, through the neo-disc to the translation plate of the skull component, would be insufficient due to a lack of contact. With this in mind, over-sized backup neo-discs are available during all implantations. In the case of different TMJ-TJR devices, the accuracy measured in the present study could also result in non-contact between the skull and condylar component during occlusion or chewing. Such a gap would be more complex, if not impossible, to correct. This also applies to stock TMJ-TJR devices where no VSP, surgical guides, or specific fit to the bone are incorporated in the surgical procedure.

Several authors have reported the shortcomings of stock TMJ-TJRs. According to Mercuri, slightly misplaced TMJ-TJR devices require a posterior stop at the fossa component to prevent the condyle from displacing posteriorly[28]. Therefore, when a patient-specific device can be positioned accurately using, e.g. surgical guides, a posterior stop is no longer required, saving space towards the auditory canal and resulting in a less bulky device. The bony anatomy of patients who require a TMJ-TJR is often damaged, which makes fitting a stock TMJ-TJR complex and generally requires bone alterations. Using a patient-specific device will reduce intraoperative bone loss, since a patient-specific fit can be obtained by removing less or no bone[29], whilst providing a stable fixation. This was described by Wolford et al. as improving long-term outcomes[30]. Due to the aforementioned, the authors consider that the use of patient-specific TMJ-TJR devices combined with surgical guides based on a VSP should be preferred at all times.

This study is novel in validating the true 3D accuracy of placing TMJ-TJR prostheses in a clinical cohort, with consistently good results. Currently, only 11 G-TMJ-TJRs have been placed in 10 patients and the clinical results appear promising. Both pain scores and maximum mouth opening improved when compared to preoperative measurements. However, it is still too early to draw conclusions about the clinical and functional outcomes due to the relatively short follow-up period of a maximum 2 years. It is hypothesized that the accuracy of patient-specific TMJ-TJRs, as described in this study, will play a key role in improved function when compared to stock G-TMJ-TJRs[21], due to the highly predictable positioning protocol. The clinical results will be investigated in terms of functional outcomes and pain scores in a future study.

The results of this study indicate that patient-specific Groningen TMJ-TJR prostheses can be applied accurately and predictably in both one-stage and two-stage surgical procedures. The workflow involving a VSP, a patient-specific TMJ-TJR, and guided surgery, as described in our prior cadaver series, was proven to be applicable and comparably accurate in patients.

Funding
No funding was received.

Competing interests
None to declare.

Ethical approval
Approval for this study was obtained from the Medical Ethics Board of the University Medical Center Groningen (METc 2016/568).

Patient consent
All patients provided their written consent.

REFERENCES

1. Sidebottom, A. J. Current thinking in temporomandibular joint management. *Br. J. Oral Maxillofac. Surg.* **47**, 91-94 (2009).
2. Johnson, N. R., Roberts, M. J., Doi, S. A. & Batstone, M. D. Total temporomandibular joint replacement prostheses: a systematic review and bias-adjusted meta-analysis. *Int. J. Oral Maxillofac. Surg.* **46**, 86-92 (2017).
3. van Loon, J. P., Otten, E., Falkenstrom, C. H., de Bont, L. G. & Verkerke, G. J. Loading of a unilateral temporomandibular joint prosthesis: a three-dimensional mathematical study. *J. Dent. Res.* **77**, 1939-1947 (1998).
4. van Loon, J. P., Falkenstrom, C. H., de Bont, L. G., Verkerke, G. J. & Stegenga, B. The theoretical optimal center of rotation for a temporomandibular joint prosthesis: a three-dimensional kinematic study. *J. Dent. Res.* **78**, 43-48 (1999).
5. Wojczyńska, A. *et al*. Alloplastic total temporomandibular joint replacements: do they perform like natural joints? Prospective cohort study with a historical control. *International Journal of Oral & Maxillofacial Surgery* **45**, 1213-1221 (2016).
6. Elledge, R., Mercuri, L. G., Attard, A., Green, J. & Speculand, B. Review of emerging temporomandibular joint total joint replacement systems. *Br. J. Oral Maxillofac. Surg.* **57**, 722-728 (2019).
7. Westermark, A. Total reconstruction of the temporomandibular joint. Up to 8 years of follow-up of patients treated with Biomet((R)) total joint prostheses. *Int. J. Oral Maxillofac. Surg.* **39**, 951-955 (2010).
8. Wolford, L. M., Mercuri, L. G., Schneiderman, E. D., Movahed, R. & Allen, W. Twenty-year follow-up study on a patient-fitted temporomandibular joint prosthesis: the Techmedica/TMJ Concepts device. *J. Oral Maxillofac. Surg.* **73**, 952-960 (2015).
9. Mercuri, L. G. & Anspach, W. E. Principles for the revision of total alloplastic TMJ prostheses. *Int. J. Oral Maxillofac. Surg.* **32**, 353-359 (2003).
10. Kanatas, A. N. *et al*. Short-term outcomes using the Christensen patient-specific temporomandibular joint implant system: a prospective study. *Br. J. Oral Maxillofac. Surg.* **50**, 149-153 (2012).
11. Wolford, L. *et al*. Temporomandibular Joint Ankylosis Can Be Successfully Treated With TMJ Concepts Patient-Fitted Total Joint Prosthesis and Autogenous Fat Grafts. *J. Oral Maxillofac. Surg.* **74**, 1215-1227 (2016).
12. Hu, Y. *et al*. Simultaneous treatment of temporomandibular joint ankylosis with severe mandibular deficiency by standard TMJ prosthesis. *Sci. Rep.* **7**, 45271 (2017).
13. Gerbino, G., Zavattero, E., Berrone, S. & Ramieri, G. One stage treatment of temporomandibular joint complete bony ankylosis using total joint replacement. *J. Craniomaxillofac. Surg.* **44**, 487-492 (2016).
14. Zheng, J. *et al*. An innovative total temporomandibular joint prosthesis with customized design and 3D printing additive fabrication: a prospective clinical study. *Journal of translational medicine* **17**, 4 (2019).
15. Bai, G. *et al*. Application of digital templates to guide total alloplastic joint replacement surgery with biomet standard replacement system. *J. Oral Maxillofac. Surg.* **72**, 2440-2452 (2014).
16. Ortho Baltic Implants. Available from URL: http://balticimplants.eu/patient-specific-medical-devices/tmj-endoprosthesis/(last accessed 6 April 2020).

17. van Loon, J. P., Verkerke, G. J., de Vries, M. P. & de Bont, L. G. Design and wear testing of a temporomandibular joint prosthesis articulation. *J. Dent. Res.* **79**, 715-721 (2000).
18. van Loon, J. P., de Bont, L. G., Spijkervet, F. K., Verkerke, G. J. & Liem, R. S. A short-term study in sheep with the Groningen temporomandibular joint prosthesis. *Int. J. Oral Maxillofac. Surg.* **29**, 315-324 (2000).
19. van Loon, J. P., de Bont, L. G., Stegenga, B., Spijkervet, F. K. & Verkerke, G. J. Groningen temporomandibular joint prosthesis. Development and first clinical application. *Int. J. Oral Maxillofac. Surg.* **31**, 44-52 (2002).
20. Falkenström, C. H. Biomechanical design of a total temporomandibular joint replacement. (1993).
21. Schuurhuis, J. M., Dijkstra, P. U., Stegenga, B., de Bont, L. G. & Spijkervet, F. K. Groningen temporomandibular total joint prosthesis: an 8-year longitudinal follow-up on function and pain. *J. Craniomaxillofac. Surg.* **40**, 815-820 (2012).
22. Kraeima, J., Merema, B. J., Witjes, M. J. H. & Spijkervet, F. K. L. Development of a patient-specific temporomandibular joint prosthesis according to the Groningen principle through a cadaver test series. *J. Craniomaxillofac. Surg.* **46**, 779-784 (2018).
23. Cicchetti, D. in *Guidelines, Criteria, and Rules of Thumb for Evaluating Normed and Standardized Assessment Instrument in Psychology* 284-290, 1994).
24. Sembronio, S., Tel, A., Costa, F., Isola, M. & Robiony, M. Accuracy of custom-fitted temporomandibular joint alloplastic reconstruction and virtual surgical planning. *Int. J. Oral Maxillofac. Surg.* **48**, 1077-1083 (2019).
25. Gerbino, G., Zavattero, E., Bosco, G., Berrone, S. & Ramieri, G. Temporomandibular joint reconstruction with stock and custom-made devices: Indications and results of a 14-year experience. *J. Craniomaxillofac. Surg.* **45**, 1710-1715 (2017).
26. Ackland, D. C., Moskaljuk, A., Hart, C., Vee Sin Lee, P. & Dimitroulis, G. Prosthesis loading after temporomandibular joint replacement surgery: a musculoskeletal modeling study. *J. Biomech. Eng.* **137**, 041001 (2015).
27. van Loon, J. P., de Bont, G. M. & Boering, G. Evaluation of temporomandibular joint prostheses: review of the literature from 1946 to 1994 and implications for future prosthesis designs. *J. Oral Maxillofac. Surg.* **53**, 984-7 (1995).
28. Mercuri, L. G. Alloplastic temporomandibular joint replacement: rationale for the use of custom devices. *Int. J. Oral Maxillofac. Surg.* **41**, 1033-1040 (2012).
29. Zhao, J., Zou, L., He, D. & Ellis, E. Comparison of bone adaptation after modification in biomet standard alloplastic temporomandibular joint prostheses. *J. Craniomaxillofac. Surg.* **46**, 1707-1711 (2018).
30. Wolford, L. M., Dingwerth, D. J., Talwar, R. M. & Pitta, M. C. Comparison of 2 temporomandibular joint total joint prosthesis systems. *J. Oral Maxillofac. Surg.* **61**, 685-90; discussion 690 (2003).

Chapter 6

Four-dimensional determination of the patient-specific centre of rotation for total temporomandibular joint replacements: *Following the Groningen principle*

Bram B. J. Merema, Max J. H. Witjes, Nicolaas B. Van Bakelen, Joep Kraeima and Frederik K. L. Spijkervet

Department of Oral and Maxillofacial Surgery, University Medical Center Groningen, University of Groningen, Hanzeplein 1, P.O. Box 30.001, 9700 RB Groningen, The Netherlands

Published:
Journal of Personalized Medicine, 2022; 12(9): 1439

ABSTRACT

For patients who suffer from severe dysfunction of the temporomandibular joint (TMJ), a total joint replacement (TJR) in the form of a prosthesis may be indicated. The position of the centre of rotation in TJRs is crucial for good postoperative oral function; however, it is not determined patient-specifically (PS) in any current TMJ-TJR. The aim of this current study was to develop a 4D-workflow to ascertain the PS mean axis of rotation, or fixed hinge, that mimics the patient's specific physiological mouth opening.

Twenty healthy adult patients were asked to volunteer for a 4D-scanning procedure. From these 4D-scanning recordings of mouth opening exercises, patient-specific centres of rotation and axes of rotation were determined using our JawAnalyser tool.

The mean CR location was positioned 28 [mm] inferiorly and 5.5 [mm] posteriorly to the centre of condyle (CoC). The 95% confidence interval ranged from 22.9 to 33.7 [mm] inferior and 3.1 to 7.8 [mm] posterior to the CoC.

This study succeeded in developing an accurate 4D-workflow to determine a PS mean axis of rotation that mimics the patient's specific physiological mouth opening. Furthermore, a change in concept is necessary for all commercially available TMJ-TJR prostheses in order to comply with the PS CRs calculated by our study. In the meantime, it seems wise to stick to placing the CR 15 [mm] inferiorly to the CoC, or even beyond, towards 28 [mm] if the patient's anatomy allows this.

INTRODUCTION

A total joint replacement (TJR) of the temporomandibular joint (TMJ) in the form of a prosthesis may be indicated for patients who suffer from severe TMJ dysfunction. Documented indications include end-stage degenerative joint disease, recurrent ankylosis, and congenital disorders affecting the TMJ when joint saving approaches do not suffice [1]. Other indications for TJRs are condylar loss as a result of trauma or neoplasia in or near the joint or to replace a failed alloplastic or autogenous reconstruction [2]. In most of these patients, mandibular movement is impaired due to either anatomical changes or surgically caused scarification, often resulting in pain, difficulties in speech, impaired oral function, and limited maximum mouth opening.

When replacing the TMJ with a TMJ-TJR prosthesis, the condyle or its remnants together with the articular disc are removed in order to fit the prosthesis. This results in the removal of the insertion of the main muscle responsible for anterior movement of the condyle, the lateral pterygoid muscle, from its insertions at the mandibular condyle and articular disc. Removal of this muscle's insertion site in order to place a TMJ-TJR is reported to decrease the amount of anterior movement of the TMJ from approximately 16 [mm] to only 2 [mm] [3] or less, thereby reducing the joint's movements to near mere rotations [4]. The consequences of placing a TMJ-TJR unilaterally are a lack of anterior movement leading to asymmetrical mouth opening movements, where the mandible deviates towards the affected side, marginal laterotrusion towards the unaffected side [5], and unnatural loading of the contralateral joint [6].

To overcome this effect, the Groningen TMJ-TJR prosthesis was developed [7,8,9]. Apart from its unique feature that allows for free translational movement of the neo-disc, the prosthesis applies a lowered centre of rotation (CR) in relation to the anatomical condylar centre [8]. Prior research suggested that a lowering of 15 [mm] in relation to the condyle would be optimal as a fixed CR for unilateral TMJ prostheses [3]. This study was, however, based on 2D optical movement tracking with no direct relation to the bony anatomy and thus the condyles of the mandible [10]. The Groningen TMJ-TJR prosthesis has been available as a patient-specific (PS) device since 2017, opening doors to also personalise the position of the CR [8]. Figure 1 illustrates the effect of a lowered centre of rotation with the Groningen TMJ-TJR prosthesis.

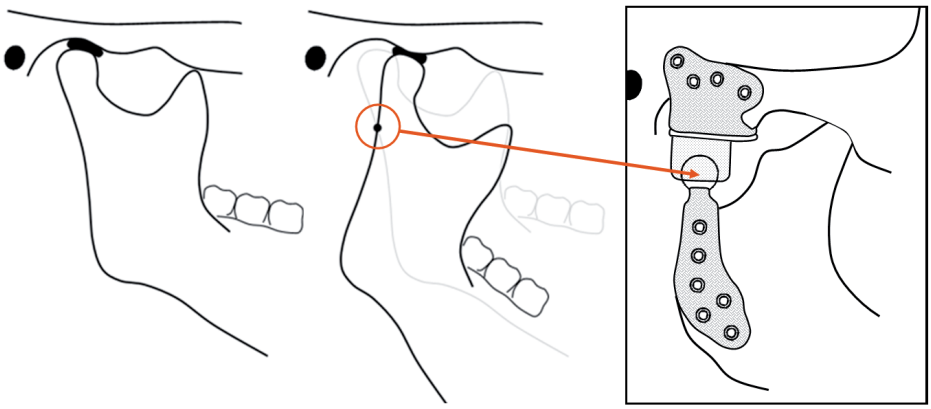

Figure 1 | This sketch shows the effect of considering a fixed centre of rotation which is positioned inferior to the centre of the condyle. This lowered centre of rotation mimics the natural translational movement of the condyle whilst merely rotating. The left sketch shows the occlusal mandibular position. Middle shows both the occlusal and maximum opened position of the mandible which is obtained by pure rotation around the dot. The right picture shows the implementation of this effect in the Groningen TMJ-TJR prosthesis, according to the *Groningen Principle*.

Physiological mandibular movement is complex and, as per definition, not truly translatable to a mere rotation around a single axis. However, as mentioned, the movement of a TMJ reconstructed by means of a TMJ-TJR prosthesis should predominantly show rotational movement [4]. Since any translational movement cannot be expected to occur in the reconstructed TMJ due to a lack in lateral pterygoid muscle function, we chose to analyse a fixed centre of rotation, even though the Groningen TMJ-TJR allows for some free translation of the neo-disc [8].

When considering a fixed CR of the mandible, placing it more inferiorly should result in increased anterior movement of the associated condyle during mouth opening. Moreover, shifting the CR in a posterior direction should enable relatively more rotation in the coronal plane and, thus, in a more inferior excursion of the condyle [3] (Figure 1).

Several prior authors have succeeded in analysing the movement of subjects' mandibles by means of tracking them in 2D (sagittal) or 3D [11,12,13,14,15,16,17,18]. Generally, incisal and condylar points are traced during mandibular movement to analyse the mandible's paths of movement, whilst in other cases the mouth opening or closing are described by a path of changing instantaneous centres of rotation throughout the

movement. The obtained movement tracking data, or four-dimensional (4D) data, of the mandible could also be used to calculate the CR in a PS manner. This, however, means the patient has to have a physiologically correct movement pattern of the mandible in order to determine these points correctly. Patients who are in need of a TJR of the TMJ often have an affected mouth opening. In such cases, a patient-specific (PS) determined CR of the prosthesis cannot be derived from mandibular movement exercises and so should be determined by alternative means.

The aim of this current study was to develop a 4D-workflow to ascertain the PS mean axis of rotation, or fixed hinge, that mimics the patient's specific physiological mouth opening. The aim was to use this 4D-workflow to find out if the aforementioned prior determined 15 [mm] lowering in CR3 is still relevant and, if not, to suggest a PS CR location.

MATERIALS AND METHODS

Twenty healthy adult patients who required cone beam computed tomography (CBCT) scanning for 3D virtual surgical planning (VSP) of their bilateral sagittal split osteotomy (BSSO) procedure between January 2020 and December 2021, were asked to volunteer for a 4D-scanning procedure. The inclusion requirements for the 4D-study were the presence of orthodontic brackets and the absence of TMJ dysfunction. Furthermore, the patient should be able to freely move the mandible without pain and other limiting factors. Before commencing with this study's protocol, approval was received from the Medical Ethical Board, file number: METc 2020/355.

The 4D-scanning was performed with a 4D optical tracking module (Planmeca 4D Jaw Motion) installed in a CBCT scanner (Planmeca ProMax, Planmeca, Helsinki, Finland). The resolution of the CBCT images was 0.4 × 0.4 × 0.4 [mm] with a field of view of 230 [mm]. The subjects had to wear a polyamide maxillary frame, which rests on the nasal bridge and ears, and an aluminium mandibular frame rigidly connected to the lower dental arch and orthodontic brackets by means of an easily removable dental bite registration putty (Exabite TT NDS, GC America INC. Alsip, IL, USA). Both the maxillary frame and the mandibular frame accommodated five optical tracer spheres which could be optically recorded by the system (Figure 2). The CBCT scan was performed in maximum dental occlusion with the patient sitting up straight and

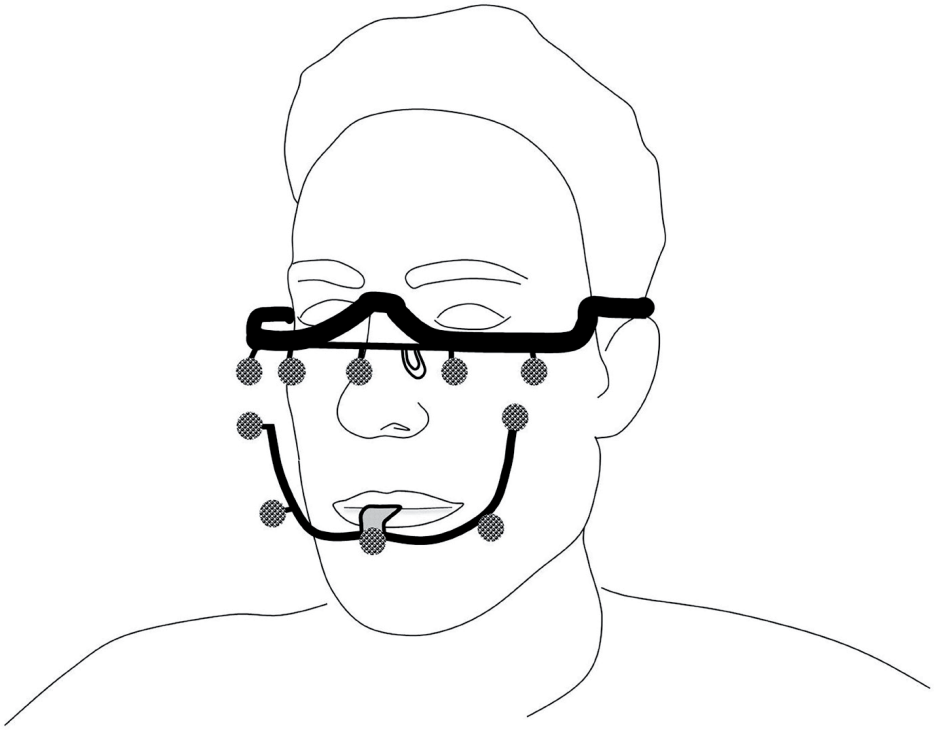

Figure 2 | Sketch showing the 4D-CBCT setup. The subject is scanned with CBCT and subsequent 4D optical scanning in one procedure. The subject wears a maxillary frame resting on the nasal bridge and ears and a mandibular frame which is rigidly connected to the dental elements. Both frames are provided with five reflective markers that are visible on both the CBCT imaging and 4D optical tracking.

in natural head position. The field of view was set to include the complete mandible and the maxilla as well as the orbits. Subsequently, movement exercises were carried out and recorded in real time with a frame rate of 24 [Hz].

The recorded experiments comprised five consecutive voluntary maximum mouth opening exercises per patient. The recorded data were exported as transformation matrices describing the transformation from the CBCT image to the mandible position in each frame. The transformation matrices were saved as .xml files and subsequently converted to .xslx format using Excel 2019 (Microsoft, Redmond, Washington, USA) to allow for easier access of the data for further analysis.

The CBCT scan segmentations were performed in the Mimics 22.0 software (Materialise, Leuven, Belgium) and 3D-models of the mandible and maxilla were created. These models were imported into the 3-Matic Medical 15.0 software (Materialise, Leuven, Belgium) to determine the Frankfurt horizontal plane (FHP) and orthogonally positioned midsagittal plane. Parallel to the midsagittal plane, planes were created in the medio-lateral middle of each condyle. These mid-condylar planes were 100 × 100 [mm] in dimension and triangulated with a maximum edge length of 0.2 [mm]. Subsequently, the mid-condylar planes were merged with the 3D-model of the mandible and exported together with the maxilla model as standard tessellation language (STL) files (Figure 3).

A program was written to develop the JawAnalyser tool in MATLAB R2020a (Mathworks, Natick, Massachusetts, USA) to analyse the recorded 4D-data and to find the instantaneous centre axis of rotation of the moving mandible. The STL models of the maxilla and mandible were imported into this tool together with the subjects' mid-condylar planes and 4D transformation matrix recordings. Start and end frames were chosen manually for each mouth opening, where the start frame was the maximal

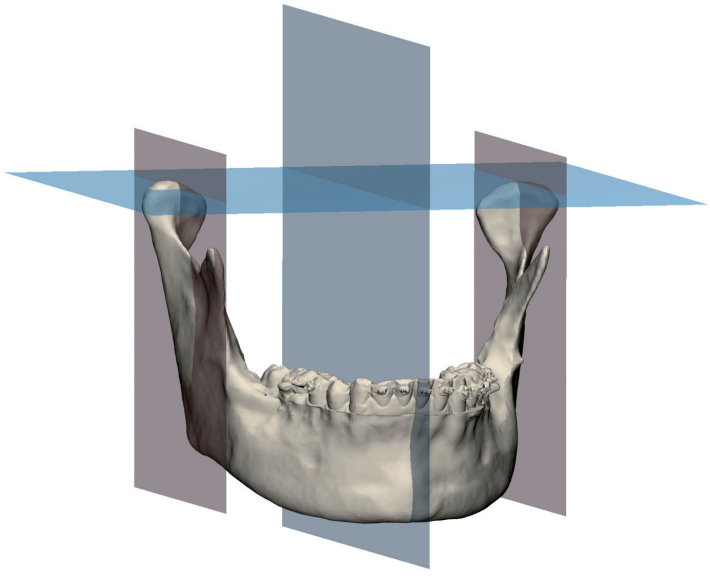

Figure 3 | An example of the assigned Frankfurt horizontal plane and matching midsagittal plane (blue). The midsagittal plane was used to create two parallel mid-condylar planes (red), which intersected the condyles in their medio-lateral middle point. These mid-condylar planes were used in the JawAnalyser tool to calculate the patient-specific centres of rotation and, thereby, the patient-specific axis of rotation for the mouth opening.

occlusal position of the mandible prior to the specific mouth opening and the end frame was the maximal open mouth position. The JawAnalyser compares the orientation of the planes of the mandibles' start frame with the opened mandible's planes and finds the point of least translation, and thus maximum rotation, on each plane. These points describe the start and endpoint of the mandible's rotation axis or instantaneous centre of rotation. This 2D technique relies on the Reuleaux method [19] and is translated to 3D by applying two planes to the mandible to find the instantaneous centre of rotation.

The accuracy of both the JawAnalyser tool and the entire workflow was validated. The JawAnalyser tool was validated by means of inputting geometries that were manually translated and rotated in space by known quantities and the results of the tool were compared to the known input translation and rotation values.

A phantom model was designed for validation purposes (Figure 4). The entire workflow, starting from the 3D-printing of the phantom, followed by the CBCT imaging, the subsequent 4D-recordings, the segmentations, and the final determined rotation axis, was validated with the aid of this 3D-printed phantom model. This model was based on the dimensions of a human head wearing the maxillary and mandibular tracer set-up, depicted in Figure 2, and was fixed to the CBCT scanner's head-supports. It included the same optical tracer sphere positions as those of our subjects (Figure 2 and Figure 4). The mandible part of the phantom was then rotated 25 degrees around a fixed axis, with ten repetitions, comparable to a mouth opening of approximately 38 [mm]. The rotation axes were then determined using JawAnalyser and compared to the known physical positions of the phantom's rotation axis. The begin and end locations of the rotation axes were determined in the mid-condylar planes and the left and right coordinate sets were registered.

Five pairs of coordinates, indicating the extremities of the axis of rotation for a specific mouth opening, were extracted for each subject from the JawAnalyser tool. The matching start and end frames of these five mouth openings were exported from the JawAnalyser tool as STL files and imported together with the extracted axes of rotation into 3-Matic. Then, all the start frames were matched to the CBCT occlusion mandible position whilst the matching axis of rotation was moved along with its mandible. This was necessary to normalise all the axes positions due to slight changes in occlusal positions. Once brought to the CBCT position, all the rotation axis coor-

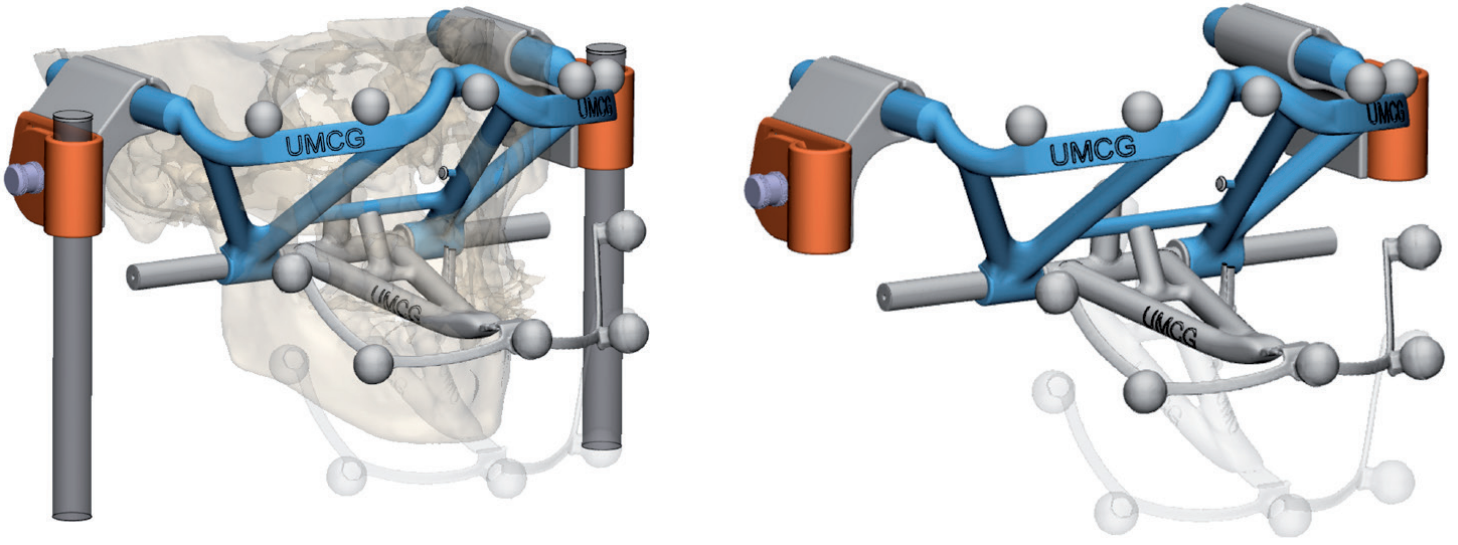

Figure 4 | The phantom model that was designed in-house (University Medical Center Groningen /UMCG) for validation of the 4D-workflow. From a subject's scan (**left**), the positions of the optical tracers were determined and the maxillary and mandibular frames were adapted to form a scaffold that could be rigidly connected to the CBCT scanner. The phantom allowed for rotation along the mandibular axis (**right**), resulting in a simulated 25 degrees opened mouth (transparent).

dinates were finalised and imported into Excel 2019 to calculate the mean x-, y-, and z-coordinates and one mean axis of rotation per subject.

Using the previously determined mid-condylar planes, a circle was sketched on the cross-section of the condyle. This circle matches the top radius of each condyle and its centre, the centre of condyle (CoC), defines the subject's zero-point, which we used to quantify the position of the patient-specific mean axis of rotation (Figure 5).

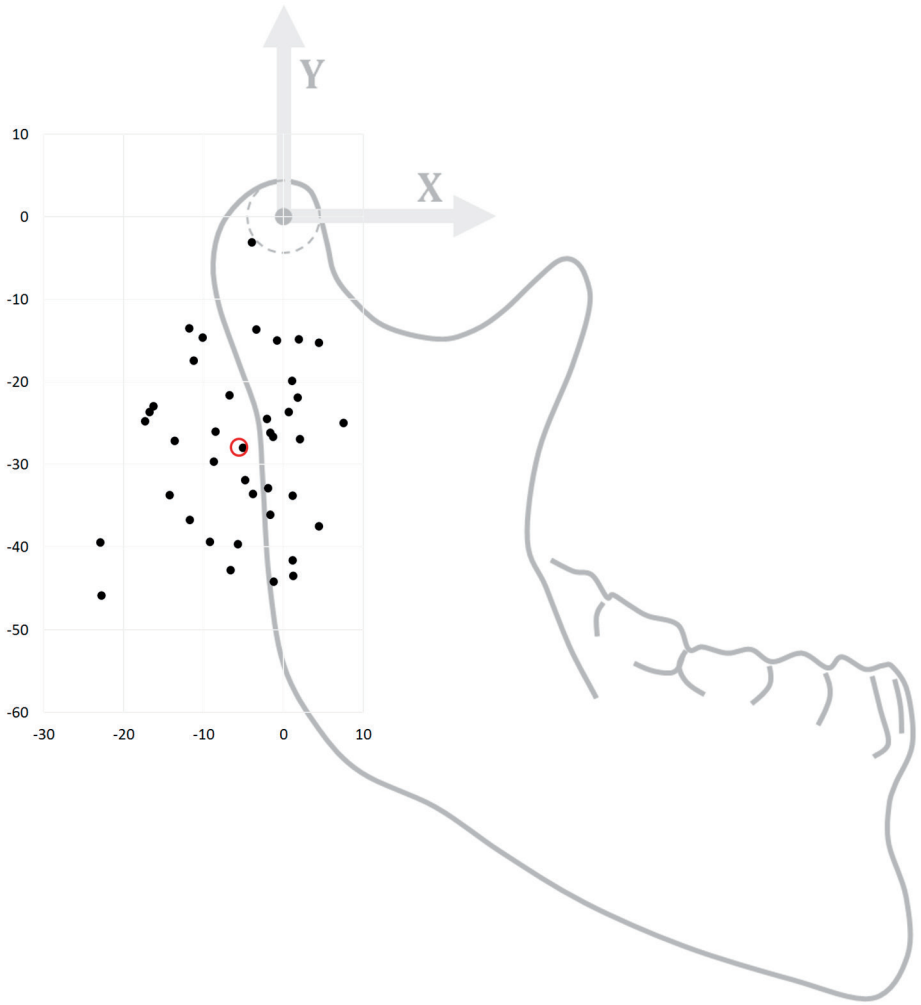

Figure 5 | A scatter plot showing the 40 patient-specific centres of rotation coordinates we determined for our cohort (left & right sides). They are overlaid onto a generic mandible for reference, where the (0, 0) point lies in the centre of condyle point (CoC). The red circle indicates the mean measurement, (−5.7, −28.3).

The PS CR calculation was carried out for both lateralities in all subjects, resulting in 40 measurements. Regarding each CR, both a Δ x- and Δ y-distance from the CoC were registered in [mm]. The positive x-axis was placed along the FHP in an anterior direction, whilst the positive y-axis was positioned orthogonally to the FHP in a cranial direction. The measured CRs per subject (left and right) were considered independently of each other due to the amount of asymmetry. The data analysis was carried out in in IBM SPSS statistics version 23 (IBM corp., Armonk, NY, USA).

The manual determination of the CoC location was repeated by a second observer for ten condyles (BM and JK). The inter-observer variability calculation was carried out in the SPSS software. The inter-observer variability was supported by calculating the interclass correlation coefficient (ICC), whereby a value of <0.40 is poor, 0.40–0.59 fair, 0.60–0.74 good, and 0.75–1.00 is excellent [20]. This statistical test is an indicator for the reproducibility of our CoC location determination between different observers.

In order to visualise the effect of the calculated mean CR for each patient, points were placed at the inter-incisal point and both CoCs. These points were moved along with the mandible's opening movements so that their coordinates formed paths. These paths, or traces, were then compared to four scenarios. The first was the physiological opening movement we measured with our 4D-tracking system. The second was a simulated opening movement with a pure rotation around the PS calculated mean CR. The third and fourth scenarios were simulations of the left condyle following its physiological path while the right joint was replaced by a fixed CR, either 15 [mm] inferiorly to the CoC or at the calculated PS mean position.

RESULTS

Twenty healthy adult subjects were included in this study. These volunteers were 12 males and 8 females, aged from 18 to 53 years, with a mean age of 29. All the subjects had complete natural dentition, wore orthodontic brackets in at least the lower front region, and had no temporomandibular joint dysfunction.

Validation of the JawAnalyser tool resulted in a perfect match between the calculated and input CRs regarding the geometries that were manually rotated and combined, as

well as rotated and translated, as is the case in mandibular kinematics. To validate the entire workflow, including the CBCT imaging, the 4D recordings, the segmentations and the final traces, the rotation axes of all ten mouth opening movements were determined for the phantom model. The mean Euclidean error of the start and end coordinates of the rotation axes to the true coordinates of the phantom was 0.81 [mm].

The 40 CR measurements were normally distributed so the mean position was considered to be a relevant indicator. The mean CR of the right-sided joints was located 28.3 [mm] inferiorly and 5.7 [mm] posteriorly, whilst the mean CR of the left joints was located 27.6 [mm] inferiorly and 5.2 [mm] posteriorly to the CoC. When both literalities were combined, the mean CR location was positioned 28 [mm] inferiorly and

Table 1 | All the calculated centre of rotation (CR) positions per subject and per laterality. The delta-Y and delta-X columns show the distance from the patient's specific centre of condyle (CoC) point, which lies in (0, 0). A negative delta-Y value indicates a shift inferiorly of the CoC and a negative delta-X value indicates a shift in the posterior direction.

Patient	Sex	Age	Right		Left	
			Δ Y	Δ X	Δ Y	Δ X
1	M	19	-39,7	-5,7	-39,4	-9,2
2	M	18	-13,7	-3,4	-14,9	1,9
3	F	53	-13,5	-11,8	-14,7	-10,1
4	F	20	-15,0	-0,8	-25,0	7,5
5	F	19	-33,6	-3,8	-21,7	-6,8
6	F	32	-26,6	-1,3	-28,0	-5,1
7	M	18	-45,9	-22,8	-39,4	-22,9
8	M	25	-3,2	-4,0	-24,5	-2,1
9	F	23	-23,7	-16,7	-24,7	-17,3
10	M	26	-29,7	-8,7	-31,9	-4,8
11	M	18	-23,0	-16,3	-33,7	-14,2
12	F	26	-19,9	1,0	-15,3	4,5
13	F	18	-33,8	1,2	-26,2	-1,6
14	M	46	-41,6	1,2	-43,5	1,2
15	M	47	-27,2	-13,6	-26,0	-8,5
16	F	47	-37,5	4,4	-26,9	2,1
17	M	23	-36,1	-1,7	-32,8	-1,9
18	M	44	-21,9	1,8	-23,7	0,6
19	M	40	-44,2	-1,2	-42,8	-6,7
20	M	29	-36,7	-11,7	-17,5	-11,2
		Mean	-28,3	-5,7	-27,6	-5,2

5.5 [mm] posteriorly to the CoC. The ranges were (–45.9/–3.2 mm) and (–22.9/+7.5 mm) for the superoinferior and anteroposterior directions, respectively. The 95% confidence interval of the calculated mean Δ y-distance from the CoC was –22.9 to –33.7 [mm] and –3.1 to –7.8 [mm] for the Δ x-distance. Figure 5 shows a scatter plot of the determined coordinates, indicating the PS positions of the CR, overlaid onto a mandible for reference. Table 1 depicts all the calculated CR positions per subject.

The manual selection of the CoC for both condyles in ten condyles was repeated by a second observer (BM and JK). The inter-observer variation was 1.47 [mm] with an interclass correlation coefficient (two-way mixed) of 0.997, indicating an excellent match for the measurements by both observers.

Patient 19's coordinate tracing throughout the mandibular opening during the four described scenarios is visualised in Figure 6. We chose this patient because of their rather inferior positioned CRs, which pronounces the differences between the four scenarios well.

DISCUSSION

The workflow and associated JawAnalyser tool developed in this study serve the purpose of determining the optimal PS fixed axis of rotation. The primary application of such PS rotation axes is in designing PS TMJ-TJRs. None of the commercially available TMJ-TJRs make use of a PS calculated CR in their designs, and their CR positions are based on, e.g., the anatomical condylar position / CoC [21] or on technical limitations, i.e., required minimal thicknesses of the used materials [22]. In the Groningen TMJ-TJR, however, the CR is placed 15 [mm] inferior to the CoC with the aim of mimicking the physiological movement [7]. In this prosthesis, the 15 [mm] CR can be easily substituted by a PS determined value due to its patient-specific design [8,9]. This is naturally within certain boundaries set by the surgical approaches used for implantation.

The PS CRs determined in this study mimic the complex physiological mandibular mouth opening movement, which consists of both translational and rotational movements, by approaching the mouth opening as merely a rotational movement around the PS calculated rotation axis.

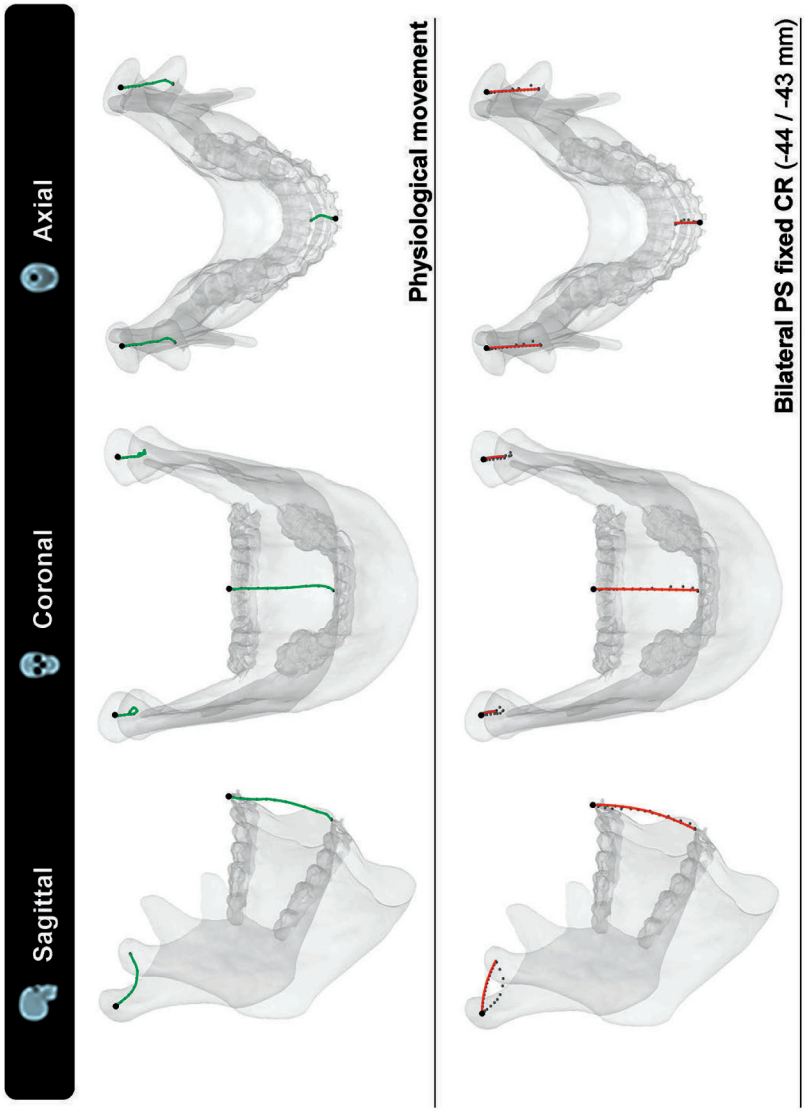
Sagittal
Coronal
Axial
Physiological movement
Bilateral PS fixed CR (-44 / -43 mm)

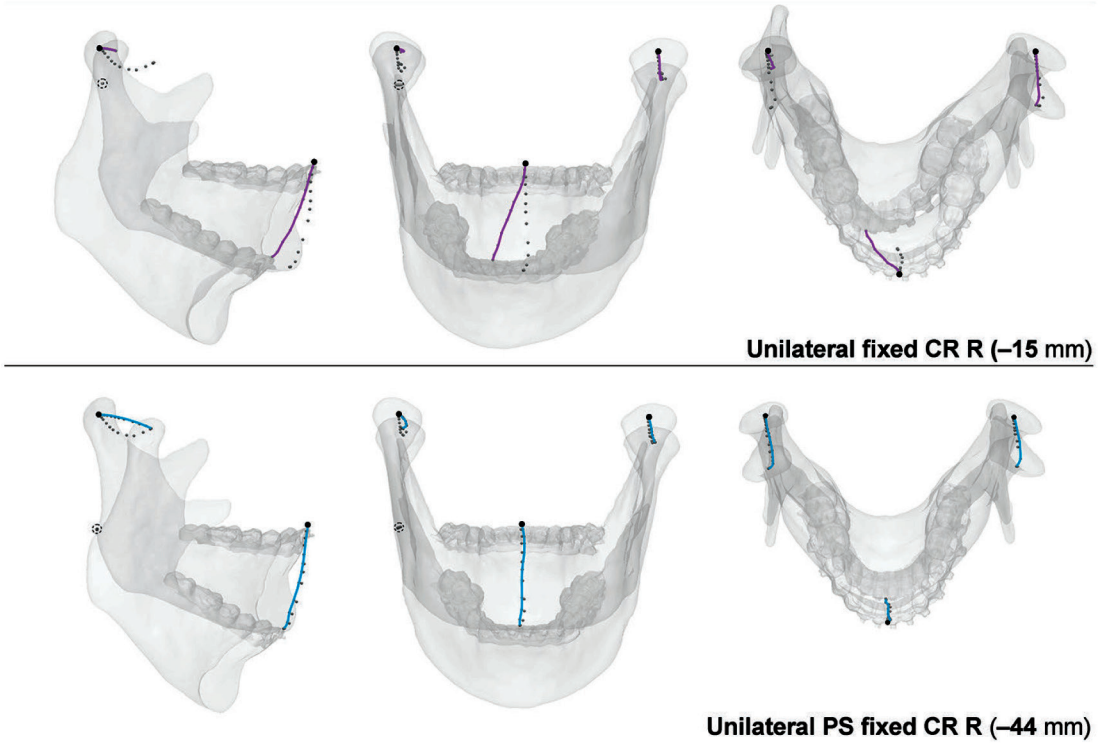

Figure 6 | Condylar and incisal point traces describing the mouth opening movement in four different scenarios. Top to bottom: Physiological movement describes the actual recorded movement pattern for this specific subject. Bilateral PS fixed CR describes a simulated mouth opening around the patient-specific (PS) axis of rotation determined with our workflow. Unilateral fixed CR R describes a simulated mouth opening with a fixed centre of rotation (CR) at 15 mm inferior to the centre of condyle (CoC) and the physiological movement of the left condyle. Unilateral PS fixed CR R describes a simulated mouth opening with a fixed CR at the PS determined position, 44 mm inferior to the CoC and the physiological movement of the left condyle. The dotted traces in the three simulated mouth openings indicate the physiological movement traces. Note the severe lateral deviation that occurs when the CR is positioned much closer to the CoC than PS determined.

By taking all the patients in our cohort into account, we determined the mean position of the CR as being 28 [mm] inferiorly and 5.5 [mm] posteriorly to the CoC. The 95% coincidence intervals for the mean indicate the probability of the majority of the measurements lie within 23 and 34 [mm] inferiorly and 3 to 8 [mm] posteriorly to the CoC. Many prior researchers have studied the kinematics of the mandible [12,13,14,15,16,17,18], but the only study which determined a mean CR position that mimicked the physiological mouth opening was the one by van Loon et al. [3]. As mentioned before, they determined an optimal CR of 15 mm inferior to the CoC. Although they did not report specific CRs per subject, they did mention that for the determination of their optimal CR, the physical boundary conditions, i.e., the prosthesis dimensions, were considered as well. This influenced the determination of their optimal centre of location, and therefore, it was not the merely anatomical optimal centre of rotation. Lowering the CR by 15 [mm] with respect to the CoC can already be challenging in some of the smaller patients. Therefore, it does not appear feasible to directly implement the mean of the PS determined CRs to the Groningen TMJ-TJR or in any commercially available prosthesis in most of our entire set of patients. Lindauer et al. also observed a great variation in rotation axes during mouth opening, and they discussed the value of PS determination of CR [23].

After replacing the TMJ with a TJR-prosthesis, it can be assumed that the reconstructed joint will show, postoperatively, rotational movement only [4]. When substituting the physiological movement of the mandible with a mere rotation around the corresponding PS axis of rotation that was calculated with our JawAnalyser, we observed that the inter-incisal point closely matched the physiological trace in all the planes. Although the CoCs matched both the start and end positions, they had an inversely shaped trace when compared to the physiological trace due to the strict rotational movement. When we replaced the right TMJ with a fixed CR located 15 [mm] inferiorly to the CoC, thereby mimicking the replacement of this joint with a Groningen-TMJ-TJR prosthesis, the simulated mouth opening in this particular patient demonstrated an obvious deviation in both the sagittal and coronal planes. The lateral deviation of the inter-incisal point at maximum mouth opening (MMO), however, was more than 12 [mm] in this scenario. The excursion that would have been made by the right condyle if had it not been replaced by the TJR would have been only 6.4 [mm] as opposed to 21.4 [mm] in the measured physiological trace. This indicates that the PS CR for this patient's joint was situated even further inferiorly than 15 [mm]. The latter scenario, where we maintained the left physiological condylar trace and substituted the right

joint with a fixed CR at the PS calculated point, showed a perfect match between both the occlusal and MMO positions of the physiological mandible, and the lateral deviation at MMO was non-existent.

The visualised effects of lateral and posterior deviations, as seen in the scenario with unilateral 15 [mm] lowering of a fixed CR (Figure 6), are less pronounced in patients with a smaller mismatch between the applied fixed CR position and the calculated PS CR position. It should be noted that these deviations are even more pronounced in TJRs with a CR that is positioned higher than 15 [mm], i.e., the Groningen principle. This applies to all commercially available TMJ-TJR prostheses.

This leaves us with three options:

- accept asymmetrical mouth openings and closing movements
- alter the current prosthesis kinematic principles
- adapt the movements of the contralateral joint

Since the latter, entailing operating on and restricting a healthy joint, would be considered unethical, this means only changing the prosthesis concept or accepting a suboptimal mandibular movement. Even though conforming to the PS axis of rotation might not be physically feasible for all cases, knowing the patient's specific axis of rotation is always valuable for predicting the outcome of the TJR procedure and to prepare the patient for the expected outcome.

To illustrate the effect of a mismatched fixed CR on the contralateral healthy joint, we used an exemplary case to compare two condylar position scenarios (Figure 7). The measured physiological MMO position was compared to a simulated MMO in a case of a unilaterally fixed CR (15 [mm] inferior to the CoC), which is comparable with a unilateral TJR. In this particular case, the calculated PS CR is approximately 44 [mm] inferior to the CoC. The contralateral healthy joint completes its full translation, whilst the replaced joint only does approximately a third. As a result of the mismatch between the PS CR and the simulated CR (44 [mm] vs 15 [mm]), the mandible rotates in the axial plane, resulting in a contralateral healthy joint with a condylar seating that is forced to rotate at an 8.2 degree angle. Figure 7 illustrates this rotational error. The patient's measured physiological maximum laterotrusive excursion, throughout the mouth opening, results only in a 1.5-degree angle, which is only 18% of the simulated forced rotation. The effect a forced rotation and change in condylar

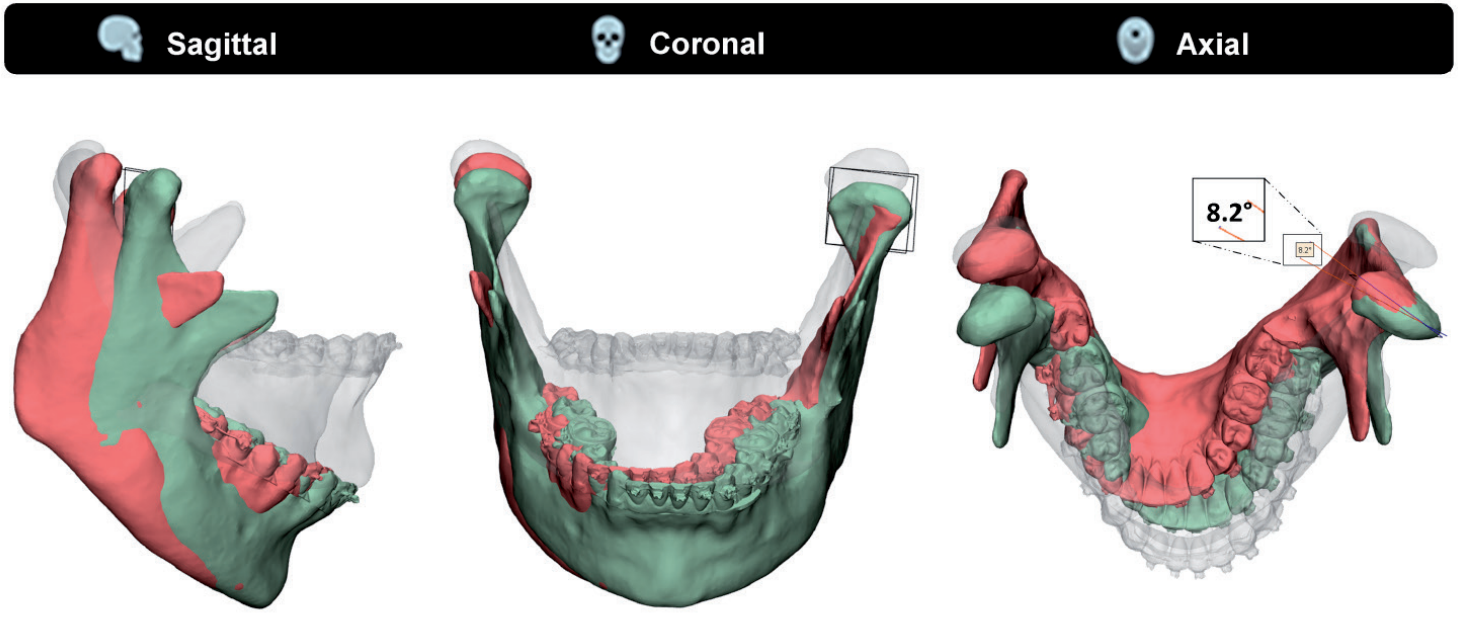

Figure 7 | An illustration showing the effect of a wrongly positioned unilateral fixed centre of rotation (CR) simulating a TMJ-TJR prosthesis on the right side, on the healthy contralateral joint. In transparent the occlusal mandibular position is shown. Green indicates the maximum opened mouth according to the recorded physiological data, and red shows the simulated mouth opening according to scenario 'Unilateral fixed CR R (–15 mm)' in Figure 6. The unilateral fixed CR R (–15 mm) scenario is where the left condyle follows the physiological path, whilst the right side has a fixed CR applied too close to the centre of condyle position for this specific patient. Note again the severe lateral deviation of the red mandible and the unnatural rotation this forces on the contralateral healthy joint. In this specific case, the left condyle is forced to rotate an 8.2 degree angle in the axial plane upon opening compared to the physiological opened condyle position.

seating has on the healthy joint, as well as the maximum acceptable forced rotation angles, is still unknown. Additionally, the fact that commercially available prostheses have an even higher CR compared to the 15 [mm] inferiorly placed CR in our case means that, according to the Groningen principle, this effect would have been even greater in those TMJ-TJR prostheses [5,14].

In patients with restricted mandibular movement, e.g., due to severe unilateral ankylosis, performing a 4D-analysis can be challenging, if not impossible, depending on the severity of the restriction of movement. Furthermore, our proposed workflow would be inapplicable for clinicians who do not have access to 4D techniques. Regarding both situations, it could be worth exploring if the PS CR is related to the morphology of the mandible and fossa and can thus be predicted instead of measured. Among our cohort, we observed that a large portion of the calculated PS CRs lay on or close to the occlusal plane. This observation is supported by prior researchers' findings [24].

In future work, we would like to test the hypothesis that PS CRs can be predicted based on the morphology of the mandible and fossa. Tools that can be applied to test such typical hypotheses are statistical shape modelling (SSM) [25,26] and principal polynomial shape analysis (PPSA) [27]. By using the segmentations of the mandible and fossa together with the calculated PS CRs from our cohort as input for the model, we can make the model predict the PS CRs of mandibles input without 4D data. Further validation of the SSM/PPSA CRs should indicate if there is any relationship between the mandible's morphology and the position of its CRs. However, in order to establish a robust model, we would need to expand our current cohort.

The main limitation of this current study, apart from the relatively small sample size of 20 patients, is the homogeneity of our cohort. Being patients who required CBCT scanning for 3D VSP of their BSSO procedure, all patients in this study had a class II or III occlusion (17 vs. 3). Whether these types of malocclusions have an effect on the movement pattern of the mandible, especially mouth opening, remains unclear, as to the best of our knowledge, this cannot be found in the current literature. Scanning a cohort of control subjects might provide us with these answers, but ethics prevent us from CBCT scanning of healthy subjects.

The strengths, on the other hand, are the fact that our well-validated method turned out a feasible workflow that is not reserved for just BSSO patients. It addresses an

issue that seems generally accepted or overlooked and to which more attention should be paid.

Conclusions

This study succeeded in developing an accurate 4D-workflow to determine a PS mean axis of rotation that mimics the patient's specific physiological mouth opening. Our results strengthen the conception that PS determination of the CR as, e.g., used in TMJ-TJR prostheses, adds value in regard to mimicking the physiological mouth opening movement. The CRs applied in the commercially available TMJ-TJR prostheses are likely positioned too cranially for the bulk of the population, causing physiologically incorrect mandibular movements. The current PS Groningen TMJ-TJR prosthesis applies a lowered CR of 15 [mm] with respect to the CoC and thereby approaches the physiological movement of the mandible to some extent. The mean optimal CR we determined in this study, 28 [mm] inferior to the CoC, however, implies that 15 [mm] of CR lowering is not sufficient for the bulk of the population. In the Groningen TMJ-TJR and perhaps other commercially available prostheses, the amount of CR can easily be lowered to a PS determined CR within certain boundaries; however, due to technical and surgical constraints this would not be far enough to comply with the PS CRs of the majority of the patients.

Therefore, a change in TMJ-TJR prosthesis concept is necessary for all commercially available prostheses in order to comply with all PS CRs calculated in our study. In the meantime, it seems wise to stick to placing the CR 15 [mm] inferiorly to the CoC, as this already partly mimics the physiological movement, or even beyond, towards 28 [mm], if the patient's anatomy allows this.

Funding

This research received no external funding.

Institutional Review Board Statement

This study was approved the Medical Ethical Board, file number METc 2020/355.

Informed Consent Statement

Written informed consent was obtained from the patients to publish this paper.

Acknowledgments

We would like to thank Floris Rotteveel for his efforts in developing the JawAnalyser tool and Haye H. Glas and Hylke van der Wel for their support in this. Additionally, we are grateful to the radiologic technician colleagues from our department for their help with the 4D-CBCT recordings.

Conflicts of Interest

The authors declare no conflict of interest.

REFERENCES

1. Sidebottom, A.J. Current thinking in temporomandibular joint management. Br. J. Oral Maxillofac. Surg. 2009, 47, 91–94.
2. Johnson, N.R.; Roberts, M.J.; Doi, S.A.; Batstone, M.D. Total temporomandibular joint replacement prostheses: A systematic review and bias-adjusted meta-analysis. Int. J. Oral Maxillofac. Surg. 2017, 46, 86–92.
3. van Loon, J.P.; Falkenstrom, C.H.; de Bont, L.G.; Verkerke, G.J.; Stegenga, B. The theoretical optimal center of rotation for a temporomandibular joint prosthesis: A three-dimensional kinematic study. J. Dent. Res. 1999, 78, 43–48.
4. Voiner, J.; Yu, J.; Deitrich, P.; Chafin, C.; Giannakopoulos, H. Analysis of mandibular motion following unilateral and bilateral alloplastic TMJ reconstruction. Int. J. Oral Maxillofac. Surg. 2011, 40, 569–571.
5. Wojczynska, A.; Gallo, L.M.; Bredell, M.; Leiggener, C.S. Alterations of mandibular movement patterns after total joint replacement: A case series of long-term outcomes in patients with total alloplastic temporomandibular joint reconstructions. Int. J. Oral Maxillofac. Surg. 2019, 48, 225–232.
6. van Loon, J.P.; Otten, E.; Falkenstrom, C.H.; de Bont, L.G.; Verkerke, G.J. Loading of a unilateral temporomandibular joint prosthesis: A three-dimensional mathematical study. J. Dent. Res. 1998, 77, 1939–1947.
7. van Loon, J.P.; de Bont, L.G.; Stegenga, B.; Spijkervet, F.K.; Verkerke, G.J. Groningen temporomandibular joint prosthesis. Development and first clinical application. Int. J. Oral Maxillofac. Surg. 2002, 31, 44–52.
8. Merema, B.J.; Kraeima, J.; Witjes, M.J.H.; van Bakelen, N.B.; Spijkervet, F.K.L. Accuracy of fit analysis of the patient-specific Groningen temporomandibular joint prosthesis. Int. J. Oral Maxillofac. Surg. 2021, 50, 538–545.
9. Kraeima, J.; Merema, B.J.; Witjes, M.J.H.; Spijkervet, F.K.L. Development of a patient-specific temporomandibular joint prosthesis according to the Groningen principle through a cadaver test series. J. Craniomaxillofac. Surg. 2018, 46, 779–784.
10. Falkenström, C.H. Biomechanical Design of a Total Temporomandibular Joint Replacement. Ph.D. Thesis, University of Twente, Enschede, The Netherlands, 1993.
11. Hall, R.E. An analysis of the work and ideas of investigators and authors of relations and movements of the mandible. J. Am. Dent. Assoc. (1922) 1929, 16, 1642–1693.
12. Ahn, S.J.; Tsou, L.; Antonio Sanchez, C.; Fels, S.; Kwon, H.B. Analyzing center of rotation during opening and closing movements of the mandible using computer simulations. J. Biomech. 2015, 48, 666–671.
13. Gallo, L.M.; Airoldi, G.B.; Airoldi, R.L.; Palla, S. Description of Mandibular Finite Helical Axis Pathways in Asymptomatic Subjects. J. Dent. Res. 1997, 76, 704–713.
14. Wojczyńska, A.; Leiggener, C.; Bredell, M.; Ettlin, D.; Erni, S.; Gallo, L.; Colombo, V. Alloplastic total temporomandibular joint replacements: Do they perform like natural joints? Prospective cohort study with a historical control. Int. J. Oral Maxillofac. Surg. 2016, 45, 1213–1221.
15. Chen, X. The instantaneous center of rotation during human jaw opening and its significance in interpreting the functional meaning of condylar translation. Am. J. Phys. Anthropol. 1998, 106, 35–46.
16. Leader, J.K.; Boston, J.R.; Debski, R.E.; Rudy, T.E. Mandibular kinematics represented by a non-orthogonal floating axis joint coordinate system. J. Biomech. 2003, 36, 275–281.

17. Leiggener, C.S.; Erni, S.; Gallo, L.M. Novel approach to the study of jaw kinematics in an alloplastic TMJ reconstruction. Int. J. Oral Maxillofac. Surg. 2012, 41, 1041–1045.
18. Chen, C.-C.; Lin, C.-C.; Hsieh, H.-P.; Fu, Y.-C.; Chen, Y.-J.; Lu, T.-W. In vivo three-dimensional mandibular kinematics and functional point trajectories during temporomandibular activities using 3d fluoroscopy. Dentomaxillofac. Radiol. 2021, 50, 20190464.
19. Moorehead, J.D.; Montgomery, S.C.; Harvey, D.M. Instant center of rotation estimation using the Reuleaux technique and a Lateral Extrapolation technique. J. Biomech. 2003, 36, 1301–1307.
20. Cicchetti, D. Guidelines, Criteria, and Rules of Thumb for Evaluating Normed and Standardized Assessment Instrument in Psychology. Psychol. Assess. 1994, 6, 284–290.
21. Zheng, J.; Chen, X.; Jiang, W.; Zhang, S.; Chen, M.; Yang, C. An innovative total temporomandibular joint prosthesis with customized design and 3D printing additive fabrication: A prospective clinical study. J. Transl. Med. 2019, 17, 4.
22. Quinn, P.D. Lorenz Prosthesis. In Oral and Maxillofacial Surgery Clinics of North America; Elsevier: Amsterdam, The Netherlands , 2000; Volume 12, pp. 93–104.
23. Lindauer, S.J.; Sabol, G.; Isaacson, R.J.; Davidovitch, M. Condylar movement and mandibular rotation during jaw opening. Am. J. Orthod. Dentofac. Orthop. 1995, 107, 573–577.
24. Terhune, C.E.; Iriarte-Diaz, J.; Taylor, A.B.; Ross, C.F. The instantaneous center of rotation of the mandible in nonhuman primates. Integr. Comp. Biol. 2011, 51, 320–332.
25. Yang, Y.M.; Rueckert, D.; Bull, A.M. Predicting the shapes of bones at a joint: Application to the shoulder. Comput. Methods Biomech. Biomed. Engin. 2008, 11, 19–30.
26. Vlachopoulos, L.; Lüthi, M.; Carrillo, F.; Gerber, C.; Székely, G.; Fürnstahl, P. Restoration of the Patient-Specific Anatomy of the Proximal and Distal Parts of the Humerus: Statistical Shape Modeling Versus Contralateral Registration Method. J. Bone Jt. Surg. Am. 2018, 100, e50.
27. Duquesne, K.; Nauwelaers, N.; Claes, P.; Audenaert, E. Principal polynomial shape analysis: A non-linear tool for statistical shape modeling. Comput. Methods Programs Biomed. 2022, 220, 106812.

Section III

Chapter 7

A contemporary approach to non-invasive 3D determination of individual masticatory muscle forces:
A proof of concept

Bram B. J. Merema, Jelbrich J. Sieswerda, Frederik K. L. Spijkervet, Joep Kraeima and Max J. H. Witjes

Department of Oral and Maxillofacial Surgery, University Medical Center Groningen, University of Groningen, Hanzeplein 1, 9700 RB Groningen, The Netherlands

Published:
Journal of Personalized Medicine, 2022; 12(8): 1273

ABSTRACT

Over the past decade, the demand for three-dimensional (3D) patient-specific (PS) modelling and simulations has increased considerably; they are now widely available and generally accepted as part of patient care. However, the patient specificity of current PS designs is often limited to this patient-matched fit and lacks individual mechanical aspects, or parameters, that conform to the specific patient's needs in terms of biomechanical acceptance. Most biomechanical models of the mandible, e.g., finite element analyses (FEA), often used to design reconstructive implants or total joint replacement devices for the temporomandibular joint (TMJ), make use of a literature-based (mean) simplified muscle model of the masticatory muscles. A muscle's cross-section seems proportionally related to its maximum contractile force and can be multiplied by an intrinsic strength constant, which previously has been calculated to be a constant of 37 [N/cm2]. Here, we propose a contemporary method to determine the patient-specific intrinsic strength value of the elevator mouth-closing muscles. The hypothesis is that patient-specific individual mandible elevator muscle forces can be approximated in a non-invasive manner.

MRI muscle delineation was combined with bite force measurements and 3D-FEA to determine PS intrinsic strength values.

The subject-specific intrinsic strength values were 40.6 [N/cm2] and 25.6 [N/cm2] for the 29- and 56-year-old subjects, respectively. Despite using a small cohort in this proof of concept study, we show that there is great variation between our subjects' individual muscle intrinsic strength.

This variation, together with the difference between our individual results and those presented in the literature, emphasises the value of our patient-specific muscle modelling and intrinsic strength determination protocol to ensure accurate biomechanical analyses and simulations. Furthermore, it suggests that average muscle models may only be sufficiently accurate for biomechanical analyses at a macro-scale level. A future larger cohort study will put the patient-specific intrinsic strength values in perspective.

INTRODUCTION

The demand for three-dimensional (3D) patient-specific (PS) modelling and simulations has increased considerably over the past decade and is now widely available and generally accepted as a part of patient care in oral and maxillofacial surgery. Clinicians throughout the world now make use of PS modelled oral and maxillofacial implants and prostheses, e.g., reconstruction plates for oncological surgery and temporomandibular joint (TMJ) prostheses for total joint replacements (TJR). These specifically designed devices are more accurate alternatives to conventional products [1,2] and a solution for complex cases where the shelf solutions do not suffice [3]. PS designs provide a patient-matched shape to ensure a proper fit to the bony anatomy. However, the patient specificity of current PS designs is often limited to this patient-matched fit and lacks mechanical aspects related to the individual situation, or parameters, that conform to the specific patient's characteristics in terms of biomechanical demands. Most biomechanical models of the mandible, e.g., finite element analyses (FEA), often used to design reconstructive implants or TJR devices for the TMJ, make use of a literature-based (mean) simplified muscle model of the masticatory muscles [2,4,5,6,7]. This is due to the complexity of the masticatory muscle anatomy and the inability to directly measure separate muscle forces in vivo. Unfortunately, this directly affects the overall biomechanical model specificity for each patient, which is a limiting factor when the model is used to develop a PS implant that should address personalised optimisation. Relying on such literature-based non-PS muscle models when developing PS implants might result in the same mechanical failures as observed with conventional osteosynthesis materials, e.g., osteosynthesis plate failure, stress shielding, and, subsequently, screw loosening [8]. The morphology of the masticatory system is subject to wide anatomical variations [9]; thus, utilising an average muscle model is only valid for general purposes.

Due to practical and ethical limitations on in vivo force output measurements of single muscles, it remains challenging to approximate the true maximum acting forces of the masticatory muscles. The jaw elevator muscles, consisting of the masseter, temporalis, and medial pterygoid muscles, are predominantly inaccessible to measurement techniques, such as intramuscular electromyography (iEMG) and surface EMG (sEMG), that could approximate the acting forces. Both can be applied to record electrical stimuli in the muscles which, when combined with the resulting force output measurements, can be used to approximate a muscle's acting force. The

iEMG technique is, however, known to cause discomfort for the subject [10] due to the needle electrodes pinching the muscle. The effect of such invasive sensors on muscular behaviour is hard to fathom, mostly because of the inability to directly measure a muscle's force in situ [11]. The sEMG technique reportedly suffers from a higher rate of crosstalk, i.e., misleading signals coming from neighbouring muscles [10,12]. Furthermore, there are many concerns regarding the sensitivity, applicability, reliability, and reproducibility of EMG measurements [10,13].

In 1846, Weber stated that the force of a muscle is related to the total cross-section of all the muscle fibres at a specified muscle length. This became known as the physiological cross-section (PCS) of a muscle [14]. It was suggested that the PCS is proportionally related to the maximum contractile force of a muscle, and thus could be multiplied by a certain constant to estimate a muscle's force. The constant is called the intrinsic strength [P] as it represents a force per unit of PCS [N/cm2]. The resulting Formula (1) is used to calculate the muscle force (F_{muscle}) and can be described as:

$$F_{muscle} = P \cdot PCS \text{ [N]} \quad (1)$$

Hitherto, many previous authors studied and suggested maximum values for the intrinsic strength of various muscle groups in order to determine the maximum separate muscle forces, but the intrinsic values varied widely [14,15,16,17,18]. Weijs and Hillen [19] reviewed the available literature on intrinsic strength and suggested a P-value of 37 [N/cm2], based on their experimental data. However, this value was determined from PCSs measured in cadavers combined with bite force data from a group of volunteers. The intrinsic strength calculation was carried out in 2D while assuming sagittal symmetry.

The P-value of 37 [N/cm2], determined by Weijs and Hillen [19], is still relevant as a general estimate for researchers who want a patient-specific model but only have the patient's muscle cross-sectional data available [20]. Another value frequently found in maxillofacial literature is 40 [N/cm2] [21,22,23,24]. This value, initiated by Koolstra et al. [21] refers, however, to Weijs and Hillen's [19] value of 37 [N/cm2].

The same relation was found using muscle cross-sectional area (CSA) [9,20,25]. The CSA, rather than the PCS of human masticatory muscles, is often used to estimate muscle force because it can be directly measured from computed tomographic (CT)

or magnetic resonance imaging (MRI) data, and has been shown to correlate strongly with the total cross-sectional area of all fibres, as determined by means of dissection or PCS [9,25,26].

With this study, we aimed to propose a contemporary method to determine the patient-specific intrinsic strength value of the elevator muscles. The hypothesis is that patient-specific individual mandible elevator muscle forces can be approximated in a non-invasive manner by combining MRI muscle cross-section data, bite force measurements and 3D finite element analysis simulations, which can be used in patient-specific designs for reconstructive implants and (TMJ) total joint replacements.

MATERIALS AND METHODS

3D Muscle Model

Our volunteers underwent an MRI scan with a 3T MRI scanner (MAGNETOM Skyra 3T, Siemens, Erlangen, Germany) using a T1 weighed sequence (PETRA, FATSAT) and 1 [mm] slice thickness, according to our centre's regular head and neck patient oncology protocol. The subjects were scanned while in a supine position and instructed to maintain dental occlusion throughout the scan. A manual 3D segmentation of the skull and mandible was subsequently performed in the Mimics 22.0 software (Materialise, Leuven, Belgium) to function as reference geometry for further muscle delineation. Using the Brainlab 2020 software (Brainlab, München, Germany), the temporalis, medial pterygoid, masseter pars profunda, and masseter pars superficialis muscles were delineated using the brush tool. The temporalis muscles' CSAs were measured 10 mm cranially to the Frankfurt horizontal plane (FHP), in accordance with the method described by Weijs and Hillen [27].

The muscles were exported as standard tessellation language (STL) files, along with the manual segmentations of the skull and mandible. Next, the STL files were imported into the 3-Matic Medical 15.0 software (Materialise, Leuven, Belgium), where the muscles were wrapped and smoothed to obtain smooth structures. Subsequently, the muscle origins and insertions were determined as the contact area between the muscle delineations and the mandible and skull. A vector was drawn between the centres of gravity for each muscle's origin and insertion surface, indicating the muscle's acting direction. The maximum CSA was determined for each individual muscle by slicing

the muscle along its defined acting direction in increments of 1 [mm] (Figure 1). The measured CSAs, in combination with the intrinsic strength values, were used to calculate the specific muscle forces. To model the muscle forces, it was necessary to assume that all muscles exert their maximum force along their determined force vectors simultaneously. A second assumption was that a single intrinsic strength value can be applied to all the simultaneously acting muscles within one subject.

The muscle delineations on MRI and the subsequent maximum muscle CSA measurements were independently performed by two individual observers (B.M. and J.S.). The inter-observer variability in cm2 CSA was calculated in IBM SPSS statistics version 23 (IBM corp., Armonk, NY, USA). The inter-observer variability was supported by the calculating the interclass correlation coefficient (ICC), whereby a value of <0.40 is poor, 0.40–0.59 is fair, 0.60–0.74 is good, and 0.75–1.00 is excellent [28]. This statistic test is an indicator for the reproducibility of our muscle delineation and CSA determination between different observers.

Bite Force Measurements

An experiment was designed to measure the total resulting force of all the elevator muscles. Intraoral scans were made of the subjects' dentitions (Trios III, 3Shape, Copenhagen, Denmark). In order to measure the maximum isometric bite force, a spacer was placed in between the subjects' central incisors to allow for a minor mouth opening of 15–20 [mm], resulting in bite sensor placement at the physiological optimum muscular length [29,30,31]. The intraoral scanning included both individual arches, both arches in natural maximum occlusion and the arches in a slightly open position with the spacer in situ. These scans were aligned with the MRI scan and, subsequently, the mandible was moved to match the lower dental scan of the opened position.

A bite force sensor was developed for this specific purpose (Figure 2), based on a FlexiForce A201 piezoresistive transducer or a force-sensitive resistor (Tekscan, Inc., South Boston, MA, USA). This 0.2 [mm] thick flexible sensor is 10 [mm] in diameter and its resistance reduces with increasing pressure. Using an Arduino Uno Rev3 microcontroller (Arduino, www.arduino.cc, accessed on 1 July 2021), data were collected and processed to read the applied normal compressive force. An apparatus was developed for accurate full-range calibration of the sensor. Calibration validation resulted in full-range linearity with a maximum error of 5%, measured from 30 to 560 N.

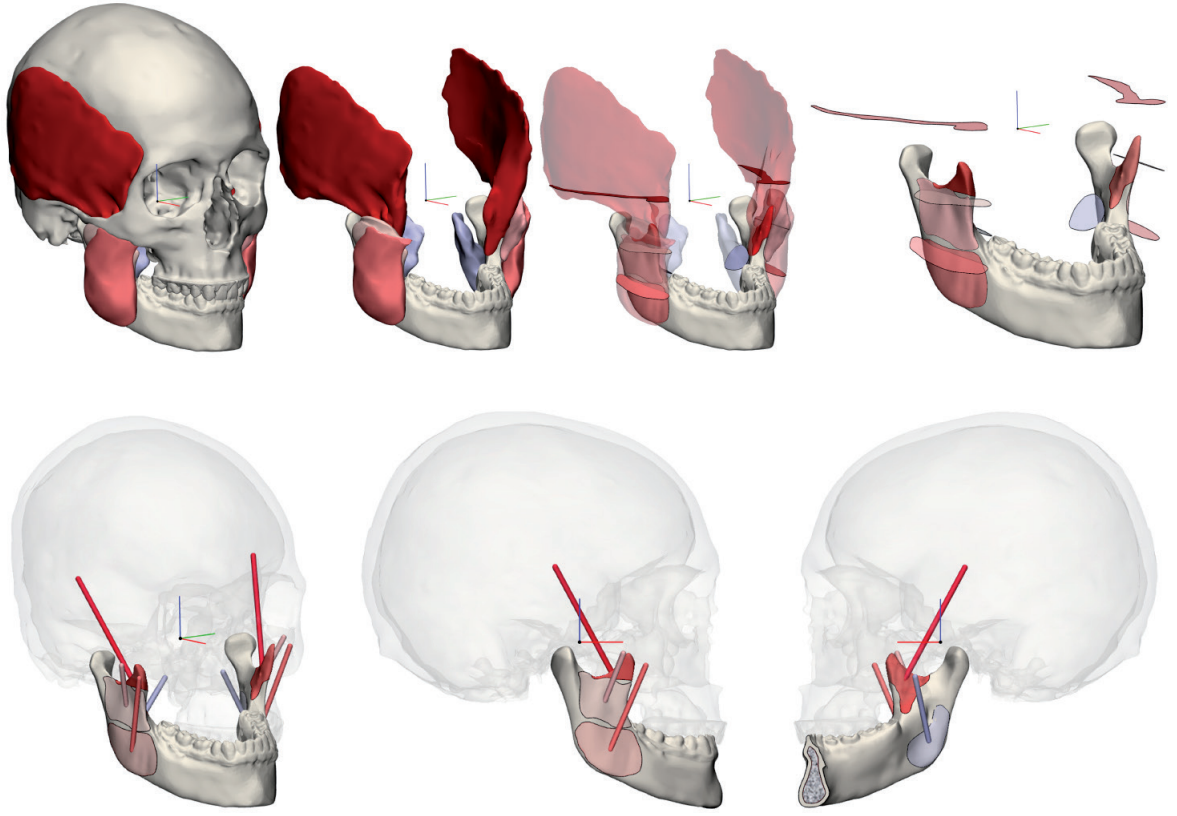

Figure 1 | Visualisation of the smooth delineated muscles obtained from MRI data. The m. masseter superficialis, m. masseter profunda, m. pterygoideus medialis, and m. temporalis were taken into account. The muscles were sliced to determine the maximum CSA (**upper**), and the force vectors were calculated between the origin and matching insertion areas for each muscle (**lower**).

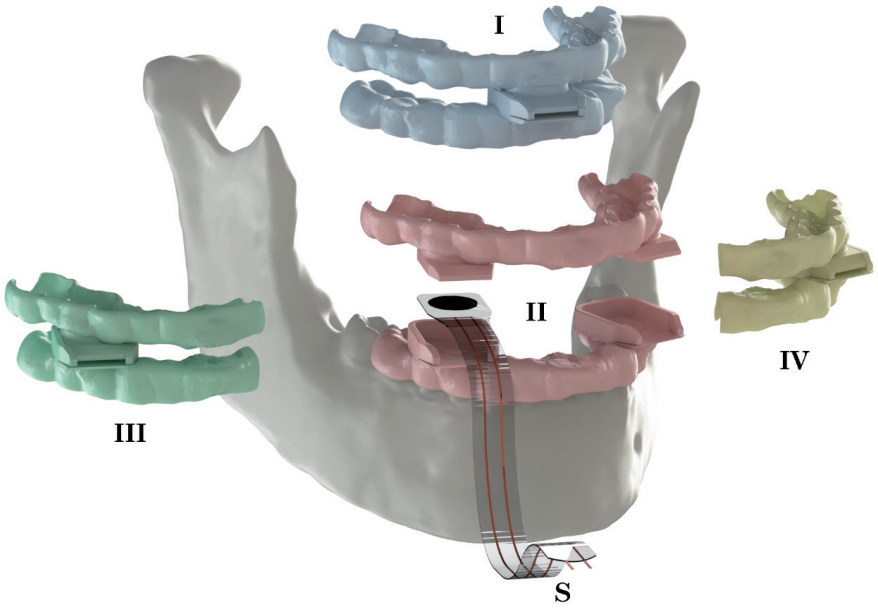

Figure 2 | An overview of the used set-up including the bite sensor (S) and corresponding sets of upper and lower splints. The violet pair **(I)** of splints was used for incisal bite force measurements, the red pair **(II)** for bilateral premolar measurements, and the green **(III)** and yellow **(IV)** pairs for unilateral measurements of the right and left side of the premolars, respectively.

Splints were designed to fit the subject's dentition in order to prevent damaging the subject's dental elements and to distribute the bite force over multiple elements. This was performed in order to lower periodontal receptor stimulation and potential pain sensations which could influence the muscles' recruitment, and to protect the dental elements, thereby encouraging the subject to apply their maximum voluntary bite force [32,33].

The sensors were located in the incisal/midline and the first pre-molar positions since these positions are relatively easily accessible and require only minimal mouth opening in order to fit the bite sensor. The sensor pockets were positioned parallel to the FHP, resulting in a registration of the bite force magnitude in a predefined direction at predefined locations. The sensor thickness was chosen so that a mouth opening of 15–20 [mm] could be established [29,30,31] (Figure 1). The splints were printed from PA12 polyamide powder (Oceanz, Ede, The Netherlands).

The maximum isometric voluntary bite force was registered in an experiment that included four separate exercises, each consisting of five load repetitions. Incisal bite force was registered, as well as both the bilateral and unilateral premolar bite forces. To avoid fatigue, a one-minute pause was taken between each measurement. For each of the four bite scenarios, the maximum bite force was determined from the five repetitions. These maximum values were used for further calculations.

Finite Element Model

A 3D finite element model was set up to first determine the resulting bite forces when calculating the muscle forces from the intrinsic strength value suggested by Weijs et al. [19]. These simulations functioned as a datum measurement. In the following simulations, the problem was inversed. The in vivo bite force measurements were now used as output objective values and each subject's muscle model was scaled in output force to match these objective values and determine the patient-specific intrinsic strength value. These simulations were based on the principle of static equilibrium of forces and moments, which can be applied to an object at rest, as is the case with isometric bites.

To briefly summarise the two scenarios:

(1) Use the subject's muscle CSA and calculate the muscle forces with the intrinsic strength (P) value of 37 [N/cm], as suggested by Weijs et al. [19], and analyse the resulting bite forces.

(2) Use the subject's muscle CSA and matching measured bite forces and calculate the patient-specific intrinsic strength value.

Regarding all the scenarios described in Section 2.2, the reaction forces were measured at both condylar supports, indicating the analysed subject's specific TMJ forces and bite force location(s).

Pre-Processing/Model Preparation

The manual 3D bone segmentations of the MRI data and the intraoral scans were combined with 3D models of the skull and mandible, including the dentition, in the 3-Matic 15.0 software (Materialise, Leuven, Belgium). A cancellous volume was assigned to the mandible by means of an internal shell function, resulting in a cortical thickness of 2 mm. To ensure the correct condylar positions in our simulations, the orientation of the mandible was matched to the slightly opened position of the man-

dible in the intraoral scan of the dentition with the spacer in situ. The final models were imported into Solidworks 2020 (Dassault Systèmes SolidWorks Corporation, Waltham, MA, USA) and converted into non-uniform rational basis spline (NURBS) solid parts using the Geomagic for Solidworks 2021 add-in (3D systems, Rock Hill, SC, USA). All the muscle insertion surfaces were copied and assigned a surface group on the mandible model so as to distribute the force equally over the entire insertion area.

Condyle supports were used as indirectly fixed buffers to avoid over-fixation, but, at the same time, to limit the allowed condylar excursion in both the x- and y-direction of the model to allow for natural strain of the mandible. These fixtures were modelled as rectangular blocks with the condylar shape subtracted, leaving a 2 mm layer in between the condyles and the top surfaces [34]. The tops of these condylar fixtures were fixed in the x, y, and z directions and the analysed bite positions of the splints, i.e., incisal, left, and right premolar unilateral or premolar bilateral, were fixed only in the z-direction to match the bite force experiments. The contact set of cortical and cancellous portions of the mandible were considered to be bonded, and thus one part, while a non-penetrating contact set was implemented between the mandible and the condylar supports and splints. Loads were applied to the muscle insertion surfaces using the prior determined Fx, Fy, and Fz muscle force components (see Table 2 in Section 3).

Homogeneous linear elastic material properties were applied. The used Young's modulus and Poisson's ratio were $E = 14.700$ MPa, $\nu = 0.3$, and $E = 300$ MPa, $\nu = 0.3$ for the cortical and cancellous bones, respectively [35]. The articular disc properties of $E = 44.1$ MPa and $\nu = 0.4$, as presented by Tanaka et al. [36] were used for the condylar supports, while the PA12 splints were assigned $E = 1.750$ MPa and $\nu = 0.4$.

Parabolic tetrahedral solid mesh elements were used to discretise the model due to the complex anatomical shape of the mandible.

Subjects

Our workflow was applied to two male Caucasian subjects, 29 and 56 years old (y.o.), who had voluntarily undergone magnetic resonance imaging (MRI) scanning for prior research and were still available for further experiments. No subject selection was applied. Both subjects had complete and well-preserved dentitions with normal

occlusions and no missing teeth apart from the third molars. None of them had clear signs of periodontal disease, pain in the temporomandibular joint or jaw muscles, or movement restrictions.

RESULTS

Muscle Model

Both subjects' CSAs were measured longitudinally along each muscle's determined force vector. The largest CSAs were registered as listed in Table 1. The 29 y.o. subject's mean CSAs for the masseter superficialis, masseter profunda, pterygoideus medialis, and temporalis muscles were 4.31 [cm2], 2.86 [cm2], 3.37 [cm2], and 6.92 [cm2], respectively, whereas the 56 y.o. subject had slightly larger CSAs of 5.47 [cm2], 2.77 [cm2], 3.98 [cm2], and 7.13 [cm2], respectively.

The mean inter-observer variation between the corresponding muscle CSAs, delineated and measured by the two observers, was 0.73 cm2 with an interclass correlation coefficient (two-way mixed) of 0.91, indicating an excellent match of measurements by both observers [28]. Since this study only includes measurements in two subjects, no further statistical analysis was carried out.

The direction of each muscle, as described by the vector in between the centres of gravity of the origin and insertion surfaces of each muscle, were found through the Fx, Fy, and Fz components in Table 2. The FHP functioned as the x–y plane with its positive x-axis pointing anteriorly, the positive y-axis pointing towards the left side of the mandible, and the z-axis pointing cranially. The origin of the coordinate system was set where the mid-sagittal plane coincided with the FHP.

Table 1 | An overview of both subjects' measured maximum cross-sectional areas per muscle.

Muscle	Subject 1, 29 y.o.			Subject 2, 56 y.o.		
	CSA [cm²]					
	Right	Left	mean	Right	Left	Mean
Masseter superficialis	4,64	3,97	4,31	5,17	5,76	5,47
Masseter profunda	3,14	2,57	2,86	2,78	2,77	2,77
Pterygoideus medialis	3,34	3,40	3,37	4,02	3,93	3,98
Temporalis	7,49	6,34	6,92	6,55	7,72	7,13

Table 2 | Both subjects' muscle force vector components for the literature-based intrinsic strength value (P = 37 [N/cm2]) and the determined patient-specific intrinsic strength values (P = 40.6 [N/cm2] and P = 25.6 [N/cm2]).

				P = 37 [N/cm²]				P = 40.6 [N/cm²]			
	Muscle	Laterality	CSA [cm²]	Σ Force [N]	Force components [N]			Σ Force [N]	Force components [N]		
					x	y	z		x	y	z
Subject 1, 29 y.o.	Masseter superficialis	Right	4,64	171,76	53,22	24,07	161,52	188,27	58,34	26,39	177,05
		Left	3,97	146,89	26,65	32,16	140,83	161,01	29,21	35,26	154,37
	Masseter profunda	Right	3,14	116,31	14,70	33,41	110,44	127,49	16,11	36,62	121,05
		Left	2,57	95,07	6,12	30,67	89,78	104,21	6,71	33,62	98,42
	Pterygoideus medialis	Right	3,34	123,53	7,04	57,22	109,25	135,40	7,71	62,72	119,75
		Left	3,40	125,71	11,28	61,27	109,19	137,80	12,37	67,16	119,69
	Temporalis	Right	7,49	277,18	139,94	55,13	232,82	303,83	153,40	60,43	255,20
		Left	6,34	234,64	113,21	47,02	200,07	257,20	124,10	51,54	219,30
				P = 37 [N/cm²]				P = 25.6 [N/cm²]			
Subject 2, 56 y.o.	Masseter superficialis	Right	5,17	191,15	57,11	33,41	179,33	126,83	37,89	22,17	118,99
		Left	5,76	213,30	67,44	49,60	196,18	141,52	44,75	32,91	130,17
	Masseter profunda	Right	2,78	102,81	17,79	31,55	96,22	68,21	11,80	20,93	63,84
		Left	2,77	102,48	14,36	39,58	93,43	67,99	9,53	26,26	61,99
	Pterygoideus medialis	Right	4,02	148,91	40,65	67,95	126,12	98,80	26,97	45,08	83,68
		Left	3,93	145,27	35,12	60,36	127,39	96,39	23,30	40,05	84,52
	Temporalis	Right	6,55	242,46	82,58	53,03	221,71	160,87	54,79	35,19	147,10
		Left	7,72	285,46	105,95	67,88	256,23	189,40	70,30	45,04	170,01

Bite Force Experiments

A total of four different bite scenarios, each including five repetitions, were recorded for each subject. All the recordings were uneventful while the subjects bit as hard as they could. Only the incisal measurements demonstrated that the subjects experienced a certain amount of insecurity or pain with the highest measured forces. The splints showed a good fit and proved to offer comfortable dental protection while guiding the subject to bite at the exact location that was used for the matching FEA. Each recording involved five repetitions of the same bite position scenario. The highest peak bite force per bite scenario was used as the maximum true in vivo bite capacity at the four specified bite locations.

All the bite forces are listed in Table 3. The ∑ F.Bite column in Table 3 describes the resultant bilateral bite force and is the sum of the right and left peak force in the bilateral experiment. The highest bite forces were registered in the 29 y.o. subject. The maximum incisal bite was 189 [N] while the maximum unilateral measurement was 345 [N] at the pre-molar location. This subject's highest overall bilateral bite force out of the four measurements was recorded as 474 [N] and thus considered the true maximum voluntary bite force at the premolar location. Regarding the 56 y.o. subject, we recorded 79 [N], 248 [N], and 342 [N] as the highest incisal, unilateral premolar, and bilateral premolar bite forces, respectively. In both our subjects, the registered bilateral bite forces were approximately 1.4 times (1.37 and 1.38) higher than the maximum voluntary unilateral measurements at the same premolar position.

Finite Element Analyses

The first FEAs, four scenarios for both subjects, were set up with an intrinsic strength value of P = 37 [N/cm2] and functioned as reference analyses for the subsequent inversed determination of the true subject-specific intrinsic strength value for each subject. The reaction forces, measured orthogonally to the FHP, are mentioned in Table 3 under "In silico", with P = 37 [N/cm2]. We observed that the intrinsic strength value used in these reference analyses was lower than the 29 y.o. subject's actual PS intrinsic strength, while it was too high for the 56 y.o. subject.

The results of the bilateral pre-molar measurements were summed and we considered the ultimate true bite capacity of the subject at the pre-molar location (∑ F.Bite). These values were used to scale the total system of the subject in the FEA. Once the right amount of scaling was achieved, the unilateral and incisal bite scenarios were

Table 3 | Bite registrations through the bite force experiments (In vivo) and finite element analyses (In silico). All the presented forces acted orthogonally to the Frankfurt horizontal plane. The boxed values were matched to determine the PS intrinsic strength values.

Subject 1, 29 y.o.

	Bite position	∑ F.Bite	Premolar laterality		Incisal	Condyle	
			Right	Left		Right	Left
	In-vivo						
	Bilat. premolar	**474**	256	218	-	-	-
	Premolar R	318	318	-	-	-	-
	Premolar L	345	-	345	-	-	-
	Incisal	189	-	-	189	-	-
	In-silico						
P = 37 [N/cm²]	Bilat. premolar	432	241	181	-	392	330
	Premolar R	426	426	-	-	326	402
	Premolar L	425	-	425	-	482	247
	Incisal	339	-	-	339	445	370
P = 40.6 [N/cm²]	Bilat. premolar	**474 (0%)**	264 (+3%)	210 (-4%)	-	429	361
	Premolar R	467	467	-	-	357	440
	Premolar L	466	-	466	-	528	270
	Incisal	371	-	-	371	488	405

Subject 2, 56 y.o.

	Bite position	∑ F.Bite	Premolar laterality		Incisal	Condyle	
			Right	Left		Right	Left
	In-vivo						
	Bilat. premolar	**342**	195	147	-	-	-
	Premolar R	197	197	-	-	-	-
	Premolar L	248		248	-	-	-
	Incisal	79	-	-	79	-	-
	In-silico						
P = 37 [N/cm²]	Bilat. premolar	520	257	263	-	360	416
	Premolar R	502	502	-	-	280	515
	Premolar L	510	-	510	-	453	333
	Incisal	409	-	-	409	415	473
P = 25.6 [N/cm²]	Bilat. premolar	**342 (0%)**	168 (-14%)	174 (+18%)	-	241	276
	Premolar R	333	333	-	-	186	341
	Premolar L	338	-	338	-	301	222
	Incisal	271	-	-	271	275	314

analysed. The subject-specific P values were 40.6 [N/cm2] and 25.6 [N/cm2] for the 29- and 56-year-old subjects, respectively. All the post-scaling results, including the joint reaction forces of the TMJs, are presented in Table 3.

Maximum Mandibular Stress

When scaling the subjects' muscular systems, FEA showed that the stresses occurring in the mandible changed drastically for the 56 y.o. subject. Even though the location of the maximum occurring stress did not change, the P = 37 [N/cm2] analysis showed an increase in maximum stress compared to the calculated subject-specific intrinsic strength analyses with P = 25.6 [N/cm2]. The maximum von Mises stresses were found in the unilateral right premolar scenarios and occurred at the contralateral side around the mandibular oblique line. The measured values were 63.8 [MPa] for P = 37 [N/cm2] compared to 42.3 [MPa] in the matching P = 25.6 [N/cm2] scenario. Figure 3 visualises this comparison.

DISCUSSION

We propose a contemporary method to determine the patient-specific intrinsic strength value of the elevator muscles of the mandible. Furthermore, we show how to patient-specifically approximate the value of the individual mandible elevator muscles in a non-invasive manner by combining the MRI volumetric data, bite force measurements, and 3D finite element analysis simulations.

We derived the CSAs of the elevator muscles of the mandible through an indirect 3D slicing approach. We did, however, choose to apply the single-slice measurement approach to the temporalis muscle, as suggested by Weijs and Hillen [27]. This was due to the muscle's complex fan shape, which makes it challenging to discriminate a single slice in space with the highest CSA. Our two subjects' values correlate well with the CSAs found in the literature [22,26,37,38]. Our approach of determining a CSA for both the masseter superficialis and the masseter profunda separately, instead of the masseter as a single unit, resulted in a slightly larger total CSA due to the different angles at which the CSAs were measured for both muscle sections. This separation of both muscle sections is important since it results in two different insertion areas and thus different mechanical arm lengths, which have been found to have more impact than CSA variation [39]. This effect is most pronounced in the masseter muscle, so a case can be made that dividing the remaining elevator muscles would only impact the model's accuracy marginally. Although several authors subdivided the temporal muscle into two or three sections, no clear anatomical separation could be observed between such portions, making the temporal multiple force vectors rather arbitrary

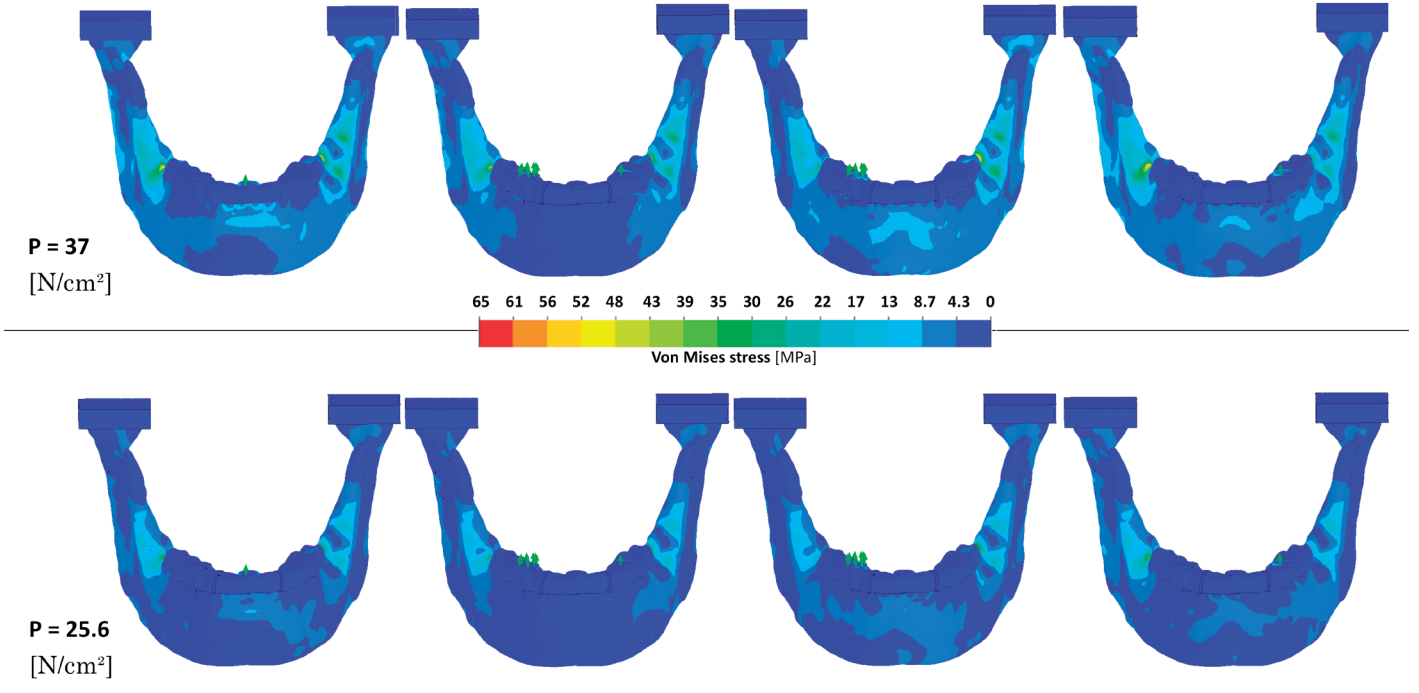

Figure 3 | Visualisation of the von-Mises stress occurring in all the FEA scenarios of our 56 y.o. subject. Left to right: incisal, bilateral premolar, unilateral premolar right, and unilateral premolar left bite.

in those cases [10,22]. Koolstra et al. [21], on the other hand, were successful and described a clear method on how to divide the temporal muscles into three sections.

An observation we made was the ratio between the total in vivo bilateral and unilateral bite force measurements. In both our subjects, the registered combined bilateral forces were approximately 40% (37% and 38%) higher. Several studies support this observation [33,40,41]. The majority of the available bite force measurements describe the molar bite positions. We also ran comparative analyses to determine the maximum theoretical bite forces for our subjects' molar positions using the muscle models with the patient-specific intrinsic strengths. The results from these analyses were corrected for unilateral bite using the aforementioned unilateral to bilateral ratio which should, by approximation, match the subjects' bite capacities. The FEA shows maximum corrected bite forces at the second molar position of around 365 N for the 56-year-old subject and around 613 N for the 29-year-old subject. These values lie within the range of healthy adults with natural teeth [41,42]. Bakke et al. described a normal incisal bite force of 120–240 [N] [43]. Our youngest subject's measures are within this range, whereas the measured force for the other subject appears rather low. Our subjects noted that regardless of the used splints, the incisal bite capacity was limited by a pain sensation around the teeth. According to our simulated incisal bite scenarios, based on the measured bilateral premolar bite, both our subjects should have been able to generate a higher bite force at the incisal position, as high as 271 and 371 [N] (Table 3). This suggests a biological inhibition which could be caused by signals from the receptors in the periodontal ligaments and mandible. This can inhibit muscle recruitment and thereby limit the generated bite force to prevent the anatomical structures from overloading [44]. The effect of local anaesthesia on the increase in bite force supports this thought [32,45]. We presume this has a greater effect on the incisal elements than on the (pre)molar elements due to their much smaller periodontal load-bearing surface, resulting in higher technical stress.

The current generally accepted intrinsic strength P values for the jaw elevator muscles in the literature are 37 and 40 [N/cm2] [19,21]. In our study, we derived P values in a subject-specific manner from FEA simulations, i.e., 25.6 and 40.6 [N/cm2] for the 56- and 29-year-old subjects, respectively. Since the MRIs were performed in maximum occlusion, our CSA measurements were performed on the corresponding muscle lengths. The bite force measurements were, however, registered at the physiologically optimum muscular length. Assuming a constant muscular volume results

in an over-approximation of the CSAs, thus giving an under-approximated intrinsic strength value. Weijs and Hillen [19] observed this as well in their experiments and suggested a gross correction. If one assumes constant muscular volume between occlusion and the physiologically optimum muscular length, a change in CSA can be calculated using the measured change in muscle length. Applying a correction factor of 10% and 15%, the measured mean muscle length difference between the occlusion and slightly opened mandible positions for our subjects resulted in a corrected P-value of 27.1 and 46.6 [N/cm2] for the 56- and 29-year-old subjects, respectively. This can be easily overcome for future cases by providing the subjects with splints that force the physiologically optimum mandibular muscular length while performing the MRI.

Even though our determined subject-specific intrinsic strength values correspond rather well with the values found in the literature, they show a broad variation between our subjects. This variation implies the necessity to determine the patient-specific capacity of the muscular system of the mandible. Our 56 y.o. subject's mandibular stress values were 63.8 [MPa] for P = 37 [N/cm2] versus 42.3 [MPa] in the corresponding P = 25.6 [N/cm2] scenario. In this case, the P = 37 [N/cm2] intrinsic strength, as was suggested in the literature, would have resulted in an overestimation of the muscle forces, leading to a stress increase of 51% in the analysis. Using the model to, e.g., design a PS implant or (TMJ) prosthesis, could result in a radical overestimation, i.e., too bulky or thick designs, of the final implant. Such overestimations lead to PS implants that are much stiffer than necessary which, in turn, is likely to result in stress shielding of the surrounding bone and could subsequently lead to screw loosening due to stress shielding-induced bone resorption [8]. Our 29 y.o. subject's corrected determined intrinsic strength is approximately 25% higher than that suggested in the literature. We simulated the reconstruction of a continuity defect in the mandible and found a comparable increase in the reconstruction plate's maximum occurring stress. Depending on the applied alloy and the actual maximum occurring stress value in the plate, this 25% stress increase could mean a decrease in a plate's life span of 10,000 to several million cycles [46], which would mean less than a week to several years of intensive loading [47].

We realise that following the protocol suggested by this study, as well as determining patient-specific intrinsic strength values, is time consuming and will therefore not always fit in with the scheduled treatment of a patient. Hence, future studies should aim to optimise and automate parts of the methods used in the protocol described

herein. For example, the delineation of the separate muscles is rather time consuming and could be overcome by applying a (semi) auto-segmentation tool. Another suggestion would be to simplify the bite force measurements by using a commercially available tool.

The variation in determined intrinsic strength values for our subjects in the current proof of concept implies that true clinical intrinsic strength determination is complex and dependent on multiple factors instead of merely the CSA of a muscle. With the results of our small cohort, presented here, we do not suggest a new general intrinsic strength value to replace the currently accepted P = 37 and 40 [N/cm2] values [19,21]. We did, however, observe the deviation between these values and the values we determined in this study, as well as the variation we found between our subjects. Therefore, it appears necessary to determine the intrinsic strength in a PS manner when critical biomechanical models or simulations are performed.

In the near future, we aim to start a study in which PS intrinsic strength determinations, as presented here, will be carried out for a large group of patients as part of the clinical evaluation. We aim to further study the spread of individual intrinsic strength values and to conclude if the intrinsic strength should indeed be calculated patient-specifically in all cases.

Conclusions

Despite using a small cohort in this proof of concept study, we show that there is great variation between our subjects' individual muscular intrinsic strength. This variation, together with the difference between our individual results and those presented in the literature, emphasises the value of our patient-specific muscle modelling and intrinsic strength determination protocol to ensure accurate biomechanical analyses and simulations. Furthermore, it suggests that average muscle models may only be sufficiently accurate for biomechanical analyses at a macro-scale level. A future larger cohort study will put the patient-specific intrinsic strength values in perspective.

Funding

No funding was received for this research.

Institutional Review Board Statement

Approval for this study was obtained from the Medical Ethics Board of the University Medical Center Groningen (METc 2016/388).

Informed Consent Statement

All the subjects provided written consent.

Acknowledgments

We are grateful to the subjects who volunteered for this study.

Conflicts of Interest

The authors have no conflict of interest to declare.

REFERENCES

1. Kraeima, J.; Merema, B.J.; Witjes, M.J.H.; Spijkervet, F.K.L. Development of a patient-specific temporomandibular joint prosthesis according to the Groningen principle through a cadaver test series. *J. Cranio-Maxillofac. Surg.* **2018**, *46*, 779–784.
2. Merema, B.B.J.; Kraeima, J.; Visscher, S.A.H.J.; Minnen, B.; Spijkervet, F.K.L.; Schepman, K.; Witjes, M.J.H. Novel finite element-based plate design for bridging mandibular defects: Reducing mechanical failure. *Oral Dis.* **2020**, *26*, 1265–1274.
3. Kraeima, J.; Glas, H.H.; Merema, B.B.J.; Vissink, A.; Spijkervet, F.K.L.; Witjes, M.J.H. Three-dimensional virtual surgical planning in the oncologic treatment of the mandible. *Oral Dis.* **2021**, *27*, 14–20.
4. Reina, J.M.; Garcia-Aznar, J.M.; Dominguez, J.; Doblare, M. Numerical estimation of bone density and elastic constants distribution in a human mandible. *J. Biomech.* **2007**, *40*, 828–836.
5. Narra, N.; Valášek, J.; Hannula, M.; Marcián, P.; Sándor, G.K.; Hyttinen, J.; Wolff, J. Finite element analysis of customized reconstruction plates for mandibular continuity defect therapy. *J. Biomech.* **2014**, *47*, 264–268.
6. Pinheiro, M.; Willaert, R.; Khan, A.; Krairi, A.; Van Paepegem, W. Biomechanical evaluation of the human mandible after temporomandibular joint replacement under different biting conditions. *Sci. Rep.* **2021**, *11*, 14034.
7. Oenning, A.C.; Freire, A.R.; Rossi, A.C.; Prado, F.B.; Caria, P.H.F.; Correr-Sobrinho, L.; Haiter-Neto, F. Resorptive potential of impacted mandibular third molars: 3D simulation by finite element analysis. *Clin. Oral Investig.* **2018**, *22*, 3195–3203.
8. Merema, B.B.J.; Kraeima, J.; Glas, H.H.; Spijkervet, F.K.L.; Witjes, M.J.H. Patient-specific finite element models of the human mandible: Lack of consensus on current set-ups. *Oral Dis.* **2021**, *27*, 42–51.
9. Weijs, W.A.; Hillen, B. Correlations between the cross-sectional area of the jaw muscles and craniofacial size and shape. *Am. J. Phys. Anthropol.* **1986**, *70*, 423–431.
10. Abdi, A.H.; Sagl, B.; Srungarapu, V.P.; Stavness, I.; Prisman, E.; Abolmaesumi, P.; Fels, S. Characterizing Motor Control of Mastication With Soft Actor-Critic. *Front. Hum. Neurosci.* **2020**, *14*, 188.
11. Wood, W.W.; Takada, K.; Hannam, A.G. The electromyographic activity of the inferior part of the human lateral pterygoid muscle during clenching and chewing. *Arch. Oral Biol.* **1986**, *31*, 245–253.
12. Farina, D.; Merletti, R.; Indino, B.; Graven-Nielsen, T. Surface EMG crosstalk evaluated from experimental recordings and simulated signals. Reflections on crosstalk interpretation, quantification and reduction. *Methods Inf. Med.* **2004**, *43*, 30–35.
13. Vigotsky, A.D.; Halperin, I.; Lehman, G.J.; Trajano, G.S.; Vieira, T.M. Interpreting Signal Amplitudes in Surface Electromyography Studies in Sport and Rehabilitation Sciences. *Front. Physiol.* **2018**, *8*, 985.
14. Weber, E. Muskelbewegung. In *Wagner, Handwörterbuch der Physiologie*; Bieweg: Braunschweig, Germany, 1846; pp. 1–122.
15. Nygaard, E.; Houston, M.; Suzuki, Y.; Jorgensen, K.; Saltin, B. Morphology of the brachial biceps muscle and elbow flexion in man. *Acta Physiol. Scand.* **1983**, *117*, 287–292.
16. Morris, C.B. The measurement of the strength of muscle relative to the cross section. *Res. Q.* **1948**, *19*, 295–303.
17. Haxton, H.A. Absolute muscle force in the ankle flexors of man. *J. Physiol.* **1944**, *103*, 267–273.

18. Franke, F. Die Kraftkurve menschlicher Muskeln bei willkiirlicher Innerration und die Frage der absoluten Muskelkraft. *Pflüg. Arch. Ges. Physiol.* **1920**, *184*, 300–323.
19. Weijs, W.A.; Hillen, B. Cross-sectional areas and estimated intrinsic strength of the human jaw muscles. *Acta Morphol. Neerl. Scand.* **1985**, *23*, 267–274.
20. Toro-Ibacache, V.; Zapata Munoz, V.; O'Higgins, P. The relationship between skull morphology, masticatory muscle force and cranial skeletal deformation during biting. *Ann. Anat.* **2016**, *203*, 59–68.
21. Koolstra, J.H.; van Eijden, T.M.G.J.; Weijs, W.A.; Naeije, M. A three-dimensional mathematical model of the human masticatory system predicting maximum possible bite forces. *J. Biomech.* **1988**, *21*, 563–576.
22. Peck, C.C.; Langenbach, G.E.; Hannam, A.G. Dynamic simulation of muscle and articular properties during human wide jaw opening. *Arch. Oral Biol.* **2000**, *45*, 963–982.
23. Hannam, A.G.; Stavness, I.; Lloyd, J.E.; Fels, S. A dynamic model of jaw and hyoid biomechanics during chewing. *J. Biomech.* **2008**, *41*, 1069–1076.
24. Sagl, B.; Schmid-Schwap, M.; Piehslinger, E.; Kundi, M.; Stavness, I. A Dynamic Jaw Model With a Finite-Element Temporomandibular Joint. *Front. Physiol.* **2019**, *10*, 1156.
25. Hannam, A.G.; Wood, W.W. Relationships between the size and spatial morphology of human masseter and medial pterygoid muscles, the craniofacial skeleton, and jaw biomechanics. *Am. J. Phys. Anthropol.* **1989**, *80*, 429–445.
26. van Spronsen, P.H.; Weijs, W.A.; Valk, J.; Prahl-Andersen, B.; van Ginkel, F.C. A comparison of jaw muscle cross-sections of long-face and normal adults. *J. Dent. Res.* **1992**, *71*, 1279–1285.
27. Weijs, W.A.; Hillen, B. Relationship between the physiological cross-section of the human jaw muscles and their cross-sectional area in computer tomograms. *Acta Anat.* **1984**, *118*, 129–138.
28. Cicchetti, D. Guidelines, Criteria, and Rules of Thumb for Evaluating Normed and Standardized Assessment Instrument in Psychology. *Psychol. Assess.* **1994**, *6*, 284–290.
29. Mackenna, B.R.; Turker, K.S. Jaw separation and maximum incising force. *J. Prosthet. Dent.* **1983**, *49*, 726–730.
30. Fields, H.W.; Proffit, W.R.; Case, J.C.; Vig, K.W. Variables affecting measurements of vertical occlusal force. *J. Dent. Res.* **1986**, *65*, 135–138.
31. Manns, A.; Miralles, R.; Palazzi, C. EMG, bite force, and elongation of the masseter muscle under isometric voluntary contractions and variations of vertical dimension. *J. Prosthet. Dent.* **1979**, *42*, 674–682.
32. van Steenberghe, D.; de Vries, J.H. The influence of local anaesthesia and occlusal surface area on the forces developed during repetitive maximal clenching efforts. *J. Periodontal. Res.* **1978**, *13*, 270–274.
33. van der Bilt, A.; Tekamp, A.; van der Glas, H.; Abbink, J. Bite force and electromyograpy during maximum unilateral and bilateral clenching. *Eur. J. Oral Sci.* **2008**, *116*, 217–222.
34. Samii, M.; Draf, W.; Lang, J. *Surgery of the Skull Base*; Springer: Berlin/Heidelberg, Germany, 1989; pp. 41–42.
35. Ramos, A.; Mesnard, M. A new condyle implant design concept for an alloplastic temporomandibular joint in bone resorption cases. *J. Cranio-Maxillofac. Surg.* **2016**, *44*, 1670–1677.
36. Tanaka, E.; del Pozo, R.; Tanaka, M.; Asai, D.; Hirose, M.; Iwabe, T.; Tanne, K. Three-dimensional finite element analysis of human temporomandibular joint with and without disc displacement during jaw opening. *Med. Eng. Phys.* **2004**, *26*, 503–511.

37. Toro-Ibacache, V.; Zapata MuNoz, V.; O'Higgins, P. The Predictability from Skull Morphology of Temporalis and Masseter Muscle Cross-Sectional Areas in Humans. *Anat. Rec.* **2015**, *298*, 1261–1270.
38. Langenbach, G.E.; Hannam, A.G. The role of passive muscle tensions in a three-dimensional dynamic model of the human jaw. *Arch. Oral Biol.* **1999**, *44*, 557–573.
39. Koolstra, J.H.; van Eijden, T.M.G.J.; Weijs, W.A. Three-Dimensional performance of the human masticatory system: The influence of the orientation and physiological cross-section of the masticatory muscles. In *International Series on Biomechanics 7-A*; Free University Press: Amsterdam, The Netherlands, 1988; pp. 101–106.
40. Tortopidis, D.; Lyons, M.F.; Baxendale, R.H.; Gilmour, W.H. The variability of bite force measurement between sessions, in different positions within the dental arch. *J. Oral Rehabil.* **1998**, *25*, 681–686.
41. Bakke, M.; Michler, L.; Han, K.; Moller, E. Clinical significance of isometric bite force versus electrical activity in temporal and masseter muscles. *Scand. J. Dent. Res.* **1989**, *97*, 539–551.
42. Hagberg, C. Assessment of bite force: A review. *J. Cranio-Maxillofac. Disord.* **1987**, *1*, 162–169.
43. Bakke, M. Mandibular elevator muscles: Physiology, action, and effect of dental occlusion. *Scand. J. Dent. Res.* **1993**, *101*, 314–331.
44. van Loon, J.P.; Otten, E.; Falkenstrom, C.H.; de Bont, L.G.; Verkerke, G.J. Loading of a unilateral temporomandibular joint prosthesis: A three-dimensional mathematical study. *J. Dent. Res.* **1998**, *77*, 1939–1947.
45. Orchardson, R.; MacFarlane, S.H. The effect of local periodontal anaesthesia on the maximum biting force achieved by human subjects. *Arch. Oral Biol.* **1980**, *25*, 799–804.
46. Fintova, S.; Dlhý, P.; Mertová, K.; Chlup, Z.; Duchek, M.; Procházka, R.; Hutař, P. Fatigue properties of UFG Ti grade 2 dental implant vs. conventionally tested smooth specimens. *J. Mech. Behav. Biomed. Mater.* **2021**, *123*, 104715.
47. van Loon, J.P.; Verkerke, G.J.; de Vries, M.P.; de Bont, L.G. Design and wear testing of a temporomandibular joint prosthesis articulation. *J. Dent. Res.* **2000**, *79*, 715–721.

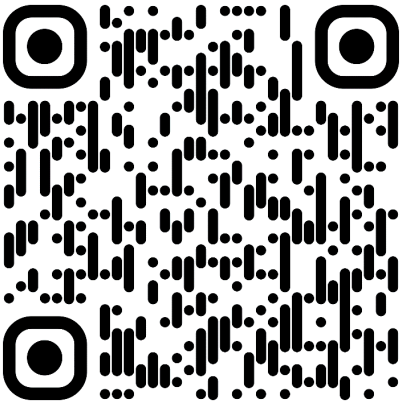

Supplementary video

Chapter 8

A topology optimisation based PEEK polymer mandibular implant design:

A non-metallic alternative for the reconstruction of large mandibular continuity defects

Bram B. J. Merema, Frederik K. L. Spijkervet, Joep Kraeima and Max J. H. Witjes

Department of Oral and Maxillofacial Surgery, University Medical Center Groningen, University of Groningen, Hanzeplein 1, 9700 RB Groningen, The Netherlands

INTRODUCTION

The preferred approach when reconstructing continuity defects of the mandible following tumour resection is generally to bridge the defect using an autogenous free vascularised bone flap, such as a fibula or scapula graft, which is fixated to the mandibular segments using osteosynthesis materials (OSM) in the form of rigid titanium reconstruction plates (RP) or mini plates. When patients are unfit to undergo a free vascularised bone flap reconstruction due to the poor quality of the donor site's vascularisation, an impaired medical condition or refusal to undergo major free vascularised bone flap surgery, the continuity defects are generally reconstructed with just a RP. These can either be manually contoured conventional plates or patient-specific implants (PSI). Reported complications in the reconstruction of continuity defects of the mandible using RPs are plate fracture, screw loosening, intra- and/or extra-oral plate exposure and stress-shielding[1-5].

As the human mandible is a complex and relatively high loaded anatomical structure, such reconstruction plates are made from high performing metals. The most used materials nowadays are commercially pure titanium and titanium alloys, as they are strong, lightweight, biocompatible and have a good resistance to fatigue. However, the titanium alloys used for mandibular reconstructions are also rather stiff when compared to the human cortical bone. These alloys have a Young's elastic modulus of approximately 110 GPa, whereas mandibular cortical bone remains around 4-20 GPa[6, 7]. As a result of this mismatch in material stiffness, the mandible can locally be subjected to under-straining upon postoperative loading of the reconstructed mandible as the neighbouring titanium is stiffer. This effect is called stress-shielding and, according to Frost's 'Mechanostat' principle, it can disturb the natural equilibrium of the local bone's strain values, and bone formation or resorption[8, 9]. As a result of stress-shielding, bone resorption can occur at or close to the bone-implant interface, ultimately leading to potential screw loosening and failure of the reconstruction[10].

Apart from the mismatch in elastic modulus between bone and the commonly applied titanium alloys, a limitation of titanium and other metallic plates is their interference with radiological imaging. Due to backscattering and metal streak artefacts, both postoperative radiological imaging and radiotherapy become suboptimal and less accurate since the signal gets absorbed or distorted due to the dense metallic material[11]. Moreover, most patients whose continuity defect has been reconstructed

after the removal of a malignity, subsequently undergo radiotherapy but the metallic reconstruction interferes with the delivery of photons or protons to the target tissues and inadvertently can increase the dose in the neighbouring areas. This complicates postoperative radiotherapy and the VSP of potential secondary reconstructions.

A solution for aforementioned limitations could be to develop a reconstruction made from a radiolucent material which is comparable in stiffness as the bone[11]. Such properties can be found in high performing polymers. Hence, polymeric implants have been discussed in the literature as potential substitutes for metallic OSM but, due to their limited strength compared to the common implant metallic materials, they are generally found unfit for the reconstruction of rather large and high loaded defects, such as a continuity defect of the mandible.

Typical examples of high performing biocompatible polymers are polyetheretherketone (PEEK) and polyetherketoneketone (PEKK), both found within the polyaryletherketone (PAEK) family. However, due to their mechanically inferior material properties, PEEK and PEKK are generally deemed unfit for highly loaded implant constructs[12]. Recently, an attempt has been made to manufacture a load bearing construct for the reconstruction of mandibular continuity defects, however, unsuccessful in terms of being able to withstand the physiological loading of the mandible[13]. In that study, a conventional strip-like plate was manufactured that was similar in shape to titanium reconstruction plates, which possibly may not have been the optimal design for a PEEK reconstruction. Alternatively, a geometrically optimal structure, designed to be manufactured from a high performing polymer, could provide a sufficiently strong load bearing construct. A method that can be used to obtain such a geometrically optimal structure is topology optimisation[14-16]. Using finite element analysis (FEA) combined with topology optimisation, a load driven design can be realised by means of a solid design space or volume from which material is removed from the lower stressed areas. This way, a design dedicated to the analysed material can be realised.

In order to thoroughly validate such a novel PEEK reconstructive PSI, we develop two apparatus, one for static experiments and one for dynamic cyclic loading. Using these, we obtain insights in both the ultimate strength and the fatigue behaviour of the PEEK reconstruction. We hypothesise that a full PEEK PSI, obtained through thorough finite element analysis and subsequent topology optimisation, can withstand the

in-vivo loading of the mandible and act as a substitute for current titanium plates in the reconstruction of continuity defects of the mandible.

MATERIALS AND METHODS

A representative deceased head and neck oncological subject with a class II Brown's[17] or Jewer L-type[18] mandibular defect was selected as an exemplar case. This 70-year-old male subject was edentulous and his mandibular body had already decreased slightly to a height of 22mm. The defect size was selected as it is most prone to failure, according to the Shibahara et al. study[5]. Based on experience, the design space, the boundary volume for the topology optimisation software, was designed at 2.5 mm and 8.5 mm lower than the resected segment at the posterior and anterior osteotomy sites, respectively to allow for space for proper soft tissue closure. A number of potential screw positions was chosen manually, in agreement with an experienced head and neck oncology oral and maxillofacial surgeon (MJHW). Based on the findings in our prior work[19], where adding screws in the osteotomy sites had a positive effect on the internal stresses in the implant, a stress-reducing screw was incorporated into both of our subject's mandibular. Two strategically chosen screws need mentioning; the bookshelf screw[19] and a newly defined dual locking sandwich-screw, which was designed to allow for a bi-cortical locking screw to be supported and locked on both the buccal and lingual side of the mandible. Due to this dual locking principle, the implant is supported on both sides of the mandible without applying resorption-inducing pressure to the sandwiched bone[20, 21]. This dual locking sandwich-screw can be inserted laterally after the guided pre-drilling of the screw pilot holes. (Figure 2). Initially, many screws, namely 23, were put in the FEA model so that any that proved unnecessary through topology optimisation could be removed at a later stage.

In order to approach the dynamic loading statically at various angles of the mouth opening, a number of scenarios was constructed. Four different mandibular orientations were chosen, i.e., maximum occlusion and 5- 10- and 15 degrees of mouth opening. Three bite positions were considered for each mandibular orientation, the incisal and left and right premolar regions. This resulted in a total of 12 different loading scenarios.

Table 1 | Muscle orientations and directions derived by means of delineation of the patient's MRI. The muscle forces were taken from the literature[23]. The three-dimensional force vectors were broken down into x, y and z components for both lateralities of the masseter superficialis (MS) and masseter profunda (MP), pterygoideus medialis (PM) and temporalis- anterior (TA), middle (TM) and posterior (TP) muscles. The Frankfurt horizontal plane (FHP) functioned as the x–z plane, with the positive x-axis pointing towards the left side of the mandible, the positive y-axis pointing cranially, and the positive z-axis pointing anteriorly. The origin of the coordinate system was set where the mid-sagittal plane coincided with the FHP.

			MS		MP		PM		TA		TM		TP	
			R	L	R	L	R	L	R	L	R	L	R	L
Literature based muscle model used in FEA models	Occlusion	x	-84,3	71,2	-20,5	18,2	53,7	-52,0	-36,0	32,6	-35,5	38,3	-55,2	56,8
		y	166,6	174,3	72,4	75,1	149,8	138,5	153,8	154,4	86,7	85,2	48,0	45,8
		z	37,7	28,9	31,9	26,3	72,5	93,3	5,6	8,6	-19,7	-20,6	-19,6	-20,1
		F.res	190,5	190,5	81,7	81,7	174,9	174,9	158,0	158,0	95,7	95,7	75,7	75,7
	5 Degrees opening	x	-90,6	78,0	-21,8	19,5	64,4	-62,1	-31,8	28,1	-34,9	37,8	-54,0	55,7
		y	163,7	171,7	72,7	75,4	147,4	137,1	154,7	155,3	87,1	85,8	49,6	47,4
		z	35,6	27,1	30,1	24,8	68,7	89,0	5,4	8,1	-18,6	-19,3	-18,9	-19,4
		F.res	190,5	190,5	81,7	81,7	174,9	174,9	158,0	158,0	95,7	95,7	75,7	75,7
	10 Degrees opening	x	-96,8	84,7	-23,3	20,9	74,5	-71,7	-28,9	24,8	-33,9	36,8	-52,7	54,5
		y	160,5	168,7	72,9	75,4	144,1	134,9	155,3	155,9	87,7	86,4	51,2	49,1
		z	33,9	25,5	28,6	23,4	65,3	85,2	5,1	7,5	-17,7	-18,2	-18,3	-18,7
		F.res	190,5	190,5	81,7	81,7	174,9	174,9	158,0	158,0	95,7	95,7	75,7	75,7
	15 Degrees opening	x	-103,0	91,4	-25,1	22,6	84,0	-80,7	-27,0	22,7	-32,7	35,6	-51,3	53,2
		y	156,9	165,4	72,8	75,3	140,2	131,9	155,6	156,2	88,3	87,1	52,8	50,8
		z	32,4	24,1	27,2	22,1	62,3	81,8	4,9	7,1	-16,9	-17,3	-17,7	-18,1
		F.res	190,5	190,5	81,7	81,7	174,9	174,9	158,0	158,0	95,7	95,7	75,7	75,7

Recently, we published a protocol for the 3D determination of PS muscle models of the jaw elevators[22]. This protocol combines MRI muscle delineation, bite force measurements and FEA in order to extract each specific PS muscle force. As we could not perform bite force measurements on the selected deceased subject, it was chosen to create a hybrid muscle model based on that protocol. This hybrid muscle model was obtained by combining the PS muscle orientations and directions together with the literature based maximum muscle forces[23]. Using the available MRI, the elevator muscles were delineated in the Brainlab 2020 software (Brainlab, München, Germany) and the origin and insertion sites were determined to find each muscle's acting direction in the form of a vector. These vectors were then scaled to match the muscle forces reported by Langenbach and Hannam[23], which were based on the work by Weijs and Hillen[24]. These muscle vectors were then recalculated for the 5-, 10- and 15 degrees mouth opening scenarios, by connecting the original muscles' origins on the skull to the insertion sites on the opened mandibles, resulting in a total of 48 unique muscle vectors. Table 1 shows the muscle vectors of this hybrid model for these scenarios at four different mandible orientations. It should be emphasised that our hybrid method uses literature based muscle forces for dentate patients and so are probably higher than this specific patient's were[22]. The Frankfurt horizontal plane (FHP) functioned as the x–z plane with its positive x-axis pointing posteriorly, the positive z-axis pointing towards the right side of the mandible, and the y-axis pointing cranially. The origin of the coordinate system was set where the mid-sagittal plane coincided with the FHP.

Following the prior PS muscle model determination protocol presented by Merema et al.[22], the muscle directions and forces were determined in a PS manner for comparison purposes. An intrinsic strength value of 37 N/cm² was used to convert the muscle cross-sectional area (CSA) from the MRI to muscle force[24]. Tables 2 and 3 describe this PS muscle model.

FEA was performed in Solidworks 2020 (Dassault Systèmes SolidWorks Corporation, Waltham, MA, USA). On each condyle, a single node was fixed in space (x, y & z) while, depending on the specific scenario, the bite region (circular area of 7mm^2) was fixed in only the z-direction, the caudal-cranial axis. Bonded intercomponent connections were chosen between all the touching components i.e., mandibular cortical and cancellous components, screw cylinders and the implant itself. The implant design space was designed to be offset at 0.1 mm to the bone and was connected to the mandibular segments by means of two-sectioned concentric cylinders to allow for a pin-

Table 2 | The cross-sectional areas (CSAs) that were determined from the MRI together with the specific muscle forces that were calculated using the intrinsic strength value (37 N/cm^2) taken from the literature[24].

Muscle	CSA [cm^2]		Muscle force [N] F = 37 * CSA	
	R	L	R	L
Masseter superficialis	4,1	3,6	152,4	134,3
Masseter profunda	2,1	2,3	78,4	86,2
Pterygoideus medialis	3,2	3,0	118,8	111,0
Temporalis	5,8	5,4	214,6	198,3

Table 3 | The three-dimensional force vectors that were used for the cyclic test were translated from the PS MRI measurements (Table 2). The muscle forces were broken down into x, y and z components for both lateralities of the masseter superficialis (MS) and masseter profunda (MP), pterygoideus medialis (PM) and middle temporalis (TM) muscles. The Frankfurt horizontal plane (FHP) functioned as the x–z plane, with the positive x-axis pointing towards the left side of the mandible, the positive y-axis pointing cranially, and the positive z-axis pointing anteriorly. The origin of the coordinate system was set where the mid-sagittal plane coincided with the FHP.

			MS		MP		PM		TM	
			R	L	R	L	R	L	R	L
Patient specific Cyclic test	15 degrees molar	x	-82,4	64,5	-24,1	23,9	57,1	-51,3	-73,3	73,8
		y	125,5	116,6	69,9	79,5	95,2	83,7	198,1	180,6
		z	25,9	17,0	26,1	23,4	42,3	51,9	-37,9	-35,8
		F.res	152,4	134,3	78,4	86,2	118,8	111,0	214,6	198,3

joint semi-contact to improve the optimisation quality after topology optimisation. The mandibular model was obtained through segmentation of the subject's CT-scan. The cortical portion was segmented in the Mimics 22.0 software (Materialise, Leuven, Belgium) and the inner cavities were assigned as cancellous bone. The homogeneously (isotropic linear elastic) mechanical properties of cortical bone (E = 14.7 GPa, ν = 0.3), cancellous bone (E = 400 MPa, ν = 0.3), Ti-6Al-4V titanium screws (E = 110 GPa ν = 0.31), PEEK (E = 3.6 GPa, ν = 0.4) were applied to the models, in agreement with the work by Mesnard and Ramos[25-29].

The results of all 12 FEA studies were exported in .INP format and imported into the ProTOp 6.1 software (CAESS, Maribor, Slovenia) for topology optimisation. The optimisation problem was set to minimum strain energy, to exhibit the lowest possible stress values. ProTOp assigns a weighing factor to each input FEA scenario, indicating the most dictating scenario in the optimisation process. In our study, the molar bite scenarios were the most dictating. After the topology optimisation was finished, resulting in an optimised implant within the provided design space and sufficient

for all 12 loading scenarios, the optimised structure was exported to the 3-Matic 15.0 software (Materialise, Leuven, Belgium) in STL format. Within 3-Matic, the design was optimised for 4-axis milling and finalised for manufacturing (Figure 1). Two identical implants were milled by Witec Medical (Stadskanaal, The Netherlands) from ZELLAMID® 1500 X PEEK (Senova, Uttendorf, Austria). The corresponding mandibular segments were manufactured and assembled to the PEEK implant using 2.7 mm ThreadLock locking screws (KLS Martin, Tuttlingen, Germany) before undergoing the static and cyclic mechanical testing (Figure 2).

Mechanical testing apparatus

As commercially available synthetic mandibles were developed for surgical training purposes, their mechanical properties deviate substantially from human bone, by a factor of 10-20[15]. Also, they are not manufactured patient-specifically, we found them to be unsuitable for our experiments. In order to allow for mechanical testing with PS shaped mandibles, we chose to develop a synthetic bone substitute. A mechanical tensile testing apparatus was developed for this purpose, the **m**andibular **uni**a**x**ial **c**ompression testing **app**aratus (MUNACAPP**)** device shown in Figure 3. The device mimics the mandibular elevator muscle forces in a simplified manner by means of one resulting force, which is applied to both mandibular angles, and is the most commonly found mandibular testing setup in the literature[15, 30-33]. Even though this is an oversimplification of the anatomical situation, it provides easily comparable data due to its minimalistic setup.

In order to carry out more anatomically correct loading experiments of the patient-specific mandible and corresponding muscle model, a mandibular dynamic bite simulator (MANDYBILATOR) apparatus was developed in-house. As the most common type of mandibular mechanical testing setup is oversimplified, as mentioned before, we decided to develop an apparatus that allows for individual mandibular muscle orientation and activation, thereby accurately mimicking the specific patient or subject's biomechanical situation. Eight elevator muscles were assigned to the current experiment: the masseter superficialis and masseter profunda, and the pterygoideus medialis and temporalis muscles from both lateralities. The pterygoideus lateralis muscles were not included as both condyles were not mobile in this experiment. Each muscle direction and force could be replicated by electro-pneumatically controlled muscles, which consisted of a bellow component (Festo, Esslingen am Neckar, Germany) and a load cell to measure the individual muscle forces. Aramide ropes, connecting the

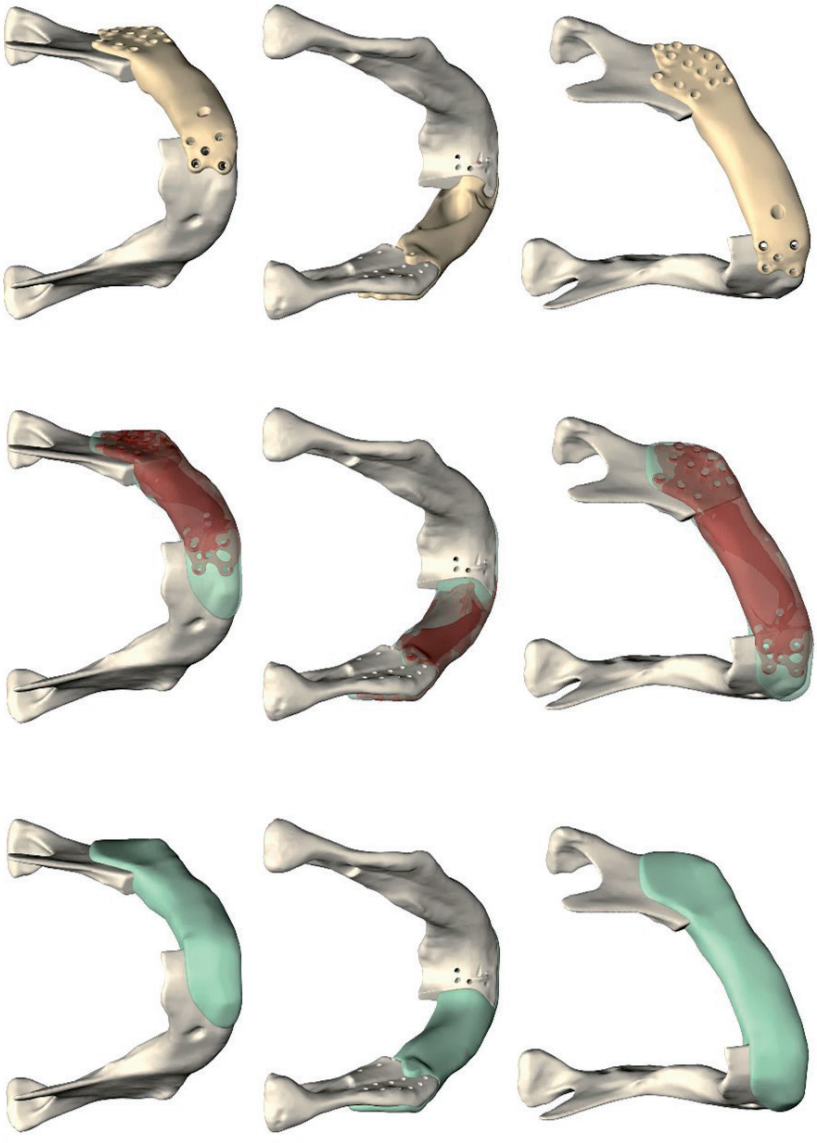

Figure 1 | Visualisation of the topology optimisation process. The design domain (green) on the left, the result of the topology optimisation (red) is in the middle and the finalised implant, adapted for manufacturing through milling (beige), is on the right.

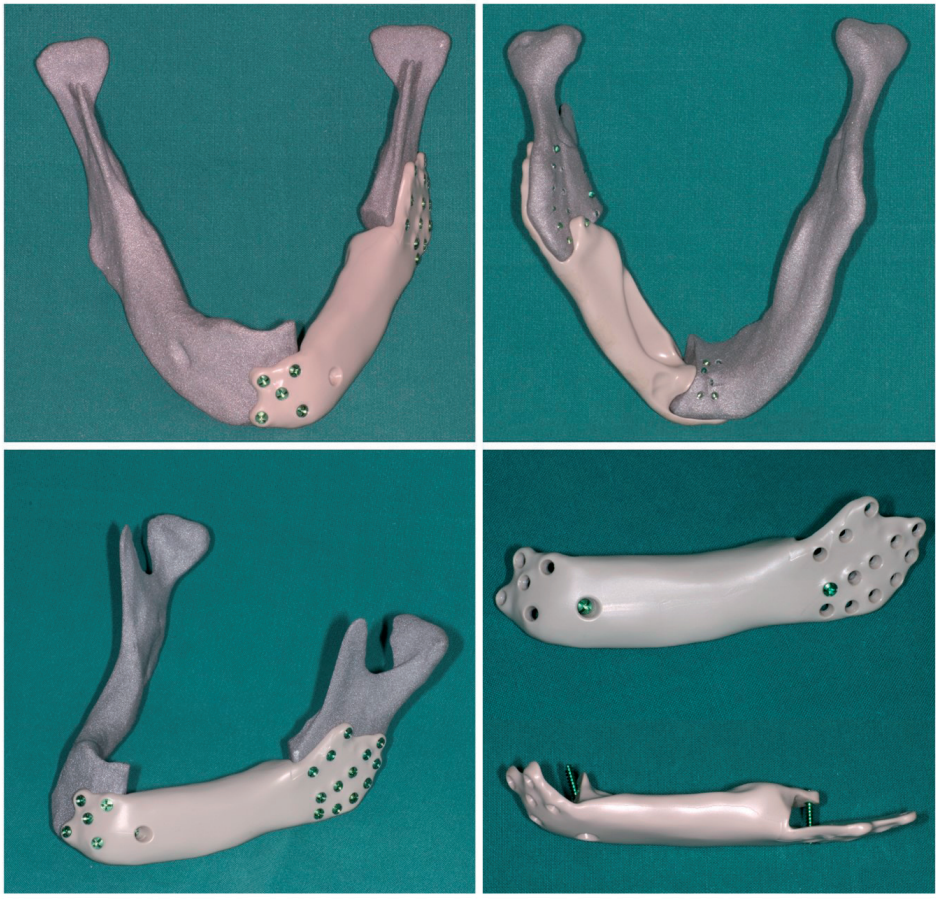

Figure 2 | One of the milled PEEK implants together with the In-VitroBone synthetic mandible. This sample was used for static testing on the MUNACAPP apparatus. The lower right image gives a good view of the two strategically placed screws.

artificial muscles to the muscle insertions, were glued to each muscle insertion area on the mandible, corresponding to the MRI data and FEA model. Both condyles were supported by artificial glenoid fossae, which were 3D printed polyamide cups (PA12, Oceanz, Ede, the Netherlands) with an imprint of the condyle connected to a seesaw construct to preserve the force direction. At the other end of the seesaw constructions, two load cells were applied to measure the resulting condylar forces. The mandible was constrained in the dental arch by means of a 3D printed (PA12) cup fixed to a sling around the alveolar process. Another load cell was applied to this sling, enabling bite force measurements. The sling could be positioned throughout the dental arch to accommodate for, e.g., incisal, canine, premolar or molar bite positions. The device

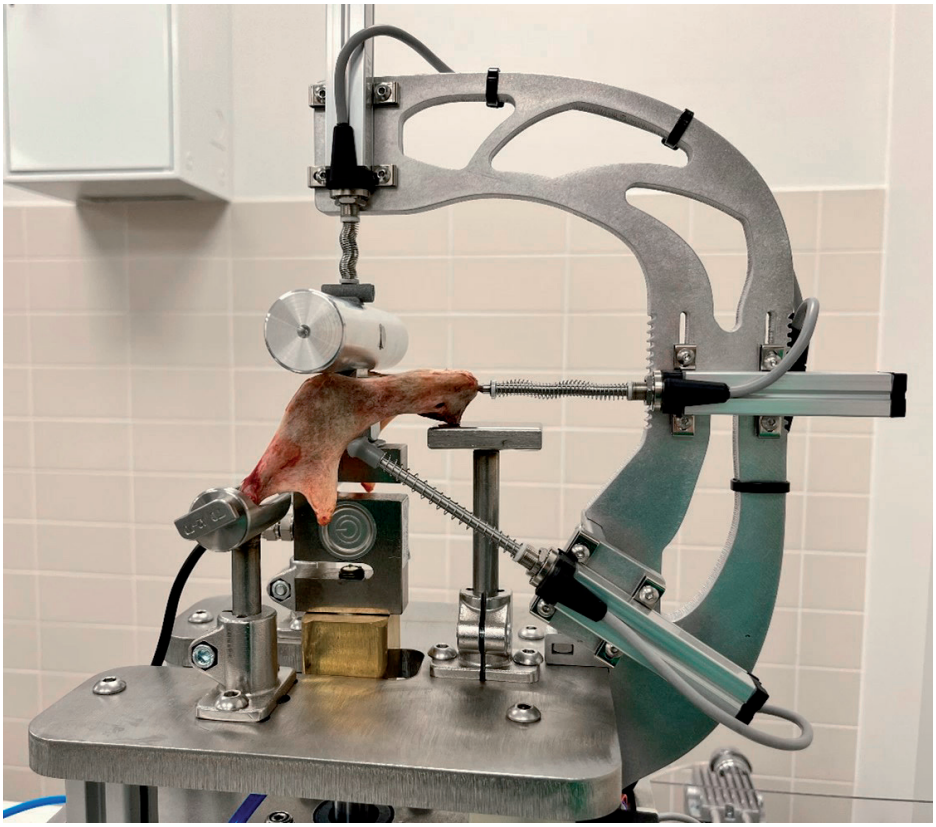

Figure 3 | A picture of the MUNACAPP apparatus ready for static uniaxial compressive testing of a cadaveric mandible.

could be deployed in both a static and a dynamic manner, enabling cyclic or fatigue testing.

A small series of fresh frozen human cadaveric mandibles were harvested, CT-scanned and frozen again. Using the CT images, synthetic, In-VitroBone clone mandibles were created. Tensile experiments were performed on the MUNACAPP apparatus by loading both the cadaveric mandibles and their synthetic In-VitroBone clones in the exact same manner. During the experiments the tensile force and corresponding vertical displacement as well as displacement at the pogonion and external oblique line of each mandible were measured and recorded. We found that the In-VitroBone mandibles failed within 1.5 percent of the ultimate tensile force of their cadaveric mandibles. Due to its lower Young's modulus of elasticity, the In-VitroBone tended to deform more prior to failure, as it was slightly less stiff than the anatomical man-

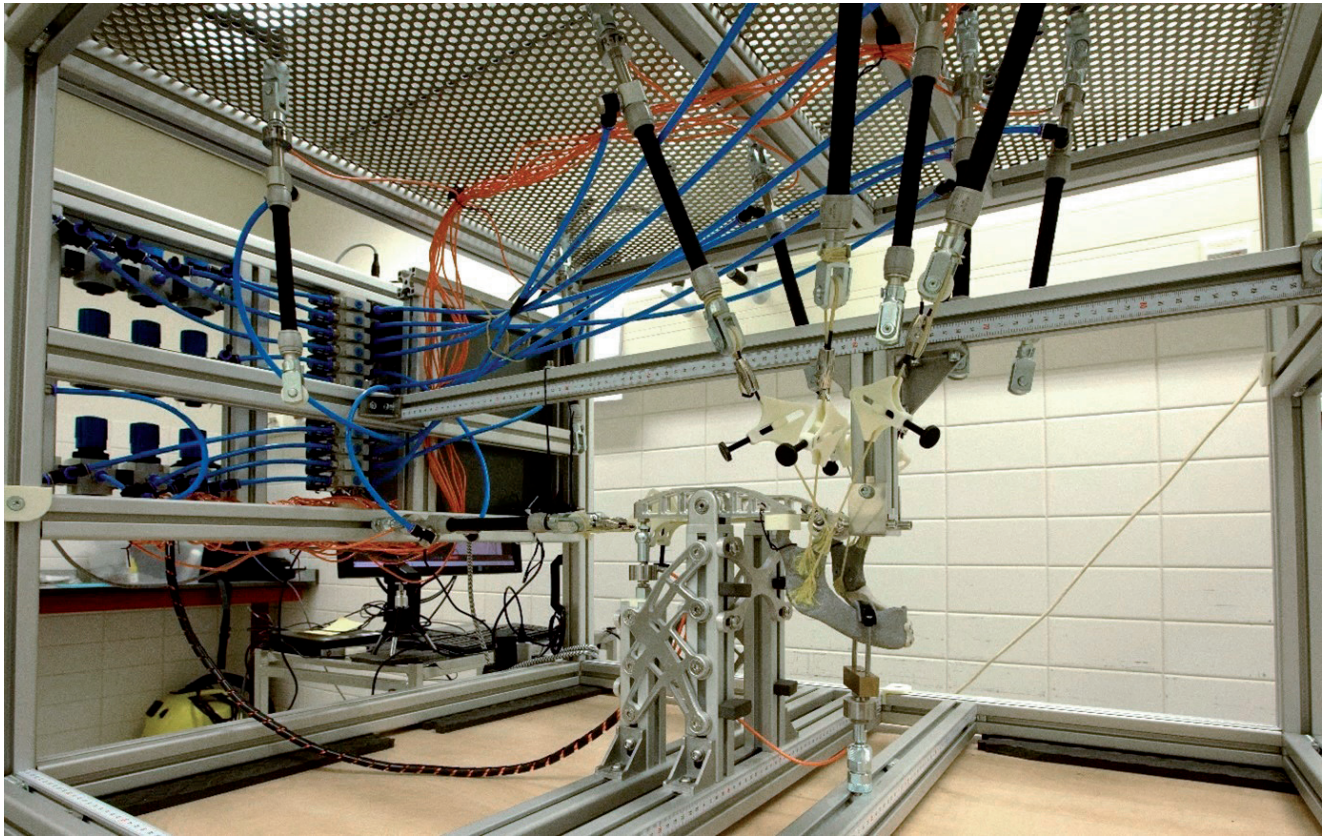

Figure 4 | Overview of the complete MANDYBILATOR apparatus with the mandible situated in the lower middle, the artificial muscles in the top middle and the electro-pneumatic controls on the left side.

dibular construct. This feature we were willing to accept as it introduced a worst-case scenario by loading the implant in a less favourable manner than the cadaveric bone. Figure 4 shows the MANDYBILATOR apparatus.

Validation of the apparatus

Directly after setting up the MANDYBILATOR apparatus with the PEEK implant reconstructed synthetic mandible test sample (see Figure 5), all the actuating muscle forces together with the resultant forces on both condyles and the bite force were measured to validate the apparatus. This was done in both a static and cyclic setting. A three second ramp load was recorded for static validation of the individual muscle forces and the resulting forces on both condyles and the molar bite position. All the recorded forces were then compared to their targets, i.e., the muscle forces that were inputs for the FEA model of the dynamic test situation (Table 2) and the resulting forces on both condyles and the molar bite position that were the results of this FEA.

Subsequently, a cyclic validation test was performed at a frequency of 1 Hz., the frequency of the dynamic experiment. In this test, the bite force and both condylar forces were measured and compared to the results of the matching predictive FEA.

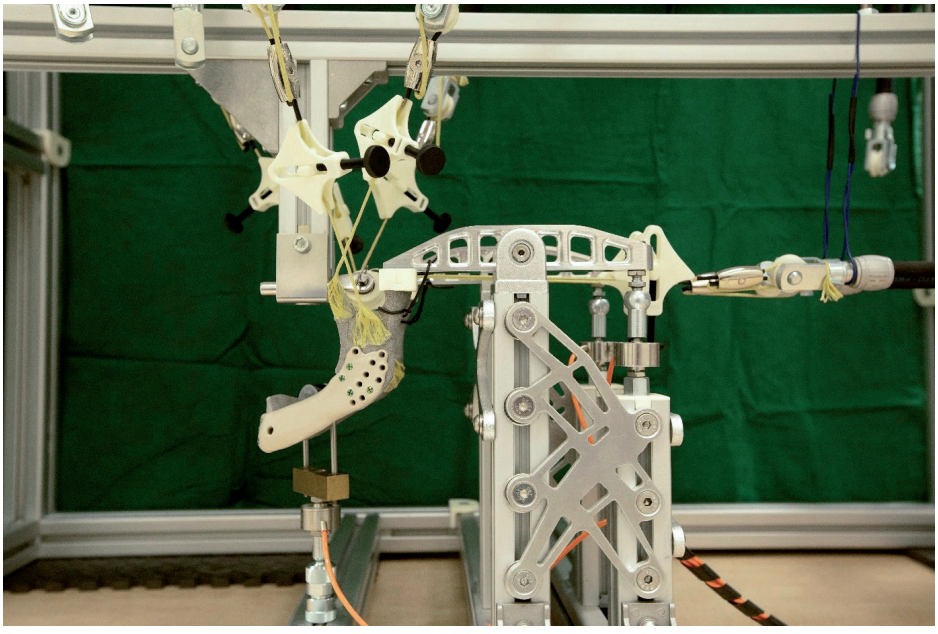

Figure 5 | Close up of the PEEK reconstructed mandible places inside the MANDYBILATOR apparatus, ready for cyclic testing.

This test was repeated directly after the initial experiment had finished, at 500,000 cycles, the equivalent number of chewing cycles with considerable bite force during approximately two years of in-vivo use[13].

Experiments

Two experiments, one static and one dynamic, were designed to assess the durability of the PEEK implants. The static ultimate performance experiment was performed first on the MUNACAPP apparatus. Three intact mandibles (n=3) and three exact duplicates with the continuity defect (n=3) were all manufactured from In-VitroBone. The continuity defects were reconstructed with the topology optimised PEEK implant and 2.7 KLS screws prior to testing in the static setup. The device was adjusted so that the mandibles rested on both condyles and the incisal position on the alveolar process was in an approximately occlusal orientation. A self-balancing round bar (D= 32 mm) was used to apply the vertical resultant muscle force to both mandibular angles equally. A pre-load of approximately 30 N was applied prior to each experiment. The load was gradually increased by approximately 17 N per second until failure occurred. Throughout the experiments, the applied vertical load (N) and displacement (mm) were registered together with linear displacements at the pogonion and mandibular lateral oblique line (mm). The applied force was registered by an S-type load cell while the displacements were measured through linear potentiometers. The ultimate load at failure was used as a measure of the mandible's strength while the ultimate displacements provided an insight into the stiffness of the mandible.

Subsequently, cyclic performance experiments were performed on the MANDYBILATOR apparatus, which had been developed in-house for this specific purpose. Another PEEK reconstructed In-VitroBone mandible was positioned in the occlusal orientation and the muscle vectors were adjusted in conformation with the vectors listed in Table 1 under *Occlusion, MRI CSAs.* The bite position was set to the right molar position at 15 degrees of mouth opening, as, according to the topology optimisation study, this represents the worst-case out of the 12 loading scenarios. The load was set to fluctuate from nearly 0 N to the subject's full bite capacity, as shown in Table 2, which is a semi-PS muscle model based on the subject's MRI CSAs, muscle directions and the intrinsic strength value of 37 N/cm^2 [24]. This resulted in the force components presented in Table 3. The load frequency was set to 1 Hz with 800 ms of 'muscle' activation, followed by 200 ms relaxation, for a maximum number of 500,000 cycles, which is in agreement with the experiments performed by Lang et al.[16]. According to

Schupp et al., this is equivalent number of chewing cycles with considerable bite force during approximately two years of in-vivo use[13]. All the inserted screws were marked using a marker prior to the dynamic experiment, allowing for the observation of early stage screw loosening. As the PEEK implant covered the insertion site of the master superficialis muscle, this muscle was not attached during the dynamic experiment in the MANDYBILATOR apparatus.

The cycle at which the reconstruction failed mechanically, irrespective of whether the cause was implant failure or screw loosening, was considered the final failure cycle.

Data collection and outcomes

The data was collected by an Arduino Mega microcontroller (Arduino, www.arduino.cc, accessed on 18th of April 2023) and written into a .CSV file in real-time. The program measured at a frequency of 10 Hz. and was programmed to loop 100 measurements followed by 900 skipped measurements, to maintain an acceptable file size.

RESULTS

Validation of the MANDYBILATOR apparatus

The ramp load, applied for static validation of the MANDYBILATOR apparatus, showed that all the set-up muscle forces lay within 1% of their target values, as depicted in Table 2. Figure 6 visualises this static validation.

The cyclic validation, performed both directly prior to and subsequently after the 500,000 cycles dynamic experiment, shows that the resulting forces on the bite position and both condyles, as measured in the MANDYBILATOR apparatus, resemble the FEA predicted values well. Prior to the 500,000 cycles dynamic experiment, the MANDYBILATOR showed forces of 139.2 N, 211.5 N and 468.3 N while the outcomes of the FEA predicted 150.6 N, 217.2 N and 475.2 N for the right condyle, left condyle and molar bite force respectively. This translates to an error of 6%, 2% and 0% respectively, between the FEA predicted values and experimentally measured values. Figure 7 visualises these results.

Directly following the dynamic experiment, the MANDYBILATOR measured forces of 154.1 N, 207.5 N and 450.3 N after 500,000 cycles for the right condyle, left

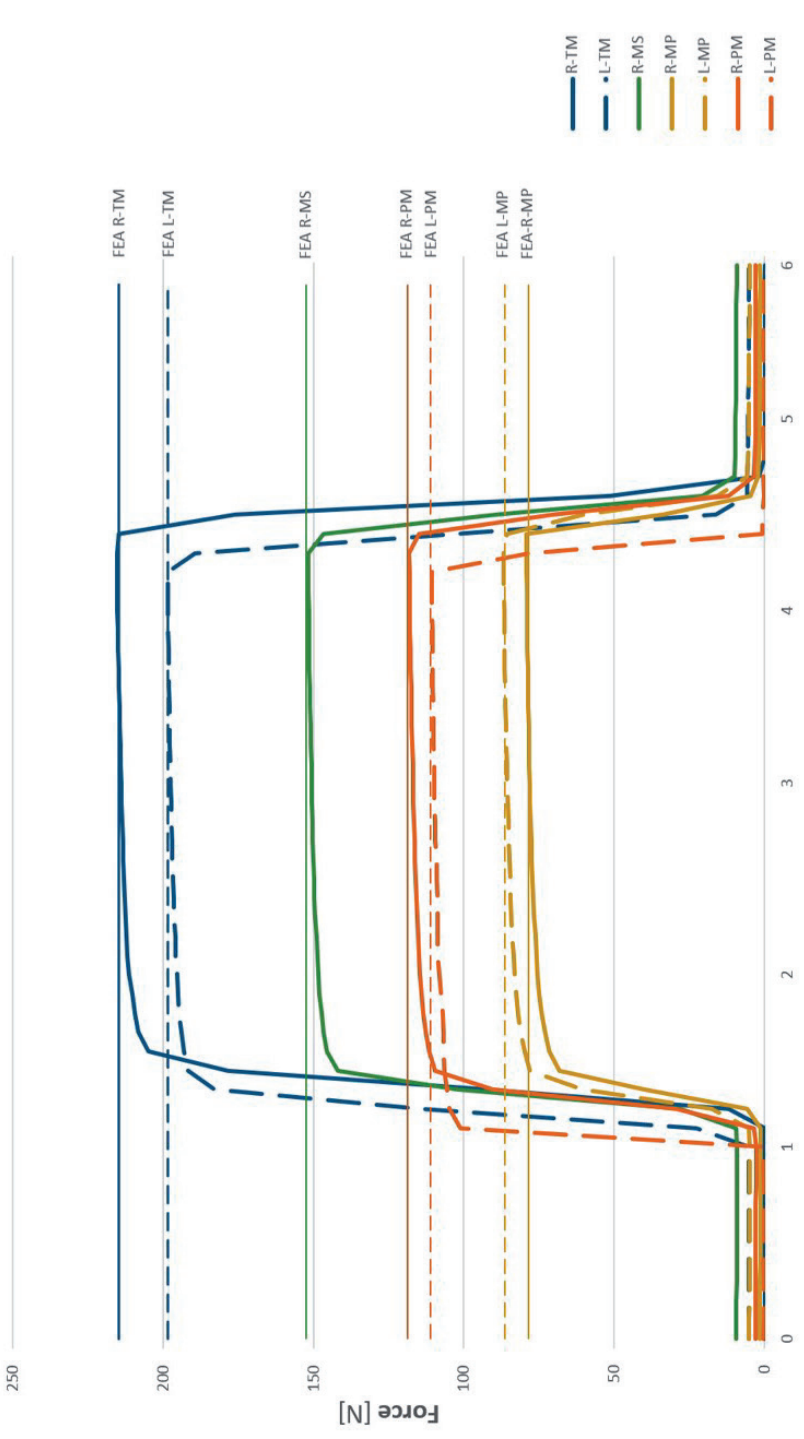

Figure 6 | Visualisation of the ramp-load used for the static validation of the MANDYBILATOR settings. The horizontal lines indicate the corresponding target values per muscle.

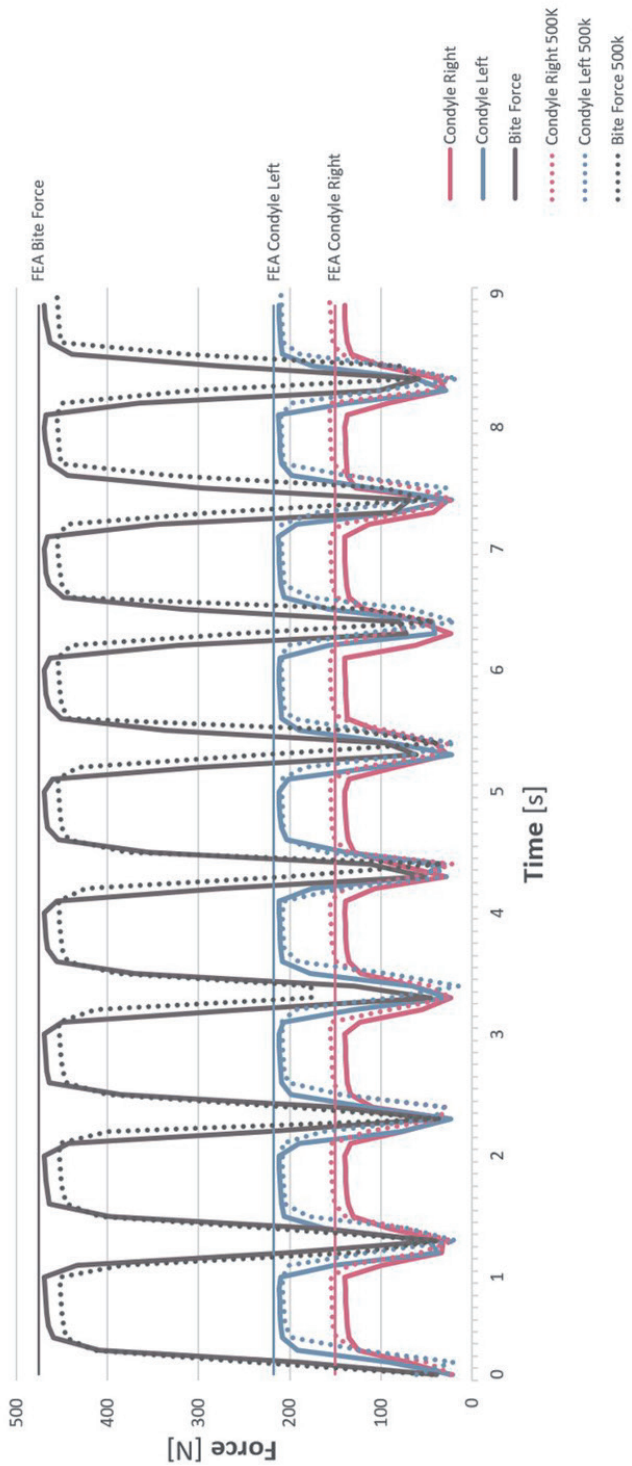

Figure 7 | Visualisation of the load cell outputs of both condylar forces and the molar bite force, generated by all the individually actuated elevator muscles of the MANDYBILATOR apparatus. The horizontal lines represent the corresponding forces that were derived from the FEA.

condyle and molar bite force, respectively. This indicates that the consistency of the MANDYBILATOR apparatus over 500,000 cycles lies within 10%.

Static experiments

The three intact synthetic In-VitroBone mandible clones that functioned as baseline samples in the static test experiments, all showed similar failure modes as in all cases the condylar neck (2x right, 1x left) failed under the ultimate load. Failure occurred at 1309 N, 1114 N and 1380 N for samples 1, 2 and 3, respectively.

The topology optimisation procedure objectively removed only one of the 23 suggested screw positions. The remainder six ventral and 16 dorsal screws were used for the first two static PEEK reconstructed mandible tests samples. This resulted in ultimate failure at 1108 N for PEEK sample 1 and 1094 N PEEK sample 2. It was then decided to only use four of the 16 dorsal screw positions in the third sample as this, clinically, would be a more reasonable number. PEEK sample 3 performed the best, failing at a load of 1212 N. In all three samples, the right condylar neck was the point of failure and the PEEK implants remained intact.

This resulted in a mean failure load of 1268 N (R:1114 – 1380 N) for the intact mandible samples and 1138 N (R:1094 – 1212) for the PEEK reconstructed samples.

The deformation of all six samples, three intact In-VitroBone mandibles and three PEEK reconstructed In-VitroBone mandibles, was measured at three corresponding points, i.e., the z-displacement of the force actuator, the external oblique line on the left side of the mandible and the pogonion. This resulted in a mean z-displacement of 3.36 mm (R:3.32 - 3.42) and 3.45 mm (R:3.27 - 3.81) for the intact and PEEK reconstructed In-VitroBone mandible samples respectively. The external oblique line measurements showed a mean displacement of 2.95 mm (R: 2.89 - 3.03) and 2.56 mm (R: 2.15 - 3.08) for the intact and PEEK reconstructed samples respectively and mean pogonion displacements of 2.98 mm (R: 2.25 - 3.62) and 2.96 mm (R: 2.39 - 3.42) for the intact and PEEK reconstructed samples respectively. Table 4 shows all the separate sample measurements. In Figure 8, all the displacements are plotted against the compression force actuated in the z-direction.

Table 4 | The results of the static uniaxial compression testing of the PEEK reconstructed In-VitroBone mandibles versus the intact In-VitroBone samples on the MUNACAPP apparatus. The ultimate compression force at failure was recorded together with the linear displacements at three points of the mandible: the z-displacement, which is the displacement of the load actuator, the external oblique line and the pogonion.

	Sample	Intact	PEEK
Force [N]	n1	1309	1108
	n2	1114	1094
	n3	1380	1212
	mean	1268	1138
Z-displacement [mm]	n1	3,32	3,27
	n2	3,42	3,27
	n3	3,33	3,81
	mean	3,36	3,45
External oblique line [mm]	n1	2,93	2,45
	n2	2,89	2,15
	n3	3,03	3,08
	mean	2,95	2,56
Pogonion [mm]	n1	3,07	3,42
	n2	3,62	2,39
	n3	2,25	3,08
	mean	2,98	2,96

Dynamic experiment

Regarding the fatigue experiment, it was decided to use only four out of the 16 screw options in the left ramus of the mandible as this appeared sufficient for the static experiment and also to stay close to the clinical situation. The PEEK reconstructed mandible survived the cyclic experiment and did not fail prior to the goal of 500,000 maximum molar bite force cycles, the equivalent of at least two years of in-vivo use. As the construct was still intact after the planned 500,000 cycle experiment had finished, it was decided to continue the experiment until failure occurred, or for1 million cycles. The experiment was stopped at 1.1 million cycles with no failure occurring or any visual signs of crack formation or screw loosening, as no rotation of the screw markings was observed.

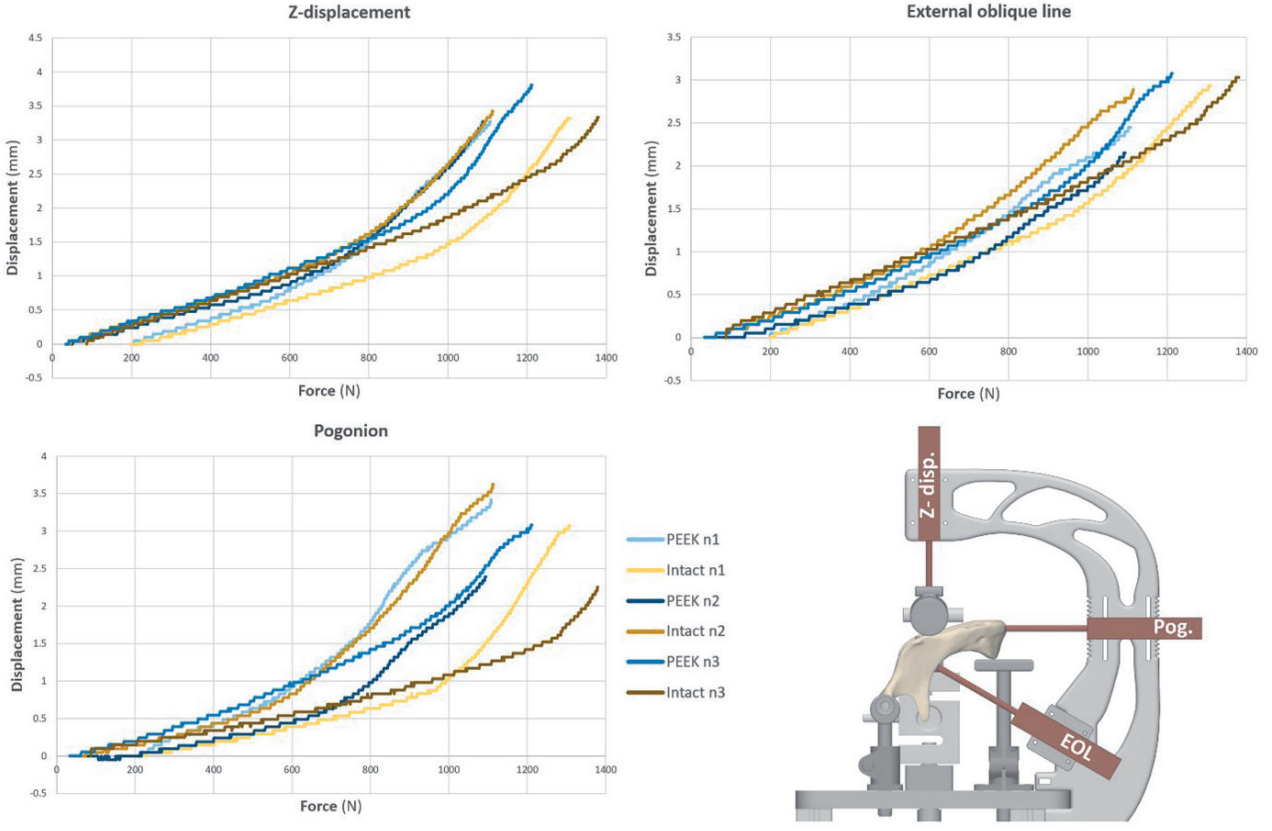

Figure 8 | Visualisation of the measured linear displacements at three positions on all the PEEK reconstructed mandible samples and all the intact mandible samples. The lower right image indicates the position and direction of the linear displacements.

DISCUSSION

This study revealed that a topology optimised PEEK PSI for the reconstruction of large continuity defects can withstand the in-vivo loading of the mandible and can act as a substitute for titanium plates in the reconstruction of continuity defects of the mandible.

Our static experiments show that the ultimate strength of the In-VitroBone mandibles that were reconstructed with the PEEK implant are comparable to the unreconstructed intact In-VitroBone mandibles. All the PEEK implants remained intact and the failure mechanism of the PEEK reconstructed mandibles was the same as in the intact non-reconstructed samples. In all cases, the condylar neck fractured under ultimate load. The dynamic, or cyclic, fatigue test we performed indicates that the PEEK implant is able to withstand multiple years (at least four/five years) of maximum in-vivo loading[13, 34], which can be considered as clinically a long term, beyond the phase where most RPs fail[4].

To the best of our knowledge, only one other study has reconstructed a mandibular continuity defect using a PEEK implant[13]. In that study, however, the implant shape was directly copied from a titanium plate and therefore not specifically designed to function when manufactured from PEEK. As a result, they observed implant failure occurring at a mean force of 592 N as opposed to a mean of 1138 N observed with the PEEK implant reconstructed mandibles in our current study. Lommen et al.'s cyclic loading study[13] is in line with a number of studies presented in the literature[30-32]. They applied 300 N distributed over both mandibular angles for 250,000 cycles without implant failure. This load of 300 N, however, is not a realistic worst-case scenario representation of the in-vivo loading of the mandible. As we wanted to test our PEEK implants under the patient's physiological maximum load, we applied the PS muscle model obtained from MRI to the PEEK reconstructed mandible in our MANDYBILATOR apparatus. When mathematically converted into a single load at both mandibular angles to enable comparisons with, e.g., Lommen et al.'s study[13], the load of our dynamic experiment was equivalent to approximately 798 N applied to the angles. This resulted in a bite force of 443 N at the molar position, much higher than can generally be clinically expected from an edentulous patient[35].

As topology optimisation was applied to optimise the implant shape to the PS load conditions and PEEK's material properties, we could easily input and combine a number of load conditions. We used twelve different load scenarios to mimic the mouth opening and the bite positions throughout the dental arch. Topology optimisation is relatively new to the field of reconstructive implant design, especially in Oral and Maxillofacial surgery, but shows excellent potential for this application[14, 32, 36, 37]. A great part of the otherwise subjective design process can be approached objectively and, using the correct PS inputs, e.g., muscle forces, directions and locations, leads to truly matching PS implants.

With the above in mind, we tried to objectify the otherwise subjective positioning of the implant screws. By adding a large number of screws (23), we expected the topology optimisation procedure would get rid of marginally loaded screw connections to the implant. This only worked in the front segment however, leaving 16 screws in the dorsal mandibular segment as the topology optimisation procedure had distributed the loads over all the potential screw positions. After manufacturing the PEEK implants and carrying out the first two static ultimate load tests, we only applied the four highest loaded screws to the third static test, according to our FEA analyses. This proved to be sufficiently strong, as this sample attained the highest ultimate load of all the PEEK samples in the static experiments. Therefore, we decided to perform our dynamic testing in line with this last static experiment and only used four screws in the dorsal mandibular segment, as it would represent the clinical situation realistically. Two screws proved important to the total strength and success of the PEEK reconstruction. The 'Bookshelf' screw, as we presented in earlier research[19], together with the new 'dual-locking screw', which locks into the implant on both the buccal and lingual side of the mandible, play a role in the implant's resistance against medial flaring of the left mandibular segment, as an effect of partial removal of the masseter, and the overall torsion of the mandible under load. Connecting screws to mandibular implants on both buccal and lingual side has been performed in the past but this has been associated with bone resorption around the screw and ultimately loosening [20, 21]. The main difference between these old applications of buccal bolts which were fixated lingually with nuts and our new 'dual-locking' principle, is that we added locking threads to both the buccal and lingual side of the implant, making it impossible for the screw to squeeze the mandible and initiate pressure related resorption.

The use of quasi-dynamic load scenarios to cover a range of bite positions and loading situations throughout the opening of the mandible in a FEA and subsequent topology optimisation appears to be an improvement over single static scenarios. In the current study, we applied different mouth opening positions and different bite locations in order to mimic the dynamic in-vivo bite options. By doing so, we found that the worst-case scenario, i.e., the scenario that influenced our PEEK implants design the most, was the molar bite due to amount of torsion this loading introduces into the implant in lateral continuity reconstructions. We therefore translated this load scenario to the dynamic cyclic test experiment.

As the subject of our exemplar case was already deceased, we could not determine the PS muscle model entirely conform our previously published protocol[22] due to lacking bite forces measurements. therefore, we chose to apply a slightly different muscle model to the FEA and subsequent topology optimisation, as was described in the Methods section. We used the PS MRI based muscle insertions and directions and combined these with the muscle forces from Langenbach and Hannam's study[23] to form a hybrid-muscle model, as these muscle forces are often reproduced in the literature as the input for FEAs of the mandible. Since we had tested intact In-VitroBone mandible samples to ultimate compression capacity, we were now interested in the equivalent compression force of this hybrid-muscle model, when translated to the MUNACAPP apparatus setup which we used for our static experiments. We found the equivalent compression force of 1364 N would represent our hybrid-muscle model. Comparing this value to the results of our static compression tests on the intact mandible models confirmed our expectations as two out of the three intact In-VitroBone mandible models had already failed, at 1268 N mean, prior to reaching the full force capacity of this hybrid-muscle model, with muscle forces taken from literature. This, together with the aforementioned ultimate strength of the In-VitroBone synthetic clones that matched the cadaveric mandibles within 1.5 %, indicates that the muscle models that are often reproduced in the literature and taken as input for mandibular experiments are not universally applicable and might drastically overestimate the specific patient's muscle model. This might be an obvious statement but it plays a big role in the underestimation of, e.g., PEEKs potential as a material for reconstructive implants.

According to van Kootwijk et al.[32], it is very challenging to mimic the in-vivo three-dimensional loading configuration of the mandible and simplifications are, therefore,

needed. This appears to be a popular conception in the literature, as performing uniaxial compression experiments on mandibles appears to be the golden standard[15, 30-33]. In such simplified experiments, the mandible is generally placed on condylar supports while supporting a point of preference in the dental arch. A bar is used to apply a compression force to both mandibular angles to represent the effect of all jaw elevator muscles. By doing so, however, all the individual effects that the separate muscles have on the mandible, and possible implant, are ignored. For example, the mediolateral force equilibrium, that exists between the mediolateral force components of the masseter and medial pterygoid muscles, is disturbed upon removal of (a part) of either of the muscles. In the literature, the effect of muscle removal on the resection side of the mandible is generally approached by offsetting the load distribution on the left and right mandibular angles. As this only changes the force distribution in predominantly the cranial-caudal direction, it does not mimic the mediolateral imbalance on the mandibular ramus. Therefore, we decided to develop a novel and more complex testing apparatus that allows one to add all the patient-specific elevator muscles and provides information beyond the oversimplified and generally accepted gold standard setup. The dynamic experiment successfully reached its target cycle count of 500,000, and the MANDYBILATOR apparatus showed no signs of failure and exorbitant wear. As mentioned in the results section, the resultant forces at both condyles and at the molar bite location did not deviate more than 10% from the initially setup values, which we consider consistent considering the number of influencing components and sensors. The 500,000 cycles target of the dynamic experiment was based on the highest number of cycles we found in the literature for mandibular testing[16]. The bulk of the cyclic experiments, generally using the aforementioned oversimplified uniaxial setup, ran up to a maximum of 250,000 cycles[15, 30-33] but the rationale behind this number of cycles was not presented. We expect this number was taken from a study in which the duration of the experiment was based on stress-strain curves for titanium or another metal in combination with a specific loading force. As we were not testing a metallic implant in the current study, we decided to use 500,000 as the target cycle count and even let the experiment continue to well past 1 million cycles (1.1 million). As already mentioned, this represents at least four to five years of maximum in-vivo loading[13, 34], where every moderate bite was assumed to represent the patient's maximum bite capacity. This is not the more likely scenario as the greatest amount of time is usually spent on chewing at lower pressures and higher pressures are only used for brief periods[38].

Within these four to five years, according to Maurer et al.[4], it is likely that if screw loosening were to occur in a reconstruction, it would have occurred already, within the first six months postoperatively. Also reconstruction plate failure due to metallic implants fracture generally occurs already within the first one to five years postoperatively[2, 5].

As PEEK has a number of derivatives within the PAEK family as well as composites[39-41], future work should aim to revaluate our choice for applying PEEK in this study and focus on gathering insights on the biological response of the hard and soft tissues to the implanted PAEK (composite) implant of choice. Cell adhesive potentials and antibacterial properties should be explored as we think these are important in the prevention of and coping with dehiscence of the reconstructions of continuity defects of the mandible. Furthermore, the effect of the implant-surrounding tissues on the irradiated implant after radiotherapy remains unknown and should be explored as well.

Conclusions

As hypothesised, a full PEEK PS implant obtained through thorough finite element analysis and subsequent topology optimisation, and provided with strategically placed screws, can withstand comparable forces to that of in-vivo loading of the mandible. It has the mechanical potential to act as a substitute for the current titanium plates used in the reconstruction of continuity defects of the mandible. This may potentially lead to optimised patient-specific reconstructions, with the implants matching the bone's stiffness and possessing radiolucent properties which are useful for radiographic follow-ups and radiotherapy. Furthermore, the addition of the dynamic/cyclic MANDYBILATOR apparatus to the common (static) uniaxial mechanical testing setup allows for more realistic application of the in-vivo loading of the mandible and can provide added insights in biomechanical behaviour of the mandible.

REFERENCES

1. Gellrich, N. C. *et al*. Comparative study of locking plates in mandibular reconstruction after ablative tumor surgery: THORP versus UniLOCK system. *J. Oral Maxillofac. Surg.* **62**, 186-193 (2004).
2. Katakura, A., Shibahara, T., Noma, H. & Yoshinari, M. Material analysis of AO plate fracture cases. *J. Oral Maxillofac. Surg.* **62**, 348-352 (2004).
3. Lopez, R., Dekeister, C., Sleiman, Z. & Paoli, J. R. Mandibular reconstruction using the titanium functionally dynamic bridging plate system: A retrospective study of 34 cases. *J. Oral Maxillofac. Surg.* **62**, 421-426 (2004).
4. Maurer, P., Eckert, A. W., Kriwalsky, M. S. & Schubert, J. Scope and limitations of methods of mandibular reconstruction: a long-term follow-up. *Br. J. Oral Maxillofac. Surg.* **48**, 100-104 (2010).
5. Shibahara, T., Noma, H., Furuya, Y. & Takaki, R. Fracture of mandibular reconstruction plates used after tumor resection. *J. Oral Maxillofac. Surg.* **60**, 182-185 (2002).
6. Vitins, V., Dobelis, M., Middleton, J., Limbert, G. & Knets, I. Flexural and Creep Properties of Human Jaw Compact Bone for FEA Studies. *Computer Methods in Biomechanics and Biomedical Engineering* **6**, 299-303 (2003).
7. Xin, P. *et al*. Material assignment in finite element modeling: heterogeneous properties of the mandibular bone. *The Journal of craniofacial surgery* **24**, 405-410 (2013).
8. Frost, H. M. Bone "mass" and the "mechanostat": a proposal. *Anat. Rec.* **219**, 1-9 (1987).
9. Frost, H. M. Bone's mechanostat: a 2003 update. *Anat. Rec. A. Discov. Mol. Cell. Evol. Biol.* **275**, 1081-1101 (2003).
10. Gefen, A. Computational simulations of stress shielding and bone resorption around existing and computer-designed orthopaedic screws. *Med. Biol. Eng. Comput.* **40**, 311-322 (2002).
11. Lommen, J. *et al*. Reduction of CT Artifacts Using Polyetheretherketone (PEEK), Polyetherketoneketone (PEKK), Polyphenylsulfone (PPSU), and Polyethylene (PE) Reconstruction Plates in Oral Oncology. *J. Oral Maxillofac. Surg.* **80**, 1272-1283 (2022).
12. Rendenbach, C. *et al*. Patient specific glass fiber reinforced composite versus titanium plate: A comparative biomechanical analysis under cyclic dynamic loading. *J. Mech. Behav. Biomed. Mater.* **91**, 212-219 (2019).
13. Lommen, J. *et al*. Mechanical Fatigue Performance of Patient-Specific Polymer Plates in Oncologic Mandible Reconstruction. *J. Clin. Med.* **11**, 3308. doi: 10.3390/jcm11123308 (2022).
14. Sutradhar, A. *et al*. Designing patient-specific 3D printed craniofacial implants using a novel topology optimization method. *Med Biol Eng Comput* **54**, 1123-1135 (2016).
15. Koper, D. C. *et al*. Topology optimization of a mandibular reconstruction plate and biomechanical validation. *J. Mech. Behav. Biomed. Mater.* **113**, 104157 (2021).
16. Lang, J. J. *et al*. Improving mandibular reconstruction by using topology optimization, patient specific design and additive manufacturing?-A biomechanical comparison against miniplates on human specimen. *PLoS One* **16**, e0253002 (2021).
17. Brown, J. S., Barry, C., Ho, M. & Shaw, R. A new classification for mandibular defects after oncological resection. *Lancet Oncol.* **17**, 23 (2016).
18. Jewer, D. D. *et al*. Orofacial and mandibular reconstruction with the iliac crest free flap: a review of 60 cases and a new method of classification. *Plast. Reconstr. Surg.* **84**, 391-5 (1989).
19. Merema, B. B. J. *et al*. Novel finite element-based plate design for bridging mandibular defects: Reducing mechanical failure. *Oral Dis.* (2020).

20. Winter, L. & McQuillan, A. S. Embedment of a Vitallium mandibular prosthesis as an integral part of the operation for removal of an adamantinoma. *The American Journ. of Surgery* **LXIX**, 318-324 (1945).
21. Freeman, B. S. The use of Vitallium plates to maintain function following resection of the mandible. *Plast. Reconstr. Surg. (1946)* **3**, 73-78 (1948).
22. Merema, B. B. J., Sieswerda, J. J., Spijkervet, F. K. L., Kraeima, J. & Witjes, M. J. H. A Contemporary Approach to Non-Invasive 3D Determination of Individual Masticatory Muscle Forces: A Proof of Concept. *J. Pers. Med.* **12**, 1273. doi: 10.3390/jpm12081273 (2022).
23. Langenbach, G. E. & Hannam, A. G. The role of passive muscle tensions in a three-dimensional dynamic model of the human jaw. *Arch. Oral Biol.* **44**, 557-573 (1999).
24. Weijs, W. A. & Hillen, B. Cross-sectional Areas and Estimated Intrinsic Strength of the Human Jaw Muscles. (1986).
25. Mesnard, M. & Ramos, A. Experimental and numerical predictions of Biomet((R)) alloplastic implant in a cadaveric mandibular ramus. *J. Craniomaxillofac. Surg.* **44**, 608-615 (2016).
26. Mesnard, M. *et al*. Biomechanical analysis comparing natural and alloplastic temporomandibular joint replacement using a finite element model. *J. Oral Maxillofac. Surg.* **69**, 1008-1017 (2011).
27. Ramos, A., Ballu, A., Mesnard, M., Talaia, P. & Simões, J. Numerical and Experimental Models of the Mandible. *Exp Mech* **51**, 1053-1059 (2011).
28. Ramos, A. M. & Mesnard, M. The stock alloplastic temporomandibular joint implant can influence the behavior of the opposite native joint: A numerical study. *Journal of Cranio-Maxillofacial Surgery* **43**, 1384-1391 (2015).
29. Ramos, A., Nyashin, Y. & Mesnard, M. Influences of geometrical and mechanical properties of bone tissues in mandible behaviour - experimental and numerical predictions. *Computer Methods in Biomechanics and Biomedical Engineering* **20**, 1004 (2017).
30. Schupp, W., Arzdorf, M., Linke, B. & Gutwald, R. Biomechanical testing of different osteosynthesis systems for segmental resection of the mandible. *J. Oral Maxillofac. Surg.* **65**, 924-930 (2007).
31. Gutwald, R., Jaeger, R. & Lambers, F. M. Customized mandibular reconstruction plates improve mechanical performance in a mandibular reconstruction model. *Comput. Methods Biomech. Biomed. Engin.* **20**, 426-435 (2017).
32. van Kootwijk, A. *et al*. Semi-automated digital workflow to design and evaluate patient-specific mandibular reconstruction implants. *J. Mech. Behav. Biomed. Mater.* **132**, 105291 (2022).
33. Gateno, J. *et al*. Biomechanical evaluation of a new MatrixMandible plating system on cadaver mandibles. *J. Oral Maxillofac. Surg.* **71**, 1900-1914 (2013).
34. Wu, C. H., Lin, Y. S., Liu, Y. S. & Lin, C. L. Biomechanical evaluation of a novel hybrid reconstruction plate for mandible segmental defects: A finite element analysis and fatigue testing. *J. Craniomaxillofac. Surg.* **45**, 1671-1680 (2017).
35. Tripathi, G. *et al*. Comparative evaluation of maximum bite force in dentulous and edentulous individuals with different facial forms. *J. Clin. Diagn. Res.* **8**, ZC37-40 (2014).
36. Lemón, L. Topology optimization process for new designs of reconstruction plates used for bridging large mandibular defects. (2016).
37. Li, C. H., Wu, C. H. & Lin, C. L. Design of a patient-specific mandible reconstruction implant with dental prosthesis for metal 3D printing using integrated weighted topology optimization and finite element analysis. *J. Mech. Behav. Biomed. Mater.* **105**, 103700 (2020).
38. Bates, J. F. & Stafford, G. D. Masticatory function-a review of the literature: (II) Speed of movement of the mandible, rate of chewing and forces developed in chewing. *J. Oral Rehabil.* **2**, 349-361 (1975).

39. Almasi, D. *et al*. Preparation Methods for Improving PEEK's Bioactivity for Orthopedic and Dental Application: A Review. *Int. J. Biomater.* **2016**, 8202653 (2016).
40. Zhao, M. *et al*. Response of Human Osteoblast to n-HA/PEEK--Quantitative Proteomic Study of Bio-effects of Nano-Hydroxyapatite Composite. *Sci. Rep*. **6**, 22832 (2016).
41. Ma, R. & Guo, D. Evaluating the bioactivity of a hydroxyapatite-incorporated polyetheretherketone biocomposite. *J. Orthop. Surg. Res.* **14**, 32-1 (2019).

Chapter 9

General Discussion

GENERAL DISCUSSION AND FUTURE PERSPECTIVES

This thesis describes both the development and implementation together with the evaluation and optimisation of 3D-virtual surgical planning (VSP) workflows and corresponding patient-specific implants (PSI) for oral and maxillofacial surgery (OMFS) purposes. The general aim was to optimise the first generation of digital PSIs and to implement a next level of patient-specificity to match the receiving patients' anatomy and physiology more closely.

The research in this thesis was carried out in order to:

- Recognise and resolve current mechanical failure principles in conventional and patient-specific implants (**Chapters 2 & 3**).
- Develop and validate a first generation of patient-specific Groningen TMJ-TJR prostheses and reconstruction plates (**Chapters 3-5**).
- Optimise the Groningen TMJ-TJR (**Chapter 6**).
- Suggest novel techniques to enable the development of the next generation of patient-specific implants and prostheses (**Chapters 6-8**).
- Present an in-vitro workflow to validate finite element models of the mandible and implants that were based on such models (**Chapter 8**).
- Develop and mechanically validate a non-metallic load bearing PEEK PSI for the reconstruction of large mandibular defects (**Chapter 8**).

Implementation of the above has led to improved 3D-VSP and subsequent improved placement accuracy PSIs and temporomandibular joint total joint replacement (TMJ-TJR) prostheses. The presented workflows enabled a higher level of tailoring of the PSIs and prostheses. Validation devices and workflows were also developed to enable the implementation of this improved tailoring after the current Ph.D.-thesis has been completed.

Oncological / Head and neck reconstructive surgery

Resection of the mandible, leading to continuity defects, is part of ablative surgery in the treatment of oral malignancies with bone ingrowth. The primary concern is to restore continuity of the remaining bone segments in the right orientation and to create a mechanically stable situation that allows for postoperative loaded oral function during mastication. These concerns have proven to be challenging, as was observed with conventional reconstructions using osteosynthesis materials (OSM) in

the last century, as described in **Chapters 2 & 3**. Intraoperative determination of the correct three dimensional orientation of the mandibular segments after a resection was challenging, resulting in suboptimal relationships between both the remaining mandibular segments and/or the remaining maxilla. The mechanically unstable reconstructions failed over time due to either screw loosening or plate fracture. The subsequently introduced of patient-specific reconstruction plates (PS-RPs), together with guided surgery, addressed both issues. We observed that most of the PS-RP's presented in the literature, are basically designed as a strip-like plate, positioned and fixated on the buccal contour of the mandible[1-6], which was found to be mechanically unfavourable in **Chapter 3** and, though not presented widely in the literature, could fail mechanically[2, 3, 7]. In **Chapter 3**, an alternatively shaped and fixated PS-RP, the so called 'bookshelf-plate', was presented and validated through finite element analysis (FEA). It should be mentioned that this type of PS-RP was and will only be considered for patients who are unfit to undergo reconstruction with a free vascularised bone flap, e.g., a fibula, due to the poor quality of the donor site vascularisation, an impaired medical condition or refusal to undergo major free vascularised bone flap surgery. This PS-RP design proved to be mechanically superior to the traditional straight plates that require manual contouring. The VSP and guided surgery procedure that was designed and presented in **Chapter 3** was validated by means of the accuracy of the implantations. It proved to be very effective with an Euclidean accuracy of approximately 1.5 mm, emphasising the value of the combination of VSP, guided surgery and PSIs. The addition of the 'bookshelf-plates' and their accompanying 'bookshelf-screws', resulted in nihil screw pull-out inducing micromotion at the bone-implant interface, an improvement compared to the traditional straight plates. Also, the stresses were relatively low due to the 'bookshelf-screws', thereby making screw loosening and plate fracture less likely.

Another concern when reconstructing a mandibular (continuity) defect is the effect of the fixated implant on the biological equilibriums in the mandible. Stress-shielding for example, may develop postoperatively and can, over time, make an initially well reconstructed mandible fail mechanically. Stress-shielding is the disturbance of the bone-formation equilibrium, often referred to with Frost's 'mechanostat'[8, 9] and is caused by implants being too stiff compared to the neighbouring bone it is fixated to. This results in an under-straining of the bone which subsequently leads to bone resorption and ultimately loosening of the implant. The current generally accepted materials for load bearing implants are titanium alloys. These alloys have an elastic

modulus of approximately 110 GPa whereas mandibular cortical bone remains around 4-20 GPa[10, 11]. To date, this discrepancy has not been resolved for such applications. The 'bookshelf' PS-RPs presented in **Chapter 3** also led, in some cases, to local stress-shielding although, up to now with a current follow-up period of 4.5 – 6.3 years, never to reconstruction failure. According to Maurer et al. [12], it is likely that if screw loosening were to occur in a reconstruction, it would occur within the first six months postoperatively. Reconstruction plate fracture generally occurs within the first one to five years postoperatively[13, 14].

During this thesis' journey, although not part of the study outcome measures, we observed that under-contouring of the 'bookshelf' PS-RPs would not exclude dehiscence of the titanium alloy implants used to reconstruct large continuity defects of the mandible. The intra- and extra-oral dehiscence of a plate is thought to be initiated by contraction of the surrounding soft tissues, because of postoperative irradiation of the area. Currently, 22 patients have been reconstructed with a 'bookshelf' PS-RP, as described in **Chapter** 3. The initial tension relief we implemented in our 'bookshelf' PS-RP design through under-contouring of the implant turned out to be insufficient in preventing dehiscence to occur in six cases (27%). There, the tops of the flanges had become dehiscent intraorally. This was resolved by reintervention with intraoperative recontouring of the dehiscent part, thereby relieving the soft tissue, up to the level where the bone could carry the soft tissue. As plate dehiscence is a well-known and reported post-reconstructive complication[15-17], occurring in up to 46% cases, we think this is not exclusively a design/shape related complication but perhaps a material-related issue. Others have postulated that reconstruction of a mandibular defect by means of a plate should be accompanied by adequate filling of the defect with a voluminous soft tissue flap[15]. The generally applied titanium alloys are known to be biocompatible, can osseointegrate and have been proven for many applications inside the body. However, in the irradiated patient, these properties alone do not seem to prevent dehiscence from occurring. Perhaps because the irradiated and damaged soft tissues do not adhere to the implants, as discussed in the literature[15].

Solutions to this complication should be sought in other implant materials, or at least the outer boundary layer of the implant by, e.g., using bio-coatings, or by means of reducing the destructive effect of radio therapy on the soft tissues in the reconstruction site. The latter can, potentially, be realised through, e.g., the use of proton-beam irradiation, a rather novel technique which can be applied more locally. What prevents

this technique from being applied to patients with a reconstructed continuity defect, however, is the amount of metal within the current reconstructions, which can change the local dose distribution. Metallic plates have backscattering effects which cause overdosage of the tissue in front of and underdosage of the tissue behind the plates, and can obstruct the localised proton beams[18-20]. Again, this results in the need for a change of implant material for cases with these indications, or at least for an alternative to the known metallic reconstructive implants.

Temporomandibular joint replacement surgery

This thesis presents a continuation of the development of the Groningen temporomandibular joint-total joint replacement (G-TMJ-TJR) PS prosthesis. The prosthesis was developed according to the Groningen principles, which includes a 15mm lowered centre of rotation together with separated translation and rotation sites[21]. The initial product was translated from the stock, confection sized and turned into a PS version that could be applied with current techniques, i.e., VSP and guided surgery (**Chapters 4 & 5)**. The stock version consisted of six components of which four needed to be selected intraoperatively based on the patient's bony anatomy[22]. A total of 72 possible combinations could be realised with all the available confection sized components. Drilling of the screw pilot holes and the condylectomy were performed free-hand and the end result was only visible when the procedure was finished. The complexity of the surgical procedure and the number of individual prosthesis parts, which must be perfectly aligned in order to function as planned, make stock TMJ-TJRs prone to errors. The work described in **Chapter 5** resulted in a design that matches the patient's anatomy perfectly, and a workflow that confines all the dimensional considerations to the preoperative VSP. Translation of the VSP to the operating theatre occurs by means of surgical guides which are fixated to the hosting bone area to maintain a proper inter-screw relationship and to allow for reliable non-orthogonal screw entry points.

Recently, a rapid increase in different TMJ-TJRs, predominantly PSs, has been presented in the literature. A recent review showed 27 different available prostheses, of which 22 were based on the two well-known designs: the custom Stryker-TMJ-Concepts[23] (Ventura, CA, USA) and the stock Biomet-Zimmer[24] (Warsaw, IN, USA) prostheses[25]. However, most of these prostheses lack their own validation studies and some are placed with the aid of non-screw-fixated surgical guides. Since information on the accuracy of TMJ-TJR prostheses placement is lacking and accurate positioning of a TMJ-TJR is crucial for TMJ-TJRs to function as planned, we performed a valida-

tion study in human cadavers with 10 prostheses (**Chapter 5**) and in the clinical setting with 11 prostheses (**Chapter 6**). This resulted in a Euclidean accuracy of around 1 mm (0.8 / 1.1 resp.) for prosthesis placement when the physical positioning was compared to the 3D VSP. Accurate positioning of a prosthesis is not only beneficial for the initial stability and function of the device but also improves osseointegration, enabling long-term stability[26, 27]. Another important aspect of positioning, which is generally overlooked in the literature, is the effect of mispositioning on the wear behaviour of the device's bearing sites. What 23 of the 27 aforementioned prostheses have in common is that their articulation occurs between a concave fossa component and a convex shaped mandibular component (Figure 1). When positioned perfectly according to plan, there is a rather large load bearing area between the two, thereby distributing the contact force. However, when marginally misaligned, this large contact area becomes a point contact, thereby increasing the local stress exorbitantly on the usually ultra-high molecular weight polyethylene (UHMWPE) material, resulting in a seriously reduced wear-life and increased wear particle formation of UHMWPE in the joint[28, 29]. The latter causes a reduced lifetime of such a prosthesis. Based on the results of our accuracy studies, and not mentioned in literature, is that, apart from these point contacts, an approximate 1 mm accuracy (perhaps more in different systems) can result in gaps between the fossa- and mandibular components from time to time. When this occurs, there is no back-up solution available for all the aforementioned reviewed PS prostheses, except the G-TMJ-TJR, and the unplanned gap between the two components remains. Clinically, this could cause malocclusions

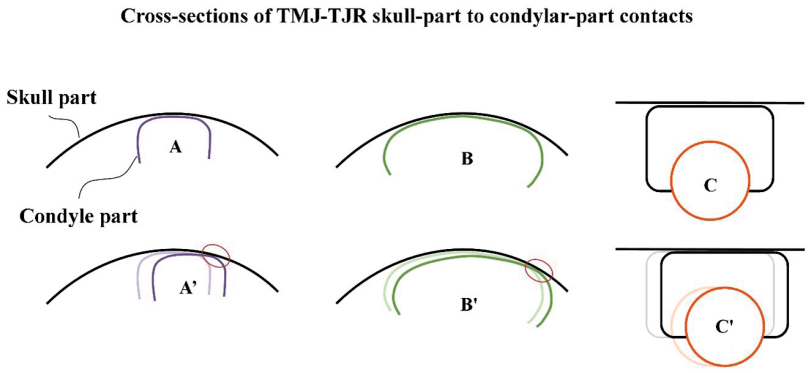

Figure 1 | Schematic examples of two prostheses with a non-spherical/non-matching contact set (A and B) at the neo-condyle to fossa component articulation site and the G-TMJ-TJR (C) with a spherical/matching contact set. The cross-sectional views illustrate the effect of a marginal shift of the neo-condylar position (A', B' and C') relative to the neo-fossa, which results in a point contact (circle) in A' and B' and increasing material stress. Note that shifting has no influence on the contact in situation C' [30].

and or unnatural loading of the mandible. Knowing the accuracy of our Groningen-TMJ-TJR device placement procedure provided us with the opportunity to add interchangeable backup neo-discs. These are 1 and 2 mm higher than the planned neo-disc height, thereby preventing gaps from occurring.

The physiological movement of the mandible is complex, with simultaneous rotation and translation movements meeting in the TMJ. When performing TMJ-TJR surgery, the condyle, or its remnants, is resected to create space for the artificial joint. By doing so, the insertion of the lateral pterygoid muscle on the condyle is lost, thereby rendering the muscle, responsible for the translation movement of the mandible, inactive. It is reported that following a unilateral TJR of the TMJ, the translational capacity of the joint disappears almost completely[31], resulting in asymmetrical mouth opening movements that deviate towards the prosthetic side. In order to mimic the physiological movements of the mandible after TJR, this lost translation should be compensated one way or another. Such physiological principles are not present in any of the well-known TMJ-TJRs. However, one of the possibilities is to lower the centre of rotation (CR) by 15 mm (the Groningen principle) with respect to the anatomical centre of the condyle, which was included when designing the G-TMJ-TJR. By lowering the CR, a pseudo-translation can be created[31]. Van Loon et al. determined that a lowered CR of 15 mm would give the optimal centre of rotation position[31]. However, a 15mm lowered CR did not prove sufficient in the clinical setting for some of the patients we provided with a G-TMJ-TJR, and (partial) asymmetry in mouth opening remained. Mimicking the physiological mouth movements in TMJ-TJR remains challenging and only little effort has been made over the last two decades to improve the post TMJ-TJR movements. Since technology has become more advanced and easily available since van Loon et al.'s measurements in 1999, we decided to develop a method to quantify the mouth opening in patients with 4D imaging and to determine the PS' optimal CR that should be applied in a TMJ-TJR device to restore the physiological mouth opening movement. We tested it on 20 patients with healthy TMJs and found the mean CR position was lowered by 28 mm rather than 15 mm. Implementing a 15 mm lowered CR into the TMJ-TJR device design can, however, be challenging in some cases due to disease related anatomy changes, restrictions for surgical approaches and limited space in-situ. Therefore, the results in **Chapter 6** do not appear to be directly applicable to the G-TMJ-TJR prostheses, or to the Stryker-TMJ-Concepts, the Biomet-Zimmer or any of the other 24 devices presented in the literature. A change of concept and, more precisely, a change in the applied kinematic

principles within the G-TMJ-TJR prosthesis, or any other future device, is necessary in order to comply with all the CRs we determined for the cohort in **Chapter 6**.

To conclude the work performed in **Chapters 4**, **5** and **6**, the use of screw-fixed surgical guides for the placement of TMJ-TJRs enables highly accurate positioning and makes both the surgical procedure and the postoperative function of the TMJ-TJR prosthesis more predictable. Furthermore, a lowering of the CR compared to the centre of the anatomical condyle should be applied in a TMJ-TJR prosthesis in order to mimic the physiological mouth opening more closely. When it is not possible to measure the CR location patient-specifically, a lowered CR of 15 to 28 mm should be applied.

Finite element model improvement for PSIs

To minimise the lacking PS inputs, which are generally substituted by generic non-PS parameters, used in FEA and subsequent in-vitro testing of the mandible, a workflow to determine individual muscle models of the mandible for a PS was presented in **Chapter 7** of this thesis. By combining the available techniques, such as MRI, CT segmentation and muscle delineation, and combining them with precisely set up bite force measurement experiments, we are now able to determine all the individual muscle forces contributing to a patient's maximum loading situation. As a result of this technique, PSIs can now be developed to cope with PS muscle models rather than only matching the shape of the bony interface of the mandible. Modelling a patient specific system entails perspective and expectations.

Without a PS muscle model, an engineer must consider the generally highest loads found in a population. In case of a highly resorbed edentulous mandible this would result in an implant that is able to withstand forces that even the (unreconstructed intact) resorbed mandible cannot cope with. In **Chapter 7**, proof of this concept was presented and tested out on two subjects. It already showed the potential deviation between individual subjects, which strengthens the case of using PS muscle models for PSI development. The variation in determined intrinsic strength values between individuals suggest that muscle force, when calculated with $F_{muscle} = P \cdot CSA$ [N], is not only dependent on the muscle's cross-sectional area (CSA) but also on the intrinsic strength (P). Thus, the intrinsic strength should be determined patent-specifically as well. This is in contrast to its use in the literature, where fixed values are generally used[32-36]. The main drawback, currently, is the labour intensity of our presented

workflow. This still prevents the PS muscle force determination from being part of the routine in the clinical setting. By optimising and automating (parts of) the workflow, we intend to resolve this drawback. Furthermore, future work should study a larger cohort to provide insight into the variety and range of the intrinsic strength values.

In-vitro validation of the FEA improvements

The bone substitutes, used in mechanical tests to judge an implant's strength or to compare different osteosynthesis materials (OSM) systems, are typically designed for surgical skill practice in bone cutting and drilling techniques. The mechanical properties of such synthetic bones have a mismatch of approximately 10-20 times in elastic modulus with the human mandible bone[10, 11, 37, 38]. As they were never designed to mechanically mimic the bone, they should not be used as mechanically correct clones of the human mandible in in-vitro testing of implants.

During this thesis, a mechanically correct synthetic bone substitute that can be produced patient-specifically and can withstand the physiological loading of the mandible was explored. Even though this is ongoing research, we managed to combine a material and an internal structure, we call In-VitroBone, that results in a PS synthetic mandible which is able to withstand the PS physiological muscle forces while failing within a very acceptable 1.5% of the failure force of the matching cadaveric mandible. Under this ultimate load, the synthetic mandible deforms more than the matching cadaveric mandible but this is an acceptable characteristic for our planned implant mechanical testing as it overloads the implants, compared to the cadaveric bone, thereby inducing a worst-case loading scenario over the anatomical. This enables similar mechanical testing using PS properties as with cadaveric mandibles. However, this In-VitroBone mandible also enables destructive mechanical testing with a sample size of more than one, which for obvious reasons would not be possible with cadaveric material. Furthermore, In-VitroBone, can be used outside the designated anatomical laboratories, and is available to any researcher requiring such testing material. The mechanical experiments described in **Chapter 8** were performed on In-VitroBone mandible specimens.

The experiments described in **Chapter 8** for the validation of the polyetheretherketone (PEEK) load bearing reconstructive PSI entailed the development of two dedicated mechanical testing apparatus. As the most common mandibular test setup in the literature uses uniaxial compression testers to apply a load to both mandibular angles[1,

[37-40], we developed a mandibular uniaxial compression apparatus (MUNACAPP) in-house to enable direct comparison of our results with those found in the literature. As mentioned in the Discussion section in **Chapter 8**, such uniaxial testing setups oversimplify the true in-vivo loading of the mandible. In such uniaxial testing, the effect of muscle removal on the resection side of the mandible is generally approached by offsetting the load distribution on the left and right mandibular angles. As this only changes the force distribution in predominantly the cranial-caudal direction, it does not mimic the mediolateral imbalance on the mandibular ramus.

Therefore, we developed a novel and more complex testing apparatus that allows for all the patient-specific elevator muscles to be added and provides information beyond the oversimplified and generally accepted gold standard setup. This in-house developed mandibular dynamic bite simulator (MANDYBILATOR) can be used to load a mandible both in a static and dynamic setting. It provides the user with the ability to apply all the specific jaw elevator muscles to their patient-specific insertion sites on the mandible. Perhaps more importantly, the user can easily leave out the specific muscles or muscle sections that have been resected. This allows for a more physiologically correct simulation compared to the uniaxial compression testing setups. Also, the loading of the mandible and its implant during a reconstruction is much closer to that seen with in-vivo loading.

The MANDYBILATOR apparatus was first applied in a long-term dynamic experiment, as described in **Chapter 8**, where it was set up to cyclically load a mandible with PEEK reconstructive PSI for 500,000 cycles. In line with the aforementioned, the superficial part of the left masseter muscle was not included in the experiment as the reconstructive implant covered its insertion area on the left mandibular ramus. After the cyclic experiment had successfully run 500,000 cycles, the individual muscle forces and resulting condylar and bite forces were recorded for validation purposes. These measured forces at t=500,000 cycles stayed within 10% of the values that were determined through the FEA, which we considered very acceptable. Finally, after almost twelve days of continuous use with a reconstructed mandible that was loaded with the full jaw elevator muscle system's capacity for every second, we stopped the experiment at a total cycle count of 1.1 million, still without signs of failure. This indicates both the potential of the new non-metallic PEEK reconstructive PSI and the reliability of the MANDYBILATOR apparatus.

The combination of a uniaxial compression tester, such as the MANUCAPP device, and a dynamic multi-muscle apparatus like the MANDYBILATOR, as presented in **Chapter 8**, provides a thorough insight into the response of the mandible under both static and dynamic loading. Although the simple uniaxial compression setup provides quick and easily comparable results due to the high level of constraints, it does not simulate the effects of the combination of individual muscles on the mandible, as found in the MANDYBILATOR. Steering clear of such apparatus because of its increased complexity compared to simple uniaxial compression devices is not the right rationale to ignore the anatomical complexity and to oversimplify it in in-vitro experiments[38].

Non-metallic load bearing PSI

Also in **Chapter 8**, the non-metallic PEEK reconstructive PSI was presented. This implant, designed to reconstruct a large continuity defect of the mandible, was obtained through topology optimisation. Several methods and findings from this thesis were combined in order to develop the unique implant. We used considerations from **Chapter 2** and included two strategically placed screws, of which one was presented in **Chapter 3**. The approach for the PS determination of the individual jaw elevator muscle forces, presented in **Chapter 7**, was used as input for the FEA and subsequent topology optimisation. The validation methods and apparatus that were developed within this thesis, as presented in **Chapter 8**, were applied to validate the PEEK implant.

With the aid of the methods and tools presented in this thesis, the PEEK reconstructive implant that we developed as an alternative to the titanium reconstruction plates proved to be sufficiently strong to withstand the expected in-vivo loading. Such a reconstruction, made from a high performing polymer from the polyaryletherketone (PAEK) family, was thought unfit in terms of strength but, knowing now that it can actually be used for relatively high load-bearing applications, opens doors for solving issues associated with metallic osteosynthesis materials.

The main advantage of PEEK over titanium and other metallic reconstructive implants, being it in combination with or without an osseous graft, lies in its radiolucent character[41, 42]. The majority of patients who need a continuity defect reconstruction due to a tumour resection receive postoperative radiotherapy, but titanium reconstruction plates interfere with the postoperative radiological imaging used for the planning of

the radiotherapy as well as with the radiotherapy itself. This interference is caused by backscattering and metal streak artefacts. Both the postoperative radiological imaging and radiotherapy become suboptimal and less accurate as the signal gets absorbed or distorted due to the dense metallic material[41] which interferes with the delivery of the photons or protons to the target tissues.

A second reason why PEEK and other PAEK polymers might prove useful in (reconstructive) implant applications is their Young's modulus of elasticity, which is close to that of mandibular cortical bone. As already mentioned in this section and discussed in **Chapter 8**, this characteristic could prevent stress-shielding from occurring in the bone neighbouring the implant.

FUTURE PERSPECTIVES

Topology optimisation

The PSIs, PS-RPs and PS TMJ-TJRs presented in this thesis were all developed with the aid of finite element analysis. This resulted in PSIs that consisted of a PS fit to the hosting bone and the designs were virtually tested on mechanical strength. The designs in **chapters 3, 4 and 5**, being fit to the patient's anatomy and are sufficiently strong, however, were subject to several subjective input variables that were chosen by the engineer or surgeon. The applied screw positions for example as well as the material thickness of the implants were decided manually and were satisfactory upon performing the FEA. What remained unknown, however, was whether the chosen positions and local material thickness were optimal for the specific designs. The tool that was used to develop the load bearing non-metallic PSI in **Chapter 8** aided in ridding such subjective decisions. Topology optimisation (TO), as it is called, is a computational method that seeks to optimise the shape or layout of a structure in a given design domain, while accounting for physical constraints such as material properties, loading conditions, and boundary conditions. The method involves iteratively modifying the distribution of material in the design domain in order to obtain a configuration that minimises a specific objective function, such as weight or stiffness, that are subject to constraints. The optimisation process is often performed using finite element analysis techniques. The resulting optimised topology can then be used as a basis for further design iterations or for manufacturing the final product.

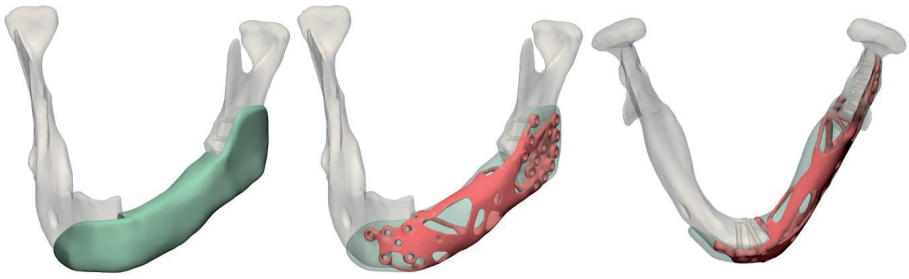

Figure 2 | An example of a topologically optimised titanium implant for the defect presented in chapter 8. The design domain is visualised in green and the final organically shaped topology optimised implant in red. The volume and weight of the design domain were reduced by 75 % though topology optimisation.

In line with this current thesis, TO could be applied in the near future for the optimisation of PSIs and TMJ-TJRs, thereby further increasing the amount of patient specificity while minimising the amount of subjective input, based on the experience of the engineer or the involved surgeon. Instead of mechanically evaluating a human design, the design should be the result of a mechanical evaluation. This is possible with TO as a large and solid design space can be sculpted into an often organic looking structure by the mathematical model behind the TO. Figure 2 shows a topologically optimised design for the defect presented in **Chapter 8** but, this time, with a titanium alloy as the input material.

By applying a TO workflow in **Chapter 8**, the PEEK polymer material that was previously found to be unfit for such high load-bearing applications, proved to be sufficiently strong. Applying TO on a larger scale should provide researchers with better insight into such alternative materials that, when shaped correctly, might be applicable for load bearing implants after all.

Lowered CR and the G-TMJ-TJR

As discussed in Chapter 6, the results obtained through our 4D study, i.e., a mean lowered CR of 28 mm, are not directly applicable to any currently available custom or stock TMJ-TJRs. This is because both the patient's anatomy and current surgical approaches do not allow for the physical positioning of the rotating bulk of TMJ-TJRs at this lowered level. The 'Groningen principle', a lowered CR of 15 mm, already improves the mimicking of the physiological mouth opening over the rest of the prostheses that do not allow for such CR lowering, however, in order to further improve

the patient's mouth opening postoperatively, in terms of mimicking the physiological movement, the kinematic concept of TMJ-TJRs needs to be changed. As a mere physical rotational point at this 28 mm lowered level would not suffice, perhaps a combination of the articulating sites is necessary in order to create a 'resultant' or instantaneous CR that is positioned outside of the rotational part of the TMJ-TJR.

When a 'posterior limit' is introduced posterior to the cranial section of the mandibular component and rigidly connected to the skull or fossa component of the G-TJ-TJR, the posterior movement of the mandibular component is locally prohibited. As the G-TMJ-TJR already has translational freedom of its neo-disc due to its unique separated articulation sites, this 'posterior limit' will force the neo-disc to translate anteriorly upon mouth opening. This results in a CR that is positioned lower than the physical neo-condyle of the G-TMJ-TJR. Figure 3 visualises this concept whereby the CR is already approximately 10 mm lower than the position of the neo-condyle, resulting in a lowering of approximately 25 mm to the CR when compared to the anatomical condyle.

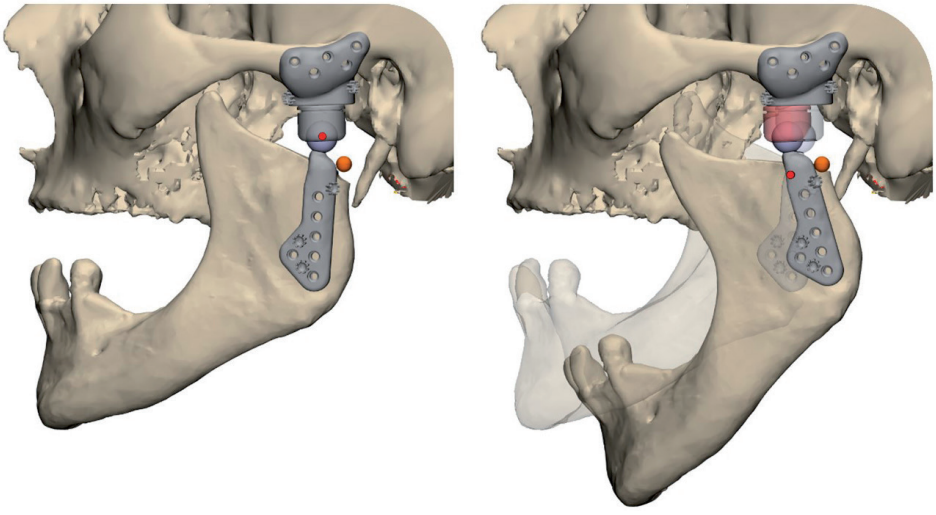

Figure 3 | Visualisation of the effect of an additional articulation on the position of the centre of rotation (CR) (red) of the mouth opening. When a 'posterior limit' (orange sphere) is introduced and rigidly connected to the fossa component of the G-TMJ-TJR, the posterior movement of the mandibular component is locally prohibited, thereby forcing the neo-disc (pink) to translate anteriorly upon mouth opening. This results in a further lowering of the CR of the G-TMJ-TJR without having to physically move the neo-condyle and neo-disc inferiorly.

Future research should explore this concept and other ways to lower the CR further so that it conforms to the PS determined CRs.

Material selection

The PAEK family, including PEEK and its derivatives, as well as composites, have demonstrated biological acceptance. Examples include polyetherketoneketone (PEKK) and hydroxyapatite infused PEEK (HA-PEEK), which promotes cell adhesion[43, 44]. The latter is particularly useful for our application, especially in the case of postoperative radiotherapy. The soft tissues around a mandibular reconstructive implant may contract after radiotherapy, leading to dehiscence of materials that do not play a bioactive role. This is a well-known complication in reconstructive surgery. Given the relatively bulky design of our current PEEK implant, it is essential that the soft tissues recognize and accept the implant to prevent dehiscence. Therefore, careful selection of the appropriate PAEK polymer and composite or surface coating that allows for sufficient mechanical strength and stiffness, while promoting cell adhesion, is crucial.

Future work should focus on gaining insight into the biological response of both hard and soft tissues to the implanted PAEK implant, in light of the necessary reconsideration of the type of PAEK (composite) used and the existing studies conducted with the chosen material. Specifically, research should investigate the cell adhesive potential and antibacterial properties of the implant, as these factors could play a crucial role in preventing and managing dehiscence of mandibular continuity defect reconstructions. Additionally, the impact of the implant's surrounding tissues on the irradiated implant after radiotherapy remains unclear and requires further exploration.

Metamaterials

A different manner to potentially mitigate the stress-shielding effect while maintaining the current titanium alloys, is to design existing materials in such a shape or structure that the bulk of the material shows (mechanical) properties that differ from the actual applied material's[45]. Such materials are generally called metamaterials (MM). MM are engineered materials designed to exhibit properties that are not typically found in naturally occurring materials. Using MM, a closer match in elastic properties between the implant and the surrounding bone might be obtained and the bulk material properties might change throughout implant. This way an implant could be engineered to be sufficiently strong and stiff to reconstruct a large continuity

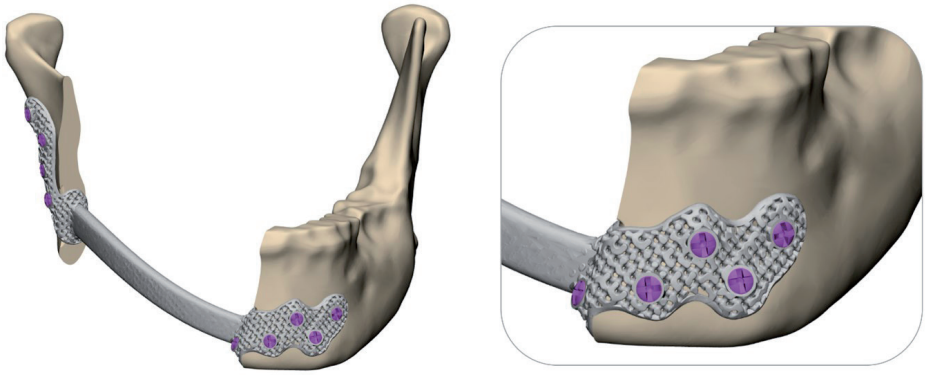

Figure 4 | An example of a metamaterial interpretation of the 'Bookshelf-plate' presented in Chapter 3. The bone sections neighbouring the reconstruction plate are made up of a lattice structure, providing these sections with a lower bulk Young's modulus of elasticity compared to the solid bridging part of this titanium reconstruction plate.

defect of the mandible in one part while allowing the bone to be sufficiently strained to prevent stress-shielding in other parts of the implant. Figure 4 shows an example of this application; our research group is currently focusing on this. The MM designs can be accurately 3D printed from e.g. biocompatible titanium alloys but still have to prove their function in the experimental setting. Another application of MM for (reconstructive) implants could be for areas where certain heterogenous deformations would be beneficial, e.g., a cranioplasty that does not interfere with the natural growth of a skull in a young child but conforms to it.

Within our research group and others, the TO, MM and subsequent applicable alternative implant material topics are currently being extensively explored[37, 41, 45, 46].

Workflow optimisation

The laborious workflows presented in this thesis, coupled with the considerable time and effort already required to make 3D designs of the PSIs, makes it nearly unfeasible to implement such processes on a large scale, especially for every patient needing a PSI. The time spent on obtaining 3D PS muscle models, perhaps applying 4D imaging, setting up FEA studies and applying TO, might be weeks for a single patient. This does not fit in with the often urgency of treatment. Therefore, the current workflows should be optimised to drastically reduce the amount of time spent on all the steps. Where repetitive steps or calculations are performed, scripting might be a helpful tool

to consider. Scripting parts of specific sub-workflows, such as parts of the PSI designs or even the setup of the FEA within certain boundaries, should be prioritised as scripting is a readily available tool in some FEA and CAD software packages, e.g., 3-Matic software (Materialise, Leuven, Belgium) and Abaqus (Simulia, Dassault Systèmes, Paris, France). Our experience is that time reductions of 75 % for certain design workflows with repetitive operations can be established. Another perk that comes with scripting (parts of) the workflows, is its repeatability. As a script will perform tasks in a predetermined order, outcomes of multiple iterations of the same (part of the) workflow should give the same results. This in turn, makes the work less user dependent and less prone to human error as important parameters can be scripted.

Regarding the determination of the PS muscle model, as presented in **Chapter 7**, vastly expanding the cohort based on the current workflow has priority. When an initial large cohort is obtained, the relationships between, e.g., the bony morphology and the muscle model, in terms of directions, forces and insertions, could be explored. If there is a relationship between multiple factors, this might be useful in terms of the prediction of muscle models based on only the shape of a mandible and skull. Such a relationship could drastically reduce time as measurements on the patient could be performed only partially or left out in toto.

A tool that could be used to search for such relationships is statistical shape modelling (SSM)[47]. SSM is a computational method used to represent the variation of shape within a given population of objects. The method involves capturing the main modes of variation in the shape of the objects by analysing a set of training data using statistical techniques such as principal component analysis. This results in a low-dimensional representation of the shape variability, which can be used to generate new shapes that conform to the statistical patterns of the training data. Medical imaging is used to model anatomical structures and to generate patient-specific models for surgical planning and simulation.

The same approach can be used to explore relationships between mandible and skull morphology and the position of the PS CR, as described in **Chapter 6**. As the main target audience of TMJ-TJR might have difficulties with opening their mouth in a physiologically correct manner, being able to predict the missing information, i.e., the PS CR based on the mandible and skull morphology, rather than determining the information from mandibular movement measurements, might be a good alterna-

tive. As to whether this statistically filled-in information is correct or not, and as to whether these statistical tools appear useful for these purposes should, naturally, be thoroughly validated.

Since artificial intelligence is becoming more readily available, machine learning and deep learning algorithms are currently being presented for applications such as auto-segmentation tools in e.g., OMFS[48, 49]. The time consuming muscle delineations, necessary for the determination of the PS muscle model, as presented in **Chapter** 7, for example, could be optimised by means of such algorithms and should be explored in the search for a true patient-specific front to back workflow that uses the techniques described in this thesis.

To recapitulate, university medical centres and other implant developers will be in the position to offer more objective and more patient-specific PSI designs over the next few years because of topology optimisation and the implementation of (semi-)automated workflows. The latter will also result in the workflows presented in this thesis becoming less laborious, which in turn will enable such workflows being deployed for every patient that might benefit. Implementing techniques such as topology optimisation and metamaterials, and by exploring non-metallic materials for proton beam irradiation following mandibular reconstruction, could help in minimising the side effects of the treatment, e.g., stress-shielding, dehiscence and soft-tissues damage. Such developments, as well as applying 4D imaging to determine PS CRs for use in TMJ-TJRs, will increase patient satisfaction due to better, more physiologically correct, oral function.

CONCLUSION

The novel approaches for three-dimensional virtual surgical planning and the development and optimisation of three-dimensional patient-specific implants and total joint replacement prostheses in Oral and Maxillofacial Surgery, presented in this thesis, should improve the treatments in terms of predictability, accuracy and better long-term concurrence between implant and body. This thesis presents novel techniques and workflows that can be implemented directly on a larger scale so that the amount of patient specificity in the next generation of patient-specific implants and prostheses are a true match, not merely due to the fit, but also their in-situ behaviours.

REFERENCES

1. Gutwald, R., Jaeger, R. & Lambers, F. M. Customized mandibular reconstruction plates improve mechanical performance in a mandibular reconstruction model. *Comput. Methods Biomech. Biomed. Engin.* **20**, 426-435 (2017).
2. Li, P. *et al*. Optimal design of an individual endoprosthesis for the reconstruction of extensive mandibular defects with finite element analysis. *J. Craniomaxillofac. Surg.* **42**, 73-78 (2014).
3. Luo, D., Xu, X., Guo, C. & Rong, Q. *Fracture Prediction for a Customized Mandibular Reconstruction Plate with Finite Element Method* (Advanced Computational Methods in Life System Modeling and Simulation, Springer Singapore, Singapore, 2017).
4. Mazzoni, S. *et al*. Prosthetically guided maxillofacial surgery: evaluation of the accuracy of a surgical guide and custom-made bone plate in oncology patients after mandibular reconstruction. *Plast. Reconstr. Surg.* **131**, 1376-1385 (2013).
5. Narra, N. *et al*. Finite element analysis of customized reconstruction plates for mandibular continuity defect therapy. *J. Biomech.* **47**, 264-268 (2014).
6. Wu, C. H., Lin, Y. S., Liu, Y. S. & Lin, C. L. Biomechanical evaluation of a novel hybrid reconstruction plate for mandible segmental defects: A finite element analysis and fatigue testing. *J. Craniomaxillofac. Surg.* **45**, 1671-1680 (2017).
7. Shi, Q. *et al*. Failure analysis of an in-vivo fractured patient-specific Ti6Al4V mandible reconstruction plate fabricated by selective laser melting. **124** (2021).
8. Frost, H. M. Bone "mass" and the "mechanostat": a proposal. *Anat. Rec.* **219**, 1-9 (1987).
9. Frost, H. M. Bone's mechanostat: a 2003 update. *Anat. Rec. A. Discov. Mol. Cell. Evol. Biol.* **275**, 1081-1101 (2003).
10. Vitins, V., Dobelis, M., Middleton, J., Limbert, G. & Knets, I. Flexural and Creep Properties of Human Jaw Compact Bone for FEA Studies. *Computer Methods in Biomechanics and Biomedical Engineering* **6**, 299-303 (2003).
11. Xin, P. *et al*. Material assignment in finite element modeling: heterogeneous properties of the mandibular bone. *The Journal of craniofacial surgery* **24**, 405-410 (2013).
12. Maurer, P., Eckert, A. W., Kriwalsky, M. S. & Schubert, J. Scope and limitations of methods of mandibular reconstruction: a long-term follow-up. *Br. J. Oral Maxillofac. Surg.* **48**, 100-104 (2010).
13. Katakura, A., Shibahara, T., Noma, H. & Yoshinari, M. Material analysis of AO plate fracture cases. *J. Oral Maxillofac. Surg.* **62**, 348-352 (2004).
14. Shibahara, T., Noma, H., Furuya, Y. & Takaki, R. Fracture of mandibular reconstruction plates used after tumor resection. *J. Oral Maxillofac. Surg.* **60**, 182-185 (2002).
15. Onoda, S. *et al*. Prevention points for plate exposure in the mandibular reconstruction. *J. Craniomaxillofac. Surg.* **40**, 310 (2012).
16. Chernohorskyi, D., Voller, M., Vasilyev, A., Chepurnyi, Y. & Kopchak, A. Clinical Efficacy of Patient-specific Implants Manufactured using Direct Metal Laser Sintering (DMLS) Technology in Patients with Mandibular Defects. *Journal of Diagnostics and Treatment of Oral and Maxillofacial Pathology* **4**, 162-177 (2020).
17. Wei, F. *et al*. Complications after reconstruction by plate and soft-tissue free flap in composite mandibular defects and secondary salvage reconstruction with osteocutaneous flap. *Plast. Reconstr. Surg.* **112**, 37-42 (2003).
18. Tams, J. *et al*. Poly(L-lactide) bone plates and screws for internal fixation of mandibular swing osteotomies. *Int. J. Oral Maxillofac. Surg.* **25**, 20-24 (1996).

19. Scher, N. *et al*. Radiotherapy of the resected mandible following stainless steel plate fixation. *Laryngoscope* **98**, 561-563 (1988).
20. Almasi, D. *et al*. Preparation Methods for Improving PEEK's Bioactivity for Orthopedic and Dental Application: A Review. *Int. J. Biomater.* **2016**, 8202653 (2016).
21. van Loon, J. P., Verkerke, G. J., de Vries, M. P. & de Bont, L. G. Design and wear testing of a temporomandibular joint prosthesis articulation. *J. Dent. Res.* **79**, 715-721 (2000).
22. van Loon, J. P., de Bont, L. G., Stegenga, B., Spijkervet, F. K. & Verkerke, G. J. Groningen temporomandibular joint prosthesis. Development and first clinical application. *Int. J. Oral Maxillofac. Surg.* **31**, 44-52 (2002).
23. Wolford, L. M., Mercuri, L. G., Schneiderman, E. D., Movahed, R. & Allen, W. Twenty-year follow-up study on a patient-fitted temporomandibular joint prosthesis: the Techmedica/TMJ Concepts device. *J. Oral Maxillofac. Surg.* **73**, 952-960 (2015).
24. Westermark, A. Total reconstruction of the temporomandibular joint. Up to 8 years of follow-up of patients treated with Biomet((R)) total joint prostheses. *Int. J. Oral Maxillofac. Surg.* **39**, 951-955 (2010).
25. Elledge, R., Mercuri, L. G., Attard, A., Green, J. & Speculand, B. Review of emerging temporomandibular joint total joint replacement systems. *Br. J. Oral Maxillofac. Surg.* **57**, 722-728 (2019).
26. Mercuri, L. G. & Anspach, W. E. Principles for the revision of total alloplastic TMJ prostheses. *Int. J. Oral Maxillofac. Surg.* **32**, 353-359 (2003).
27. Kanatas, A. N. *et al*. Short-term outcomes using the Christensen patient-specific temporomandibular joint implant system: a prospective study. *Br. J. Oral Maxillofac. Surg.* **50**, 149-153 (2012).
28. Kim, Y. Comparison of polyethylene wear associated with cobalt-chromium and zirconia heads after total hip replacement. A prospective, randomized study. *J. Bone Joint Surg. Am.* **87**, 1769-1776 (2005).
29. Tsukamoto, R. *et al*. Improved wear performance with crosslinked UHMWPE and zirconia implants in knee simulation. *Acta Orthop.* **77**, 505-511 (2006).
30. Merema, B. J., Kraeima, J., Witjes, M. J. H., van Bakelen, N. B. & Spijkervet, F. K. L. Accuracy of fit analysis of the patient-specific Groningen temporomandibular joint prosthesis. *Int. J. Oral Maxillofac. Surg.* **50**, 538-545 (2021).
31. van Loon, J. P., Falkenstrom, C. H., de Bont, L. G., Verkerke, G. J. & Stegenga, B. The theoretical optimal center of rotation for a temporomandibular joint prosthesis: a three-dimensional kinematic study. *J. Dent. Res.* **78**, 43-48 (1999).
32. Weijs, W. A. & Hillen, B. Cross-sectional areas and estimated intrinsic strength of the human jaw muscles. *Acta Morphol. Neerl. Scand.* **23**, 267-274 (1985).
33. Koolstra, J. H., van Eijden, T. M., Weijs, W. A. & Naeije, M. A three-dimensional mathematical model of the human masticatory system predicting maximum possible bite forces. *J. Biomech.* **21**, 563-576 (1988).
34. Peck, C. C., Langenbach, G. E. & Hannam, A. G. Dynamic simulation of muscle and articular properties during human wide jaw opening. *Arch. Oral Biol.* **45**, 963-982 (2000).
35. Hannam, A. G., Stavness, I., Lloyd, J. E. & Fels, S. A dynamic model of jaw and hyoid biomechanics during chewing. *J. Biomech.* **41**, 1069-1076 (2008).
36. Sagl, B., Schmid-Schwap, M., Piehslinger, E., Kundi, M. & Stavness, I. A Dynamic Jaw Model With a Finite-Element Temporomandibular Joint. *Front. Physiol.* **10**, 1156 (2019).

37. Koper, D. C. *et al*. Topology optimization of a mandibular reconstruction plate and biomechanical validation. *J. Mech. Behav. Biomed. Mater.* **113**, 104157 (2021).
38. van Kootwijk, A. *et al*. Semi-automated digital workflow to design and evaluate patient-specific mandibular reconstruction implants. *J. Mech. Behav. Biomed. Mater.* **132**, 105291 (2022).
39. Schupp, W., Arzdorf, M., Linke, B. & Gutwald, R. Biomechanical testing of different osteosynthesis systems for segmental resection of the mandible. *J. Oral Maxillofac. Surg.* **65**, 924-930 (2007).
40. Gateno, J. *et al*. Biomechanical evaluation of a new MatrixMandible plating system on cadaver mandibles. *J. Oral Maxillofac. Surg.* **71**, 1900-1914 (2013).
41. Lommen, J. *et al*. Reduction of CT Artifacts Using Polyetheretherketone (PEEK), Polyetherketoneketone (PEKK), Polyphenylsulfone (PPSU), and Polyethylene (PE) Reconstruction Plates in Oral Oncology. *J. Oral Maxillofac. Surg.* **80**, 1272-1283 (2022).
42. Almasi, D. *et al*. Preparation Methods for Improving PEEK's Bioactivity for Orthopedic and Dental Application: A Review. *Int. J. Biomater.* **2016**, 8202653 (2016).
43. Zhao, M. *et al*. Response of Human Osteoblast to n-HA/PEEK--Quantitative Proteomic Study of Bio-effects of Nano-Hydroxyapatite Composite. *Sci. Rep.* **6**, 22832 (2016).
44. Ma, R. & Guo, D. Evaluating the bioactivity of a hydroxyapatite-incorporated polyetheretherketone biocomposite. *J. Orthop. Surg. Res.* **14**, 32-1 (2019).
45. de Jonge, C. P., Kolken, H. M. A. & Zadpoor, A. A. Non-Auxetic Mechanical Metamaterials. *Materials (Basel)* **12**, 635. doi: 10.3390/ma12040635 (2019).
46. D'Alessandro, L., Krushynska, A. O., Ardito, R., Pugno, N. M. & Corigliano, A. A design strategy to match the band gap of periodic and aperiodic metamaterials. *Sci. Rep.* **10**, 16403-3 (2020).
47. Klop, C. & MAGIC Amsterdam. A three-dimensional statistical shape model of the growing mandible. *Sci. Rep.* **11**, 18843-x (2021).
48. Qiu, B. *et al*. Automatic segmentation of the mandible from computed tomography scans for 3D virtual surgical planning using the convolutional neural network. *Phys. Med. Biol.* **64**, 175020-6560/ab2c95 (2019).
49. Heo, M. *et al*. Artificial intelligence in oral and maxillofacial radiology: what is currently possible? *Dentomaxillofac. Radiol.* **50**, 20200375 (2021).

Appendices

SUMMARY

This thesis focuses on the development, implementation, evaluation, and optimization of 3D-virtual surgical planning (VSP) workflows and patient specific implants (PSI) for oral and maxillofacial surgery (OMFS). The studied fields are: head and neck reconstructive surgery (***Section I***) and temporomandibular joint (TMJ) replacement surgery (***Section II***). ***Section III*** of this thesis focuses on optimisation and validation workflows and intertwines with both aforementioned fields. Current conventional osteosynthesis reconstruction plates (RPs) and PSIs are accompanied by complications, such as, mechanical instability, screw loosening, plate fracture and inaccurate positioning. In TMJ total joint replacement (TMJ-TJR) surgery, correct positioning of TMJ-TJR prostheses and their movement behaviour are focus areas. The general aim of the research described in this thesis was to solve these complications and focus areas by means of mechanical reconsiderations, developing patient-specific (PS) solutions to be used in guided surgery and optimising current workflows in order to enhance the current generation of PS-RPs and TMJ-TJR prostheses by increasing their level of patient-specificity, making them more specific to the patient than currently is the case.

Chapter 2 of this thesis focuses on the use of Finite Element Analysis (FEA) of the human mandible, used in a biomechanical setting. As FEA can be applied to virtually test an implant or mandible mechanical behaviour, thereby reducing time and costs when compared to physical mechanical testing. In order to rely on a FEA model, however, they should be properly validated for its intended purpose. We found a lack of consensus on the input variables required for representative FEA models of the mandible. To address this, the literature was reviewed. The analysis revealed that only a few FEA models have been validated, and there is significant variation in described material properties and FEA approaches. The available validations are not strong enough to establish a general consensus concerning the input parameters that should be used in order to obtain representative FEA models of the mandible. As a result, this chapter concludes that further validations are needed, preferably using the same measuring workflow, to obtain insight into the wide range of mandibular variations and to establish validated FEA settings.

The mechanical challenges associated with reconstructing mandibular continuity defects, resulting from ablative surgery of oral malignancies are addressed in **Chapter 3.** The results of conventional reconstructions using stock osteosynthesis reconstruc-

tion plates are often suboptimal, resulting in mechanical instability, screw loosening, and plate fracture. To overcome these issues, patient specific reconstruction plates PS-RPs and guided surgery techniques have been introduced, including an alternative PS-RP design called the "Bookshelf-plate". The latter was validated in this chapter to be mechanically superior to conventional reconstruction osteosynthesis plates. The combination of VSP, guided surgery and PSIs appears to be highly accurate, with an average Euclidean accuracy of approximately 1.5 mm after implantation. The use of "Bookshelf-plates" with the accompanying screws reduces screw pull-out and micromotion, leading to lower stresses and a decreased risk of screw loosening and plate fracture. However, concerns regarding stress-shielding and plate dehiscence remain. Stress-shielding can occur when the implants are stiffer than the surrounding bone, leading to bone resorption and implant loosening. This effect is noted with the use of titanium alloys, the current standard for load-bearing reconstruction plates.

To address stress-shielding and plate dehiscence, this thesis suggests exploring alternative implant materials or incorporating bio-coatings. This led to the description in **Chapter 8** of an alternative implant developed with a non-metallic material.

In addition to mandibular reconstructions, this thesis focuses on the development of patient-specific (PS) TMJ-TJR prostheses (**Chapter 4**). Stock prostheses often have a suboptimal fit to the hosting bone, require recontouring of the bone and are prone to mispositioning. Reported complications related to stock prostheses are mechanical instability, malocclusion or suboptimal function. The current available TMJ-TJRs, including custom and stock designs, lack validation studies of positioning accuracy. Therefore, this thesis presents a PS TMJ-TJR design based on the Groningen principles, with a lowered centre of rotation (CR) and separate translation and rotation sites. **Chapters 4 and 5** show the use of VSP and guided surgery for precise placement of the prosthesis, with a Euclidean accuracy of around 1 mm in both a cadaver study and a clinical setting.

Chapter 6 adds to the patient-specificity of the newly developed PS Groningen TMJ-TJR by determining PS lowered CR positions. By lowering the CR, pseudo-translation can be achieved which enhances the restoration of physiological mandibular movements after placement of a TMJ-TJR. Temporomandibular joint movements were recorded in 20 subjects, without TMJ-related complaints, through four-dimensional scanning of the skull and mandible. The mean optimal CR position was lowered by

28 mm compared to the anatomical condyle centre. As positioning the CR at a prior determined 15 mm lowered position can be challenging in current designs, having the ability to implement a lowered CR of 28 mm in TMJ-TJR designs requires a change in kinematic principles of TMJ-TJRs but is crucial for restoring natural mouth opening movements.

In **Chapter 7** of this thesis, a workflow is presented to address the limitations of using generic non-PS parameters in FEA and in-vitro testing of the mandible. The goal was to determine PS muscle models for the mandible, enabling the development of PS implants that are dictated by the patient's specific maximum bite capacity. By combining techniques like MRI, CT scanning, muscle delineation, and bite force measurements, the workflow provides a comprehensive approach to determine the forces exerted by individual muscles on the patient's mandible.

This approach highlights the importance of considering PS muscle models rather than solely focusing on the bony interface of the mandible when developing PS implants. This chapter demonstrates the potential variation between individual subjects, emphasising the need to consider PS muscle models to account for these differences. **Chapter 7** challenges the conventional practice of using the fixed muscle strength values found in the literature by suggesting that intrinsic muscle strength should be determined on a patient-specific basis. Studying a larger cohort is expected to provide valuable insights into the variety and range of intrinsic strength values among individuals.

Chapter 8 describes the limitations of using synthetic bone substitutes for the mechanical testing of implants. These substitutes, designed primarily for surgical skill practice, do not mimic accurately the mechanical properties of the human mandible. To address this issue, the exploration of a patient-specific synthetic mandible, we call In-VitroBone, is initiated in this thesis. This current synthetic mandible can withstand physiological muscle forces, fails within an acceptable range of forces compared to cadaveric mandibles, however, is less stiff. However, it has the advantage of enabling destructive mechanical testing with multiple identical samples, which is not feasible with cadaveric material. In-VitroBone also provides researchers outside anatomical laboratories with a reliable testing material for implant-related studies. For the mechanical experiments performed in **Chapter 8**, In-VitroBone mandibles were used.

To evaluate the strength and fatigue resistance of PSIs, **Chapter 8** describes two mechanical testing apparatus. Although the mandibular uniaxial compression apparatus (MUNACAPP) allowed for direct comparison with existing literature results, it oversimplified the in-vivo loading of the mandible. To address this limitation, we developed the mandibular dynamic bite simulator (MANDYBILATOR), a more complex apparatus capable of loading the mandible in both a static and dynamic manner. The MANDYBILATOR takes the patient-specific jaw elevator muscles into consideration and allows for the exclusion of resected muscles, thereby providing a more physiologically accurate simulation of mandibular loading. Using the MANDYBILATOR apparatus, we successfully validated a non-metallic polyetheretherketone (PEEK) reconstructive PSI, demonstrating it has sufficient strength to withstand the expected patient-specific in-vivo loading. PEEK implants offer advantages over metallic implants, such as radiolucency, and their mechanical properties are much closer to that of mandibular cortical bone. Using the PEEK material for large load bearing reconstructive implants for the mandible was considered impossible but, on applying the techniques described in **Chapters 6 and 8** we proved, through thorough mechanical validation using the MANDYBILATOR apparatus, that such an implant is strong enough to withstand the in-vivo static and dynamic loading of the mandible.

General conclusion

This thesis addresses conventional osteosynthesis reconstruction plates and temporomandibular joint total joint replacements, including their complications in oral and maxillofacial surgery. Improvements were made by developing patient specific alternatives, which were experimentally and clinically validated. Furthermore, by presenting workflows that allow for improvements in the development of patient specific implants and temporomandibular joint total joint replacements, and by presenting enhanced mechanical testing methodologies, the research presented in this thesis will come together in a next, even more patient specific generation of patient specific implants and temporomandibular joint total joint replacements.

SAMENVATTING

Dit proefschrift beschrijft de ontwikkeling, implementatie, evaluatie en optimalisatie van 3D virtuele chirurgische planning (VCP) workflows en patiënt-specifieke implantaten (PSI) binnen het vakgebied van de mondziekten, kaak- en aangezichtschirurgie (MKA-chirurgie). De specifieke aandachtsgebieden zijn: hoofd/hals reconstructieve chirurgie bij patiënten behandeld vanwege een kwaadaardige tumor in dit gebied (**Sectie I**) en kaakgewrichtsvervangende chirurgie door middel van gewrichtsprotheses (**Sectie II**). In **Sectie III** van dit proefschrift worden optimalisatie en validatie van de werkprocessen beschreven die aansluiten bij beide eerdergenoemde aandachtsgebieden. Huidige conventionele en patiënt-specifieke (PS) reconstructieplaten (RP) gaan gepaard met complicaties, zoals, mechanische instabiliteit, schroefloslating, plaatbreuk en inaccurate plaatsing. Bij kaakgewrichtsvervangende chirurgie zijn de correcte plaatsing van kaakgewrichtsprotheses en het bewegingspatroon aandachtsgebieden. Het algemene doel van het onderzoek beschreven in dit proefschrift was het verhelpen van deze complicaties en aandachtsgebieden door middel van mechanische heroverwegingen, het ontwikkelen van PS oplossingen voor gebruik in '*guided* surgery' en het optimaliseren van de huidige werkprocessen. Dit alles om de huidige generatie PS-RP en kaakgewrichtsprotheses te verbeteren door hun mate van patiëntspecificiteit te verhogen.

Hoofdstuk 2 van dit proefschrift focust op het gebruik van de eindige elementen methode (Eng. Finite Element analysis FEA) in biomechanische analyses van de menselijke onderkaak. Hier werd een gebrek aan consensus gevonden betreft de te gebruiken input variabelen die nodig zijn voor representatieve FEA modellen van de onderkaak. Om dit te verbeteren werd een literatuuronderzoek opgezet. De analyse liet zien dat slechts enkele FEA modellen gevalideerd zijn en dat er een ruime variëteit is aan toegepaste materiaaleigenschappen van de onderkaak en aan FEA instellingen.

De mechanische uitdagingen gerelateerd aan het reconstrueren van continuïteitsdefecten in de onderkaak, ten gevolge van oncologische (ablatieve) chirurgie voor de behandeling van kwaadaardige aandoeningen in de mond, worden onderzocht in **Hoofdstuk 3**. De resultaten van conventionele reconstructies, gebruikmakend van standaard, niet-PS, osteosynthese reconstructieplaten, zijn vaak suboptimaal, wat resulteert in mechanische instabiliteit, schroefloslating en plaatbreuk. Om deze complicaties te verhelpen werden patiënt-specifieke reconstructieplaten (PS-RP) en '*guided*

surgery' technieken geïntroduceerd, inclusief een alternatief PS-RP ontwerp, genaamd de 'Boekensteunplaat'. Deze werd in dit hoofdstuk in-silico en in een klinische setting gevalideerd en bleek mechanisch superieur aan de conventionele osteosynthese reconstructieplaten. De combinatie van VCP, '*guided surgery*' en PSI blijkt erg accuraat met gemiddelde afwijkingen van 1.5 mm tussen de op het beeldscherm geplande situatie en de postoperatieve resultaten. Het gebruik van de 'Boekensteunplaten' inclusief bijbehorende boekensteunschroeven reduceert schroefuittrekking en microbeweging, resulterend in lagere spanningen in het materiaal van de plaat en een verminderd risico op schroefloslating en plaatbreuk. Echter, het risico op '*stress-shielding*' en dehiscentie, het blootraken van de plaat, blijft bestaan. *Stress-shielding* kan optreden wanneer het geplaatste implantaat beduidend stijver is dan het bot waarop het aanligt en kan leiden tot botresorptie en uiteindelijk schroefuittrekking of schroefloslating en losraken van de reconstructieplaat. Dit effect wordt opgemerkt met het gebruik van titanium(legering), de huidige standaard voor dergelijke zwaarbelaste reconstructieplaten.

Om de kans op *stress-shielding* en dehiscentie van de plaat te verminderen wordt in dit proefschrift voorgesteld om alternatieve implantaatmaterialen en biocoatings te verkennen. Dit heeft geleid tot de beschrijving van een alternatief implantaat dat werd ontwikkeld uit een niet-metalen materiaal (**Hoofdstuk 8**).

Naast onderkaakreconstructies focust dit proefschrift tevens op de ontwikkeling van een PS kaakgewrichtsprothese voor gewrichtsvervangende chirurgie (**Hoofdstuk 4)**. Standaard, niet-PS, protheses hebben vaak een slechte pasvorm op de kaak en schedel en vergen handmatige aanpassingen van het bot voorafgaand aan de plaatsing. Ook zijn ze gevoelig voor verkeerde positionering en hieraan gerelateerde gerapporteerde complicaties zijn dan ook mechanische instabiliteit, grotere slijtage, malocclusie (het niet goed op elkaar passen van de tanden en kiezen in boven- en onderkaak) en suboptimale functie van de gewrichtsprothese. Het ontbreekt de huidige kaakgewrichtsprotheses, zowel de standaard als PS, aan validatiestudies van de plaatsingsaccuratesse. Daarom wordt in dit proefschrift een PS kaakgewrichtsprothese gepresenteerd die werd gebaseerd op de 'Groningen-principes', met een verlaagd rotatiepunt en een separate translatie- en rotatieplaats. **Hoofdstukken 4 en 5** tonen het effect van VCP en plaatsing met behulp van individuele boor/zaagmallen, zgn. '*guided surgery',* in combinatie met deze PS Groningen kaakgewrichtsprothese op de plaatsingsaccura-

tesse. Allereerst in een kadaverstudie en later in klinische toepassing. In beide studies werden de kaakgewrichtsprotheses met een accuratesse van rond 1 mm geplaatst.

Hoofdstuk 6 verhoogt de mate van patiënt-specificiteit van de nieuw ontwikkelde PS Groningen kaakgewrichtsprothese door het rotatiepunt van de prothese op PS wijze te bepalen. Door het verlagen van het rotatiepunt van de prothese ten opzichte van de kaakkop kan een pseudo-translatie worden bewerkstelligd waarmee de fysiologische kaakbeweging na het plaatsen van een kaakgewrichtsprothese beter kan worden nagebootst. In 20 proefpersonen zonder kaakgewrichtklachten werd de beweging van de onderkaak geregistreerd door middel van een vierdimensionale scan van de schedel en onderkaak. Het gemiddelde optimale rotatiepunt lag hierbij 28 mm lager dan het anatomische middelpunt van de kaakkop. Omdat het implementeren van een eerder beschreven 15 mm verlaagd rotatiepunt in een kaakgewrichtsprothese al uitdagend bleek in alle huidige beschikbare kaakgewrichtsprotheses, is een verandering in kinematische principes die worden toegepast in kaakgewrichtsprotheses, noodzakelijk om een rotatiepuntverlaging van 28 mm te bewerkstelligen. Dit is echter cruciaal voor het nabootsen van de natuurlijke kaakbeweging en de functionele uitkomsten na het plaatsen van kaakgewrichtsprotheses te vergroten.

In **Hoofdstuk 7** van dit proefschrift wordt een workflow gepresenteerd waarmee de beperkingen worden behandeld van het toepassen van generieke, niet-PS, parameters in FEA en in-vitro (mechanische) testen van de onderkaak. Het doel was om PS spiermodellen voor de onderkaak te kunnen bepalen, waarbij elke afzonderlijke spierkracht wordt benaderd. Dit maakt het mogelijk om PSI te ontwikkelen die gedicteerd zijn door de specifieke maximale bijtcapaciteit van de patiënt. Door o.a. technieken als MRI, CT, spierintekeningen en bijtkrachtmetingen te combineren kwam een uitgebreide workflow tot stand die op niet-invasieve wijze de maximale kracht van de kauwspieren afzonderlijk benadert.

Deze aanpak benadrukt de toegevoegde waarde van het toepassen van PS spiermodellen en niet enkel te focussen op het benige contactvlak bij het ontwikkelen van PSI. Dit hoofdstuk laat zien wat de potentiële onderlinge variatie is van spierkrachten tussen individuen, wat de waarde van het PS bepalen van kauwspiermodellen benadrukt. **Hoofdstuk 7** bekritiseert het conventionele gebruik van vaste spierkrachten die worden gepresenteerd in de literatuur door voor te stellen dat intrinsieke spierkracht op PS wijze bepaald dient te worden. Het uitbreiden van het huidige cohort zal inzicht

moeten geven in de mate van onderlinge variëteit in de afzonderlijke spierkrachten van patiënten.

Hoofdstuk 8 beschrijft de beperking van commercieel verkrijgbare synthetische kaakmodellen wanneer deze worden toegepast in mechanische (implantaat) testen. Deze botvervangers, die primair zijn bedoeld voor het oefenen van chirurgische vaardigheden, bootsen de mechanische eigenschappen van het bot van de onderkaak niet nauwkeurig na. Gedurende dit proefschrift werd een studie geïnitieerd waarin wordt getracht om een synthetische botvervanger voor de onderkaak te ontwikkelen (In-VitroBone) met overeenkomstige eigenschappen als menselijke (kadaver)kaken. De huidige versie van deze synthetische onderkaken kan de fysiologische spierkrachten weerstaan, breekt bij overeenkomstige belasting als de kadaverkaken die het nabootst echter, is minder stijf. In-VitroBone heeft echter ten opzichte van kadavermateriaal als groot voordeel dat het identiek te dupliceren is voor experimenten waarbij meerdere samples benodigd zijn. Daarnaast biedt het hebben van een mechanisch geschikte synthetische botvervanger perspectieven voor onderzoekers die geen beschikking hebben over een anatomisch laboratorium waar testen met kadavermateriaal kunnen worden uitgevoerd. Voor de mechanische testen die in **Hoofdstuk 8** zijn uitgevoerd werden In-VitroBone onderkaken gebruikt.

Om de sterkte en bestendigheid tegen vermoeiing van PSI te evalueren werden twee testapparaten ontwikkeld. Deze zijn beschreven in **Hoofdstuk 8**. De *mandibular uniaxial compression apparatus* (MUNACAPP) werd ontwikkeld voor het uitvoeren van statische experimenten. De uitkomsten van dit apparaat laten zich direct vergelijken met die van vergelijkbare appraten die eerder werden beschreven in de literatuur. Echter, bootst dit apparaat een sterk versimpelde belasting van de onderkaak na. Het tweede apparaat dat wij ontwikkelden, de *mandibular dynamic bite simulator* (MANDYBILATOR), is beduidend complexer en belast de kaak op een fysiologisch meer correcte wijze. De MANDYBILATOR is in staat om zowel statisch als dynamisch te belasten, waardoor ook vermoeiingstesten kunnen worden uitgevoerd. Ook is het mogelijk om in dit apparaat alle patiënt-specifieke spieren, richtingen en krachten, toe te passen op te testen kaak. Hierdoor is het in de MANDYBILATOR mogelijk om delen van, of hele spieren weg te laten waarmee de resectie van botdelen met spieraanhechtingen kan worden nagebootst, zoals vaak het geval is in oncologische reconstructies. Dit geeft een uitgebreider en meer fysiologisch correct inzicht in de

belasting en vervorming van de, al dan niet met PSI gereconstrueerde, onderkaak in de patiënt.

Met de MANDYBILATOR werd onze niet-metalen polyetheretherketon (PEEK) reconstructieve PSI succesvol gevalideerd en werd hiermee aangetoond dat een PEEK PSI voor deze toepassing voldoende sterk kan zijn om de verwachte in-vivo belasting in de patiënt te weerstaan. PEEK implantaten bieden verscheidene voordelen ten opzichte van titanium reconstructieplaten. Zo is het materiaal radiolucent, het is niet zichtbaar op CT, en liggen de materiaaleigenschappen veel dichter bij dat van corticaal bot dan bij titanium het geval is. Het toepassen van PEEK als implantaatmateriaal voor grote, last dragende, reconstructieve implantaten voor de onderkaak werd eerder onmogelijk geacht. Echter, met het toepassen van de technieken beschreven in **Hoofdstuk 6 en 8** toonden wij door middel van uitgebreide mechanische validaties aan dat een dergelijk implantaat wel degelijk sterk genoeg kan zijn om te worden toegepast in de patiënt.

Algemene conclusie

Dit proefschrift beschrijft conventionele osteosynthese reconstructieplaten en kaakgewrichtsprotheses en de complicaties waarmee zij gepaard gaan in de mondziekten, kaak- en aangezichtschirurgie. Verbeteringen werden aangebracht door patiënt-specifieke alternatieven te ontwikkelen, die zowel experimenteel als in de kliniek werden gevalideerd. Methodieken werden geïntroduceerd die verbeteringen in de ontwikkelingen van patiënt-specifieke reconstructieve implantaten en kaakgewrichtsprotheses mogelijk maken en uitgebreide, meer complexe, mechanische test methodieken werden hieraan ter validatie toegevoegd. Het onderzoek dat in dit proefschrift wordt gepresenteerd zal bijeenkomen in een volgende, nóg patiënt-specifiekere, generatie van patiënt-specifieke reconstructieve implantaten en kaakgewrichtsprotheses.

DANKWOORD

Dit proefschrift is mede tot stand gekomen dankzij de vele mensen die de afgelopen jaren aan mijn onderzoek hebben meegewerkt. Hiervoor wil ik jullie allen hartelijk danken. In het bijzonder wil de ik de volgende personen bedanken:

Prof. dr. F.K.L. Spijkervet, beste Fred, van stagebegeleider tot eerste promotor van mijn proefschrift. Het G-TMJ-TJR project lag stil en je kon toevallig iemand als ik gebruiken om het samen met Joep nieuw leven in te blazen. Ik ben nog altijd erg dankbaar dat ik deze kans heb gekregen. Je bent vanaf het begin nauw betrokken geweest bij mijn werkzaamheden op onze afdeling en van je nauwkeurige en kritische blik heb ik een hoop mogen leren, waarvoor veel dank. In mijn optiek is mede hierdoor de huidige versie van onze prothese een succes.

Prof. dr. M.J.H. Witjes, beste Max, jouw enthousiasme voor nieuwe ideeën werkt aanstekelijk. In mijn tijd met jou als promotor en ook daarvoor heb jij mij aangespoord tot het verkennen van een hoop verschillende onderwerpen. Of dit altijd bewust was weet ik niet maar dit doet er in zoverre niet toe. Ook op persoonlijk vlak heb ik van jou een hoop mogen leren en ik hoop dat we nog tal van onze plannen samen mogen uitwerken.

Dr. J. Kraeima, beste Joep, al sinds mijn eerste dag in het UMCG nam jij mij op sleeptouw. Je begeleidde mijn dagelijkse werkzaamheden tijdens mijn afstudeerproject, dat was gefocust op de G-TMJ-TJR, en hebt mij wegwijs gemaakt in het ziekenhuis en op onze afdeling. Op zowel technisch, medisch als academisch vlak heb ik alles van je mogen leren, waar ik erg dankbaar voor ben. We gaan nog een hoop mooie dingen doen in de toekomst.

Promotores, Beste Fred, Max en Joep, bedankt voor het vertrouwen dat ik van jullie krijg om zelfstandig zaken te verkennen en uit te werken. Zowel in de patiëntenzorg als bij nieuwe onderzoeksideeën.

Leden van de manuscriptcommissie: **Prof. dr. ir. Verkerke, Prof. dr. dr. Kessler, Prof. dr. Santos**, bedankt voor het vrijmaken van uw tijd voor de zorgvuldige beoordeling van mijn proefschrift en de interesse in het onderwerp. Tevens bedankt voor de inspiratie op het gebied van (3D) technologie binnen de medische wetenschap en

hoofd-hals oncologie. Het was mij een genoegen om de afgelopen jaren met u of uw directe collegae samen te werken aan verdere implementatie van 3D-technologie in de zorg.

[ENG] Thank you for investing your time in careful and critical reading and your appreciation of my manuscript. Also, thank you for your inspiration in the field of technology within medical science. It has been my pleasure to work with you or your immediate colleagues over the past few years to further implement (3D) technology in healthcare.

Prof. dr. R.R.M. Bos, beste Ruud, bij jou is het echt allemaal begonnen. Via mijn minor Biomedical Engineering kreeg ik jouw contactgegevens toen ik zocht naar een afstudeerplek. Was ik toen niet met jou in contact gekomen dan had ik deze tekst nu niet geschreven. Dank voor je tomeloze optimisme, enthousiasme en gezelligheid de afgelopen jaren. En niet te vergeten, de heerlijke stukjes vlees.

Prof. dr. G.M. Raghoebar, beste Gerry, je bent altijd mee te krijgen in het proberen van iets nieuws en geeft ons (3D lab) hier veel vrijheid in. Bedankt voor je vertrouwen, enthousiasme en de je participatie als behandelaar en co-auteur in een aantal van mijn publicaties.

Prof. dr. A. Vissink, beste Arjan, dank voor je hulp bij de review en andere zaken die terloops of bij de koffieautomaat werden behandeld. Jouw hulp stel ik erg op prijs.

Prof. dr. J.L.N. Roodenburg, beste professor, gedurende mijn hele promotietraject heb ik een onverminderd enthousiasme ervaren wanneer we in gesprek waren over 3D-technologie of onderzoek. Dit was erg stimulerend en ook van waarde om nieuwe ideeën inhoudelijk aan te scherpen, dank hiervoor.

Dr. K.P. Schepman, Dr. B. van Minnen, Dr. S.A.H.J. de Visscher, beste Kees Pieter, Baucke en Sebastiaan, dank voor jullie participatie als behandelaar en co-auteur in enkele van de studies uit dit proefschrift. Jullie dragen de 3D-technologie een warm hart toe en innoveren graag, waarvoor dank.

Dr. C. Saridin, **Dr. N.B. van Bakelen**, beste Carrol, beste Nico, dank voor jullie enthousiasme en input omtrent de G-TMJ-TJR. Met name de precisie van deze

ingreep en de plaatsing van de prothese vind ik fascinerend. Jullie wijze van werken draagt hier sterk aan bij. Zowel op de OK als op het podium zijn we volgens mij op elkaar ingespeeld. Bedankt.

Dr. J. Jansma, **Dr. R.H. Schepers,** beste Johan, beste Rutger, 'die twee', altijd samen en nu helaas niet meer onderdeel van ons team. Bedankt voor wat ik van jullie heb mogen leren en wat we hebben gedaan in de afgelopen jaren. Ook voor jullie aandeel in de 4D studie ben ik erg dankbaar

Drs. J. Alberga, beste Jamie, kamergenote, met name in de afronding van onze proefschriften hebben we veel kunnen sparren over de inhoud van onze stukken. Dank hiervoor, voor de goede sfeer en vele zoete versnaperingen.

Dr. J. Drouven-Kamstra, beste Jolanda, dank voor je inzet voor de 3D toepassingen in de implantologie. Jouw duidelijke blik maakt ons (3D lab) werk makkelijker.

Ron de Graaf, beste Ron, dank voor je werk voor het 3D-lab en de afdeling. Je draagt het lab en de afdeling een warm hart toe en dit deel ik met je. Dank voor je hulp.

Maikel Beerens, beste Maikel, jarenlang hebben wij bijna wekelijks contact gehad tijdens de ontwikkeling van de G-TMJ-TJR. Jouw aandeel hierin mag natuurlijk niet ongenoemd blijven. Gelukkig zag jij, nog voor ik op het project kwam, potentie in de prothese en durfde jij, met je bedrijf Xilloc, het aan om verder te ontwikkelen. Het is ons gelukt, bedankt.

3D Lab: Peter, Anne, Nick, Hylke, Miriam, Lisanne, Katrijn, Haye, Jorn-Ids, en Sander, Zeinab, Reinier, Willemijn, bedankt voor de fijne samenwerking. Altijd is er wel ruimte om te sparren over ideeën of voor even dat handje hulp. We zijn een goed team en krijgen een hoop voor elkaar voor de patiëntenzorg, de wetenschap en bij de Buurvrouw.

Ahswin Beekes, beste Ashwin, veel tijd hebben we doorgebracht in 'jouw hok'. Altijd als er ge-Willie Worteld moet worden kom ik bij jou en laat ik mij verrassen. Dit door of je tips en ideeën, of door een goed en/of slap verhaal. Dank voor alle hulp, ook als dit even niet goed uitkomt.

Klaas van Linschoten[†]**, Steve, Janniko, Carola, Peter, Florian** en overige medewerkers verbonden aan het Anatomisch lab UMCG. Met jullie hulp heb ik door de jaren heen een hoop dingen mogen en kunnen doen die onmisbaar zijn geweest voor zowel mijn onderzoek als dat van anderen. Altijd kunnen wij rekenen op jullie hulp en inzet en voor mijn laatste mechanische testen bleken jullie zelfs de enige faciliteit in heel het UMCG waar ik welkom was. Dank hiervoor.

Drs. N. Vosselman, beste Nathalie, jouw vernuft heeft mij met regelmaat uit de brand geholpen. Dank voor je hulp en de fijne samenwerking in zowel het onderzoek als de patiëntenzorg.

Sanne Scholten, Barbara Eijkelenborg, Beste Sanne en Barbara, jullie wil ik bedanken voor jullie hulp bij het fixeren van de bitjes ten behoeve van de 4D studie. Erg fijn dat jullie konden en wilden helpen.

Gert Seubers, beste Gert, dank voor je organisatorische hulp bij meerdere studies. Je hebt perfect op je netvlies wanneer we specifieke patiënten verwachten en dit heeft mij meermaals gered.

Angelika, Lisa, Fieke en Nienke, beste dames, dank voor alles de afgelopen jaren. Er is geen ruimte om alles specifiek te benoemen maar bijna elke dag weer heb ik iets nodig waarbij of waarmee jullie kunnen helpen. Fijn dat ik altijd bij jullie mag aankloppen.

Röntgendames, dank voor jullie hulp bij de 4D studie. Zonder jullie was dit niet gelukt. Ook voor alle vlugge hulp bij de korte '*binnenloop-scans*', erg bedankt.

CBT, in de patiëntenzorg en daar omheen hebben wij veel met elkaar te maken gehad. Bedankt voor de altijd fijne samenwerking.

Research Instrumentmakerij UMCG, heren van de RI, al sinds 2014 werken wij samen en kom ik naar jullie voor prototypes, frees, draai en printwerk. Met jullie hulp heb ik de experimenten kunnen doen die dit proefschrift hebben gemaakt tot wat het is. Dank hiervoor.

AIOS en jongklaren, bedankt voor de fijne samenwerking, de vele mooie congresbezoeken, afdelingsuitjes en andere momenten.

Jerry en Boukje, bedankt voor jullie hulp bij mijn talloze verzoekjes en afwijkende dingen.

Alle overige MKA- medewerkers, onderzoekers, en stagiaires, dank voor jullie interesse, betrokkenheid en hulp in mijn onderzoek.

Dave, David, thank you for providing us with the perfect spot for '*Thesis-Friday',* good company and a healthy portion of Guinness and humbleness every week.

Koekhuis, Abel, Bart Willem, Leon, Sep, Simon, Tim, amigos, dank voor jullie interesse in mijn onderzoek en fijn dat ik hier met jullie vaak ook niet mee bezig hoef te zijn.

Roti-club, pals, bovenstaande geldt ook voor jullie, dank voor zowel het kunnen bespreken van mijn onderzoek als het kunnen laten liggen hiervan. De woensdag koester ik.

Kobus, van alle personen in deze lijst heb jij de meeste uren van mijn onderzoek meegemaakt. Je was gedurende de COVID pandemie onderdeel van mijn thuislaboratorium en hebt mijn ontwikkelingen op de voet gevolgd. Dank voor je steun. **Kees**†, je was iets minder geïnteresseerd, je wordt gemist.

Paranimfen, **Abel, Bart Willem en Guido,** vrinden, dank dat jullie tijdens de verdediging van dit proefschrift en ook de rest van de dagen aan mijn zijde staan.

Dr. G. Trentadue, of eigenlijk, Lord dr. dr. G. Trentadue, jou dien ik los van bovenstaande te bedanken omdat je juist in dit proefschrift een groot aandeel hebt gehad. Sinds we elkaar in 2015 ontmoetten, in wat nu het 3D Lab is, zijn wij vrienden geweest. We zaten in eenzelfde schuitje wat het promoveren betreft, al liep je iets op mij voor. In onze wekelijkse *'Thesis-Friday'*-uitjes, een excuus voor de nodige Guinnii, werd al ons wetenschappelijke werk aan de tand gevoeld en door elkaar van de nodige kritiek voorzien. Ik heb een hoop van je mogen leren op dit vlak. Ook als persoon sta je altijd voor mij/ons klaar, je bent een goede vriend, dankjewel.

Lieve Mam en Pap, bedankt voor jullie onvoorwaardelijke steun. Ik heb hier altijd op kunnen rekenen, of het nu mijn voetbalcarrière, het verbouwen van ons huis of hobby's betrof. Bedankt voor alle kansen. Lieve **Debby**, ook jij bedankt dat bovenstaande mogelijk was.

Lieve Else, bedankt voor je serieuze interesse in de ontwikkeling en met name werking van de MANDYBILATOR. Het was zo nu en dan lastig voor je om overal af te blijven maar het is niet voor niets geweest. Hopelijk mag dit boek ooit een interesse voor de wetenschap en/of techniek in je aanwakkeren.

Lieve Emma, je staat al sinds mijn studie aan mijn zijde en ik kan altijd rekenen op je steun. Zij het van mentale aard of een meer logistieke (sorry dat je meerdere jaren je werkkamer/mijn thuis-laboratorium hebt moeten missen). Met het verschijnen van dit proefschrift ronden we wederom een hoofdstuk af. Ik kan niet wachten op de vele volgende die we samen nog gaan meemaken. Falafel, ik hou van je.

CURRICULUM VITAE

Bram Merema was born in Assen on the 6th of March 1992. He finished high school in 2010 (Dr. Nassau College, Assen) and started with Mechanical Engineering at the Hanze University of Applied Sciences in Groningen in 2010 and graduated in 2016 after finishing the Biomedical Engineering Minor. Hereafter he continued with his work at the department of Oral and Maxillofacial Surgery at the University Medical Center Groningen. He started here as a researcher and Engineer at the 3D Lab, which had just been founded in late 2015, and has been working here since.

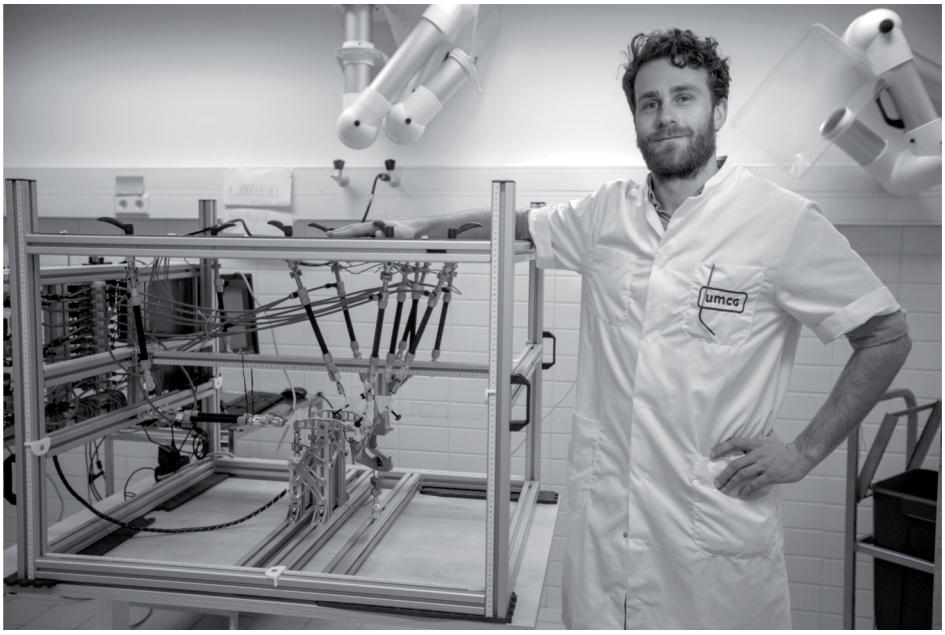

Address for correspondence

B.J. Merema
University Medical Center Groningen
Department of Oral and Maxillofacial Surgery
P.O. Box 30.001
9700 RB Groningen
The Netherlands
Phone: +31 50 3613481
E-mail: b.j.merema@umcg.nl

LIST OF PUBLICATIONS

Book chapters

Replacing temporomandibular joints.
F.K.L. Spijkervet, **B.J. Merema**, N.B. Van Bakelen, J. Kraeima
Editor(s): Peter Revell, In Woodhead Publishing Series in Biomaterials, Joint Replacement Technology (Third Edition), Woodhead Publishing, 2021, Pages 675-697, ISBN 9780128210826

Articles

The design, production and clinical application of 3D patient-specific implants with drilling guides for acetabular surgery.
Merema BJ, Kraeima J, Ten Duis K, Wendt KW, Warta R, Vos E, Schepers RH, Witjes MJH, IJpma FFA.
Injury. 2017 Nov;48(11):2540-2547. doi: 10.1016/j.injury.2017.08.059. Epub 2017 Aug 30.

Development of a patient-specific temporomandibular joint prosthesis according to the Groningen principle through a cadaver test series.
Kraeima J, **Merema BJ**, Witjes MJH, Spijkervet FKL.
J Craniomaxillofac Surg. 2018 May;46(5):779-784. doi: 10.1016/j.jcms.2018.03.004. Epub 2018 Mar 14.

Patient-specific sub-periosteal zygoma implant for prosthetic rehabilitation of large maxillary defects after oncological resection.
Vosselman N, **Merema BJ**, Schepman KP, Raghoebar GM.
Int J Oral Maxillofac Surg. 2019 Jan;48(1):115-117. doi: 10.1016/j.ijom.2018.06.010. Epub 2018 Jul 2

Differences in approach for sub-periosteal zygoma implant designs.
Vosselman N, **Merema BJ**, Raghoebar GM, Vissink A.
Int J Oral Maxillofac Surg. 2019 Dec;48(12):1605-1606. doi: 10.1016/j.ijom.2019.03.005. Epub 2019 Mar 26.

Novel finite element-based plate design for bridging mandibular defects: Reducing mechanical failure.
Merema BBJ, Kraeima J, de Visscher SAHJ, van Minnen B, Spijkervet FKL, Schepman KP, Witjes MJH.
Oral Dis. 2020 Mar 16;26(6):1265-74. doi: 10.1111/odi.13331. Online ahead of print.

Experimental Multicenter and Multivendor Evaluation of the Performance of PET Radiomic Features Using 3-Dimensionally Printed Phantom Inserts.
Pfaehler E, van Sluis J, **Merema BBJ**, van Ooijen P, Berendsen RCM, van Velden FHP, Boellaard R.
J Nucl Med. 2020 Mar;61(3):469-476. doi: 10.2967/jnumed.119.229724. Epub 2019 Aug 16.

Utilising the nasal aperture for template stabilisation for guided surgery in the atrophic maxilla.
Onclin P, Kraeima J, **Merema BBJ**, Meijer HJA, Vissink A, Raghoebar GM.
Int J Implant Dent. 2020 Jun 26;6(1):23. doi: 10.1186/s40729-020-00221-x.

Patient-specific finite element models of the human mandible: Lack of consensus on current set-ups.
Merema BBJ, Kraeima J, Glas HH, Spijkervet FKL, Witjes MJH.
Oral Dis. 2021 Jan;27(1):42-51. doi: 10.1111/odi.13381. Epub 2020 Jul 9.

Three-dimensional virtual surgical planning in the oncologic treatment of the mandible.
Kraeima J, Glas HH, **Merema BBJ**, Vissink A, Spijkervet FKL, Witjes MJH.
Oral Dis. 2021 Jan;27(1):14-20. doi: 10.1111/odi.13631. Epub 2020 Sep 28.

Feasibility of Imaging-Based 3-Dimensional Models to Design Patient-Specific Osteosynthesis Plates and Drilling Guides.
IJpma FFA, Meesters AML, **Merema BBJ**, Ten Duis K, de Vries JPM, Banierink H, Wendt KW, Kraeima J, Witjes MJH.
JAMA Netw Open. 2021 Feb 1;4(2):e2037519. doi: 10.1001/jamanetworkopen.2020.37519.

Accuracy of fit analysis of the patient-specific Groningen temporomandibular joint prosthesis.
Merema BJ, Kraeima J, Witjes MJH, van Bakelen NB, Spijkervet FKL.
Int J Oral Maxillofac Surg. 2021 Apr;50(4):538-545. doi: 10.1016/j.ijom.2020.08.012. Epub 2020 Sep 14.

Immediate implant-retained prosthetic obturation after maxillectomy based on zygomatic implant placement by 3D-guided surgery: a cadaver study.
Vosselman N, Glas HH, de Visscher SAHJ, Kraeima J, **Merema BJ**, Reintsema H, Raghoebar GM, Witjes MJH.
Int J Implant Dent. 2021 Jun 14;7(1):54. doi: 10.1186/s40729-021-00335-w.

Three-Dimensional Guided Zygomatic Implant Placement after Maxillectomy.
Vosselman N, Glas HH, **Merema BJ**, Kraeima J, Reintsema H, Raghoebar GM, Witjes MJH, de Visscher SAHJ.
J Pers Med. 2022 Apr 6;12(4):588. doi: 10.3390/jpm12040588.

Four-Dimensional Determination of the Patient-Specific Centre of Rotation for Total Temporomandibular Joint Replacements: Following the Groningen Principle.
Merema BBJ, Witjes MJH, Van Bakelen NB, Kraeima J, Spijkervet FKL.
J Pers Med. 2022 Aug 31;12(9):1439. doi: 10.3390/jpm12091439.

A Contemporary Approach to Non-Invasive 3D Determination of Individual Masticatory Muscle Forces: A Proof of Concept.
Merema BBJ, Sieswerda JJ, Spijkervet FKL, Kraeima J, Witjes MJH.
J Pers Med. 2022 Aug 2;12(8):1273. doi: 10.3390/jpm12081273.

The sketch on the right provides a clear view on the organic and seemingly disorganized structure of topology optimized volumes. In this case, a titanium alloy was considered during the process. Due to the complex structure, this implant should be manufactured through 3D-printing and cannot be milled from a solid block without further modifications.

The model on the left was prepared for milling operations. As the result of topology optimization was a typical organic structure, sharp and abberant positions needed filling in order to make the highest possible surface approximation in this design.

To reconstruct a large continuity defect in the mandible, th specific implant can be obtained through the application o optimization. This technique results in geometries that re organic topology as the material follows the stress within t The implants depicted here are prepared for milling (le 3D-printing (right).